The effects of secretagogues and bile salts on calcium signalling and NFkB activation in pancreatic acinar cells.

Thesis submitted in accordance with the requirements

of

The University of Liverpool

for the degree of

Doctor in Philosophy

by

Esme Rebecca Longbottom

September 2002

Abstract

The main function of the pancreatic acinar cell is to synthesize and secrete digestive enzymes. Gut hormones and neurotransmitters binding to their respective receptors stimulate the secretion of the digestive enzymes. One of the second messengers involved in secretion stimulated by cholecystokinin (CCK) and acetylcholine (ACh) is Ca^{2+}. The Ca^{2+} is released from internal stores as a consequence of IP_3 production. Ca^{2+} influx is triggered as a result of store depletion and Ca^{2+} efflux occurs in order to reduce the cytoplasmic Ca^{2+} levels back to normal resting levels. The first aim of this thesis was to investigate the influence of CCK and ACh on these two processes. The main finding from this section of my work was that, in cells with depleted calcium stores and elevated cytosolic [Ca^{2+}], secretagogues CCK, ACh and JMV-180 all induced a reduction in cytosolic Ca^{2+} levels. The reduction was due to an activation of extrusion. The reduction was independent of external sodium excluding any involvement of the Na^+/Ca^{2+} exchanger, and was therefore mediated by stimulation of the PMCA. Importantly calcium extrusion was stimulated by low "physiological" concentrations of CCK and ACh, proposing a role for this action in normal pancreatic acinar cell signalling. The investigation of the signalling pathway involved in this secretagogue-induced activation of Ca^{2+} extrusion examined a wide variety of signalling molecules. The findings of my experiments suggest a possible role for tyrosine phosphorylation in the actions of the secretagogues on the PMCA.

The second area of work reported in this thesis was an examination of the influence of a bile acid, TLC-S on Ca^{2+} signalling in the pancreatic acinar cell. Reflux of bile acids into the pancreas is considered to be a trigger for acute pancreatitis (Opie,

1901). A recent report suggested that bile acids caused a release of Ca^{2+} from internal stores (Voronina *et al.*, 2002). My experiments demonstrated that in conditions of elevated cytosolic [Ca^{2+}] after store depletion, TLC-S induced three types of responses: 1. A further Ca^{2+} increase, 2. A Ca^{2+} increase followed by a reduction to below the starting level, and 3. A reduction in the cytosolic Ca^{2+} level. The main focus of these investigations, was the identification of the source of Ca^{2+} revealed by TLC-S application in conditions of an elevated cytosolic Ca^{2+} plateau. The findings of my experiments eliminate any involvement of the mitochondria or granules in the TLC-S induced Ca^{2+} transient increase. The study of the Golgi apparatus was inconclusive. The TLC-S transient was found to be somewhat dependent on calcium entry, since it was partially attenuated by La^{3+} application. The response was however not abolished completely. It seems that TLC-S enhances Ca^{2+} influx, however, it may also mobilise calcium from another source, possibly an internal Ca^{2+} store with a low Ca^{2+} affinity.

The aim of the third section of the work reported in this thesis was to establish a method for fast measurement of Nuclear Factor kappa beta (NFκB) activation in living pancreatic acinar cells. NFκB plays an important role in development of pancreatitis. The method aimed to measure activation of NFκB by nuclear translocation of Green Fluorescent Protein (GFP) conjugates of a transcriptionally active subunit of NFκB, p65. The initial experiments were performed in HeLa cells in order to establish compatibility of translocation and Ca^{2+} measurements. Nuclear accumulation of the NFκB construct was observed upon stimulation in HeLa cells. To investigate NFκB activation in pancreatic acinar cells, the construct was microinjected into freshly isolated cells. Successfully expressed GFP-p65 was found

predominately in the nucleus of pancreatic acinar cells even before stimulation. No further nuclear accumulation could be measured after stimulation with supramaximal concentrations of CCK which have been previously reported to activate NFκB in the pancreatic acinar cell (Han & Logsdon, 1999). Attempts to remove GFP-p65 from nuclei or reduce its nuclear accumulation were unsuccessful. Attempts to measure NFκB activation via the rate of inhibitor protein degradation (using GFP conjugated IκBα protein) were also unsuccessful. These experiments were difficult due to cell movement artefacts and the low rate of survival of microinjected cells. The probability of successful expression of GFP constructs in microinjected cells was also low. Further methodological work, possibly including usage of viral transfection, is necessary for developing the technique of fast measurements of NFκB activation in pancreatic acinar cells.

This thesis reports that secretagogues activate PMCA and reduce sustained calcium levels in cells with depleted thapsigargin sensitive calcium stores, whilst TLC-S can enhance calcium levels. The effect of TLC-S is mediated by increasing Ca^{2+} influx and possibly by releasing calcium from a thapsigargin insensitive calcium stores. These findings have important implications in understanding the onset and development of acute pancreatitis.

For my family, friends and other animals.

Acknowledgements

I would like to thank Alexei Tepikin for all his support, patience, advice and supervision through the course of this project, for answering my endless queries and his troubleshooting skills when things weren't going exactly to plan. I would also like to thank Mike White for provision of the GFP constructs, invaluable discussion, belief and encouragement. I would also like to thank Professor Petersen for his advice and discussion during the project and allowing me the opportunity to work in his laboratory.

I would also like to thank all those that have help me through the course of my work and time here in Liverpool, those of whom have provided valuable assistance. To my colleagues in blue block, Dr Oleg Gerasimenko for help with the steep learning curve of microinjection, Alex Harmer and Jose Cancela who between them taught me electrophysiology techniques, Mike for his advice and instruction with the confocal and scientific debate, Paul for his help with the imaging system. I should like to thank Dr Camille Vaillant for advice and discussion and Mrs Julie Henry for her time processing tissue and technical advice on electron microscope operation. The software used to perform the analysis for the EM work was kindly loaned by Dr P Djali and Dr M Browne at kinetic imaging.

A big thanks to everyone who has worked in Blue Block during my stay there and members of Mike Whites group who also answered my questions and gave up their time to help.

I also need to thank my friends and family without whom I would not have got this far. Special thanks go to my housemates Jane, Mark, Shirley and Io for putting up with me for so long; to Sarah and Adelina for their sympathetic ears, honest advice and refuge provisions. To everyone else you know who you are, at work, hockey, cricket and otherwise (;-)), THANK YOU. And last but certainly not least my family for their support, grammatical knowledge, red-cross parcels, mechanical abilities and unwavering belief.

Thank you to the Wellcome trust for providing the prize studentship making this all possible.

Abbreviations

2-APB	2-aminoethoxydiphenylborate
AA	Arachidonic acid
$AACOCF_3$	Arachidonyl triflioromethyl ketone
ACh	Acetylcholine
AM	Acetoxymethyl
AOTF	Acousto-Optical Tuneable Filter
ATP	Adenosine triphosphate
BAPTA	1,2-bis-(2-aminophenoxyethane-N, N, N', N')-tetraacetic acid
BoNT/A	Botulinum neurotoxin A
BZiPAR	bis-(CBZ-Ile-Pro-Arg)-R110
cADPr	cADPribose
cAMP	Cyclic adenosine monophosphate
CCCP	Carbonyl cyanide 3-chlorophenylhydrazone
CCD	Charged coupled device
CCK	Cholecystokinin
cGMP	Cyclic guanosine monophosphate
CHO	Chinese hamster ovary
CICR	Calcium induced-calcium release
CIF	Calcium influx factor
CPA	Cyclopiazonic acid
CRAC	Calcium-release activated current
DAG	Diacylglycerol
DNA	Deoxyribose nucleic acid
EGTA	Ethylene glycol-bis(2-aminoethylether)-N,N,N¢,N¢-tetraacetic acid
EM	Electron microscopy
ER	Endoplasmic reticulm
GFP	Green fluorescent protein
HEK	Human embryonic kidney
HEPES	4-(2-Hydroxyethyl)piperazine-1-ethanesulfonic acid
I_{CRAC}	Ca^{2+} release-activated Ca^{2+} current
I_{CRANC}	Calcium-release-activated non-selective cation current
IκB	Inhibitor kappa Beta -IκB
IKK	Inhibitory Kappa Kinase
Il-1β	Interleukin 1beta
IP_3	Inositol 1,4,5-trisphosphate
IP_3R	Inositol 1,4,5-trisphosphate receptor
IP_4	Inositol-1,3,4,5-tetrakisphosphate
LMB	Leptomycin B
LRD	Lipid raft domains
LSM	Laser scanning microscope
MAP	Mitogen activated protein

Na^+/Ca^{2+} exchanger	Sodium/calcium exchanger
NAADP	Nicotinic acid adenine dinucleotide phosphate
NAC	N-acetylcysteine
NADH	Nicotinamide adenine dinucleotide (reduced form)
NFkB	Nuclear Factor kappa Beta
NMDG	N-Methyl-D-glucamine
NO	Nitric oxide
NP-EGTA	Nitrophenyl EGTA
PA	Phosphatidic acid
PDTC	Pyrrolidine dithiocarbamate
PDZ	PSD-95/Dlg/ZO-1
PI (3,4,5)P_3	Phosphatidylinositol 3,4,5-trisphosphate
PIP_2	Phosphatidylinositol 4,5-bisphophate
PKC	Protein kinase C
PLA_2	Phospholipase A_2
PLC	Phospholipase C
PLD	Phospholipase D
PMA	Phorbol-12-myristate-13-acetate
PMCA	Plasma membrane Ca^{2+}- ATPase
RANTES	Regulated upon activation, normal T-cells expressed and secreted
ROI	Region of interest
RyR	Ryanodine receptors
S.E.	Standard error
SERCA	Sarco/endoplasmic reticulm Ca^{2+}-Mg ATPase
SNAP	Soluble NSF attachment protein
SOC	Store operated calcium
SOCC	Store operated calcium channels
TA	Taurolithocholic acid
tBuBHQ	2,5-di-(*tert*-butyl)-1,4-benzohydroquinone
TCA	Taurocholate
TCDC	Taurochenodeoycholate
TDC	Taurodeoxy-cholate
TeNT	Tetanus neurotoxin
TLC-S	Taurolithocholic acid 3-sulfate
TMB-8	8-(Diethylamino)octyl 3,4,5-trimethoxybenzoate hydrochloride
TNFα	Tumour necrosis factor alpha
TRP	Transient receptor potential
UV	Ultra Violet
VAMP	Vesicle associated membrane protein
VIP	Vasoactive intestinal polypeptide
VOCC	Voltage operated calcium channels
VSCC	Voltage sensitive calcium channels
Xest C	Xestospongin C

Contents

Chapter 1

Introduction

The pancreas

Structure, function and location of the pancreas

The pancreas is a gland located in the upper abdominal cavity. The name pancreas comes from the Greek, 'pan' meaning all and 'kreas' meaning meat. This describes the fleshy nature of the organ, which is made up of mainly water with a smaller amount of protein and fat. The pancreas is divided into four regions, head, neck, body and tail. The head is the largest portion that is in close contact with the duodenum. The pancreas tapers towards the tail, which lies behind the stomach adjacent to the spleen. The blood supply to the pancreas is from the coeliac and superior mesenteric arteries that branch from the aorta. Venous drainage is via the hepatic portal vein from the splenic and superior mesenteric veins. The pancreas has an extensive lymphatic drainage system which is not particularly active under normal physiological conditions, though its role in fluid drainage is increased in conditions of pancreatitis (Bockman *et al.*, 1973).

Both the parasympathetic and sympathetic branches of the autonomic nervous systems supply the pancreas. The parasympathetic branch is involved in secretory stimulus of the exocrine pancreas. Another mechanism of secretory stimulus is by means of hormonal control. The pancreas is a lobular organ and within these lobules there are a large proportion of acinar cells (exocrine), a smaller number of ductal cells and endocrine tissue, islets of Langerhans. This series of studies was performed on acinar cells (exocrine pancreas), which account for the majority of cells in the pancreas. Further description and discussion will focus on the acinar unit.

The exocrine unit (referred to as acini, from the Latin acinus, meaning berry), the main function of which is to synthesize and secrete digestive enzymes, surrounds a common lumen. There are intralobular ducts and interlobular ducts. The intralobule ducts are situated in lobules and drain pancreatic juices from acinar units, and the interlobule ducts connect the individual lobules running along the regions of connective tissue connecting eventually to the main pancreatic duct. This eventually joins the common duct that enters the duodenum at the Ampulla of Vater (Motta *et al.*, 1997). The pancreatic juice consists of fluid containing bicarbonate and chloride ions secreted by the ductal system. This acts a transport medium for the digestive enzymes secreted by the acinar cells. The pH of the pancreatic juice is of importance in achieving an environment in which the digestive enzymes can function. The pancreatic juice has a pH of between 7.6 and 8.2. This neutralises the acidity of the chyme received into the intestine from the stomach, and raises the pH to a range that is optimal for the activity of the digestive enzymes (Williams, 1980).

Digestive enzymes

An acinar unit is comprised of acinar cells, which secrete the digestive enzymes responsible for the breakdown of carbohydrate, fat, nucleic acids and proteins. The enzymes amylase, lipase, nucleases (ribonuclease and deoxyribonuclease), trypsin and chymotrypsin are all synthesised and secreted by the acinar cells. They are secreted in the form of proenzymes (zymogens). The presence of trypsin inhibitor prevents their activation during transit to the duodenum. The enzymes are activated upon arrival in the intestine by enteropeptidase found in the brushborder of the small intestine. Enteropeptidase cleaves a lysine-isoleucine bond within the trypsinogen

molecule activating a small proportion of the secreted trypsinogen, which in turn cleaves and activates other proenzymes chymotrypsinogen, proelastase and procarboxypeptidase. This results in simultaneous activation of the full range of digestive enzymes in the small intestine where they can act on their specific substrates.

Structure of the acini unit

Acinar cells exist in an acini unit as described earlier with an encompassing basal laminae that surrounds each acini unit covering the basal membrane of each acinar cell within the unit, insulating them from neighbouring acini units. Other cells in the acini are centroacinar cells, which form the initial part of the intralobular duct (figure1.1). These cells have a less electron dense cytoplasm as they lacks secretory granules, however within the cytoplasm there are a large number of mitochondria. These cells are thought to be involved in the transport of fluid and ions into the lumen of the acini unit (Gorelick & Jamieson, 1994). The lumen of the acini is sealed from the intercellular space by a series of junctions. The closest of which to the lumenal space is that of an occluding junction or tight junctions. These are followed by a belt desmonsomes and a spot desmonsomes (figure 1.1). The tight junctions form a continuous belt around the whole of the acinar cell where there is a fusion of the adjacent cell membranes. This prevents the movement of fluid and ions and also maintains the different membrane composition of the basal and apical membranes, the basal membrane containing a greater number of proteins in comparison to the apical membrane. The belt desmonsomes form a band around each acinar cell where there is thickening of the plasma membrane in this region due

to a dense network of thin filaments containing a protein vinculin through which the actin filaments attach to the plasma membrane. The spot desmonsomes are more rivet-like structures that bridge the intercellular gap where two plaques from adjacent plasma membranes of two cells meet. Intermediate filaments have been shown to terminate at spot desmonsomes (Gorelick & Jamieson, 1994).

Another type of cell-cell junction is a gap junction. These have been shown to form a pore structure that is complemented in the juxtapose membrane, which together form a channel between the two cells. These channels have a pore size of 16-20Å allowing the passage of ions, metabolites, and nucleotides but not macromolecules. Electrical communication between acinar cells was demonstrated by the use of microelectrodes in two separate cells. Depolarisation of one cell changed the polarisation of the neighbouring cells to an equal extent (Petersen, 1975). The direct transfer of dyes between cells has also been performed to demonstrate the connection between cells. Fluorescein and procion yellow have been shown to pass from an injected cell into neighbouring cells. The connected units were shown to be quite extensive consisting of over 100 cells (Findlay & Petersen, 1983;Iwatsuki & Petersen, 1979a). The uncoupling and recoupling of cells has been demonstrated by high concentrations of secretagogues (Findlay & Petersen, 1982). Intracellular injection of calcium or intracellular acidification have also been shown to induce reversible isolation of cells (Iwatsuki & Petersen, 1978;Iwatsuki & Petersen, 1979b). Secondary messengers Ca^{2+}, inositol 1,4,5-trisphosphate (IP_3) and cAMP have been shown to pass through gap junctions (Saez *et al.*, 1989;Sandberg *et al.*, 1992). Thus gap junctions represent a potentially important means of coordinating responses in groups of individual cells. This has been demonstrated for IP_3 in epithelial cells

(Boitano *et al.*, 1992) and between neurons and astrocytes (Nedergaard, 1994). Calcium wave transmission has been shown to be intercellular in rat pancreatic acinar cells within an acini unit. The study suggests that this is due to diffusion of IP_3 through gap junctions as the injection of $CaCl_2$ alone was not enough to propagate a wave within the unit (Yule *et al.*, 1996). This study also demonstrates the uncoupling of cells at supramaximal concentrations of agonist. The diffusible distance of Ca^{2+} as an effective range for intercellular communication is questioned by Allbritton and colleagues owing to the presence of intracellular buffering proteins (Allbritton *et al.*, 1992). This coordination of signals between cells may account for the more efficient secretion from groups of cells in comparison to single cells (Stauffer *et al.*, 1993).

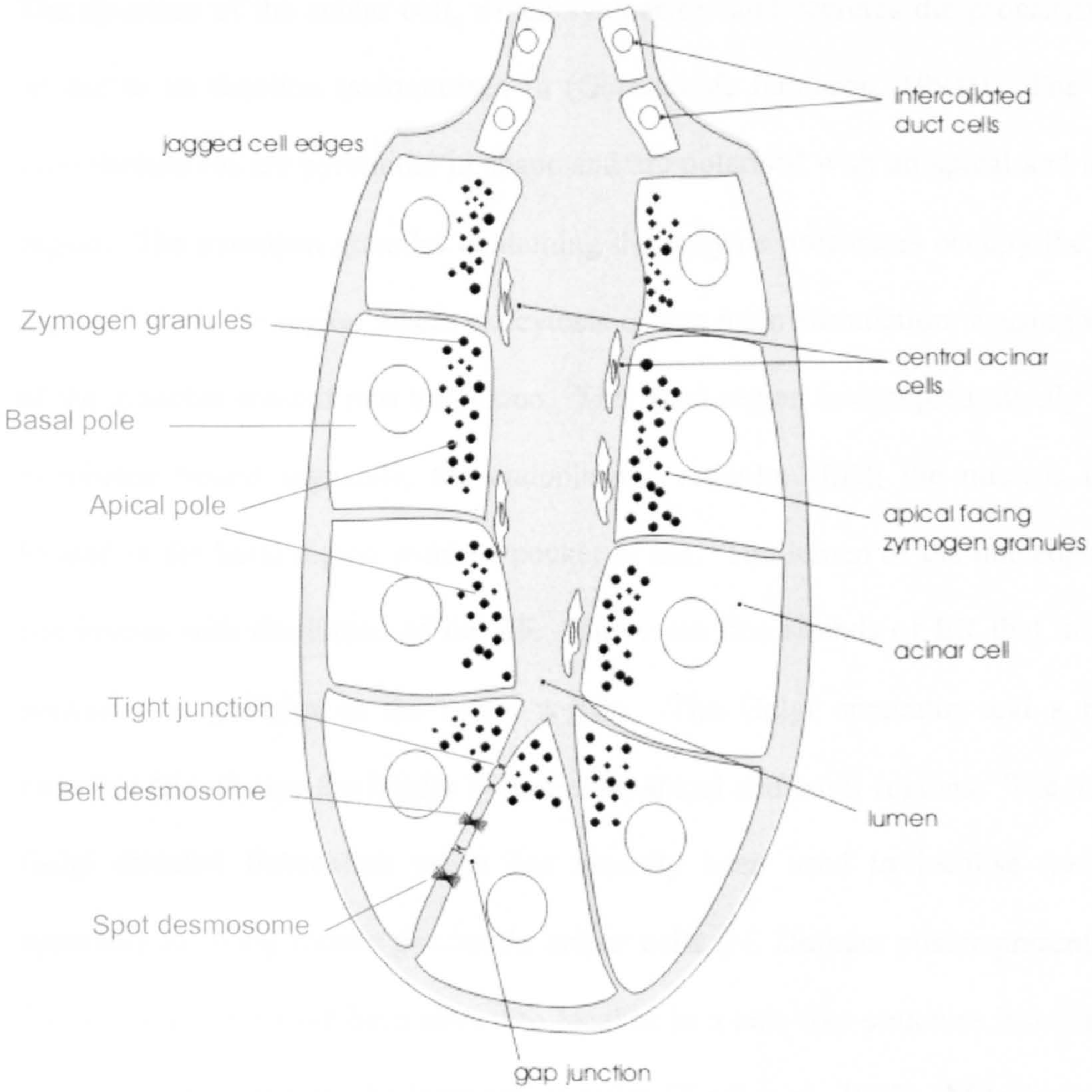

Figure 1.1. **The acini unit**. The cartoon represents the structure of the acini unit. The acinar cells arranged around a common lumen into which the zymogens are secreted upon stimulation. The cartoon shows the location of cells within the acini unit. The acinar cells are connected by gap junctions and tight junctions as indicated on the cartoon, and tight junctions. The junctions are important for maintaining the structure of acinus and also for separating content of apical and basal membranes of acinar cells (adapted from Craske 1999).

Structure of the acinar cell

The structure of the acinar cell, which synthesises and secretes the proenzymes, is related to its function (summarised in (Gorelick & Jamieson, 1994)). The acinar cells themselves are pyramidal in shape and are polarised with an apical and a basal region. The zymogen granules containing the enzyme precursors occupy the apical region. This is the region where exocytosis occurs upon stimulation, causing release of the granules content into the lumen. The basal region is occupied mainly by the membrane bound organelle, the endoplasmic reticulm (ER); the nucleus is also located in the basal region within a pocket of ER. The lumen of the nucleoplasm is continuous with the lumen of the ER. There are fine strands of ER that interpose between the granules in the apical region. The Golgi apparatus and a belt of mitochondria occupy the border between the apical and basal regions. The use of a Golgi directed fluorescent probe has recently been used to localise the Golgi apparatus in living mouse pancreatic acinar cells (N. Dolman poster presentation). The mitochondria have been shown to localise in a belt–like structure insulating the apical region containing the secretory granules (Tinel *et al.*, 1999). Mitochondria are also located in a perinuclear and sub-plasmalemmal locations and their location has an impact on local calcium homeostasis (Park *et al.*, 2001).

Calcium signalling

Calcium is involved in the regulation of numerous processes in cells such as contraction, proliferation, gene expression, regulation of metabolism and secretion. The versatility of calcium in its role of a secondary messenger within the cell relies

on the ability of the cells to generate different spatial and temporal calcium signals. The characteristics of different calcium signals elicit different outcomes for example different frequencies of calcium oscillations activate different transcription factors (Dolmetsch *et al.*, 1998). The main function of pancreatic acinar cells is to produce and secrete digestive enzymes. This is regulated by secretagogues acting through secondary messengers Ca^{2+}, diacylglycerol (DAG) and cAMP. The next section provides a brief overview of the role of calcium, the different patterns of calcium signals produced, and the mechanisms involved in the production of calcium signals in the pancreatic acinar cell.

Calcium and secretion

Secretion is activated by the gut hormones cholecystokinin (CCK) and secretin, and the neurotransmitters acetylcholine (ACh) and vasoactive intestinal polypeptide (VIP). The binding of agonists to their receptors in the basal membrane of the acinar cell stimulates secretion from the lumenal pole. The messenger involved in agonist-stimulated secretion generated by CCK and ACh, is Ca^{2+}. It was first shown that in the absence of extracellular calcium the secretion stimulated by agonist was impaired (Kanno, 1972). Subsequently an increase in cytosolic calcium was sufficient to induce enzyme secretion (Eimerl *et al.*, 1974;Williams & Lee, 1974). The observations of Hokin and Hokin that phosphatidylinositol turnover increased upon stimulation (Hokin & Hokin, 1953), suggested a link between receptor occupation, calcium mobilisation from stores and led to the discovery of the intracellular messenger IP_3. Berridge made the identification of IP_3 production as the event immediately following receptor occupation in 1981 (Berridge, 1981). This was

followed by the demonstration that hormonal stimulation and IP_3 evoke a calcium release from the same intracellular store (Streb *et al.*, 1983). VIP and secretin both cause an increase in the levels of cAMP through adenylate cyclase activation leading to an increase in enzyme or fluid and electrolyte secretion (Gardner & Jensen, 1986). The schematic in figure 1.2 shows a model of stimulus-secretion coupling in the pancreatic cell.

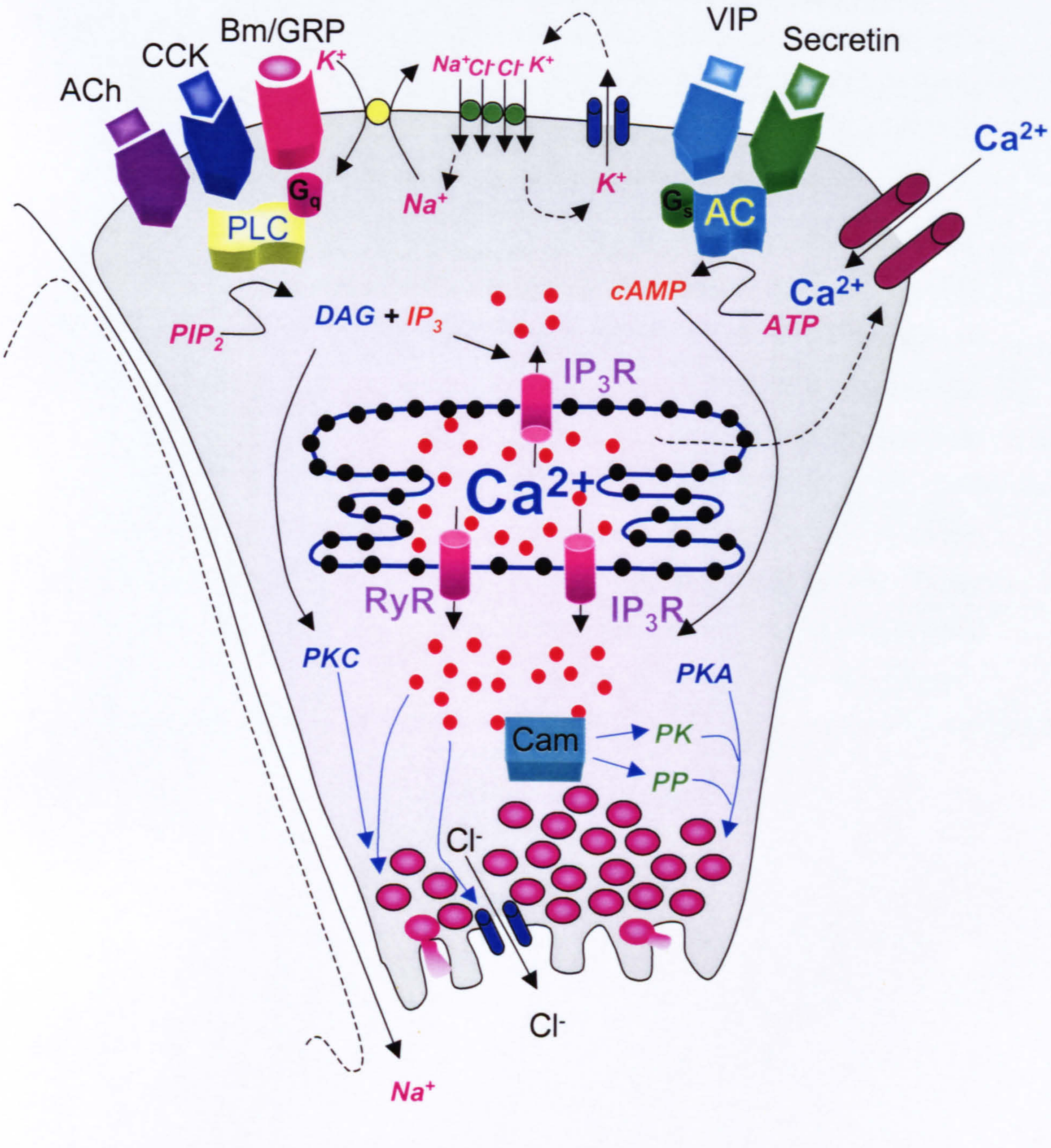

Cam-Calmodulin, PP-protein phosphatase, PK- protein kinases, PKC-Protein kinase C, PKA -Protein kinase A, RyR- ryanodine receptor, IP_3R-IP_3 receptor, PLC-phospholipase C, AC-Adenylate cyclase, Bm/GRP- bombesin/gastrin releasing peptide

Figure 1.2 **A stimulus-secretion model in the pancreatic acinar cell.** The binding of ACh,CCK or bombesin (GRP) activates PLC through the G protein coupled receptor that causes an increase in IP_3 and DAG. IP_3 via its receptors induces calcium release from stores accompanied by activation of calcium influx. DAG activates PKC. Calcium activates exocytosis and Ca^{2+}-activated chloride channels in the apical membrane only (Park, *et al.*, 2001). Calmodulin-calcium complex either directly or indirectly activate calmodulin dependent kinases (CaMK) and calmodulin dependent phosphatases (CaMPP). VIP and secretin binding activates adenylate cyclase that increases cAMP production which in turn activates PKA. The activated CaMK, PKC, PKA and CamPP can then alter the phosphorylation state of proteins involved in exocytosis. There are Ca^{2+} activated non-specific cation channels in the pancreatic cell membranes. It is thought that the electroneutral Cl^-, Na^+, K^+ transport replenishes the Cl^- in the cell.

Agonists ACh and CCK bind to their receptors, which are G protein coupled membrane proteins that have seven membrane-spanning regions. There are two types of CCK: receptor A (alimentary) and B (brain), both bind CCK; type B also binds gastrin. Type A receptors are the only type of CCK receptor expressed in mouse pancreatic acinar cells and the subsequent description concentrates on the type A. They have two binding sites for CCK on the receptor, a high and a low affinity site. The muscarinic cholinergic receptor present in the acinar cell is the M3 isoform. These are coupled to phospholipase C (PLC) that catalyses the formation of IP_3 and DAG from phosphatidylinositol 4,5-bisphophate (PIP_2) breakdown. Several isoforms of PLC are expressed in the acinar cell, PLCβ_1, -β_3, -γ_1 and –δ_1 (Piiper *et al.*, 1997). Antibodies against PLCβ_1 blocked CCK stimulation of the PLC activity. IP_3, a mobile molecule within the cell cytoplasm, migrates and binds to its receptor which functions as a ligand-gated Ca^{2+} channel allowing the release of sequestered Ca^{2+} from the ER.

CCK receptor

The occupancy of the high affinity site of the CCK receptor is thought to stimulate enzyme secretion, protein synthesis and calcium oscillations; whereas the occupancy of the low affinity site inhibits secretion, and induces a large global calcium transient (Williams & Hotman, 1986). The use of a CCK analogue JMV-180, which binds to both sites of the CCK A receptor, but only acts as an agonist at the high affinity site, allowing dissection of the roles of the two sites. Matozaki and colleagues found that activation via the high affinity site induced calcium oscillations but no measurable IP_3 production. However the effect of JMV-180 at this site can be blocked by

heparin, an IP_3 receptor antagonist. The injection of antibodies against $G\alpha_q$ subunit which is coupled to the PLC receptor, inhibited the responses to 20pM CCK a concentration that would only bind to the high affinity site of the CCK receptor (Yule *et al.*, 1999). Activation via the low affinity site leads to IP_3 generation. DAG production was measured upon occupancy of the high affinity site. The application of CCK at a concentration which resulted in occupancy of both the high and low affinity sites of the receptor (1nM) induced a rapid increase in IP_3 peaking within seconds which then plateaus and a biphasic DAG production. DAG levels show an initial peak which coincides with the IP_3 peak and then a slower sustained increase (Matozaki *et al.*, 1989;Matozaki *et al.*, 1990). JMV-180 induced a monophasic sustained increase in DAG (Matozaki *et al.*, 1990). The second phase of DAG production is thought to result from activation of phospholipase D (PLD) via the low affinity site resulting in phosphatidylcholine metabolism. The secretion dose response to CCK is biphasic with low concentrations of CCK stimulation amylase release and higher concentrations inhibiting amylase release (Jensen, 1994). JMV-180 also stimulates amylase secretion to the same extent as low concentrations of CCK. However JMV-180 blocks the inhibition of amylase secretion by higher concentrations of CCK. This is achieved by JMV-180 binding but not activating the CCK receptor at the low affinity site hence blocking the CCK access to this site. It has therefore been suggested that the slow sustained production of DAG from the high affinity site stimulates secretion, and the rapid increase in DAG from the PLC activation via the low affinity site induces the inhibitory effects on secretion, suggesting a role for protein kinase C (PKC) in the regulations of secretion (Pollo *et al.*, 1994).

There is also evidence for the high and not the low affinity site of the CCK receptor being coupled to phospholipase A_2 (PLA_2) (Lankisch *et al.*, 1999;Gonzalez *et al.*, 1999). Investigation of wave speed propagation in pancreatic acinar cells found that inhibition of PLA_2 by $AACOCF_3$ (arachidonyl triflioromethyl ketone) increased the speed from 5 μm/s to 10 μm/s of waves mediated by occupation of the high affinity site of the CCK receptor, with no effect on waves induced by occupancy of the low affinity site. Arachidonic acid (AA), produced as a result of PLA_2 mediated hydrolysis of phosphatidylcholine, was found to decrease the speed of low affinity site induced waves but had no effect on the waves induced by high affinity site occupancy. This implies that the high affinity was coupled to PLA_2, as AA had no additional effects (Gonzalez *et al.*, 1999).

PLD activation and its effects on wave speed propagation was also investigated in the acinar cell (Gonzalez *et al.*, 1999). They found that the low affinity site of the CCK receptor is coupled to PLD and PLC by the use of n-butanol which produces an ineffective phosphatidylbutanol instead of phosphatidic acid (PA) that is then dephosphorylated to DAG (Gonzalez *et al.*, 1999) (Pfeiffer *et al.*, 1998).

ACh receptor

The Acetylcholine receptor is also expressed on the pancreatic acinar cell in the M3 isoform (Williams, 2001). The ACh receptor is coupled to PLC; production of IP_3 has been measured upon receptor binding. The relationship between ACh concentration and secretion is biphasic. With increasing concentrations there is an increase in amylase secretion followed by an inhibition of secretion at even higher

concentrations. That shows a maximal secretory response to ACh at concentrations 10-14μM (Jensen, 1994). This is consistent with a receptor having two different affinity binding sites. PLA_2 activation is involved in ACh receptor stimulation; inhibition of PLA_2 affected ACh induced calcium wave propagation speeds, calcium waves induced by bombesin were not affected (Siegel *et al.*, 2001). The propagation speed of ACh induced calcium waves was suggested to be dependent mainly on calcium induced calcium release mechanisms, which are inhibited by ruthenium red and reduced the wave speed (Pfeiffer *et al.*, 1998).

Figure 1.3 summarises the different pathways activated by occupancy of the different receptors.

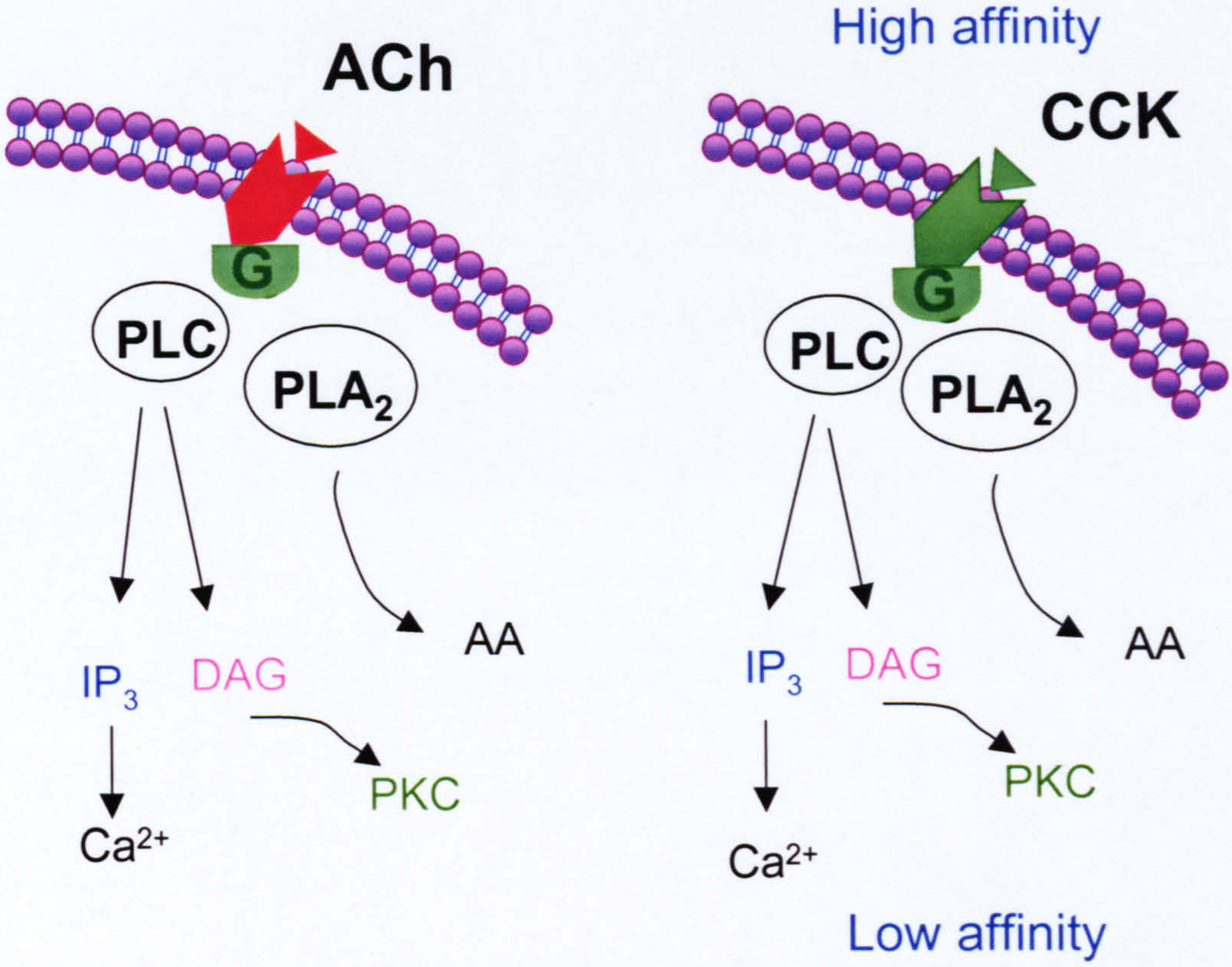
ACh
G
PLC
PLA2
AA
IP3
DAG
PKC
Ca2+
High affinity
CCK
G
PLC
PLA2
AA
IP3
DAG
PKC
Ca2+
Low affinity

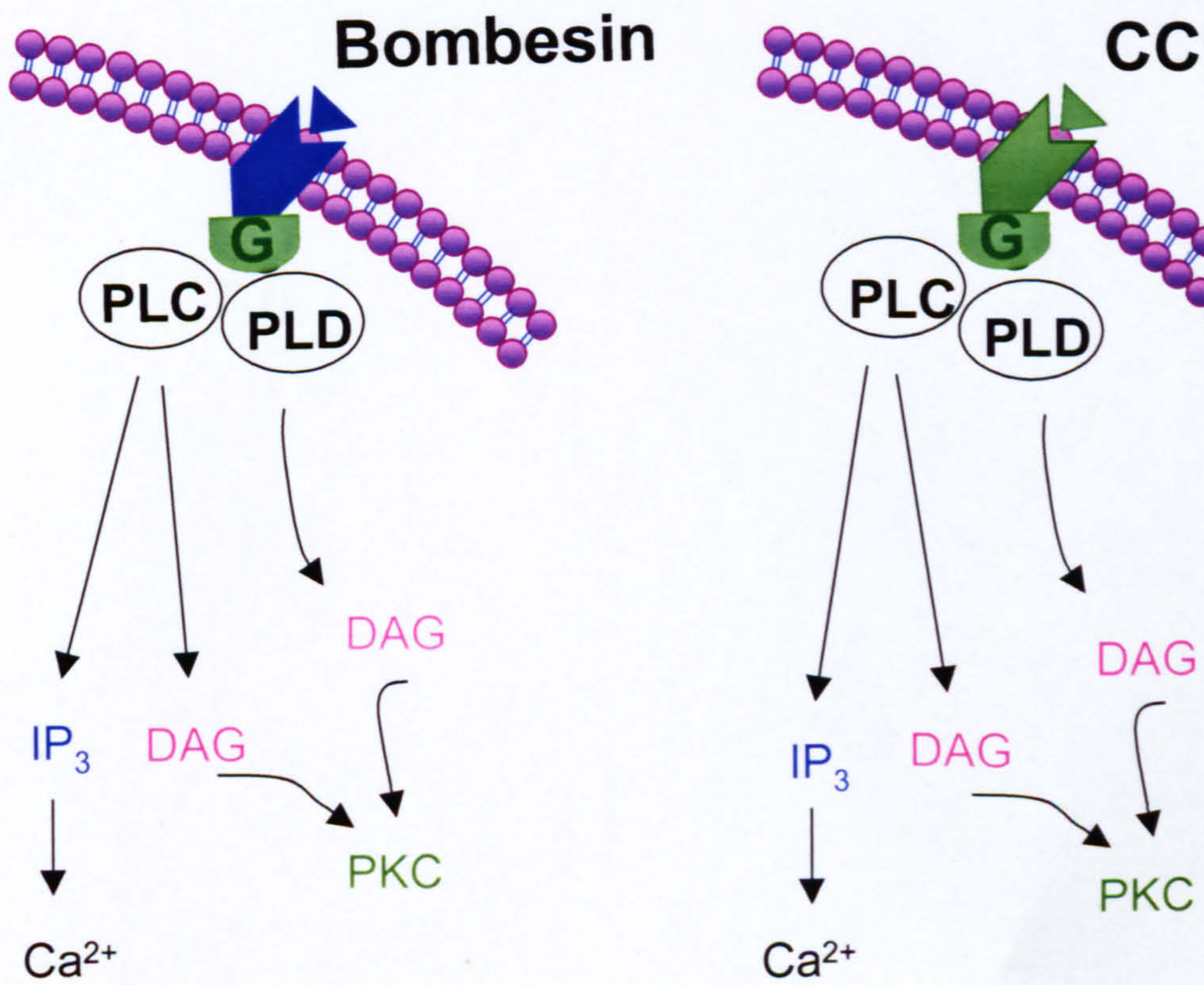
Bombesin
G
PLC
PLD
DAG
IP3
DAG
PKC
Ca2+
CCK
G
PLC
PLD
DAG
IP3
DAG
PKC
Ca2+

Figure 1.3 **Coupling of the receptors to second messenger cascades in the pancreatic acinar cell.** The receptors the ACh, high and low affinity sites of the CCK and bombesin are shown. The production of IP_3 leads to a release of calcium from internal store. The co production of DAG activates PKC. There is also AA production due to activation of ACh and high affinity CCK receptors.

Intracellular calcium signals

The investigation of secretagogue induced calcium signalling has demonstrated the different responses to different concentrations of secretagogue. High supramaximal concentrations of CCK and ACh induce a large rapid increase in $[Ca^{2+}]_i$, which declines to an elevated plateau in the presence of extracellular calcium. In the absence of external calcium the calcium recovers back to the baseline, thus indicating the initial rise is due to a release from intracellular stores and that the plateau phase is attributed to calcium influx. Lower concentrations of CCK (1-20pM, physiological) and ACh (25nM) induced calcium oscillations. The frequency of these oscillations range from 0.5 to 5/min, in the case of ACh this is sometimes superimposed on an elevated baseline (Thorn & Petersen, 1993) (Petersen *et al.*, 1991). The mechanism of oscillation regulation is unknown. It was initially proposed that the levels of IP_3 were oscillating, however delivery via the patch pipette of a non-metabolizable IP_3 analogue was able to induce oscillations hence a constant IP_3 concentration can induce oscillations in calcium (Wakui *et al.*, 1989). Oscillations can be blocked by the application of the IP_3 receptor antagonist heparin (Wakui *et al.*, 1989) (Thorn *et al.*, 1993b). As a result of this, it was then proposed that a constant level of IP_3 production induces the primary calcium release, which then induces calcium induced-calcium release (CICR). Another messenger cADPribose (cADPr) was shown to elicit short lasting calcium spikes in pancreatic acinar cells. ACh and CCK responses were also blocked by ryanodine (Thorn *et al.*, 1994;Cancela & Petersen, 1998). The enzyme ADPribosyl cyclase, which catalyses the formation of cADPr can also form NAADP, a messenger that elicits calcium release in sea urchin eggs (Chini *et al.*, 1995). It has also been shown to release calcium in the pancreatic

acinar cell (Cancela *et al.*, 2000). It has since been proposed that a cooperation between the three messengers IP_3, cADPr, NAADP and Ca^{2+} are responsible for the generations of calcium spikes (Cancela *et al.*, 2000) and the primary Ca^{2+} release that triggers CICR which has been shown to require both IP_3 and ryanodine receptors (RyR) (Ashby *et al.*, 2002). Ca^{2+} has also been shown to regulate the IP_3 (Bezprozvanny *et al.*, 1991;Adkins *et al.*, 2000) and ryanodine receptors (Gyorke, 1999). This may also be involved in oscillation generation. The Ca^{2+} sensitivity of the IP_3 receptor may also play a role in the propagation of waves between cells. The small amount of Ca^{2+} transmitted between cells through the gap junctions may serve to sensitise the IP_3 receptors, decreasing the amount of IP_3 required for those channels to release Ca^{2+}. Experiments where injection of $CaCl_2$ does not induce intercellular propagation unless there is a background of IP_3, support this hypothesis (Yule *et al.*, 1996).

Initiation of the calcium transient

The maintenance of resting calcium in cells is important for the function and responsiveness of the cells to stimulus i.e. the ability to produce a transient increase in calcium in order to stimulate secretion. The pancreatic acinar cell maintains a resting calcium level of 150nM (Muallem, 1989). This is achieved by sequestering calcium into intracellular stores, namely the ER, by Ca^{2+}-Mg ATPase in the ER membrane (SERCA), extrusion of Ca^{2+} out of the cell through the plasma membrane Ca^{2+}- ATPase PMCA and Na^{+}/Ca^{2+} exchanger, and cytosolic calcium buffers. Upon stimulation by an agonist binding to its receptor, a series of events are initiated that result in a transient increase of Ca^{2+}(discussed above). The binding of messengers

open the ligand-gated Ca^{2+} channels, and Ca^{2+} leaves the ER down its concentration gradient into the cytoplasm. The reduction of store calcium has been visualised by the loading of the ER lumen with calcium indicators Mag Fura-2 and Mag-Fluo-4 (Gobel *et al.*, 2001;Park *et al.*, 2000). The release of calcium from internal stores is counter balanced by the movement of K^+ into the ER to balance the charge released. The inhibition of K+ movement through replacement by NMDG or K+ channel blockers prevents the IP_3 mediated release from internal stores (Camello, unpublished data) (Palade *et al.*, 1989;Abramcheck & Best, 1989).

The ACh and CCK response initiation site has been mapped to the secretory pole. Where there is a higher abundance of type 3 IP_3 receptors in comparison to the basalateral region (Nathanson *et al.*, 1994), the sensitivity of the IP_3 receptors in that region is also proposed to be higher (Thorn *et al.*, 1993a;Kasai *et al.*, 1993). The involvement of different messengers in the responses to ACh and CCK has been studied in detail; the initiation site remains the same and resides in the "trigger" zone within the apical pole (Cancela *et al.*, 2000). The expression of the RyRs in the pancreatic acinar cells have been confirmed and their distribution appears to be homogeneous throughout the cell (Fitzsimmons *et al.*, 2000). Though these receptors are known to be involved in CICR and hence wave propagation, their role in the formation of a trigger zone is unknown. There are three different subtypes of RyR and the expression pattern of these subtypes may influence the kinetics calcium responses within the trigger zone.

Termination of the calcium signal

The termination of the calcium signals is an important process; long sustained elevation of calcium has been shown to be toxic to cells (Raraty *et al.*, 2000). The first event in termination is the decrease in calcium efflux from the ER, i.e. a reduction in the calcium permeability of the ER membrane. This is thought to be due to closure of the ligand gated calcium channels possibly mediated by receptor desensitisation. The calcium is removed from the cytosol by ER Ca^{2+} ATPase (SERCA) which pumps Ca^{2+} back into the ER lumen and calcium removal out of the cell by Na^{+}/Ca^{2+} exchanger and PMCA. In the pancreatic acinar cell the primary removal mechanism is the PMCA as shown by the relative insensitivity of the removal processes to the absence of Na^{+} (Muallem *et al.*, 1988a). Tepikin and colleagues confirmed these findings by measuring calcium extrusion after agonist stimulation in the presence and absence of Na^{+} (Tepikin *et al.*, 1992). Camello and colleagues investigated the calcium dependency of calcium extrusion by the simultaneous measurements of external and internal calcium. A high co-operativity was found with a Hill coefficient of 3, with extrusion mechanisms saturated at intracellular calcium concentrations higher than 400nM (Camello *et al.*, 1996).

The plasma membrane Ca^{2+} ATPase regulation

The regulation of the PMCA in the pancreatic acinar cell is therefore of importance, as this is the primary mechanism of calcium removal. The PMCA is a "P-type" ATPase of which there are 4 different genes PMCA1-4. Further variation is produced by the existence of splice variants of these genes, which are expressed in a

tissue specific pattern. PMCA1 is known as the house keeping isoform owing to its wide tissue expression profile. The regulation and the properties of the isoforms have been investigated. They differ in their affinities for calmodulin and calcium responsiveness and kinase regulation site availability (Penniston & Enyedi, 1998).

The investigation of PMCA localisation in the pancreatic acinar cell has demonstrated a polarisation of expression of the PMCA with a higher level of protein in the lumenal membrane, with some punctate staining at the basal and lateral membranes (Lee *et al.*, 1997). This correlates well with studies that measure the calcium extrusion rate by simultaneous internal and external calcium measurements. Belan and colleagues measured the majority of calcium extrusion occurring at the lumenal pole (Belan *et al.*, 1996;Belan *et al.*, 1997). It has also been reported that PMCA concentrates within caveolae in some cell types (Penniston & Enyedi, 1998).

The PMCA has been identified as a target for protein kinase C (PKC), cAMP-dependent protein kinase, cGMP-dependent protein kinase and tyrosine protein kinase. The phosphorylation of isoform PMCA 4 by PKC alters the rate of pump activity whilst retaining its potential for calmodulin regulation (Hofmann *et al.*, 1994;Enyedi *et al.*, 1996). However, phosphorylation of other isoforms of PMCA by PKC occurs within or near the calmodulin-binding domain altering their calmodulin dependent regulation (Enyedi *et al.*, 1997). PKC dependent activation of the PMCA 4 has been shown in neurons (Usachev *et al.*, 2002). The regulation of the PMCA by another kinase, cAMP-dependent protein kinase has been shown in platelets (Johansson & Haynes, 1992) and erythrocytes (James *et al.*, 1989;Dean *et al.*, 1997). The phosphorylation by cAMP-dependent protein kinase has been shown to alter the

K_m for Ca^{2+} and the V_{max} of the PMCA. The site of cAMP-dependent protein kinase is near but not within the calmodulin-binding site in the C terminus auto inhibitory domain. If calmodulin was bound, the PMCA was no longer phosphorylated by cAMP-dependent protein kinase (James *et al.*, 1989). The autoinhibitory domain is proposed to overlap a calcium-binding site or the ATP binding site that once bound to calmodulin swings out of the way allowing access to the calcium binding site and/or the ATP binding site (Enyedi *et al.*, 1989;Falchetto *et al.*, 1991).

The phosphorylation of the PMCA by cGMP-dependent protein kinase was found to increase the calcium affinity and enhance the pump activity (Furukawa & Nakamura, 1987). In contrast to these findings Zolle and colleagues found that activation of particulate guanylate cyclases at the plasma membrane inhibited ATP stimulated calcium extrusion through the PMCA in epithelial cells (Zolle *et al.*, 2000). They did not investigate whether this effect was mediated through cGMP-dependent protein kinases. Work by Dean and colleagues showed tyrosine protein kinase dependent inhibition of the PMCA activity (Dean *et al.*, 1997).

The affinity for calmodulin differs between the isoforms of the PMCA (Elwess *et al.*, 1997;Filoteo *et al.*, 1997). The removal of the calmodulin-binding domain by Ca^{2+}-dependent protease calpain generates a fully active PMCA; this may be of physiological relevance (James *et al.*, 1989). These effects of proteases have been described as "a last line of defence against sustained high levels of calcium" (Rosado & Sage, 2000). At low cytoplasmic calcium levels, the pump is maintained in an inactive conformation by the binding of the auto inhibitory site in the C terminus to the first and second cytoplasmic loops (Falchetto *et al.*, 1991). It is the C terminus

region in which the isoforms can differ substantially (Penniston & Enyedi, 1998). Activation of the PMCA by calmodulin is probably by displacement of the auto inhibitory domain. Ba-Thein and colleagues investigated the differences between isoforms PMCA 2b and PMCA4b; PMCA 2b had a higher affinity for calmodulin and higher basal activity in the absence of calmodulin. By interchanging the C terminal regions of the two isoforms on the catalytic cores it was found that the calmodulin binding was not solely influenced by the calmodulin binding domain (which have only 2 amino acids different between the two isoforms but a four fold difference in calmodulin affinity) and the C terminal autoinhibitory region, but that calmodulin interacts with multiple regions of the PMCA. This makes the regulation by calmodulin very complex and the potential influence of phosphorylation of the PMCA unpredictable (Ba-Thein *et al.*, 2001).

The N terminal of the PMCA contains the phospholipid interaction sites, in the absence of calmodulin the PMCA is activated by acid phospholipids. The location of the pump in a phospholipid rich environment indicates that this may mediate the basal activity of the PMCA (Carafoli, 1994). There are theories linking this property of phospholipid activation of the PMCA to PIP_2 metabolism as a means of coordinating efflux and calcium release, influencing the characteristics of the calcium responses to agonists (Penniston & Enyedi, 1998;Carafoli, 1994). The recently identified PDZ domain that mediates interactions with other enzymes to form multifunctional complexes poses another means of PMCA regulation (Kim *et al.*, 1998). The regulation of the PMCA pump activity is important in cells for maintaining resting calcium levels, especially in cells such as the pancreatic acinar cell where it is the major route for calcium extrusion out of the cells. Therefore the

regulation of the pump activity could have consequences on temporal and spatial aspects of calcium signals created by agonist stimulation. The calcium extrusion rate in agonist stimulated pancreatic acinar cells was demonstrated to be three times faster than in control cells (Zhang *et al.*, 1992). This is the only evidence to my knowledge in the pancreatic acinar cell of direct regulation of the PMCA by agonists. The work of Zhang and colleagues studied the effects of agonists at high supramaximal concentrations. The first results chapter (chapter 3) in my thesis describes experiments, which confirm these findings, and extend the range of the agonist concentration studied to the physiological range.

Calcium influx during the calcium response

Ca^{2+} influx across the plasma membrane is also induced during stimulation. Calcium influx through non-capacitative channels as part of a cellular response can occur via voltage operated calcium channels (VOCC) in excitable cells, ligand-gated non-specific cation channels and receptor activated Ca^{2+} channels (reviewed in Barritt, 1999). Arachidonic acid has been shown to activate non-capacitative calcium entry during oscillations in exocrine avian nasal gland cells (Shuttleworth, 1996). The activation of calcium influx as part of a response to agonist has been reported in a RBL-2H3 cells where an involvement of phosphatidylinositol 3-kinase due to its products phosphatidylinositol 3,4,5-trisphosphate ($PI(3,4,5)P_3$) direct induction of Ca^{2+} influx, independent of PLC activity and store depletion (Ching *et al.*, 2001). In the pancreatic acinar cells Camello and colleagues propose that there are two pathways which may mediate calcium entry in these cells (Camello *et al.*, 1999). They suggest that the two pathways carry calcium influx under different conditions.

During stimulation they propose that the initial calcium influx is via a non-specific cation channel that is sensitive to flufenamic acid and tyrosine kinase inhibitors but insensitive to La^{3+}. The second phase of calcium influx during the response is via a moderately Ca^{2+}-selective channel, which is sensitive to La^{3+} and Mn^{2+}. This is in agreement with a study that describes a calcium-release-activated non-selective cation current (I_{cranc}) in pancreatic acinar cells, which was also sensitive to tyrosine kinase inhibitor genistein (Krause *et al.*, 1996). The pH sensitivity of these two calcium influx mechanisms was found to be identical. An increase in pH increased the rate of influx and a decrease in pH reduced the rate of influx measured by analysis of a sustained plateau during agonist stimulation or by the time taken to refill the store after stimulation (Tsunoda & Tashiro, 1999). Again this study confirmed the 2 types of calcium influx, an initial phase that was Mn^{2+} permeable and a second Mn^{2+} impermeable.

ER reloading and calcium influx

After termination of the calcium transient, Ca^{2+} influx mechanisms remain active to achieve the complete refilling of the calcium store. The refilling of the store is dependent upon the presence of extracellular calcium (Putney, Jr., 1986;Muallem *et al.*, 1988b;Pandol *et al.*, 1987). The entry of calcium induced by store depletion is termed "capacitative calcium entry" (CCE) or "store operated calcium" (SOC) entry (Putney, Jr., 1986). This can be induced by depletion of the store using the SERCA specific inhibitor thapsigargin (Putney, Jr. & McKay, 1999). This phenomenon has been observed in a number of cells including the pancreatic acinar cell (Bahnson *et al.*, 1993) (summarised in Parekh & Penner, 1997).

Ca^{2+} release-activated Ca^{2+} current, (I_{crac})

The measurement of calcium influx current after store depletion was first made in mast cells and was termed Ca^{2+} release-activated Ca^{2+} current, (I_{crac}) (Hoth & Penner, 1992). I_{crac} is mediated by channels that are not gated by changes in membrane potential and has a reversal potential of approximately +50mV. The channel is calcium selective showing a reduction of current when Ca^{2+} is replaced with Ba^{2+} or Sr^{2+}. There is no significant monovalent cation current unless the calcium concentration is lowered (from 10mM to 2mM). The single channel conductance is very low for I_{crac}. I_{crac} is blocked by some divalent cations $Zn^{2+} > Cd^{2+} > Be^{2+} = Co^{2+} = Mn^{2+} > Ni^{2+} > Sr^{2+} > Ba^{2+}$ and is blocked by trivalent cation La^{3+}(Parekh & Penner, 1997). Inactivation of I_{crac} is regulated by cytosolic calcium, due to a rise in local calcium as it re-enters the cell. The inactivation occurs with a rapid time course of 10-100ms. The inclusion of BAPTA in the pipette suppresses the current inactivation. The inactivation of I_{crac} has also been shown to be sensitive to the state of the store refilling. I_{crac} is inactivated once the store is refilled. However this only accounts for part of the I_{crac} inactivation, as there is a 50% inactivation of I_{crac} in the presence of thapsigargin which prevents store refilling (Zweifach & Lewis, 1995). A role for phosphorylation has been suggested in I_{crac} inactivation. The use of non-hydrolysable ATP analogues differing in their kinase utilisation suggests, that phosphorylation and dephosphorylation are involved in the inactivation process. PKC is one kinase that has been implicated in this process (Parekh & Penner, 1995). Store depletion activated currents have been measured in pancreatic acinar cells by Bahnson and colleagues and Pandol and colleagues (Pandol & Schoeffield-Payne,

1990;Bahnson *et al.*, 1993). Other store operated currents have also been described their ion selectivity differ from that of I_{crac} (Parekh & Penner, 1997).

The process of SOC entry is a subject of much debate; the molecular identity of the channel/channels responsible for the calcium entry has remained elusive, as has the nature of the signal from the internal calcium stores that activates the channel.

The molecular identity of the SOC channel

The TRP family of proteins are prime candidates for this job. The Drosophila *trp* mutant is incapable of producing a sustained receptor depolarisation required for light detection, hence the term "transient receptor potential" trp mutants. These mutants were also found to have a defect in SOC entry. Cloning and expression of the TRP protein in mutant flies could restore wild type function (Harteneck *et al.*, 2000). The TRP sequence analysis revealed homology to the mammalian voltage-dependent calcium channels and a number of mammalian homologue proteins TRP1-7 have been identified (Harteneck *et al.*, 2000). Investigation of the TRP proteins are summarised by Putney and McKay (Putney, Jr. & McKay, 1999). Most studies investigate the properties by over expression of the proteins in cell lines. TRP3 expressing cells were shown to respond to thapsigargin application with a larger calcium entry than vector only control cells, demonstrating an increase in SOC entry. However the selectivity of the channel for calcium varies between the family members, being calcium selective in some circumstances (Warnat *et al.*, 1999) and non-selective cation channels in others (Kamouchi *et al.*, 1999). The single channels

conductance also varied in comparison to the current measurements previously made for I_{crac} reviewed in (Harteneck *et al.*, 2000).

Two proteins ECaC1 and CaT1 (also called ECaC2) both of which are members of the TRP family have also been put forward as prospective candidates for the SOC channel, though both were initially identified as a result of their role in calcium transport from the lumen to the blood in the intestine and kidney. The expression of CaT1 in Chinese hamster ovary (CHO)-K1 cells demonstrated CaT1 currents with very similar properties to those exhibited by I_{crac}. A similar reversal potential, ion selectivity and La^{3+} sensitivity were described. CaT1 currents were induced in strong (10mM EGTA) and not weak (0.05mM EGTA) intracellular buffering with a similar time course of activation and inactivation as described in similar conditions for I_{crac}. The induction of CaT1 currents was achieved by the inclusion of IP_3 in the patch pipette or thapsigargin in the intracellular solution in weak buffering conditions. This demonstrates activation of CaT1 by both passive and active store depletion (Yue *et al.*, 2001). A subsequent report by Voets and colleagues suggest that there are some significant differences between the properties of I_{crac} and CaT1 channels (Voets *et al.*, 2001). However the difference of CaT1 currents to the properties or I_{crac} currents may reflect the existence of a multimer, which forms the I_{crac} channel, and maybe made up of many combinations of subunits.

ECaC1 has a 75% homology with CaT1 and both are expressed in the pancreas (Peng *et al.*, 1999;Hoenderop *et al.*, 2001). ECaC1 when expressed in human embryonic kidney (HEK) 293 cells (Vennekens *et al.*, 2000) or oocytes (Hoenderop

et al., 1999) was shown to be a Ca^{2+} selective channel demonstrating Ca^{2+} dependent feedback with fast inactivation.

The physiological relevance of I_{crac} has been questioned by the inability to measure the currents without strong intracellular calcium buffering. If the CRAC channels are important in physiological circumstances, they must be sensitive to and be activated during agonist exposures, which result in a small degree of store depletion. The majority of studies measuring I_{crac} currents have been done under strong intracellular calcium buffering conditions. This buffering removes the local calcium negative feedback on the CRAC channels. The inability to measure I_{crac} currents in weak calcium buffers was suggested to be a result of IP_3R inactivation terminating release, the store being refilled and therefore no I_{crac} activation occurring (Broad *et al.*, 1999). However this was inconsistent with the findings of Bakowski and Parekh, they found that the inclusion of IP_3 in the pipette did not prevent subsequent Icrac induction by thapsigargin. They also found that the use of Ba^{2+} as an I_{crac} carrier, but one that is not taken up into the store or involved in IP_3R inactivation did not facilitate I_{crac} in weak buffering conditions. They proposed that the SERCA pumps activity prevented the activation of I_{crac} currents as they are continuously reloading the store (Bakowski & Parekh, 2001). This is also suggested by the measurement of bursts of Ca^{2+} influx during agonist stimulation in human submandibular gland, which was attributed to the SERCA activity refilling the store and turning off the influx that is subsequently induced by IP_3R activation (Liu & Ambudkar, 2001). It has however been shown that I_{crac} can be measured under physiological conditions i.e. near normal intracellular buffering, by using an energised mitochondrial cocktail (Gilabert & Parekh, 2000). It has also been shown that lower concentrations of IP_3

than previously used were able to induce activation of I_{crac} in the presence of energised mitochondria (Gilabert *et al.*, 2001). The explanation for this is that energised mitochondria are able to take up calcium suppressing calcium inactivation; the mitochondria also compete with the SERCA pumps; therefore the store is able to induce I_{crac} activation. The mitochondria residing close to the plasma membrane, sub-plasmalemmal mitochondria, have been shown to take up calcium during calcium influx, generated by emptying the calcium stores (Park *et al.*, 2001). A study that reported measurements of the calcium content of the ER by trapped calcium sensitive dye (Mag-fura-2) and I_{crac} simultaneously, observed a clear grading of I_{crac} activation and calcium store content (Hofer *et al.*, 1998).

Mechanism of regulation of SOC entry has been the subject of intensive research. There have been numerous models proposed to account for the activation of calcium entry upon store depletion reviewed in (Berridge, 1995;Elliott, 2001). There are presently three main models; conformational coupling, vesicle insertion and diffusible messenger. Each will be briefly discussed below.

Conformational coupling model

The conformational coupling model first proposed by Irvine (Irvine, 1990) suggests that there is a direct interaction between the IP_3 receptors on the surface of the intracellular store and the SOC entry channels at the plasma membrane. The intra lumenal portion of the IP_3R detects the lumenal levels of calcium within the store. Lumenal calcium has previously been shown to modulate the IP_3R (Sienaert *et al.*, 1996). Conformational changes within the IP_3R upon store depletion are translated

through to the SOC entry channel, which is activated to allow store refilling. Evidence in support of this model comes from the co-immunoprecipitation of TRP3, a candidate for the SOC channel and IP_3R. The subsequent identification of the domains within TRP3 and IP_3R proteins involved in the interaction and the ability of corresponding peptides to inhibit calcium influx lends further support to this model (Boulay *et al.*, 1999). This is not entirely consistent with observations of Kiselyov and colleagues, who were unable to co-immunoprecipitate the two proteins. They found that channel activity activated by IP_3 application in excised patches from TRP3 expressing cells, was abolished by extensive washing of excised patches. Implicating a weak interaction between the IP_3R and TRP3 protein. TRP3 activity could be restored in these extensively washed excised patches by application of microsomes containing native or recombinant IP_3R protein. They also found that deletion of the 154 amino acids at the C-terminal of the IP_3R did not affect the ability of the receptor to restore TRP3 activity (Kiselyov *et al.*, 1998). Other studies have also found a requirement for a functional IP_3R through the use of IP_3R antagonists 2-APB and Xest C (Ma *et al.*, 2000). The antagonistic abilities on the IP_3R of these two compounds are questionable (Ashby *et al.*, 2002). The promotion of actin polymerisation by the Jasplakinolide (cell permeant phalloidin analogue), which prevents close contacts between the ER and the PM, was shown to inhibit the activation of SOC entry. This polymerisation of actin had no effect on the IP_3 production and the subsequent calcium release from stores, in response to agonists. Depolymerisation of the actin re-established the SOC entry (Patterson *et al.*, 1999). Association of TRP3 with lipid raft domains (LRD) and caveolae have been reported and that within these domains there are also other molecules involved in calcium signalling. The co-immunoprecipitation of IP_3R and $G_{\alpha q/11}$ with TRP3 from these

detergent insoluble domains, was also reported from human submandibular gland cells (Lockwich *et al.*, 2000). In the same study it was shown that disruption of these LRD attenuated the thapsigargin-induced SOC entry. They also that reported carbachol-induced calcium release was also inhibited by LRD disruption.

All these studies suggest an interaction between the SOC entry channel and the IP_3R, as proposed in the conformational coupling model. However a problem that still existing with this model of SOC entry activation is the induction of SOC entry by depletion of the stores through the use of SERCA pump inhibitors, thapsigargin, where no IP_3 is generated. However binding of local IP_3 may be all that is required to involve conformational coupling of IP_3R to the SOC entry channel. The presence of IP_3R are however required. Studies that use cells where IP_3R expression has been abolished or reduced but still demonstrate a thapsigargin-induced SOC entry are more difficult to reconcile with the conformational coupling model (Jayaraman *et al.*, 1995;Sugawara *et al.*, 1997).

Vesicle insertion

Another model to explain the mechanism or SOC entry regulation is the vesicle insertion theory. This involves the insertion of vesicles into the plasma membrane, which contain the SOC channel. The evidence for this model is based mainly on the evidence that modifications of the cytoskeleton or enzymes involved in cytoskeleton remodelling are involved in the regulation of SOC entry. Rosado and Sage reported the involvement of phosphatidylinositol 3-kinase and phosphatidylinositol 4-kinase in SOC entry through cytoskeleton rearrangement (Rosado & Sage, 2000). The

involvement of cytoskeleton is not mutually exclusive to the vesicle insertion model. As discussed above the cytoskeleton rearrangement has also been used to support the conformational coupling model. There are studies that use the injection of botulinum neurotoxin A (BoNT/A), and tetanus neurotoxin (TeNT) which proteolyse SNAP25 and synaptobrevin/VAMP respectively, to interfere with vesicle docking and fusion. These investigations show an inhibition of SOC entry (Alderton *et al.*, 2000). This confirms findings that previously have implicated vesicle fusion and docking in the activation of SOC entry (Yao *et al.*, 1999). These two studies strongly support the vesicle insertion model of SOC entry regulation.

Diffusible messenger

The activation of SOC entry has been proposed to be mediated by a soluble diffusible factor, which is released by the ER or generated as a result of calcium store depletion. The identification of such a factor has led to three popular candidates inositol-1,3,4,5-tetrakisphosphate (IP_4), a cytochromes P450 metabolite and a as yet unidentified calcium influx factor (CIF). The choice of IP_4 as the factor stems from the observation that its production is a direct result of IP_3 production and hence agonist stimulation. Early studies suggested a role for IP_4 and SOC entry, though it has been more recently suggested that IP_4 acts through increasing IP_3 mediated release (Hermosura *et al.*, 2000). Hermosura and colleagues suggest that this occurs via inhibition of IP_3 metabolism, therefore increasing the effects of IP_3 on SOC entry (Hermosura *et al.*, 2000)(summarised in Elliott, 2001). P450 and its metabolites were implicated in SOC entry via the use of inhibitors and their effects on Ca^{2+} entry. The activating effects on SOC entry by P450 or addition of its metabolites, further

increased the credibility of this as a possible mechanism of SOC entry regulation. However there have been reports that K^+ channels are the channels directly activated and that the increase in calcium is owing to the subsequent effects of the increase in K^+ ions on calcium channels. This is summarised in (Elliott, 2001). Application of the cytosol harvested from activated cells to "test" cells which then demonstrated an activation of SOC entry, was the first evidence to suggest the existence of CIF. Microinjection of activated cell cytosol rather than extracellular application also showed SOC entry activation. The use of genetic mutants of yeast, which are unable to load a calcium store, were postulated to be continually synthesising or releasing CIF. The application of these mutant yeasts extracts was shown to induce SOC entry without inducing any calcium release. Studies using inside out patches from smooth muscle were also shown to be stimulated by the application of both activated mammalian cytosol extract and the mutant yeast cytosol (Trepakova *et al.*, 2000) (summarised in Elliott, 2001). Though without isolation and identification of the CIF the acceptance of such a model is unlikely.

Tunnelling

In pancreatic acinar cells the reloading of the ER by calcium influx through SOC channels occurs without measurable changes in the cytoplasmic calcium levels (Muallem, 1989). It was therefore suggested that the site of calcium entry, i.e. is the source for ER reloading, is localised to a region where there is a very close association of the ER and the plasma membrane and therefore the overall cytosolic calcium remains unchanged. In the pancreatic acinar cell the calcium release site as discussed earlier is in the apical pole. However the reloading of the calcium store

occurs mainly through the basal membrane (Toescu & Petersen, 1995). After a period of time, which allowed the store to refill, ACh could then evoke another calcium response again initiating in the apical region, which was abolished in the presence of thapsigargin. It was proposed that the calcium was reloaded into the store and moved through the store to the release sites in the apical region by "tunnelling" through the ER (Mogami *et al.*, 1997). This was further supported by work of Park and colleagues, which showed the movement within the lumen of the ER by photobleaching of fluorescent substances and uncaging locally of substances trapped in the lumen of the ER (Park *et al.*, 2000).

The role of organelles in calcium homeostasis

The main organelle involved in calcium signalling and homeostasis is the ER as previously discussed. However other organelles are also involved in the generation and propagation of calcium responses as (reviewed in Rutter *et al.*, 1998). Figure 1.4 demonstrates the different organelles that may participate in calcium homeostasis in the pancreatic acinar cell.

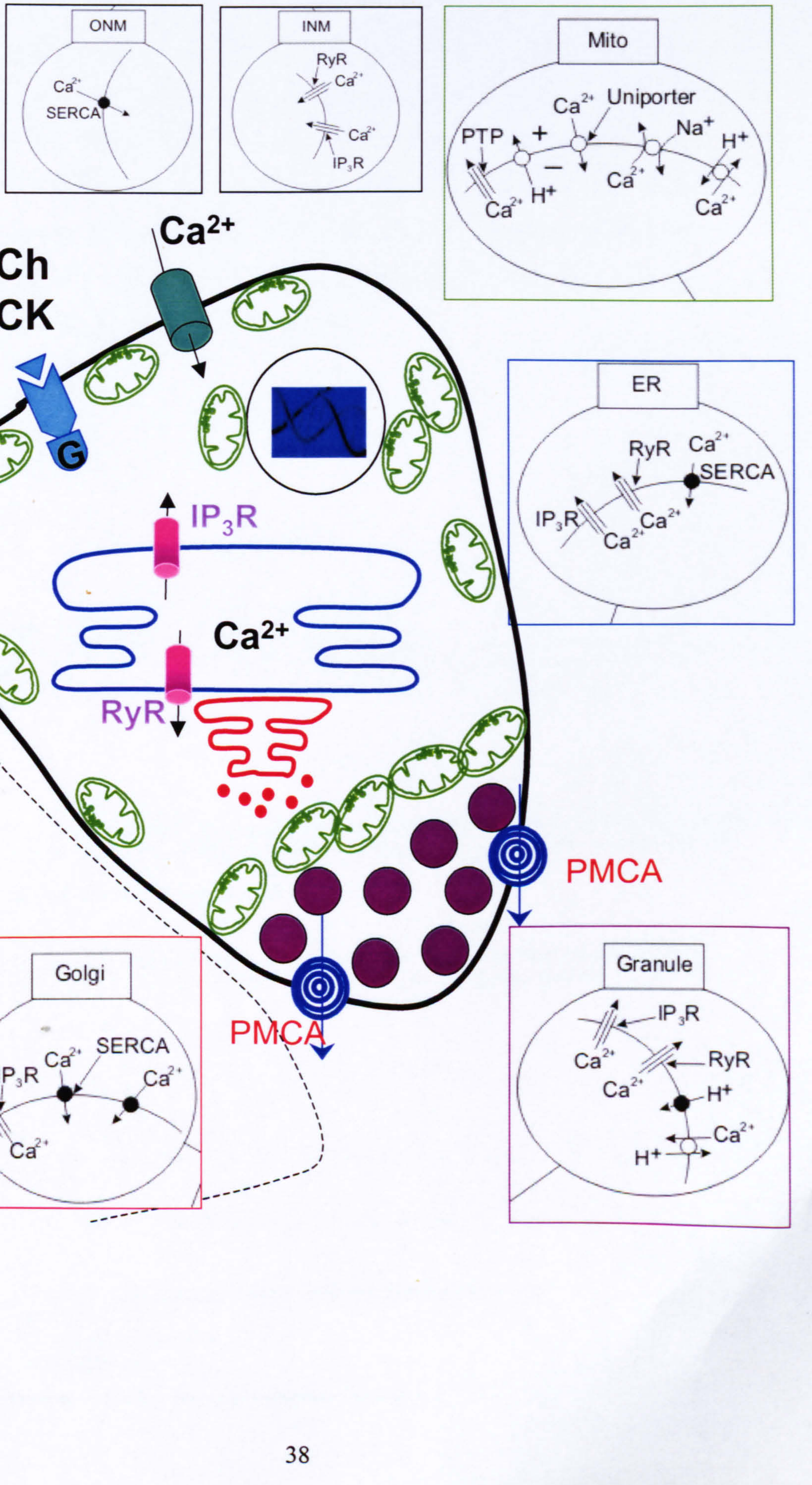
ONM
Ca2+
SERCA
INM
RyR
Ca2+
Ca2+
IP3R
Mito
Ca2+
Uniporter
PTP
+
Na+
H+
—
Ca2+
H+
Ca2+
Ca2+
ACh
CCK
Ca2+
G
Ca2+
IP3R
Ca2+
RyR
ER
RyR
Ca2+
SERCA
IP3R
Ca2+
Ca2+
PMCA
PMCA
Golgi
IP3R
Ca2+
SERCA
Ca2+
Ca2+
Granule
IP3R
Ca2+
RyR
Ca2+
H+
Ca2+
H+

Figure 1.4. **The cellular distribution of organelles in the acinar cell and the pumps and channels within their membranes.** The cartoon shows the subcellular distribution of organelles within the cell and channels and pumps in the different organelles that are involved in calcium homeostasis. The insets correspond to the different organelle membranes with pumps and channels involved in calcium homeostasis in these organelles. (INM-inner nuclear membrane and ONM-outer nuclear membrane)

Mitochondria

Mitochondria take up and release calcium; this has been measured directly using mitochondrial target calcium sensitive probes (Rizzuto *et al.*, 1995). In the pancreatic acinar cells, mitochondria lie in distinct locations as discussed earlier. It has also been shown that calcium regulates the rate of metabolism of the mitochondria, measured via changes in NADH autofluorescence. Increases in mitochondrial calcium are followed by an increase in NADH autofluorescence, indicating an increase in the rate of metabolism (Voronina *et al.*, 2002b). The calcium sensitivities of the dehydrogenases which are involved in the Krebs cycle have been described (McCormack & Denton, 1990;Robb-Gaspers *et al.*, 1998). It is therefore proposed by Park and colleagues that the strategic localisation of the mitochondria is to provide a local energy source to drive cellular processes such as calcium extrusion at the plasma membrane (via the PMCA)(Park *et al.*, 2001). The mitochondrial uptake and release of calcium also alter the temporal characteristics of calcium signals. The speed of wave propagation in response to agonist stimulation is changed if the mitochondria are inhibited using RU360, removing them from the calcium homeostasis equation (Johnson *et al.*, 2002). This further supports a role for mitochondria in calcium homeostasis within the pancreatic acinar cell.

Secretory granules

Secretory granules/vesicles are known to contain calcium and their potential role in calcium signalling within the pancreatic acinar cell has been the subject of investigation (Gerasimenko *et al.*, 1996). The apical pole of these cells is densely

packed with granules containing the zymogens. The calcium signals also always originate within the apical pole in the "trigger zone" (Kasai *et al.*, 1993), which is also known to contain a high density of IP_3Rs (Thorn *et al.*, 1993b). The granules therefore are in a prime location to participate in calcium signals, which are important for the function of the acinar cell. The presence of IP_3 receptors on secretory granules was reported by Blondel and colleagues by the use of immunogold electron microscopy (Blondel *et al.*, 1994). Gerasimenko and colleagues demonstrated the ability of messengers IP_3 and cADPribose to release calcium from granule preparations and they suggest that this calcium release from granules plays an important role in secretion (Gerasimenko *et al.*, 1996). This study measured intragranular calcium decreases in response to messengers and calcium release from granules by measurement of the external calcium changes. The measurement of calcium uptake during a response to agonists has been achieved by the use of vesicle-targeted aequorin in MIN6 β-cells, attributed to an ATP sensitive mechanism (Mitchell *et al.*, 2001). Uptake of calcium into granules remains a subject of investigation, two mechanisms having been proposed; one through a Na^+/Ca^{2+} exchanger and the second through a Ca^{2+}/H^+ exchanger. The use of inhibitors monensin (Na^+/H^+ exchanger inhibitor) bafilomycin (H^+-ATPase inhibitor) and FCCP (protonophore) had no effect on Ca^{2+} vesicular uptake (Mitchell *et al.*, 2001). The participation of granules in calcium homeostasis remains disputed (Muallem & Lee, 1997). However studies using specifically target probes clearly suggest active uptake of calcium during stimulation (Mitchell *et al.*, 2001;Emmanouilidou *et al.*, 1999)

The Golgi apparatus

The Golgi apparatus is mainly thought of as an organelle involved in trafficking of proteins within the cell. However studies have also shown it to have a role as an internal calcium store. This store is IP_3 sensitive but is partially insensitive to thapsigargin the SERCA inhibitor (Pinton *et al.*, 1998;Missiaen *et al.*, 2001;Van Baelen *et al.*, 2001;Missiaen *et al.*, 2002). The pump responsible for the calcium loading of the Golgi store is proposed to be Pmr1, first identified in yeast. This was found to be expressed and functional i.e. involved in responses to IP_3 and agonists in two cell lines (one rat aortic smooth muscle and human bronchial mucosal cells) (Missiaen *et al.*, 2002). The calcium stored in the Golgi is released by higher concentrations of IP_3 (five times higher) than those required to induce release from the ER and only 33% of the ionophore releasable calcium pool was released by maximal IP_3 (>100μM) application (Missiaen *et al.*, 2001). Golgi calcium is thought to be involved in trafficking processes undertaken by the organelle (Porat & Elazar, 2000). However, further studies are required to identify the role the Golgi may play in cellular calcium responses to agonists.

Nucleus

The consequence of nuclear calcium fluctuations has been demonstrated in studies investigating the effects on gene expression (Hardingham *et al.*, 2001;Dolmetsch *et al.*, 1998;Li *et al.*, 1998). The role of the nucleus in generating calcium signals has also been investigated. The nuclear membranes are continuous with the membranes of the ER, as is the lumen. Therefore release from the common lumen could

influence nuclear processes and the patterns of cellular calcium signals. Work with isolated nuclei and direct microinjection of IP_3 into the nuclei of oocytes, demonstrates the localisation of functional IP_3 receptors on the inner nuclear membrane (Gerasimenko *et al.*, 1995;Hennager *et al.*, 1995). This was confirmed by detection of IP_3 receptors on a preparation of inner nuclear membranes (Humbert *et al.*, 1996). cADP ribose has also been reported to induce increases in calcium within the nucleus (Gerasimenko *et al.*, 1995;Santella & Kyozuka, 1997).

Calcium signalling in the pancreatic acinar cell has been investigated in relation to the cells' secretory function. However calcium can also play a role in the diseases involving these cells. Sustained elevations of calcium have been implicated in the development of pancreatitis, a condition where the auto digestion of the pancreas occurs. A trigger for this elevated calcium is required, and a theory referred to as the "common duct theory" proposes a role for bile salts in the disease process. The next section introduces bile salts, the condition pancreatitis and finally the transcription factor NFκB that has a possible role in the development of the disease.

Bile Salts and their putative role in pancreatitis

Bile is produced in the liver, and contains excretory products, cholesterol and bile pigments from the breakdown of haemoglobin and cytochromes, and secretory products, which are important in digestion; bile salts and bicarbonate. Bile salts are important in the digestion and absorption of fats and fat-soluble vitamins and are the major constituent of bile (Strange, 1984).

The concentration of bile salts has been reported between 2 and 45mM (10mmol in humans) in mammals. Their structure is based on cholic acid (24 carbon compound). The commonly occurring bile acids have differing numbers of hydroxyl groups; cholate has three, chenodeoxycholate has two and lithocholate has one. The number of hydroxyl groups affects the salts aqueous solubility. Lithocholate is less soluble than cholate, however its amino acid conjugates (taurine and glycine) increase the solubility. There are a variety of bile salts that make up the bile salt pool in mammals. The most abundant bile salt being glycine-conjugated cholate. Lithocholate makes up 2% of the pool. Bile salts are secreted in the small intestine where unmodified and modified (sulphation by bacteria) bile salts are reabsorbed. They return to the liver via the portal circulation, between 90-99% of bile salts being retained for re-circulation. The amount of bile salts taken up by the liver from the portal blood is a means of regulating bile synthesis (Strange, 1984;Hofmann, 1994a).

Bile salts initially secreted by hepatic cells are concentrated and stored in the gallbladder. The cystic duct from the gallbladder joins the common duct before entering the duodenum at the ampoule of Vater. The pancreatic duct and the common duct join a short distance from the entrance to the duodenum. This part of the common duct allows the transport of digestive secretions of the pancreas containing digestive enzymes, to enter the duodenum (figure 1.5). The balance of bile constituents is crucial; too much cholesterol or insufficient bile salts can lead to the formation of cholesterol precipitates. Migration of clusters of these precipitates, microcrystals, into the common duct can cause obstruction at the level of the ampoule of Vater. The scenario described above can lead to acute pancreatitis, and is termed "The common duct theory", first described by Eugene Opie in 1901 (Opie,

1901). This occurs where the blockage of the common duct at the ampoule of Vater leads to reflux of the duct content into the pancreas resulting in bile penetration of the pancreas. In support of this theory an investigation by Kohut and colleagues examined the microcrystal density in bile from acute pancreatitis patients at different times from disease onset. They found a higher density of microcrystals on the first day after disease onset, with the density decreasing as the period between disease onset and sample collection increased (Kohut *et al.*, 2002). This suggests that the microcrystals are causative rather than resultant of acute pancreatitis. Another study performed on a group of patients suffering from acute pancreatitis also found an increase in microcrystals, both cholesterol and bilirubinate granules (Perez-Martin *et al.*, 1998). Bilirubin has been found to stimulate pancreatic amylase secretion, which is partially inhibited by PKC inhibition. This is a potential mechanism involved in the induction of pancreatitis via bilirubin penetration of the intra-acinar space (Hirohata *et al.*, 2002).

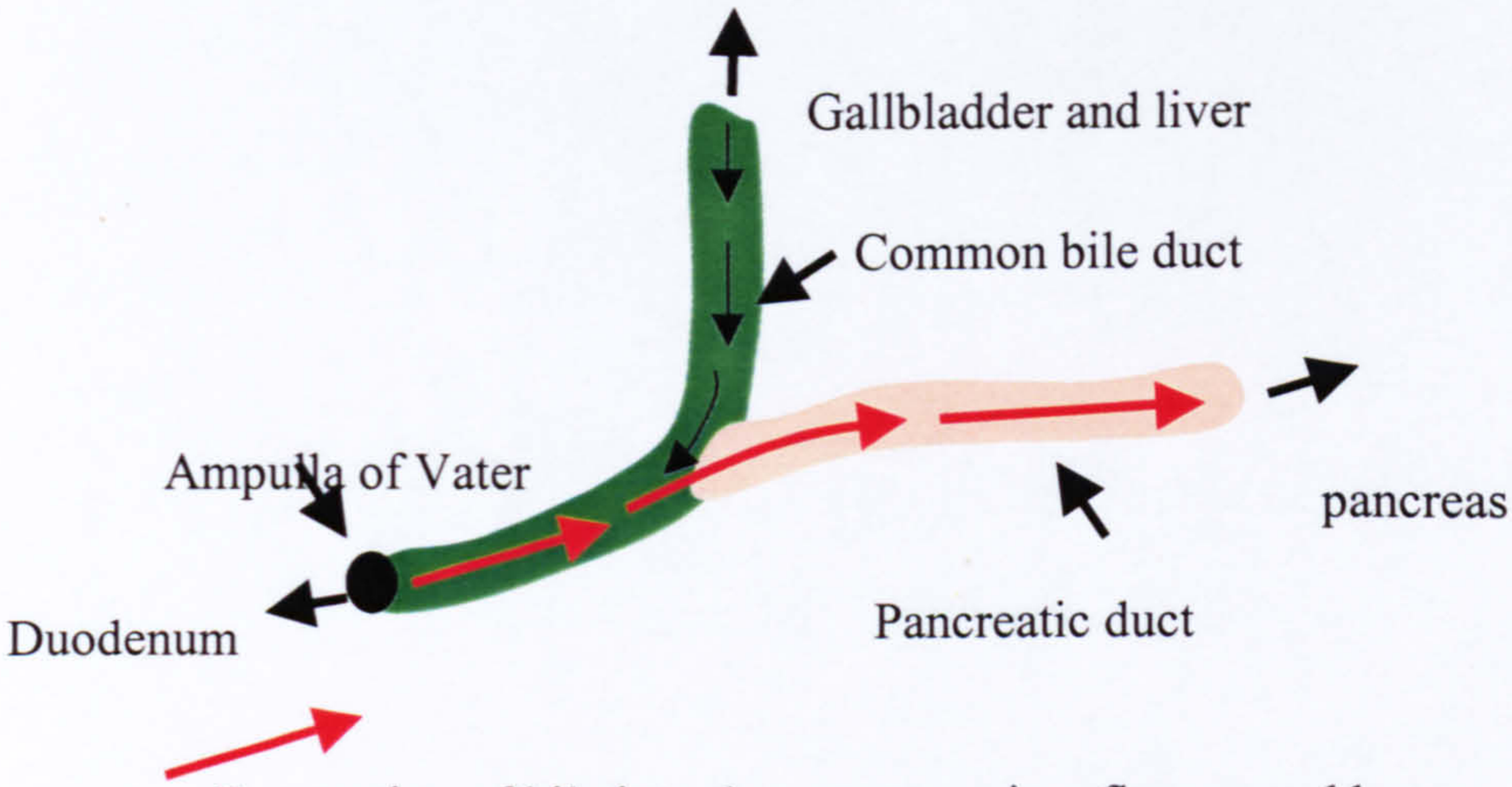

Figure 1.5 **The "common duct" theory of pancreatitis proposed by Opie, in 1901** This is a schematic demonstrating the situation proposed by Opie to explain the development of acute pancreatitis. The common duct (green) is the duct that links the gallbladder and liver to the duodenum at the Ampulla of Vater. This also links the pancreatic duct to the duodenum. The migration of microcrystals from the gallbladder down the common duct may cause blockage in the ampulla of Vater. Reflux of bile salts released from the gallbladder into the pancreas (red arrows) is proposed to trigger acute pancreatitis this is the termed the "common duct theory ".

Bile salts and their effects on cellular calcium signalling

The effects of bile salts and cellular signalling have been studied in the hepatocytes by a number of groups. In particular the role of bile in the regulation of its own transport of bile across the cell and secretion for re-circulation has been considered (Bouscarel *et al.*, 1999). Taurolithocholic acid (TLC) was found to release calcium from internal stores of hepatocytes but did not affect the IP_3 levels (Combettes *et al.*, 1988;Combettes *et al.*, 1990). TLC-S has been found to initiate oscillations in hepatocytes, which was again dependent upon internal calcium stores, not external calcium, and was not affected by heparin an IP_3 receptor antagonist (Capiod *et al.*, 1991;Marrero *et al.*, 1994). Anwer and colleagues found increases in response to bile salts were dependent upon the presence of external calcium and that no increase in response to TLC was seen in the absence of external calcium (Anwer *et al.*, 1988). The differences between this and other studies are explained by experimental conditions depleting the internal store before TLC application.

Bile salts have also been shown to cause calcium fluxes in rat pancreatic acinar cells by activating calcium uptake and efflux (Duan & Erlanson-Albertsson, 1988). These studies looked at the effects of bile salts taurodeoxy-cholate (TDC) and taurochenodeoycholate (TCDC) in mM concentrations. Voronina and colleagues studied the effects of bile salts in pancreatic acinar cells. They found that TDC caused increases in calcium at mM concentrations however the bile salt taurolithocholic acid 3-sulphate induced a calcium increase at μM concentrations. The increase to TLC-S was found to be oscillatory at 200μM gradually running down in zero external calcium. Some responses exhibited a plateau phase that was

dependent on external calcium. These responses to TLC-S in pancreatic acinar cells were also suggested to be dependent upon on IP_3 receptors (Voronina *et al.*, 2002a).

Pancreatitis and trypsinogen activation in acinar cells

Acute pancreatitis was first characterised in 1889 by Reginald Fitz (Fitz, 1889) and it was proposed that an autodigestive process where the gland was consumed by its own enzymatic content was responsible for the progression of pancreatitis (Chiari, 1896). The pancreatic acinar cells' primary function is to synthesize and secrete digestive enzymes. The digestive enzymes are secreted as inactive precursors, zymogens. They remain inactive until entry into the duodenum; activated trypsinogen activates the other zymogens. The inappropriate activation of the zymogens within the granules of pancreatic acinar cell is hypothesised to be the cause of the cell damage associated with pancreatitis. This is further supported by the observation that, some forms of hereditary pancreatitis are due to a mutation in the trypsin gene which renders it resistant to inactivation (Whitcomb *et al.*, 1996). However the exact mechanism of the inappropriate activation is still the a matter of debate. One theory to account for this intracellular activation of the zymogens, is the "co-localisation hypothesis". This theory dictates that the normal segregation of the lysosomal enzymes and the digestive granule zymogens malfunctions, resulting in the co-localisation of the lysosomal hydrolase cathepsin B with zymogens. Cathepsin B can activate trypsinogen, which in turn can activate the other zymogens. Studies concentrating on the co-localisation hypothesis have examined the ability of Cathepsin B inhibitors to prevent the activation of trypsinogen. They used E64 a cathepsin B inhibitor, in a secretagogue-induced *in vivo* model of pancreatitis. This failed to prevent full inhibition of cathepsin B (Steer, 1999). However in an *in vitro*

model of pancreatitis, using freshly isolated acinar cells and a highly cell permeant cathepsin B inhibitor E64D, full inhibition was achieved, which in turn prevented intracellular activation of pancreatitis (Saluja *et al.*, 1997). Further work supporting the co-localisation theory, found that lysosomal and digestive enzymes both localise to the same cellular fraction in preparations where secretagogue-induced pancreatitis was initiated and activation of trypsin activity was detected (Grady *et al.*, 1996).

Involvement of External Calcium in Pancreatitis

Investigations using isolated pancreatic acinar cells as an *in vitro* model of pancreatitis have found a requirement for external calcium in the intracellular activation of trypsinogen. Activation of trypsinogen was not observed in the absence of external calcium (Saluja *et al.*, 1999), indicating a role for calcium influx in the development of pancreatitis. It has been shown that in the presence of JMV-180 there is an inhibition of secretagogue-induced pancreatitis (Saluja *et al.*, 1989). The application of JMV-180 alone did not itself induce any trypsin activation. It is known that JMV-180 acts at both sites on the CCK_A receptor, the high and low affinity, however it acts as an agonist at the high affinity site and an antagonist at the low affinity site (Matozaki *et al.*, 1990)(discussed earlier). These findings suggest that the pathological calcium influx induction is via occupancy of the low affinity site of the CCK_A receptor. Other studies have also shown an involvement of calcium influx in the development of pancreatitis. Raraty and colleagues found that sustained elevation of calcium induced by either supramaximal secretagogue or thapsigargin (A SERCA pump inhibitor), induced the formation of vacuoles and trypsin

activation. This activation was prevented by the presence of BAPTA, a fast high affinity calcium chelator (Raraty *et al.*, 1999) (Raraty *et al.*, 2000).

Other studies have also found that an increase in calcium is required for intracellular activation of trypsinogen. Krüger and colleagues found that a sustain elevation in the apical region was required. The duration of the increase was required to be greater than 100s. Oscillations or spikes of a greater intensity of calcium increase were ineffective activators of intracellular trypsin if the elevation was less than 100s in duration. They also report that ionomycin and cyclopiazonic acid (CPA) (SERCA pump inhibitor) did not induce trypsinogen activation, their explanation being that there is a required localisation of the calcium increase (Kruger *et al.*, 2000). However this is in disagreement with Raraty and colleagues findings that thapsigargin did induce activation of intracellular trypsinogen measured simultaneously with BZiPAR (fluorescence trypsin substrate) and calcium (Fura-2). Calcium measurements made in this study were taken from the whole cell and question the opinion, that SERCA pump inhibition does not cause a calcium release not experienced in the apical region. It has also been shown by Frick and colleagues that both high calcium and supramaximal secretagogue stimulation was required to induce an increase in trypsinogen activation in isolated cells (Frick *et al.*, 1997).

Hypercalcaemia in rats has been found to lower the threshold of caerulein concentration required to induce the development of pancreatitis, by the process of intrapancreatic infusion (Zhou *et al.*, 1996). An explanation for this is that high levels of extracellular calcium may hinder calcium extrusion, preventing the restoration of normal intracellular calcium levels. The same study showed the use of

a calcium channel blocker verapamil was protective against the development of pancreatitis in rats, though the absence of voltage-gated calcium channels on these cells makes this finding difficult to explain. However the results have been repeated in isolated acinar cells and isolated perfused pancreas suggesting that this is not due to actions of the blocker on blood flow or other physiological components potentially mediated in the *in vivo* model. The role of calcium influx in the pathogenesis of acute pancreatitis is supported by clinical evidence that hypercalcaemia can lead to pancreatitis. The calcium mobilisation in acinar cells in response to physiological concentrations of agonists is reported to be mainly a result of release from intracellular stores. However supra-physiological concentrations of secretagogues cause calcium influx in addition to release from internal stores (Yule *et al.*, 1991), again implicating calcium influx in the development of pancreatitis.

Examination of the calcium homeostasis in cells during the early development of pancreatitis was achieved by using an *in vivo* model that involved administration of hourly injections of caerulein. Cells were isolated from the pancreas after a different number of injections. It was found that abnormal calcium responses in acinar cells, to application of agonists post isolation, increased with increasing number of injections in comparison to saline injected controls (Ward *et al.*, 1996). The disruption of calcium signals occurred in a spatial as well as temporal manner. The absence of oscillatory responses or any responses in some cases and the change of point of origin, (which would normally localise to the secretory pole region) to the basalateral region are indications of interference of calcium signalling. However the ER calcium content was unaffected. Comparable amounts of calcium were released after inhibition of the SECRA pumps from both treated and control cells. Other

studies have also reported impairment of calcium homeostasis where levels of cytosolic calcium increase with prolonged pancreatic duct obstruction (Urunuela *et al.*, 2002).

The disruption of calcium homeostasis in cells, which have been subjected to conditions such as those experienced during the induction of pancreatitis, shows the potential for a calcium-mediated mechanism of inappropriate enzyme activation. Disruption of normal secretion of enzymes after supramaximal stimulation has been observed. Apical exocytosis of zymogen granular content appears to be blocked and aberrant exocytotic events occur at the basal lateral membranes (Scheele *et al.*, 1987;Gaisano *et al.*, 2001). Gaisano and colleagues have studied the localisation of proteins involved in exocytosis in the pancreatic acinar cells. They found that the non-neuronal SNAP-25 isoform, SNAP-23, is localised predominately to the basal lateral membranes in the pancreatic acinar which co localises with syntaxin-4. Syntaxin-2 is found at the apical membrane where the physiological secretion occurs and syntaxin-3 is found on the granular membranes (Gaisano *et al.*, 1997). Munc18 also known as nSEC-1, has been described to prevent SNARE complex formation by binding to syntaxin. The phosphorylation of mun18 by PKC causes the disassociation of munc18 from syntaxin and removal of its inhibitor effect (Rizo & Sudhof, 2002). Munc18 localises to the basal lateral membranes in non-stimulated pancreatic acinar cells. Stimulation by physiological concentrations of CCK does not effect munc18's cellular distribution. However stimulation with supraphysiological concentration of CCK-8 caused a redistribution of munc18 in pancreatic acinar cells to a cytosolic location, which was dependent upon PKC activation. The presence of munc18 at the basal lateral membranes is suggested to be

a protective role preventing exocytosis at this site. Activation of PKC by supraphysiological concentrations of CCK results in the removal of munc18 from the basal lateral membranes. This in conjunction with high cytosolic calcium across the cell allows exocytosis to occur abnormally at the basal lateral membranes (Gaisano *et al.*, 2001).

Inflammation and the involvement of transcription factor NFκB in the development of pancreatitis.

Inflammation is another factor involved in the development of pancreatitis. Acinar cell damage leads to a local inflammatory response. The role of inflammatory mediators in pancreatitis have been extensively studied using inhibitors, neutralising antibodies and genetic approaches (review in Bhatia *et al.*, 2000). However experiments with applications of TNFα and Il-1β on both isolated acinar cells and perfused isolated pancreas show no co-localisation of granules and lysosomes and no activation of trypsin. This implies that the inflammatory mediators are a symptom of pancreatitis development owing to cell damage not causative of the pancreas damage (Norman, 1998). Cellular regulation of these inflammatory regulators involves the transcription factor NFκB. Activation of the transcription factor NFκB has been observed in secretagogue-induced pancreatitis models (Steinle *et al.*, 1999).

NFκB a transcription factor

The following is a brief description of the NFκB activation pathway. Further details are review in (Ghosh & Karin, 2002;Silverman & Maniatis, 2001;Schmid & Adler,

2000). The transcription factor NFκB represents a family of transcription factors made up of 5 members to date: Rel (c-Rel), p65 (RelA), RelB, NF-κB1 (p50 and its precursor p105) and NF-κB2 (p52 and its precursor p100). The functional unit exists as either homo or heterodimers; most dimers are transcriptionally active, the exception being p50/p52 or p50 and p52 homodimers, which repress transcription of the target genes. The precursors of p50 and p52, p105 and p100 respectively, have also been shown to participate and form dimers with other members of the family. Dimers involving these subunits (p105 and p100) are however not transcriptionally active. The transcriptionally active protein binds to κB sites within the DNA. The κB site is a consensus sequence, which is 10base pairs in length; there is diversity within the κB sequences of different promoters. The varieties of dimers have different affinities for the κB sites. The complexity of the genes and promoters regulated by NFκB/Rel proteins is immense. There are so far few identified subsets of genes or genes that are preferentially regulated by one combination of NFκB proteins. The ability of different NFκB combinations to bind the same sequence produces overlap in their spectrum of genes. The NFκB/Rel proteins can also interact with other transcription factors and repressors to add another layer of control. Phosphorylation of the NFκB/Rel proteins are thought to be involved these interactions.

In unstimulated cells the NFκB/Rel proteins are inhibited and anchored in the cytoplasm by inhibitor proteins, IκBs. The inhibitors consist of IκBα, IκBβ, IκBγ and IκBε. They possess an ankyrin repeat in the C terminus. This domain mediates the interaction with the NFκB/Rel proteins masking the nuclear localisation signal

causing their retention in the cytoplasm. The most widely studied IκB is IκBα, serine phosphorylation of the IκBα protein in response to stimuli, results in ubiquitination and eventual degradation by the 26S proteasome pathway. Degradation of the IκBα reveals the nuclear localisation signal on the NFκB/Rel protein. This allows NFκB translocation to the nucleus.

The activation of NFκB is transient. This is due to NFκB mediated transcription of the gene that encodes for IκBα. NFκB controls the production of its own inhibitor. The newly synthesised IκBα translocates to the nucleus and binds to the NFκB protein hiding the nuclear localisation signal. The complex is subsequently removed from the nucleus back into the cytoplasm.

The IKKα and IKKβ are two of the kinases identified which phosphorylate the IκB proteins. It has been suggested that these kinases are themselves phosphorylated; the MAP kinase cascade has been implicated in the activation of the IKKs and subsequently NFκB. Tyrosine kinase activity has also been associated with NFκB activation not only in the upstream activation of the MAP kinase pathways but direct tyrosine phosphorylation of the IκB proteins. This tyrosine phosphorylation, unlike serine phosphorylation, does not cause degradation of the protein but does induce IκB proteins to disassociate from the NFκB/Rel protein (Imbert *et al.*, 1996). NFκB induction due to tyrosine phosphorylation associated with cytoskeleton disruption in pancreatic lobules has been suggested (Algul *et al.*, 2002). This was not the only pathway of NFκB activation reported in the pancreas.

Activation of NFκB has been linked to the onset of pancreatitis. CCK or its analogue caerulein have been shown in numerous studies to activate NFκB (Han & Logsdon, 2000;Tando *et al.*, 1999;Han & Logsdon, 1999;Steinle *et al.*, 1999;Gukovsky *et al.*, 1998). The activation is rapid, detectable within 15mins of stimulation and disappears at ~6hrs. The activation and inactivation of NFκB correlate well with the degradation and subsequent resynthesis of the IκBα inhibitor protein (Steinle *et al.*, 1999). In two studies the blockade of NFκB activation with inhibitors, which act through their antioxidant properties, attenuate the symptoms of the hormone induced pancreatitis (Gukovsky *et al.*, 1998;Demols *et al.*, 2000) and in another exacerbate the symptoms (Steinle *et al.*, 1999). An in vivo study, which involves the intrapancreatic injection of an adenovirus expressing an active NFκB subunit, p65 (RelA), induced activation of NFκB in a population of the acinar cells. The activation of NFκB was measured by monitoring abundance of a *mob-1* mRNA, a gene whose transcription is under the control of NFκB. Cellular damage, such as vacuole formation and swelling of the pancreatic tissue, both associated with pancreatitis, were induced upon expression of the p65 subunit. Further to this, inflammation was detected in the lungs of animals injected with the adenovirus; this is consistent with systemic complications observed with pancreatitis (Chen *et al.*, 2002). Trypsin activation was unaffected by the adenoviral mediated expression of p65. This is in agreement with a study indicating that CCK activates trypsinogen and NFκB by independent pathways (Han *et al.*, 2001).

NFκB activation is also thought to be involved in bile salt, taurocholate-induced pancreatitis (Vaquero *et al.*, 2001;Satoh *et al.*, 1999). The inhibition of NFκB activation by an inhibitor pyrrolidine dithiocarbamate (PDTC), an antioxidant,

improved the survival rates of rats that underwent experimental taurocholate-induced pancreatitis (Satoh *et al.*, 1999). The stimulation of chemokine gene expression has also been shown as a result of bile treatment (Grady *et al.*, 1997). Interestingly bile acids have been implicated in the regulation of RANTES (a chemokine) transcription via NFκB binding sequence in the RANTES promoter region (Hirano *et al.*, 2001).

The pathways found to mediate the CCK-induced NFκB activation in the pancreatic acinar cell are PKC and calcium dependent (Tando *et al.*, 1999;Han & Logsdon, 2000). Treatment with Ca^{2+} chelators TMB-8 and BAPTA both inhibit NFκB/Rel activation by inhibition of IκB degradation in response to CCK (Tando *et al.*, 1999;Han & Logsdon, 2000). Treatment with PKC inhibitors GF109203X could also block transcription of an NFκB dependent gene (Han & Logsdon, 2000). Agonist activation of NFκB has only been detected at high supraphysiological concentrations of agonists. Physiological concentrations of agonists are unable to activate NFκB (Tando *et al.*, 1999;Han & Logsdon, 2000). Interestingly CCK analogue JMV-180 was unable to induce pancreatitis (Saluja *et al.*, 1989) Bombesin also does not promote the development of pancreatitis or activate NFκB (Grady *et al.*, 1997;Han & Logsdon, 1999) (Powers *et al.*, 1993). This could be linked to the degree of PKC activation through DAG production; bombesin stimulation has been shown to produce very little DAG (Pandol & Schoeffield, 1986). It was found that calcium increase and PKC activation synergistically lead to the activation of NFκB (Han & Logsdon, 2000;Tando *et al.*, 1999). The activation of PKC alone by phorbol ester treatment slightly decreased the levels of IκB proteins whereas ionomycin alone had no effect. In combination ionomycin and phorbol ester treatment activated IκB degradation to a similar extent to that seen with CCK (Han & Logsdon, 2000).

Activation of p38 MAP kinase has also been linked to cytokine upregulation in the pancreas and pancreatitis development (Blinman *et al.*, 2000;Wagner *et al.*, 1999). Inhibition of p38 MAP kinase by SB 204580 reduced the degree of cytokine activation (Blinman *et al.*, 2000). A role for p38 MAP kinase activation has been described in CCK-induced cytoskeleton reorganisation in the pancreatic acinar cell at physiological concentrations of agonists (Schafer *et al.*, 1998).

Aims

The aims of my studies were, firstly **to investigate the effects of secretagogues CCK and ACh on calcium efflux.** Efflux, mediated by calcium pumps of the plasma membrane, is an important mechanism in protecting the cells from unwanted sustained calcium elevations. The investigation of the effects of secretagogues on efflux mechanism is addressed in chapter 3. The regulation of efflux mechanisms by secretagogues creates an interesting situation of additional modulation by the secretagogue on the calcium signal, induced be these very secretagogues. We found an activation of efflux by ACh and CCK. This effect was further characterised and the signal transduction pathway involved was investigated. The protocol of an elevated calcium plateau was used to investigate this function of the secretagogues stimulation. The extra advantage of this protocol was that it emulated the conditions of elevated cytosolic calcium, postulated by Raraty and colleagues to be involved in the development of pancreatitis (Raraty *et al.*, 2000).

The initial trigger of pancreatitis is still a matter of some debate. However the influence of bile salts on the disease is of interest, especially in light of the association of gallstones or crystals with the incidence of pancreatitis. The effects of bile salts on calcium signals in the hepatocytes has been described, but information on bile acids and calcium signalling in the pancreas is only just emerging (Voronina *et al.*, 2002a). **The description of the influence of a bile salt, taurolithocholic acid 3-sulfate on cytosolic calcium was the second aim of my work** (results discussed in chapter 4). Particular emphasis of this part of the project was on TLC-S effects on sustained calcium plateau. The long-term goal of this component would be to reveal

possible influence of bile acids on the development of pancreatitis and the mechanism of its action.

The transcription factor NFκB was reported to play an important role in the development of pancreatitis. **I aimed to develop a method, which would enable the measurement of NFκB activation in single cells** and to apply this method to study calcium-dependent activation of NFκB in pancreatic acinar cells (results reported in chapter 5). These experiments utilised GFP conjugated proteins of the p65 subunit of the NFκB dimer, to measure activation through localisation of the transcriptionally active unit, and a GFP conjugated IκBα protein to measure the abundance of IκBα inhibitor protein.

Chapter 2

Materials and Methods

2.1 Preparation of isolated Pancreatic acinar cells

Adult, Male CD1 mice (approximately 30grms) were killed by stunning by a blow to the head followed by cervical dislocation. A left transverse subcostal incision was made exposing the spleen and stomach. The pancreas can be found under the spleen, and was excised and placed in a dish containing standard extracellular solution, trimmed free of fat. Collagenase (Worthington, 200units/ml in 1ml of standard extracellular solution 1mM Ca^{2+}) pre-warmed to 37°C was injected into the lobes of the pancreas until tissue was flooded. The tissue and excess collagenase solution were transferred to a 1.5ml ependorf and incubated in a shaking water bath at 37°C for a period 10-18mins.

After incubation the tissue was removed from the collagenase solution and placed in a 15ml tube containing standard extracellular solution. Vigorous shaking disrupted the tissue, the solution containing the smaller clusters and single cells was removed from the upper portion and the fluid partially replaced with standard extracellular solution. After this was repeated several times the remaining tissue was discarded. The dispersed cells were washed by centrifugation at 1000rpm for 1min, the supernatant discarded and pellet resuspended in extracellular solution. This washing processed was repeated and the remaining pellet resuspended in standard extracellular solution.

2.2 Primary acinar Cell culture

Cells were cultured after microinjection to allow expression of the protein. Cells were cultured in a serum free system, the effects of serum on calcium signals and protein expression were unknown, and serum was found to be unnecessary for cell

survival. The cell culture procedure was adapted from Brannon et al., 1985 (Brannon *et al.*, 1985): Waymouths medium (Gibco) was used with 1x antibiotic/antimytotic mix (Gibco), 0.1mg/ml of Soya bean trypsin inhibitor and 10% Chick embryo extract (Sera laboratories). Cells were re-suspended in the culture medium and placed on sterilised cover slips (in a 6 well dish (nunc)) that had been coated in poly-L lysine. After a short period allowing the cells to adhere, further culture medium was added to prevent drying out.

For imaging experiments, the cover slips were carefully removed and placed in a dish containing 5μM Fura-2 AM in Na^+ HEPES solution for 30mins at room temperature. The cover slips were then attached to the bottom of a perfusion chamber with vacuum grease.

For microinjection experiments, cells were re-suspended in the culture medium and then placed on a cover slip which had a border around the edge in vacuum grease to prevent the cell containing solution from running off the edge. Microinjection was performed as described in section 2.10 and the location of the microinjected cells recorded by sketching and markings on the edge of the cover slip. The cover slip was then placed in a specially designed chamber that consisted of a petri dish with a small reservoir of water and an elevated platform to support the cover slip. This was then placed in a humidified incubator at 37°C and 5% $C0_2$.

2.3 Description of cell chamber and Perfusion System

A small volume of suspended cells (100-200μl) was placed in a Perspex chamber with a disposable glass coverslip attached to the bottom and held in place by vacuum grease (silicon grease). Figure 2.1 shows a chamber and the perfusion inflow and suction (for removal of solution) tubes positioned on an inverted microscope stage. A gravity fed perfusion system was used with 20ml syringe barrel attached to polythene tubing that contained the perfusate. All the inflow tubes were fed into a single adaptor that was attached to the chamber through a specifically designed holder on the chamber. The rate of solution exchange is determined by the height of the supply barrels relative to the level of inflow, the diameter of the tubing used and the volume of the cell bath. On the confocal microscope system the gravity fed perfusion system flow rate was approximately 600μl/min, which fed into a bath of a 150μl volume. This was used for all confocal experiments unless otherwise stated.

The perfusion system on the imaging set-up was of a similar design, a gravity fed perfusion with a common single inflow, and this was held by a manipulator arm that allowed positioning on the inflow close to the cells of interest. The flow rate of this system was 500μl/min, which fed into a bath of a 300μl volume. The suction removed waste solution from the edge of the chamber, the suction tube has been positioned opposite the perfusion inflow.

For microinjection and electrophysiological experiments the coverslips were coated with poly-L lysine to help the cells adhere to the glass more effectively. The coverslips were covered with a 1 in 10 solution of poly-L lysine in distilled water for 10-20mins then rinsed with distilled water and allowed to air dry. All experiments were performed at room temperature ~25°C controlled by air conditioning.

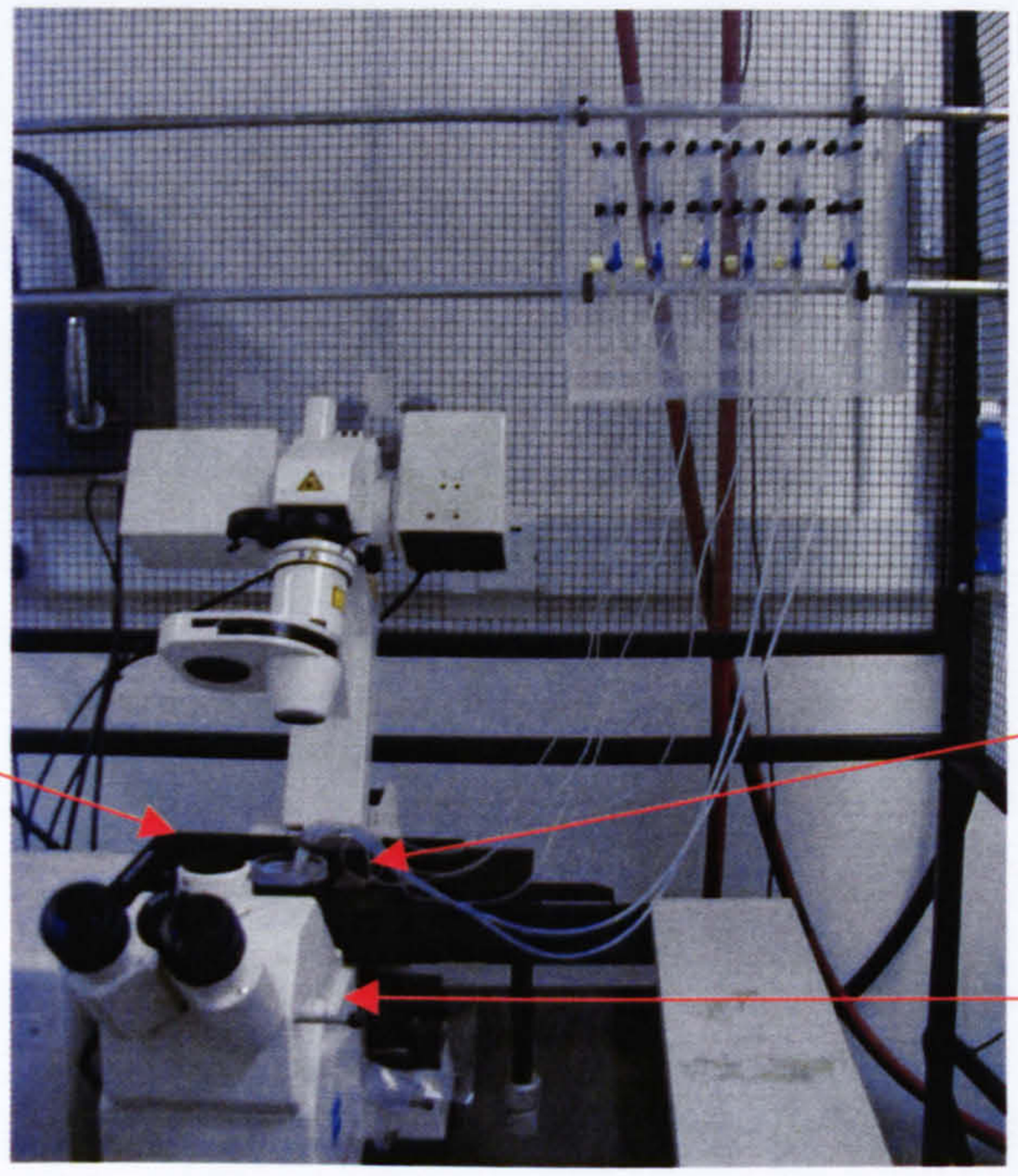
Gravity fed
Perfusion system
Inverted
Microscope
stage
Perfusion chamber
Inverted microscope

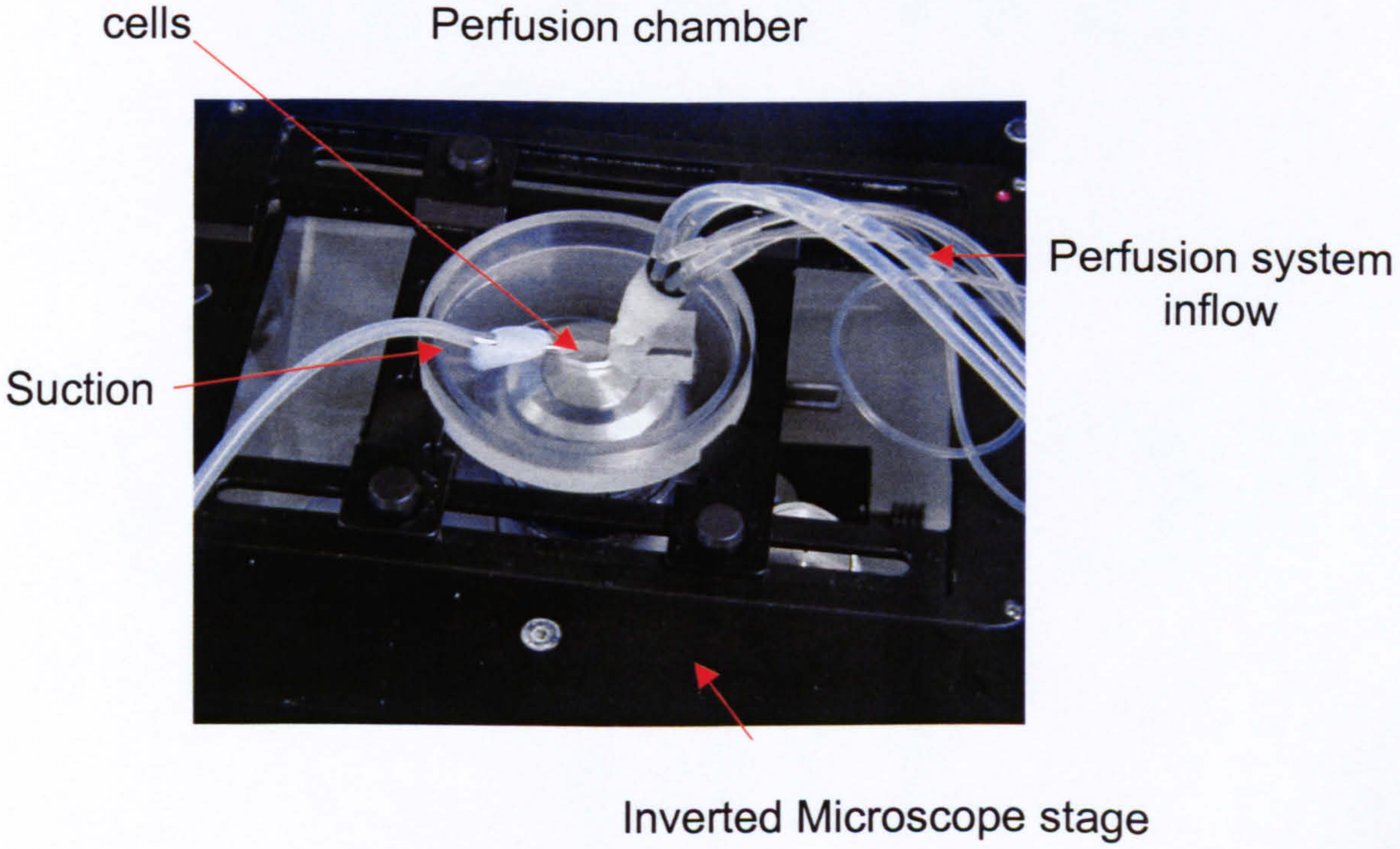
cells
Perfusion chamber
Perfusion system
inflow
Suction
Inverted Microscope stage

Figure 2.1 **Examples of the perfusion systems used on both confocal and imaging systems** The upper photograph shows the gravity fed perfusion system to the right of the inverted microscope. The lower photograph shows the perfusion chamber on the inverted microscope stage. The perfusion supply is on the right and the suction for solution removal is on the left.

2.4 Confocal Microscopy

The superior spatial or temporal resolution was required for some experiments. The confocal experiments were performed on a Zeiss laser scanning confocal microscope (LSM 510). The confocal microscope first patented in 1957 by Minsky, is a system that improves resolution with a reduced background by the use of a pinhole that removes extraneous light (blur). By inserting a pinhole in the emission light path of the microscope this allows one to illuminate and collect light from a specific focal plane within the specimen. This coupled together with scanning mirrors, allows the precise collection of light from a defined point. A number of Ca^{2+}-sensitive indicators are suitable for laser excitation and can be used in conjunction with laser scanning confocal microscopy. The schematic 2.2 shows the basis of the confocal excitation and emission pathways. The excitation light (Blue lines) passes through an excitation pinhole and reflected by a dichroic mirror to pass through the lens. The lens focuses the light to a point within the specimen. After excitation emitted light (Red lines) from the specimen, both in focus and out of focus light, is collected by the objective lens. Emitted light passes through the dichroic mirror, however only in focus light is detected as the emission pinhole blocks the out of focus light from passing through to the detector. The scanning of the whole field is achieved by rotation of the dichroic mirror and other scanning mirrors (not shown) to achieve point-by-point, line-by-line, excitation and emission of the entire field, this is termed raster scanning. The resolution of the scan dictates the length of time taken to complete the scan; higher resolution demands a longer scan time. The requirements of the experiment determine the degree of spatial resolution offset against the

temporal resolution required (A region of interest (ROI) within a field can be defined, to reduce the scan time before starting the experiment).

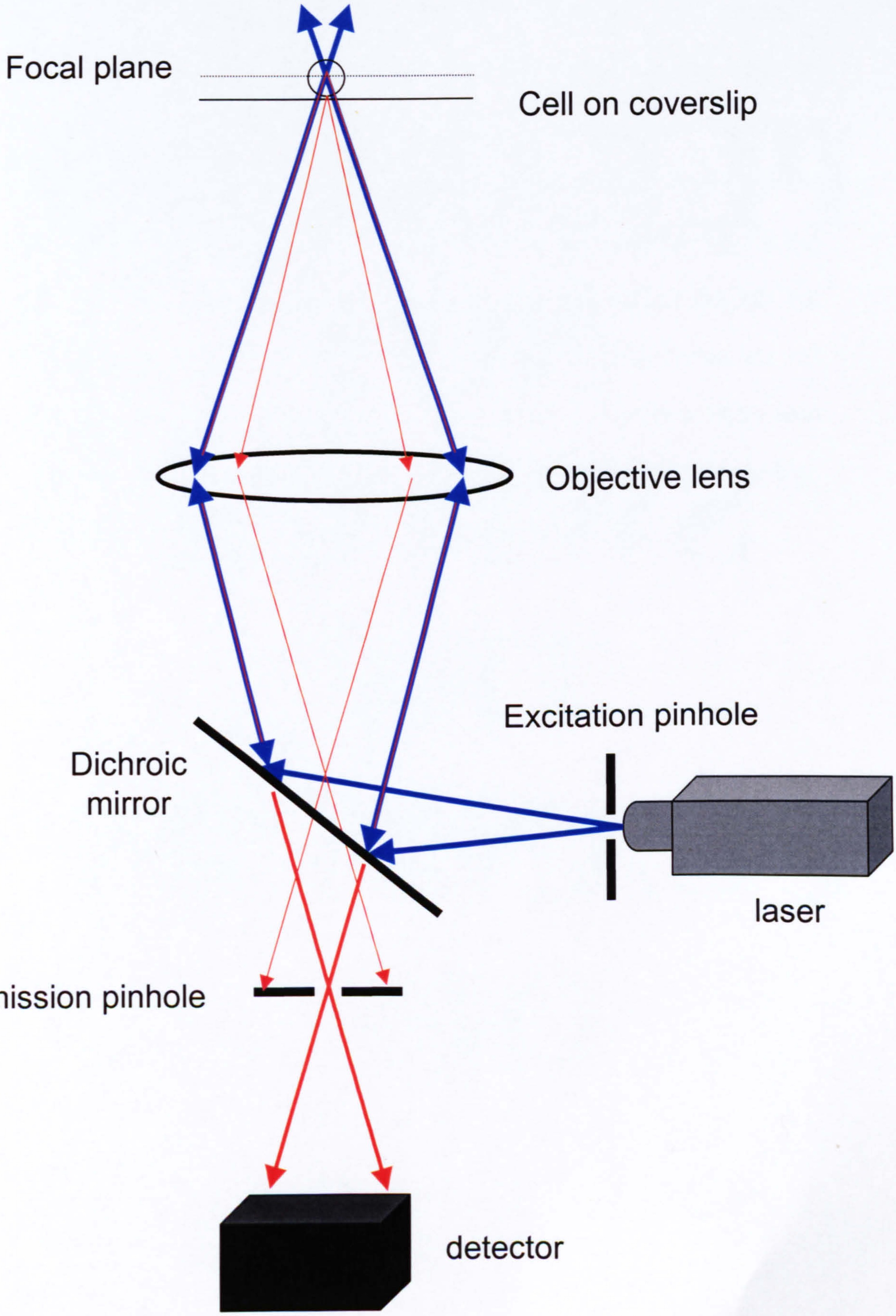
Focal plane
Cell on coverslip
Objective lens
Excitation pinhole
Dichroic mirror
laser
Emission pinhole
detector

Figure 2.2 **A schematic depicting the principle of confocal microscopy** The blues line demonstrates the excitation light pathway from the source to the specimen. The red lines represent the pathway of the emission light through to the detector. The redlines that originate from the focal plane and follow the same path as the excitation light to the dichroic mirror that then pass through the dichroic mirror through the emission pinhole and fall on the detector is in the focus emission, the red lines that originate from beneath the focal plane (out of focus light) also pass through the dichroic mirror however they are blocked form reaching the detector by the presence of the emission pinhole.

The resolution both temporal and spatial is controlled through the software that also allows you to change the intensity of excitation light and the size of the pinhole. A larger pinhole aperture allows more light and a thicker confocal section, however at a loss of z-axis resolution, a smaller pinhole aperture reduces the thickness of the confocal section increasing z-axis resolution however the amount of light collected is reduced. This can be compensated to a degree by increasing the intensity of excitation, however increasing the amount of photodamage to the fluorophore and the specimen.

Z-axis scanning is achieved by changing the focal plane in steps. The user determines the step size. The confocal computer software can be used to recombine the z-section images to produce a 3D reconstruction of the specimen.

The Zeiss LSM 510 is equipped with an Acousto-Optical Tuneable Filter (AOTF), that allows very fast (non-mechanical) changes of a excitation light. This could be used for almost simultaneous dual-excitation of a point in a specimen by two different lines of excitation. This allows simultaneous excitation and therefore measurements from two different dyes/probes.

The analysis of the experiments was performed in the LSM software, where ROIs within the image captured can be applied. This allows analysis within discreet areas of a single cell or individual cells within a cluster. This also allows the same ROI to be analysed for both probes where simultaneous acquisition has been performed.

2.5 Caged Compounds

Caged compounds are engineered molecules that can be loaded into the cell but within a molecular cage (chemical group inhibiting biological activity) and hence undetectable to the cell until released by destroying the molecular cage with UV light. Uncaging is conceptual rather than a chemically accurate term. In most cases a covalent bond has to be broken by UV illumination to unmask biological active substance. In the case of the two molecules that have used within the course of these studies both caged calcium and caged IP_3 uses the 1-(2-Nitrophenyl) (NP or NPE (ethyl)) system. This system is compatible with a large number of functional groups, is reasonably light sensitive and easy to synthesize (Adams & Tsien, 1993).

Caged calcium-NP-EGTA is a modified EGTA molecule that is introduced to the cell utilising the AM ester form, or loaded into the cell via the patch pipette where the NP-EGTA (Molecular Probes) is co-loaded with a proportion of calcium. Absorption of the UV light release of the uncaging group and decreases the calcium affinity of the probe. As a result calcium is released into the cytosol (figure 2.3).

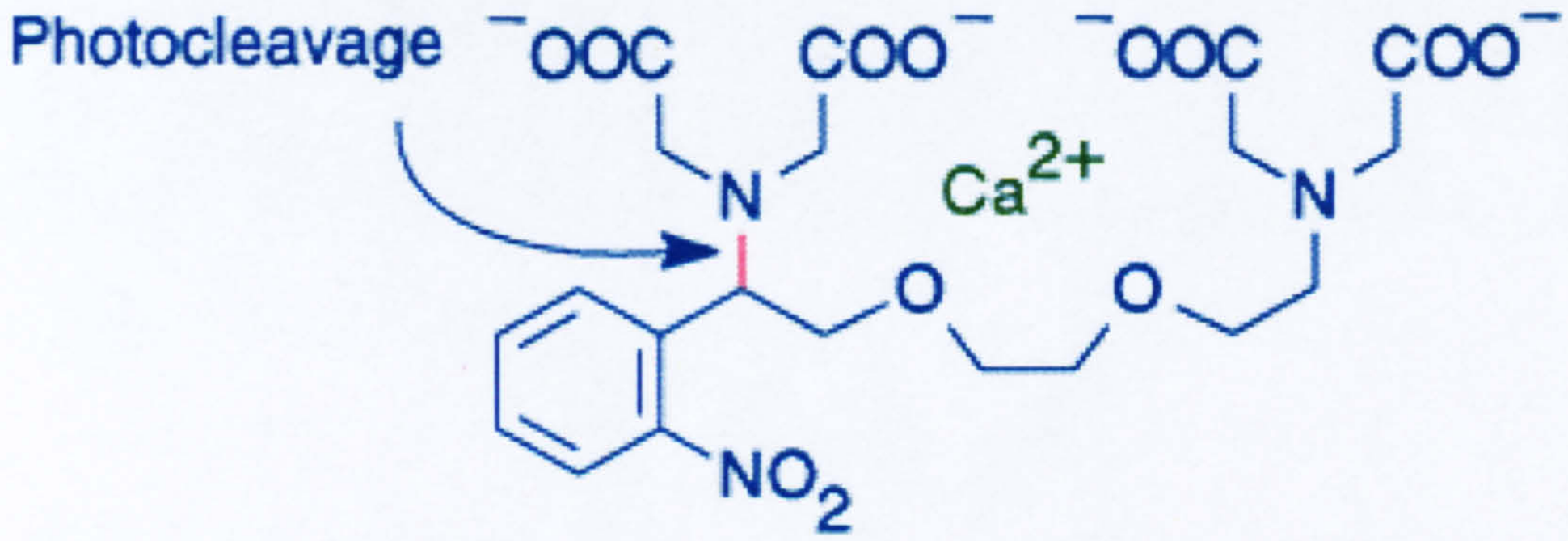

Figure 2.3 **NP-EGTA or caged calcium molecule**.

Shows a molecule of caged calcium bound to a calcium ion. The bond in red indicates the bond destroyed by photo cleavage resulting in liberation of the calcium ion.

The other caged compound used during these studies is caged IP_3 (Molecular Probes), which is a cell impermanent molecule and has therefore to be loaded via the patch pipette. Again this uses the NPE caging group. Loading through the patch pipette has the advantage of monitoring cytosolic calcium by measuring the calcium dependent chloride and non-specific cation currents. This can be done whilst monitoring the calcium and performing the uncaging within a discreet ROI within the scan field that is set through the LSM software.

2.6 Selection of Calcium sensitive dye

The development of fluorescent probes that show a change in their spectral properties upon binding of calcium have enable researchers to investigate the changes in intracellular calcium. Ca^{2+} sensitive indicators developed by Roger Tsien and colleagues are usually based on Ca2+ chelators EGTA and BAPTA. The indicators developed by Roger Tsien and colleagues have lower affinities, faster responses and brighter fluorescence than previously used dyes. The choice of dye is dependent upon the excitation lines available and the expected range of calcium concentrations to be investigated and hence the k_d of the dye. Dyes with a lower k_d are used for measuring calcium within the endoplasmic reticulm where the concentration of calcium is higher than that measure in the cytosol where dyes with a higher k_d are used. Table 2.1 shows a list of the dyes used in my work, information on the k_d and loading conditions. The use of ratiometric (two wavelength) dyes is an advantage, as this allows measurements that are independent of the amount of dye loaded into the cells and artefacts e.g. bleaching and leakage, effect both wavelengths equally are eliminated. Most of the dyes used are available in membrane-permeant acetoxymethyl (AM) ester form, which utilises esterases within the cells. After

crossing the membranes the AM forms of indicators undergo cleave of the AM group rendering them impermeable and hence captured with the cell (Tsien, 1981). Cell impermeant probes (free acid) have to be loaded by a more invasive technique (patch clamp or microinjection) though AM loading of dyes is not without its drawbacks such as organelle compartmentalisation and incomplete ester hydrolysis. In the experiments where microscopy is combined with whole cell patch clamping, probes are loaded via the patch pipette in a free acid form. This also allows continuous refilling of cytosolic probe from the pipette, so for processes such as uncaging over a long period of a time there is a constant supply of caged compound. Substances used in experiments can affect some dyes; fura-2 and fluo-4 are quenched by caffeine, which is also used as an IP_3 receptor antagonist in the pancreatic acinar cells. So for experiments that require the use of caffeine, fura-red must be used, as the effect of caffeine on this dye fluorescence is small.

Name of dye	Excitation wavelength (nm)	Emission wavelength (nm)	Kd for calcium	Loading concentration (μM)	Loading temperature	Loading time (min)
Fura-2 AM	340/380	505LP	~145 nM	2-5	RT	35-40
Fluo-4 AM	488	505-550BP	~345 nM	5	RT	25
Fura-red AM	543	650LP	~140 nM	5	RT	30
Mag-fluo-4 Am	488	505LP	~22 μM	5	37°C	20
Lysotracker AM	488	505LP	-	2 (added to bath)	RT	2-4
Indo-1*	364	400LP	~230 nM	1mM (in pipette)	-	-
Fluo-4	488	505-550BP	~345 nM	2.5	RT	30

*Used for co-injection of DNA in the microinjection studies

Table 2.1 Conditions and properties of the fluorescent probes used during these studies.

2.7 Imaging measurement of intracellular Calcium using fura-2.

Cells Loaded with fura-2 suspended in normal 1mM Ca^{2+} containing Na^{+} HEPES extracellular solution, were placed in a perfusion-slide chamber on the stage of a Nikon Diaphot inverted microscope. Cells were constantly perfused with solutions through a gravity fed perfusion system. Solutions were placed in a series of inverted 50ml syringe barrels, by opening a tap valve the solution flowed into the chamber through capillary tubing (550μl/min). Solution was removed by suction from a vacuum line allowing efficient exchange of solutions.

Perfusion-slide chamber consisted on a perspex slide with a diamond (300µl volume) removed from the centre. A circular poly-L-lysine coated coverslip (22mm) was attached with silicon grease to the underside of the chamber. Approximately 100µl of cells were placed in the chamber and allowed to adhere for ~2 min. Perfusion of normal Na^+ HEPES before the beginning of the experiment washed away any debris.

The temperature in the room was maintained by air-conditioning system, at 25°C.

The schematic 2.4 illustrates the basis of the imaging system. A xenon light source produces excitation light where selection of 340 and 380nm were alternated through a rotational excitation filter wheel. The excitation light is reflected by a dichroic mirror through the objective lens that focuses the light onto the specimen (cells on a coverslip). Emission images are collected by the objective lens, the light then passes through the dichroic mirror and emission filter (510nm) and through a series of moveable mirrors onto an intensified CCD camera or up to the eyepiece dependent upon the position of the mirrors. The images were recorded by an imaging analysis system running on a Magical computer (Tardis, Visitech international, Sunderland, UK), Background subtraction was performed independently at both wavelengths, ratios (340/380nm) were then calculated for each individual image. This was followed by calculation of $[Ca^{2+}]_i$ values.

Figure 2.4 **A schematic of the imaging set-up used to measure fura-2 fluorescence** The blue line represents the excitation light pathway and the red the emission light pathway.

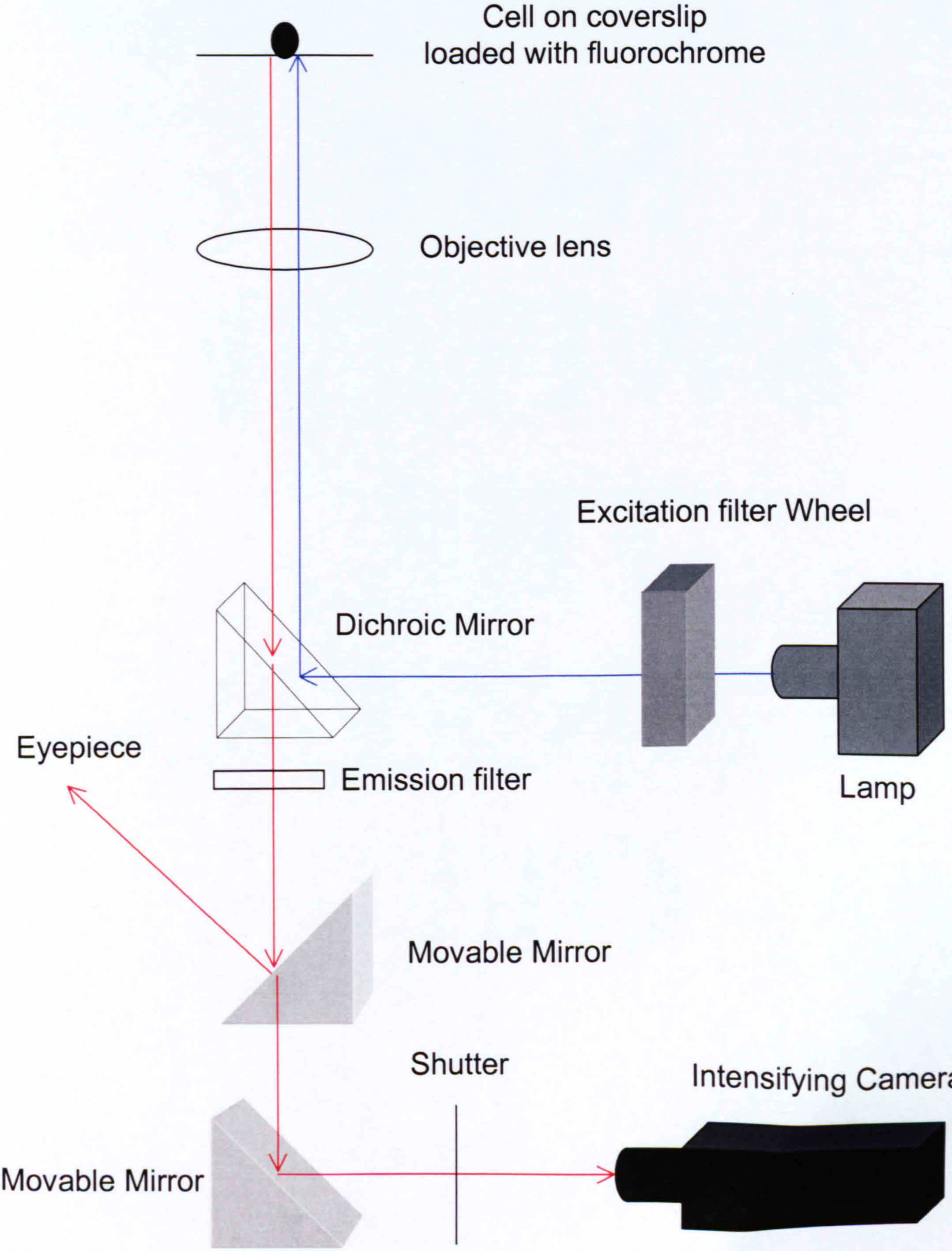

2.8 Calibration of Fura-2

Calibration of calcium sensitive dyes is required for quantitative evaluation; use of the Grynkiewicz equation (Grynkiewicz *et al.*, 1985) gives the relationship between fluorescence intensity and calcium concentration.

Grynkiewicz equation for a ratiometric dye:

$$[Ca^{2+}] = \beta \times K_d \times (R - R_{min}) / (R_{max} - R) \qquad (1)$$

Where for Fura-2:

$$\beta = F_{max}380 / F_{min}380 \qquad (2)$$

$$R_{min} = F_{min}340 / F_{max}380 \qquad (3)$$

$$R_{max} = F_{max}340 / F_{min}380 \qquad (4)$$

K_d = 150nM (Neher & Augustine, 1992)

The environment affects the properties and behaviour of calcium sensitive dyes and therefore an *in vivo* calibration was performed. The measurement of R_{max} and R_{min} are performed by exposing the cells loaded with Fura-2 to external solution containing ionomycin and either high calcium or calcium and EGTA. Zero Ca^{2+}, 10mM EGTA and 10μM ionomycin was applied for 20 minutes to determine R_{min}. Application of external solution with 10mM $[Ca^{2+}]$ and 10μM ionomycin was performed for measurements of R_{max}. Figure 2.5 shows a trace that results from such a protocol. Initially the cells are at low calcium showing that the 380nm fluorescence is high (red and blue traces) and the 340nm fluorescence is low (green and black trace). Then after application of high external calcium, 10mM, the high calcium saturates the dye giving a low signal from the 380nm (red and blue traces) and high from the 340nm (green and black trace) fluorescence. These measurements

were used to calculate R_{min}, R_{max} and β values, 0.51, 3.0 and 2.63 respectively (values averaged from 10 different cells). This then allows calculation of the corresponding calcium concentrations using equations 1, 2, 3 and 4 described above.

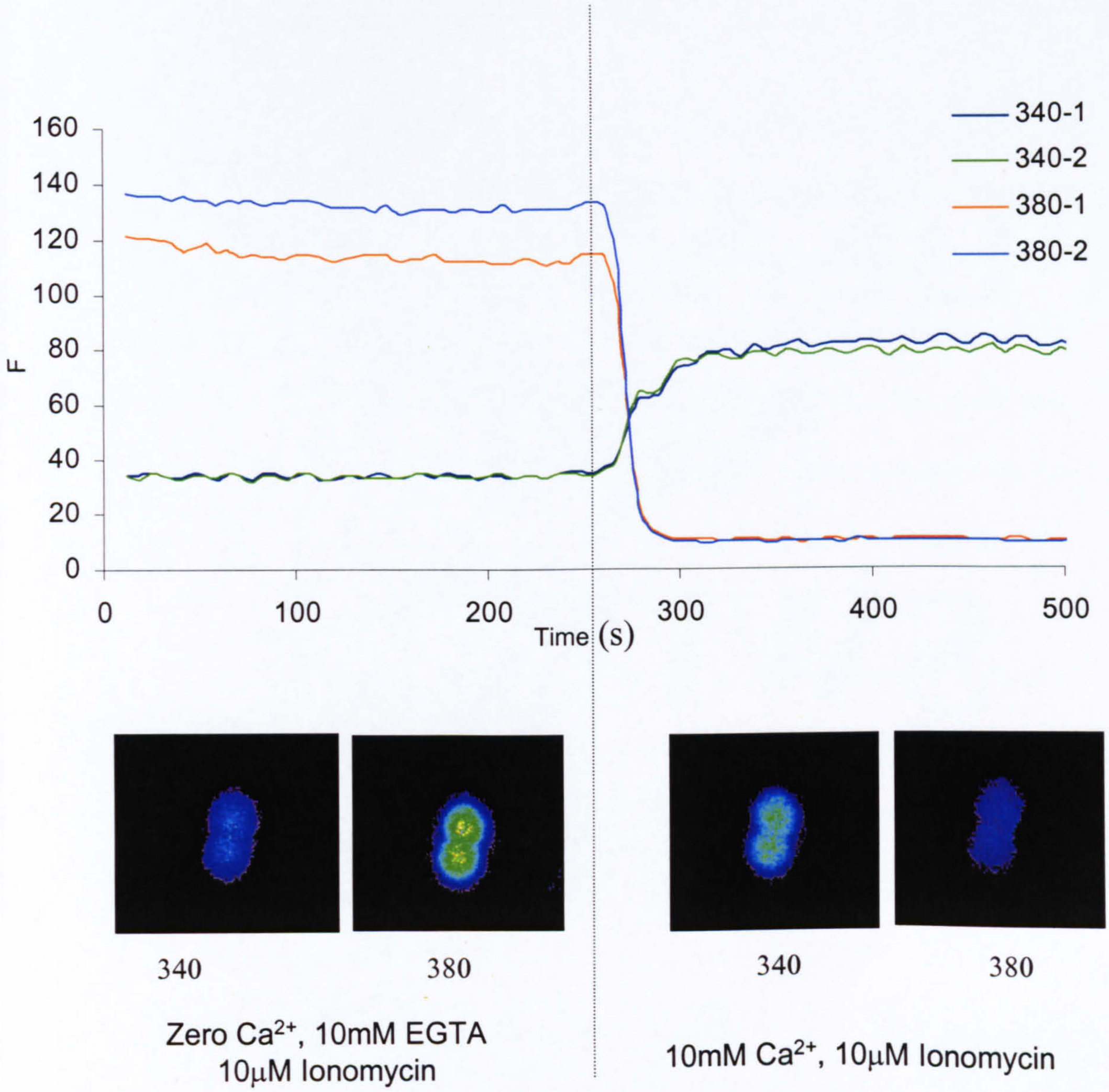

Figure 2.5 **Fura-2 Calibration protocol** The cells are previously incubated in zero calcium, 10μM ionomycin, 10mM EGTA (pH 7.6) for 20minutes then placed on the imaging system, 250s of fluorescence are recorded then the solution is changed to 10mM calcium and 10uM Ionomycin (pH7.6) as indicated by the dashed line. The lines are the fluorescence for both excitation wavelengths for two cells shown in the images below. The dark blue and green lines represent the 340 emission and red and light blue lines represent the 380 emission.

2.9 Electrophysiology

Patch clamp pipettes were produced from borosilicate glass capillary tubing with an outer diameter of 1.5mm and an inner diameter of 1.17mm (Harvard Apparatus Ltd, Kent). A DMZ Universal pipette puller (Germany) was used to pull pipettes and the heat settings for elongation steps could be varied to suit the requirements of the experiment. Pipettes used typically had a resistance of 2-4MΩ. The final step involved is polishing the pipette to clean and smooth the tip surface, this facilities the formation of a giga seal between the glass of the pipette and the cell membrane.

Pipettes were back filled with intracellular solution containing various dyes and compounds as indicated, and then placed in a pipette holder. The pipette holder is fixed to the head-stage. Using a micromanipulator (Burleigh instruments, Victor, USA), the pipette was positioned close to the cell with a slight positive pressure to prevent mixing of the extracellular solution with the internal pipette solution. The pipette was the placed gently on the surface of the cell and suction applied to achieve a high resistance GΩ seal. The holding potential clamp was then applied and further suction was used to break through the cell membranes, achieving a whole cell configuration. At this point, dyes and other compounds within the intracellular solution would diffuse in to the cell and equilibrium between the pipette and inside the cell would be attained (figure 2.6).

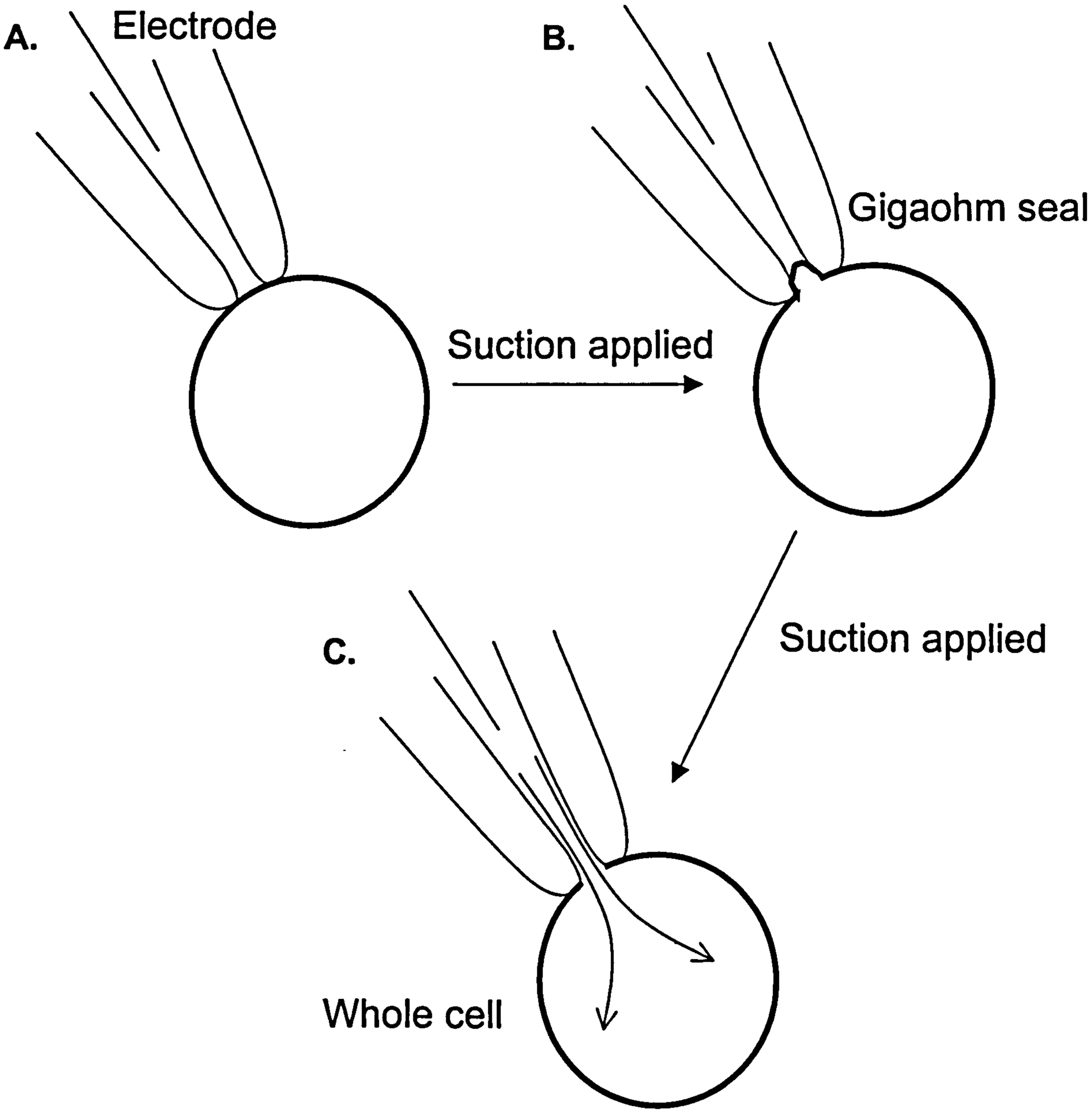

Figure 2.6 The a schematic represent the stages of gaining whole cell patch clamp configuration (**A**) The pipette is placed gently on the cell. (**B**) Suction is applied and a high resistance seal termed a giga seal is achieved. (**C**) Gentle suction is then applied to rupture the membrane and gain whole cell access, where the contents of the pipette is allowed to diffuse freely into the cytoplasm of the cell and an equilibrium is reached.

The resting membrane potential of a mouse pancreatic acinar cell is approximately -40mV. This was originally measured using a glass microelectrode inserted into a cell in a section of pancreas (Nishiyama & Petersen, 1974). There are Ca^{2+}-activated Cl^- channels and non-selective cation channels in the pancreatic acinar cell, both of which provide a sensitive measurement of calcium changes within the cell. Whole cell patch clamp configuration was used, where the total currents of the cell are recorded. Membrane potential was held at –30mV unless otherwise stated. A protocol where depolarising steps to 0mV membrane potential are applied every 150ms was used in my experiments. At 0mV the net flux of ions is very small as there is equilibrium between cations fluxes across the cell membrane and no driving force for Cl^- movement. However at –30mV inward currents, carried mainly by Cl^- ions can be measured (Park *et al.*, 2001). That result from the conductance through calcium activated Cl^- and calcium activated non-selective cation channels.

Whole cell membrane current measurements were made using an EPC-8 patch clamp amplifier (HEKA, Lambrecht, Germany). The signals were recorded from whole cell patch clamp configuration were digitised via an IST-16 A/D interface (Instrutech, Long Island, USA) and recorded on a PC (Research Machines) and stored on disc. The software used was Pulse (HEKA) and the currents were charted online using X-chart software (HEKA).

To minimise electrical noise from external sources the microscope and patch set up were enclosed in a faraday cage. The microscope and attached patch pipette holder and manipulators were placed on an air table to isolate from any vibrations.

Internal patch solution:

140mM KCl; 10mM HEPES; 1.13mM MgCl2; 2mM ATP; 0.1mM EGTA solution was adjusted to pH 7.2 using potassium hydroxide.

2.10 Microinjection.

Microinjection is a method used to introduce impermeant molecules in to the cell. One of the applications of this technique is the delivery of DNA constructs into cells that are difficult to transfect (Mulderry, 1996).

Microinjection pipettes were made from X glass with an inner diameter of 0.94mm and an outer diameter of 1.2mm (Clark electromedical instruments, Reading, UK). A DMZ Universal pipette puller was used to pull pipettes and the heat settings for elongation steps could be varied to suit the requirements of the experiment. Generally cells, which successfully expressed protein after being injected, were in medium to large clusters, cells in small clusters were unable to survive the pressure injection. The positive backpressure and the injection pressure were maintained by a FemtoJet® unit (Eppendorf, Germany), a tuneable pressure supply. The values of positive backpressure and injection pressure changed between cell preparations and pipettes (300-600 hPa). The pipette was placed in a holder, positioned at approximately a 45° angle; this was connected to a micromanipulator (Eppendorf 5171, Germany), which was used to position the tip of the pipette just touching the surface of the cell, Cells were situated on a cover glass on an inverted microscope (Nikon). A Z-level setting, where isolated nuclei inherent to the cell preparation were used as markers, is set within the manipulator; this indicates the level that the tip will move to when injection is initiated. The length of injection varied depending upon the cell preparation and injection pipette (range 0.1s to 20s). Some required only a

short injection time, which could be done with the semi-automatically facility. In some cases however a longer injection period was required, 10-20sec. Injections of the longer length of time were normally done under a manual control and successful injection was visualised by the co-injection of Indo-1 free acid at 1mM concentration in the pipette and visualised by fluorescence. With both semi-automatic and manual injection the successful injections were confirmed by Indo-1 fluorescence (364 excitation, coherent laser on Noran confocal).

The concentration of DNA in the pipette was ~50ng/µl in the injection solution, diluted with distilled H_20, which had been cleaned using a filter with a 2 µm pore diameter (See section 2.11 for DNA amplification and purification). DNA was centrifuged for 15min at 13,000rpm; this was to remove debris that may cause blockage of the pipette during injections. The top fraction of the DNA solution was used as a stock for further dilution.

2.11 DNA amplification and purification for microinjection

Plasmids for the GFP conjugated IκB and p65 proteins were kindly donated by Dr M. White. The plasmids were transformed into chemically competent cells, (XL1-blue Stratagene). The transformation was performed by incubation with 1-10ng of plasmid DNA on ice for 30mins, followed by heat shocking at 42°C for 45sec and transferring back to ice for 2 minutes, followed by addition of 0.9ml SOC medium pre-warmed to 42°C, then cells were allowed to recover at 37°C for 1 hour, whilst shaking at 250rpm. The transformation mixture was then plated out at different concentrations made up in SOC medium on LB plates with the appropriate antibiotic selection and grown up overnight at 37°C. Individual Colonies were selected the

following day and 5ml cultures in LB broth were cultured with antibiotic selection. Glycerol stocks were prepared by mixing a 1:4 ratio of culture:80% glycerol solution, and stored at -70°C.

3ml of the culture was used for mini preps using a Qiagen™ mini prep kit, following the protocol provided (Qiagen™, Crawley, UK). The purification of DNA in this kit was based on an ion exchange methodology, kits that used a DNA binding resin, as a means of purification showed a decrease in efficiency of subsequent expression of successfully injected cells. Fresh DNA was prepared weekly; this greatly improved frequency of successful expression in injected cells. The difference in the quality of DNA made no detectable difference in expression efficiency after transfection of the same protein in HeLa cells. The concentration and quality of DNA was determined by absorbance at 260nm and 280nm.

LB Broth: 10grm NaCl; 10grm tryptone and 5grm yeast extract in 1 litre of distilled water.

LB Agar: 10grm NaCl; 10grm tryptone; 5grm yeast extract and 5grm agar in litre of distilled water.

SOC Media: 0.3grm NaCl; 20grm tryptone; 5grm yeast extract in litre of distilled water. Immediately before use add 1ml of 40% (w/v) glucose per 100ml (0.2μm filtered).

All reagents were purchased from Sigma.

2.12 Electron microscopy

Electron microscopy (EM) utilises the properties of electron beams to improve resolution in comparison to a light microscope. The wavelength of electron beam is inversely proportional to the velocity of the electrons and focusing of the beam by passing through a magnetic field is the principle behind operation of the electron microscope. The source of electrons is a tungsten filament, which when heated up emits electrons. These electrons are then accelerated by a creation of a high potential difference between an anode and the filament. In the anode there is an aperture through which some of the electrons pass. These electrons are focused by a magnetic lens, the condenser lens, onto the specimen. Some electrons pass through without deviation, however tissue stains used that contain compounds and ions with a high atomic number scatter some of the electrons. The binding of these substances to lipids and proteins enhance the electron-scattering ability of the tissue and produce a better contrast image. The electrons that pass through without deviation are focused by the objective lens and enlarged by the projector lens onto a fluorescent screen. Swinging of the fluorescent screen out of the way allows one to expose a photographic plate recording the images. The areas of dark are where electrons have been knocked out of the beam entirely. This occurs where there is a high density of proteins or lipids i.e. membranes or cellular compartments.

The analysis of the EM images was carried out using Histometrix software (kindly loaned by kinetic imaging). Photographs from the EM were scanned in at 300 dpi and saved as TIFF files, a format supported by the Histometrix software. Only sections of cells that displayed an apical pole and a nucleus were considered. The fraction area of the section of the apical region occupied by granules and vacuoles

was calculated by the analysis software. The apical region was defined using the cell apical membrane on one side and the most basal granules or vacuoles and mitochondria on the other. The analysis software was then told to define the dark structures as granules (dense regions where the electrons have been knocked out) and the light regions as vacuoles (regions that the electrons transmitted through). Other structures such as mitochondria that are also electron dense, though distinguishable by their structure and shape were manually eliminated from analysis of the granular area. Vacuole region classification was also manually corrected to include only large vacuole structures and eliminate small translucent vesicles.

All fixation and tissue processing was performed by Mrs J Henry, veterinary faculty.

Fixative: 2% glutaraldehyde; 4% paraformaldehyde in 0.1M Sodium cacodylate buffer.

2.13 HeLa cell culture and Transfection

HeLa cells were kindly donated by Dr M. White; they were used between passages 20 and 30 only. HeLa cells were culture in Minimal essential medium with Earle's salts (Gibco) with 5% foetal calf serum (Harlan Seralab) and essential amino acids (1x, diluted from 100x) (Gibco) at 37°C, 5% CO_2 humidified incubator. Cells were spilt 1:4 every 2 days.

For transfection, HeLa cells were plated at a $2x10^4$ cells/ml (total volume 2ml) density in matex dishes (Matex corporation, USA) that were sterile plastic culture dishes with glass coverslips 15mm attached to the underside of the dish where a hole had been removed. Transfection was performed using Fugene 6™ (Bohringer

Mannheim) reagent. The transfection reagent was used at 1ug of DNA to 1.5ul of reagent. The Fugene 6™ was added to 100µl (per dish of cells) of serum free media, mixed and left to stand for 5minutes. The DNA was then added and mixed, left to stand for a minimum of 15mins (15-40mins). The mixture was then added drop wise directly from above to the cells on the glass coverslip region of the matex dish. The cells were then placed back in the incubator for 24hrs.

2.14 Reagents

All reagents for buffers were purchased from sigma. The following list indicates where other chemicals were purchased.

1,2-bis-(2-aminophenoxyethane-N, N, N', N')-tetraacetic acid (BAPTA)-Sigma
10% Chick embryo extract-Sera laboratories
8 Br cGMP - Sigma
8-Br cAMP– Sigma
$AACOCF_3$ –Calbiochem
Acetylcholine – Sigma
Ampicillin – Sigma
Antibiotic/antimycotic mix-Gibco
Brefeldin A–Calbiochem
BSA- Sigma
Caffeine –Sigma
Caged IP3 – Molecular probes
Calmidazolium chloride -Sigma
CCCP (Carbonyl cyanide 3-chlorophenylhydrazone)–Sigma
CCK-8 -Sigma
Collagenase -Worthington
Cytochalsin D-Sigma
DC_{10}-Sigma
Dibutyryl cAMP –Sigma
Dibutyryl cGMP–Sigma

Essential amino acids –Gibco

ET-18-OCH_3 –Calbiochem

Fluo-4 AM and free acid – Molecular probes

Foetal calf serum-Harlan Seralab UK

Fugene 6Ô -Bohringer

Fura-2 -Sigma

Fura-red –Molecular probes

Genistein –Calbiochem

Genistin (negative control) –Calbiochem

Indo-1 free acid –Molecular probes

Ionomycin – Sigma

JMV-180 – Research plus Inc, New Jersey, USA

Kanamycin - Sigma

Lanthanum Chloride –Sigma

Matex dishes -Matex Corporation

Minimal essential medium –Gibco

NFkB antibody –Santa Cruz

Normal goat serum- Sigma

NP-EGTA Am and free acid – Molecular probes

Oligomycin–Sigma

Paraformaldehyde - Sigma

PD908059 (solution) –Calbiochem

PMA (phorbol-12-myristate-13-acetate) –Calbiochem

Rotenone–Sigma

Soybean trypsin inhibitor - Sigma

Taurolithocholic acid 3-sulfate (TLC-S) –Sigma

Thapsigargin– Sigma

Waymouths medium 752/1-Gibco

Chapter 3

The effects of secretagogues on calcium efflux

Introduction

In 1992 Zhang and colleagues reported the activation of extrusion by the secretagogues. In stimulated cells, calcium extrusion was 3-fold faster than that of non-stimulated cells. They also showed that this increase was independent of the cytosolic calcium changes. The same activation of calcium extrusion was observed in the presence of 1,2-bis-(2-aminophenoxyethane-N, N, N', N')-tetraacetic acid (BAPTA). Calculations of rates of calcium extrusion at different cytosolic calcium concentrations (BAPTA loaded and fully stimulated without BAPTA) indicate that the pump is 88% saturated at relatively low calcium concentrations (129nM) and that a calcium-independent mechanism is responsible for the activation of extrusion (Zhang *et al.*, 1992). However the concentrations of agonists involved in the above studies were all supra-physiological. It was decided to investigate this effect and the potential role of this phenomenon at physiological concentrations of secretagogues.

CCK stimulated reduction in the calcium plateau level

Thapsigargin depletion of the internal stores followed by re-admittance of high external calcium to create a cytosolic calcium plateau, dependent upon the balance between calcium efflux and influx, was used to examine the effects of CCK on these mechanisms in the mouse pancreatic acinar cell. Firstly application of high supramaximal concentrations on the plateau was performed. As is shown in figure 3.1A a reduction in the level of the plateau was observed at supramaximal concentrations. Application of 10nM CCK produced an average drop 66 ± 4.2 nM (drop ± S.E.) (n=6). This confirmed the observations published by Zhang and colleagues in 1992. A range of CCK concentrations was then investigated. Figure

3.1B-D show a range of CCK concentrations 1nM –20pM, which induce a reduction in the plateau level. Application of 20pM CCK produced an average drop 15 ± 3.2 nM (drop ± S.E.) (n=36). Figure 3.1e shows that sequential addition in increasing concentration of CCK can induce a stepwise reduction in the plateau level. The level of reduction for each concentration is summarised in table 3.1. Upon removal of the agonist there are in some cases a recovery of the plateau level to pre-stimulation level, evident in figures 3.1c and 3.1d.

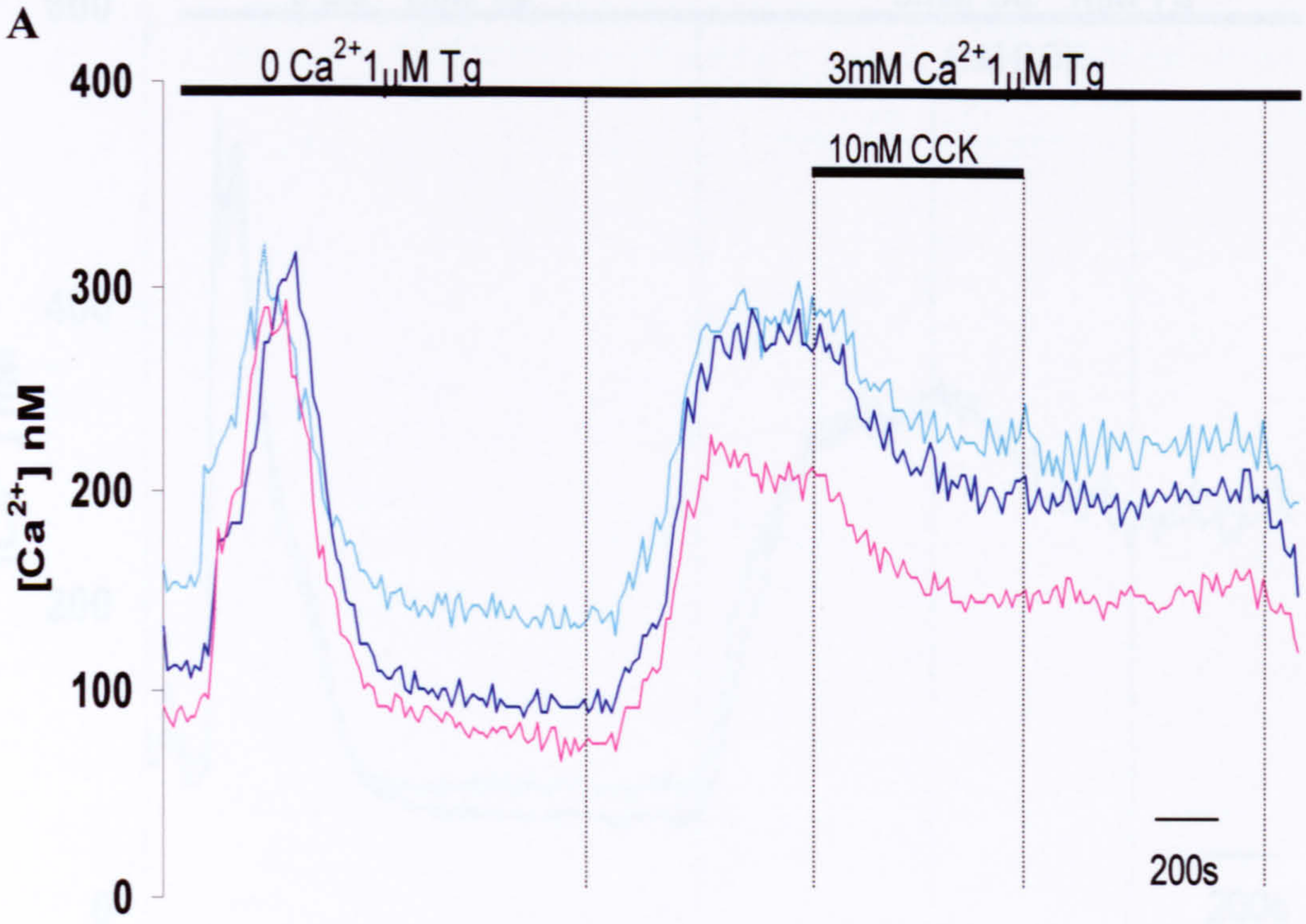

Figure 3.1 **The effect of CCK on a thapsigargin-induced cytosolic calcium plateau** Calcium responses in fura-2 loaded cells after thapsigargin depletion of the stores and creation of a cytosolic calcium plateau by exposure to high external calcium (3mM). Representative responses to (**A)** 10nM CCK application (B-E are shown on following pages) (**B)** 1nM CCK **(C)** 100pM CCK followed by 1nM CCK **(D)** 20pM CCK and **(E)** sequential application of 20pM, 100pM and 1nM CCK. Each line represents an individual cell.

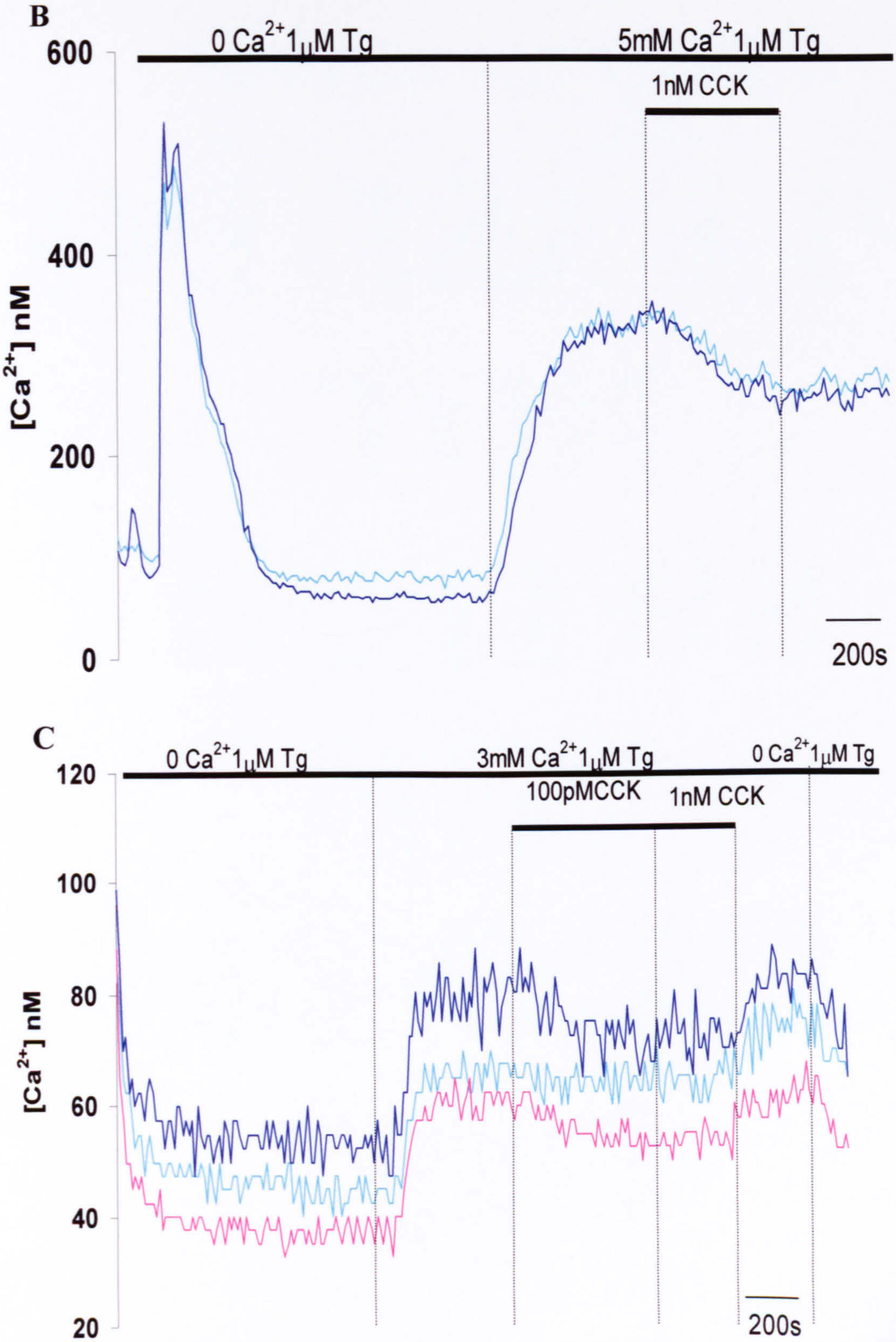
B
0 Ca2+ 1μM Tg
5mM Ca2+ 1μM Tg
1nM CCK
600
400
200
0
[Ca2+] nM
200s
C
0 Ca2+ 1μM Tg
3mM Ca2+ 1μM Tg
0 Ca2+ 1μM Tg
100pMCCK
1nM CCK
120
100
80
60
40
20
[Ca2+] nM
200s

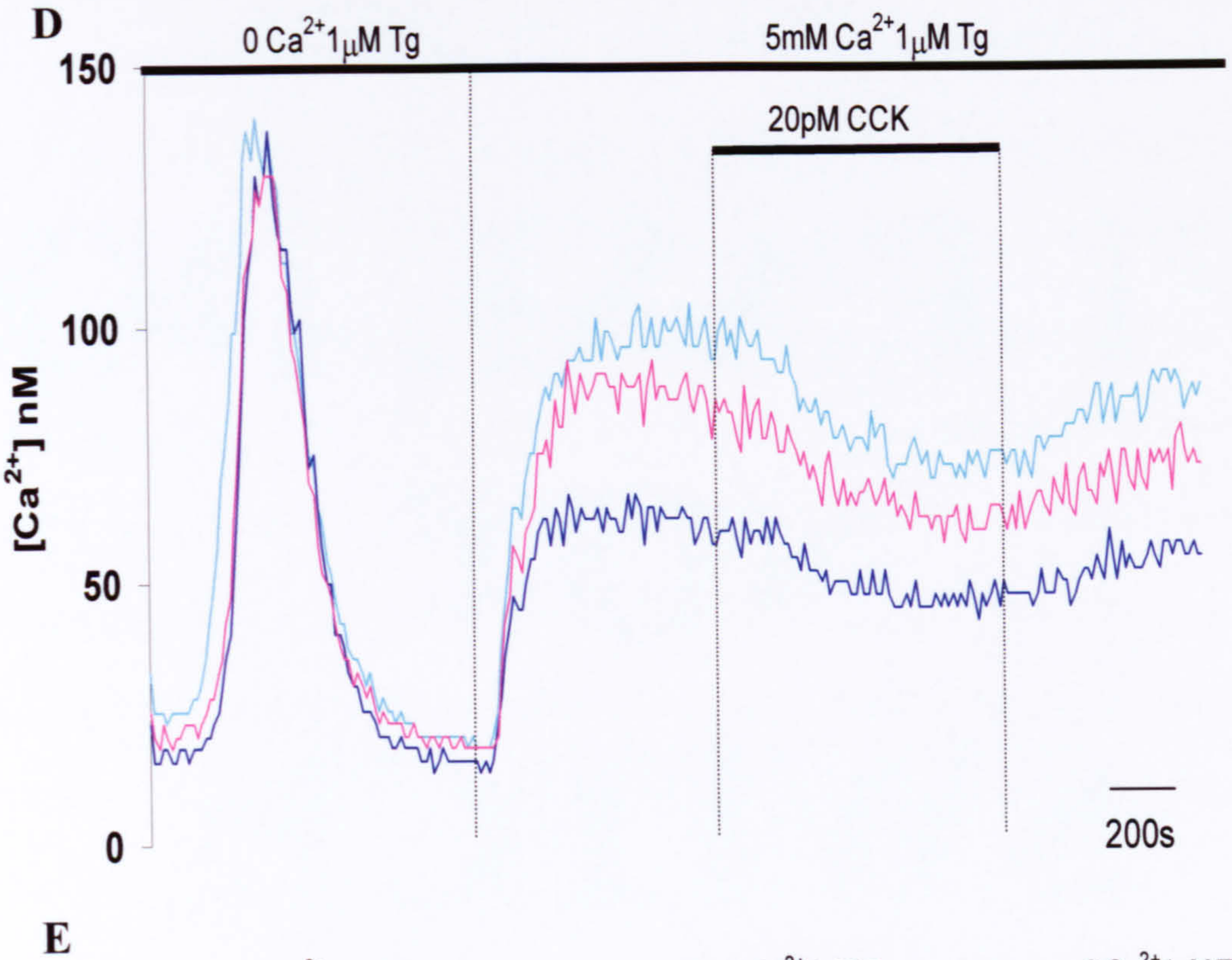
D
0 Ca2+1μM Tg
5mM Ca2+1μM Tg
20pM CCK
150
100
50
0
[Ca2+] nM
200s

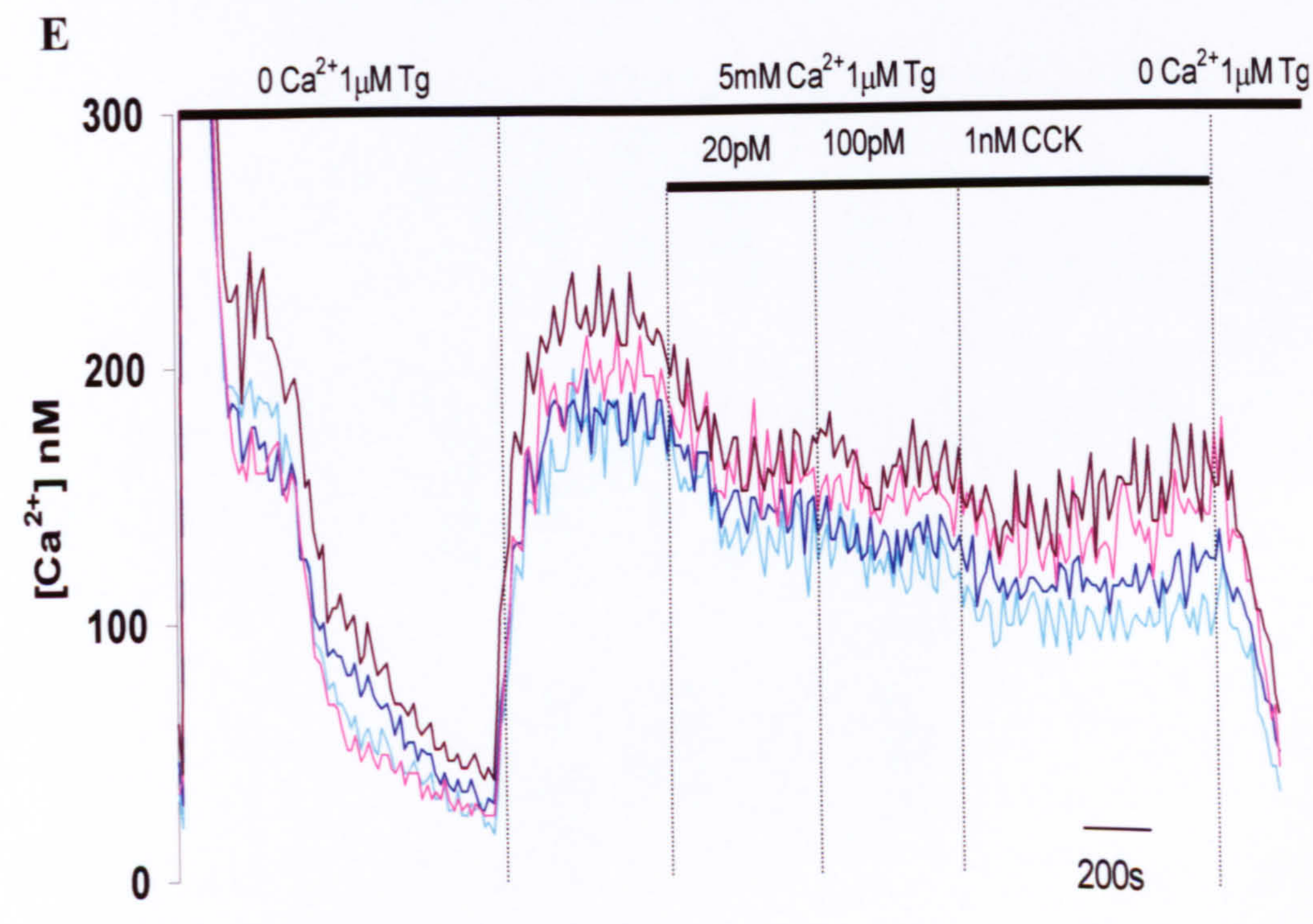
E
0 Ca2+1μM Tg
5mM Ca2+1μM Tg
0 Ca2+1μM Tg
20pM
100pM
1nM CCK
300
200
100
0
[Ca2+] nM
200s

ACh stimulated reduction in the calcium plateau level

Effect of ACh on the efflux and influx mechanisms in the pancreatic acinar cell was also examined using the same protocol as that use to investigate the CCK effects. Application of 10μM ACh shown in figure 3.2a, produced an average drop of 11 ± 4.4 nM (drop ± S.E.) (n=11) and figures 3.2b and c demonstrate that the effect could be induced at 1μM and 100nM ACh respectively. Application of 100nM ACh produced an average drop of 29 ± 4.6 nM (drop ± S.E.) (n=11). Figure 3.2d shows that sequential addition of increasing concentration can produce stepwise reductions in the plateau level; there is no measurable reduction in response to 100nM ACh: however 1μM then causes a reduction and a further reduction to 10μM ACh is apparent. Recovery was also seen in some cases upon removal of the agonist as is shown in figure 3.2b where upon removal of 1μM ACh there is a recovery of the plateau to pre-stimulation level. The degree of plateau level reduction to different concentrations of ACh is summarised on table 3.1.

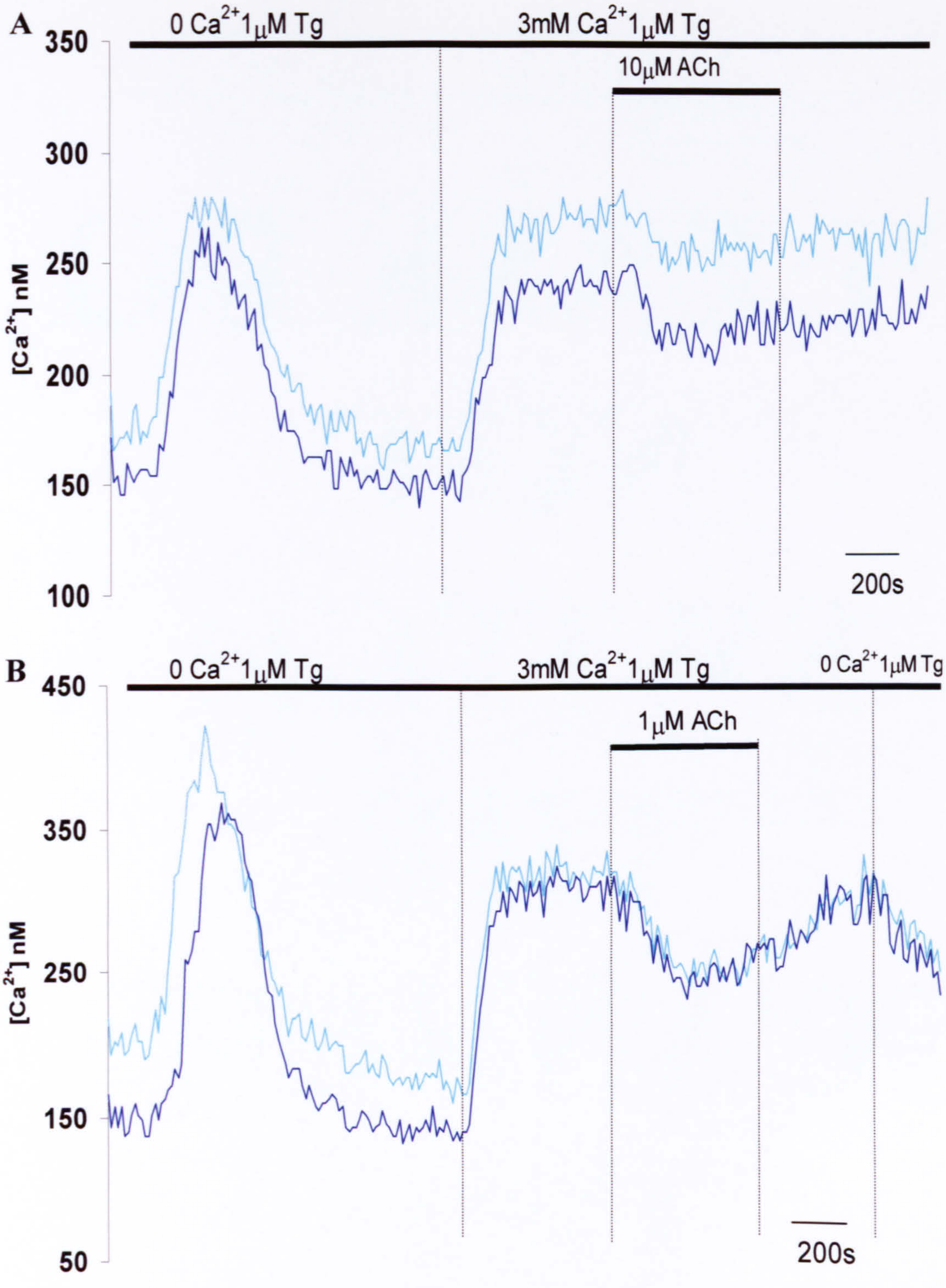

Figure 3.2 **The effect of ACh on a thapsigargin-induced cytosolic calcium plateau** Calcium responses in fura-2 loaded cells after thapsigargin depletion of the stores and creation of a cytosolic calcium plateau by exposure to high external calcium (3mM). Representative responses to (**A)** 10μM ACh application (**B)** 1μM ACh (panels C and D are shown on the next page) **(C)** 100nM ACh **(D)** sequential application of 100nM, 1μM and 10μM ACh. Each line represents an individual cell.

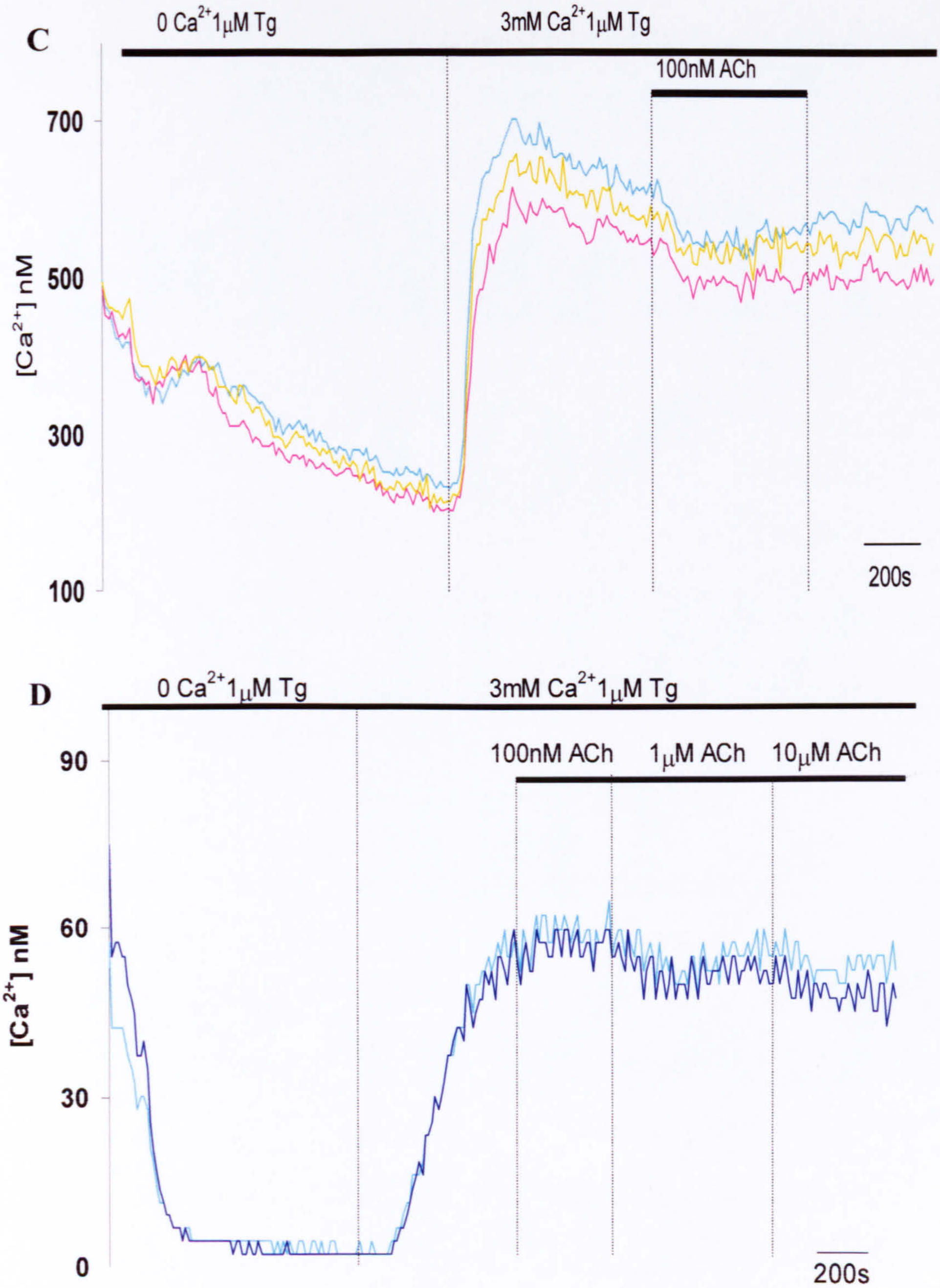
C
0 Ca2+1μM Tg
3mM Ca2+1μM Tg
100nM ACh
700
500
300
100
[Ca2+] nM
200s
D
0 Ca2+1μM Tg
3mM Ca2+1μM Tg
100nM ACh
1μM ACh
10μM ACh
90
60
30
0
[Ca2+] nM
200s

Agonist	Number of cells which responded (n/total n)	Decrease as a percentage of the original plateau (Average)	Statistical comparison of the plateau induced by agonist to the original plateau. (Wilcoxon signed rank test)
10nM CCK	6/6	24.2	P = 0.0313
1nM CCK	41/42	26.7	P <0.0001
100pM CCK	10/11	30.3	P = 0020
20pM CCK	23/36	14.7	P <0.0001
10μM ACh	8/11	9.1	P = 0.0420
1μM ACh	32/39	20.2	P <0.0001
100nM ACh	11/11	9.0	P = 0.0010

Table 3.1. Summary of the effects on the thapsigargin induced plateau of agonists CCK and ACh at different concentrations.

Investigation of the role of mitochondria in the reduction of the cytosolic calcium plateau induced by secretagogues

The mitochondria in the pancreatic acinar cell have been shown to take up calcium when the cells undergo stimulation (Park *et al.*, 2001). The ability of mitochondria to store calcium under the conditions used to establish a plateau is shown in figure 3.3. Where oligomycin an ATP synthase inhibitor and Rotenone an electron transport inhibitor were used to collapse the mitochondrial proton gradient, these prevented further uptake of calcium and caused release of any calcium stored in the mitochondria. As is shown in figure 3.3 upon application of oligomycin and rotenone, a gradual increase in calcium on the plateau is observed which reaches a new steady state in the time frame of this experiment. Collapse of the mitochondrial

proton gradient also compromises the energy state of the cell. Therefore application of the agonist on the plateau after collapse of the mitochondria would be difficult to interpret, as the effect maybe due to ATP depletion rather than removal of the mitochondria from the situation.

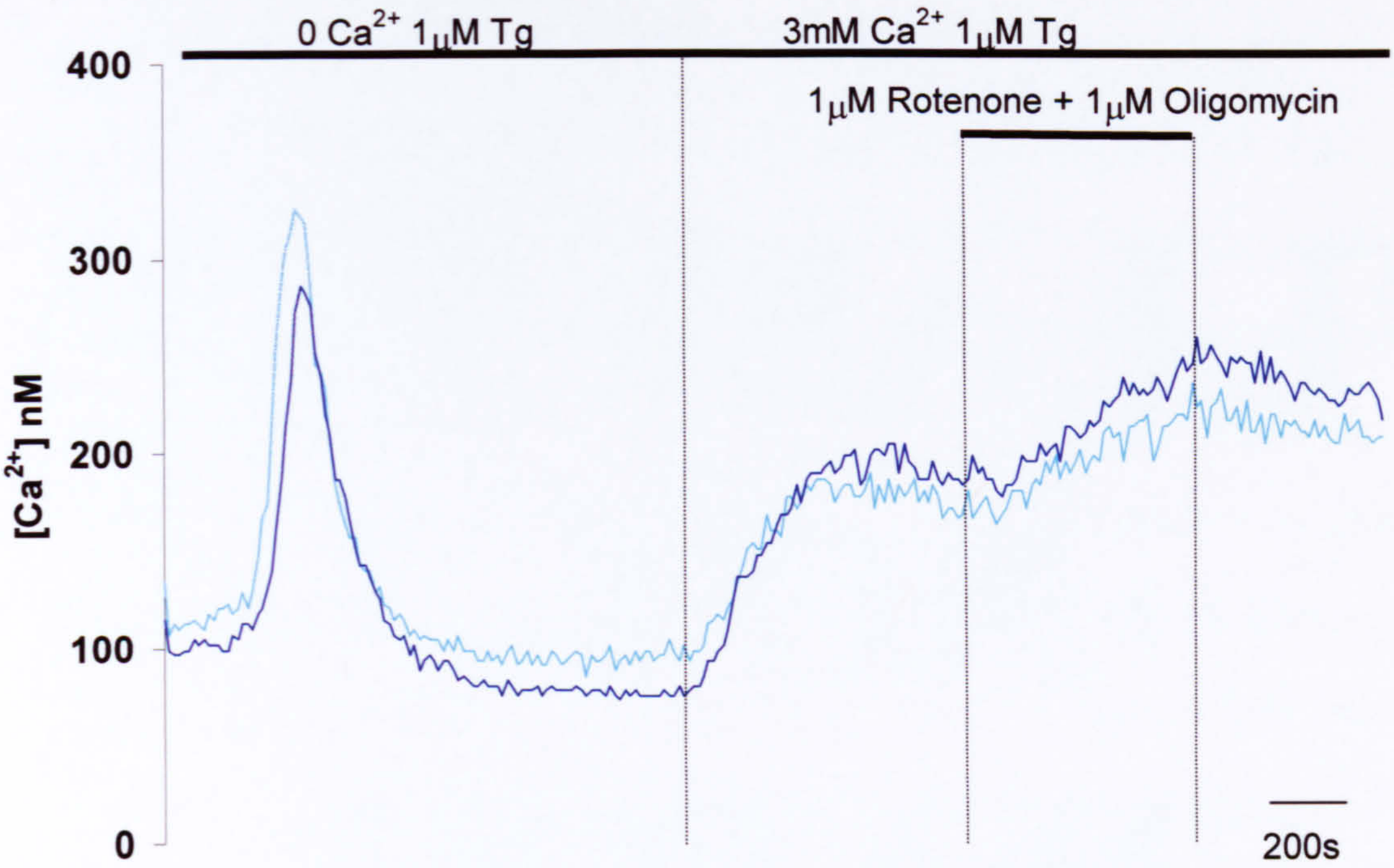

Figure 3.3 **The effect of mitochondrial inhibitors Rotenone and Oligomycin on the thapsigargin-induced cytosolic calcium plateau**

A trace from fura-2 loaded cells that have been treated with thapsigargin in zero external calcium, 3mM external calcium reintroduced and a cytosolic calcium plateau built. 1μM Rotenone and 1μM Oligomycin was applied on the cytosolic calcium plateau. Individual cells represented by each line.

Measurements of NADH autofluorescence as an indirect indicator of mitochondrial calcium

However, Voronina and colleagues show a correlation between the NADH and Ca^{2+} signals in the pancreatic acinar cell (Voronina *et al.*, 2002). So indirect means of measuring mitochondrial calcium and its possible role in the agonist-induced reduction in the plateau level is by measuring the NADH autofluorescence during the protocol. An increase in NADH correlates to an increase in mitochondrial calcium due to the calcium sensitivities of the mitochondrial dehydrogenases (McCormack & Denton, 1990;Robb-Gaspers *et al.*, 1998). As is shown in figure 3.4 the NADH transiently increases upon application of thapsigargin in zero calcium, and then increases again to a plateau level after the re-introduction of external calcium, which would create a cytosolic calcium plateau. Upon application of agonist on the plateau a reduction in the NADH autofluorescence was observed in (n=15/17). This was detected preferentially in the mitochondria which are located under the plasma membrane, 8 of 15 cells. Figure 3.5 shows the autofluorescence from subplasmalemmal (pink trace) and belt regions (blue) from the same cell. In figure 3.6 the cells were loaded with fura-red and simultaneous measurements of cytosolic calcium and NADH autofluorescence were performed. The red trace represents the fura-red signal and the green NADH autofluorescence; the open square symbols are measurements from the peripheral mitochondrial region and the closed diamond symbol from the belt region. This shows that the drop in NADH autofluorescence correlates with the drop in calcium induced by agonist application on the calcium plateau. Although there is some degree of recovery in calcium level after the removal of the agonist, there is a plateau in the NADH autofluorescence but no significant recovery.

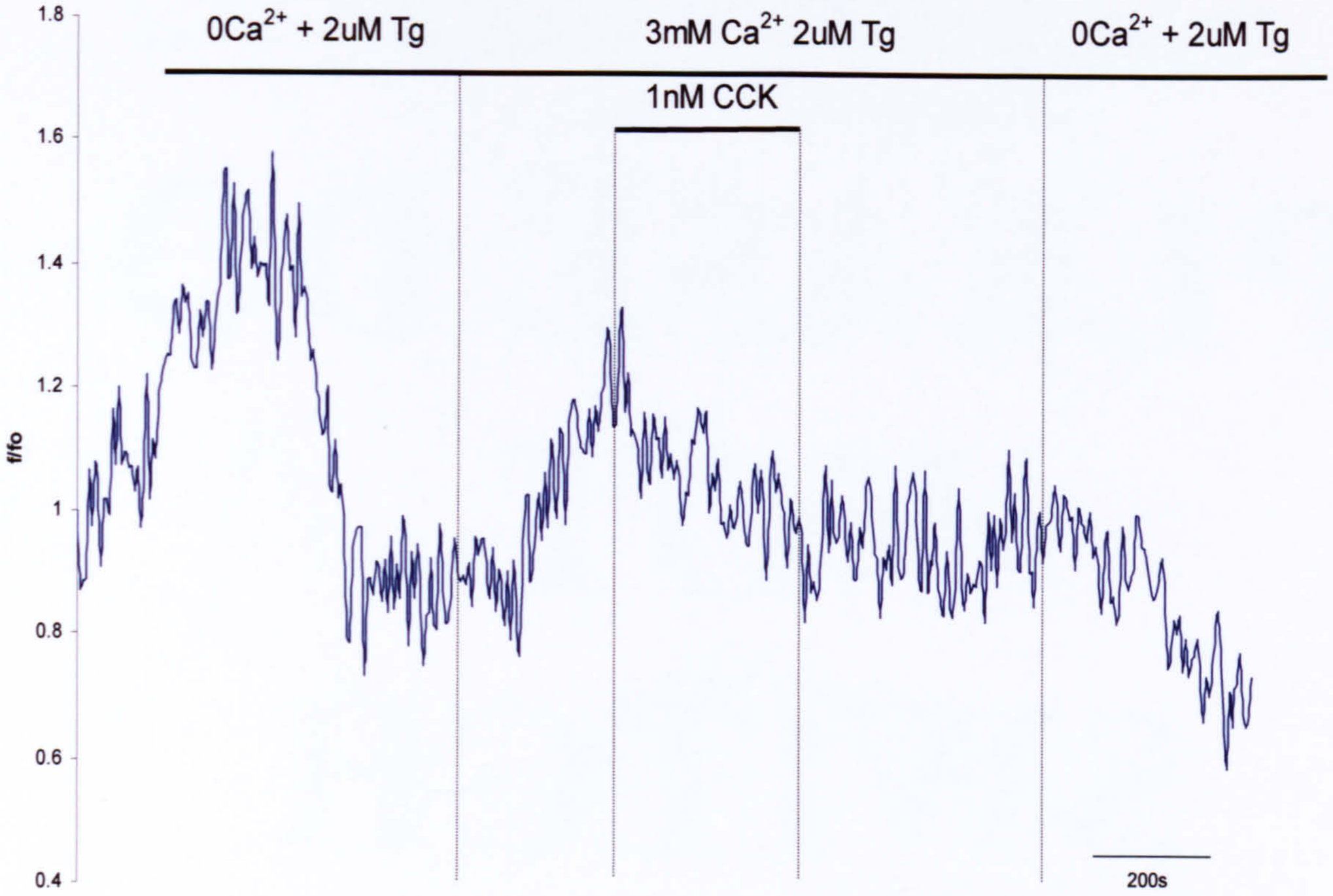

Figure 3.4 **The effect of a secretagogue on mitochondrial NADH levels** Measurements of NADH autofluorescence from a whole cell that has been treated with thapsigargin in zero external calcium. 3mM of external calcium was reintroduced at the moment shown on the upper bar to create a cytosolic calcium plateau after that 1nM CCK was applied for ~300s, then agonist was removed and finally external calcium was removed. The autofluorescence measurements were normalised to the value of autofluorescence recorded at the beginning of the experiment (f_0).

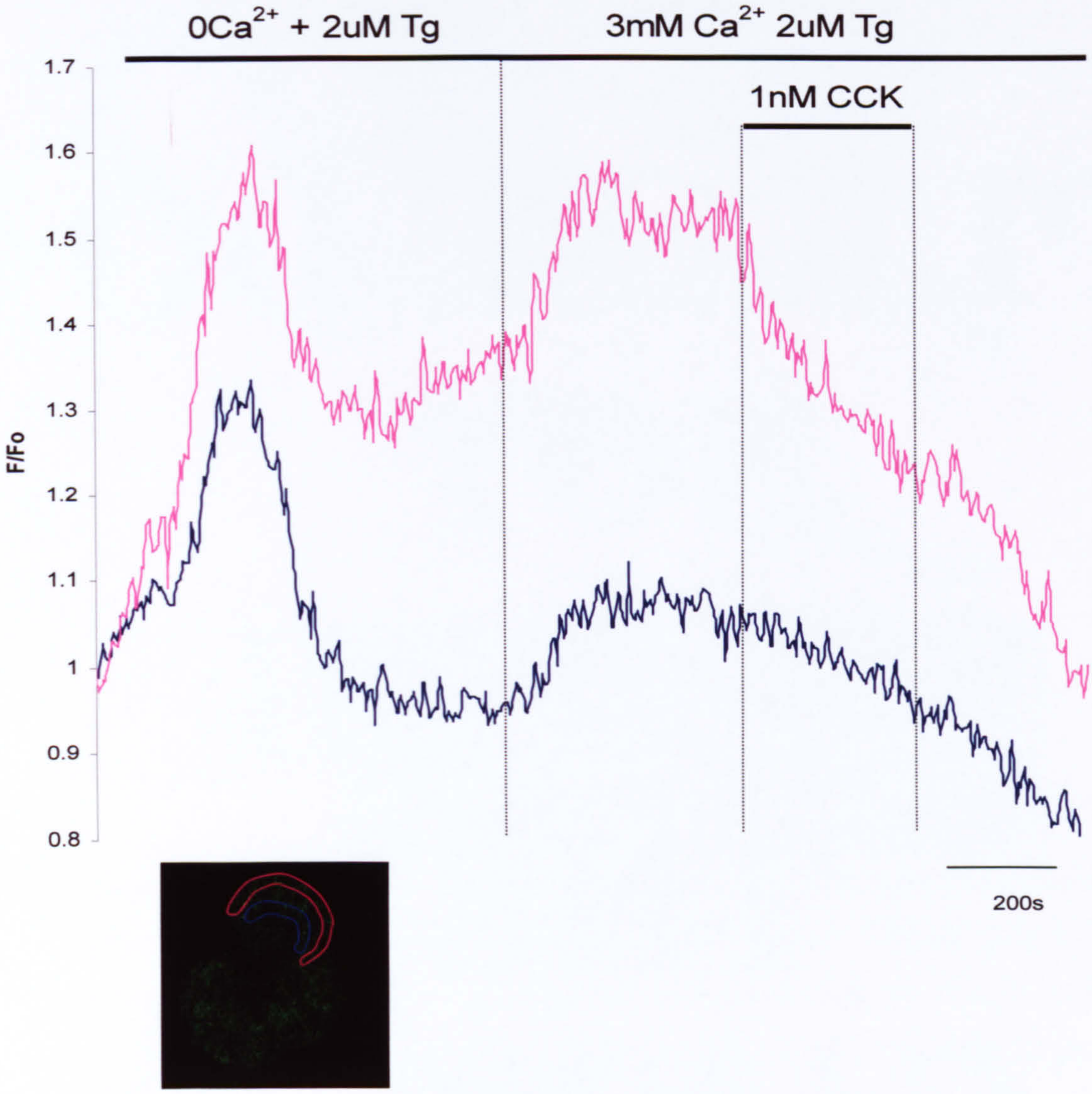

Figure 3.5 **The effect of a secretagogue on mitochondrial NADH levels** A trace from a single cell that has been treated with thapsigargin in zero external calcium, 3mM external calcium was reintroduced at the moment shown on the upper bar to form a cytosolic calcium plateau. This was followed by application of 1nM CCK for ~300s, then agonist was removed. Measurements of NADH autofluorescence from the peripheral (pink line) from the belt region (blue line) were made from the same cell. The autofluorescence measurements were normalised to F_0 value. Image below shows the NADH fluorescence with the ROI indicated in the corresponding colour.

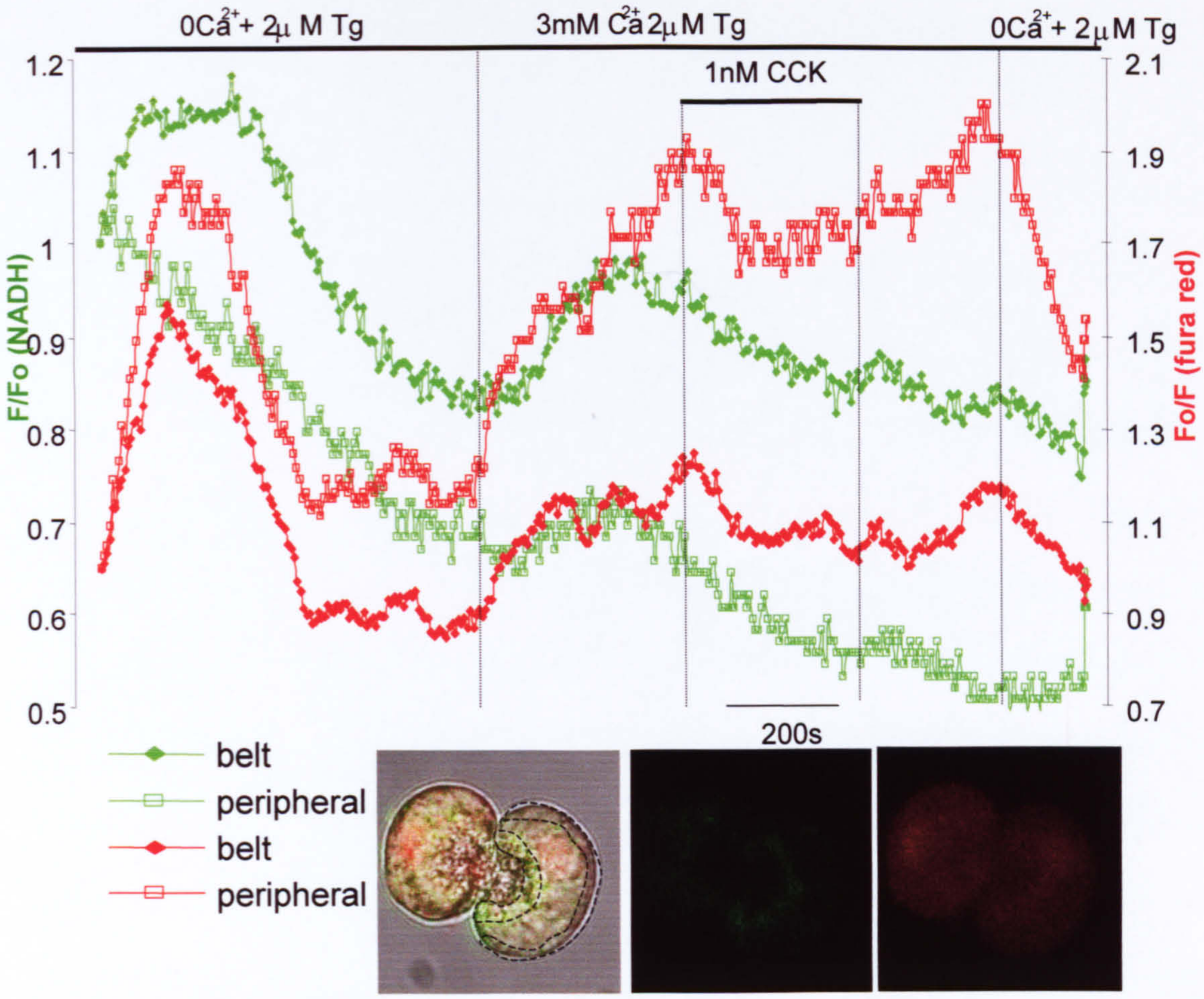

Figure 3.6 **The effect of a secretagogue on the thapsigargin-induced cytosolic calcium plateau and the mitochondrial NADH levels – simultaneous measurements of calcium and NADH** A trace from a single fura red loaded cell that have been treated with thapsigargin in zero external calcium, 3mM external calcium was reintroduced at the time shown on the upper bar and a cytosolic calcium plateau built. 1nM CCK was applied on the cytosolic calcium plateau for 300s then agonist was then removed followed by the removal of external calcium. Measurements of Fura red (red lines) from the belt region (closed diamonds) and the peripheral region (open squares) and NADH autofluorescence (green lines) from the belt (closed diamonds) and peripheral region (open squares) were made. The autofluorescence measurements were normalised to F_0 value and the fura red measurements were also normalised to the value for fluorescence measured in the beginning of the experiment and inverted (fura red fluorescence decreases upon binding calcium). The images below show the transmitted light (ROI marked), NADH (central image) and fura red fluorescence (right image).

Effect of membrane holding potential on the calcium plateau level

Figure 3.7 demonstrates the effect of changing the membrane potential on the level of calcium plateau under patch clamp conditions, which allows the membrane potential to be artificially controlled. The cells have been treated with thapsigargin in zero external calcium, and then 3mM calcium applied externally. Changing the membrane holding potential changes the level of the calcium plateau. The pink arrows at the bottom of the trace indicate the point at which the holding potential has been changed. Changing to 0mV from –30mV (1st pink arrow) lowers the level of the calcium plateau (blue trace represents calcium levels (fluo-4 fluorescence) and the red trace current measured at –30mV). Changing from –30mV to –60mV (3rd pink arrow) increases the calcium plateau level. This occurs because of a change in the driving force for the entry of calcium into the cell. The more negative holding potential results in increased calcium entry, and the more positive holding potential produces decreased calcium entry.

The application of 1nM CCK (supramaximal concentration with a robust response on the calcium plateau) where the membrane potential was held at –30mV was performed to confirm that the reduction in calcium plateau level occurred under voltage clamp conditions (n=5/5). Figure 3.8 shows the result of this experiment when 1nM CCK is applied there is a decrease in the calcium plateau level and upon removal of the agonist the plateau level recovers to pre-stimulation level.

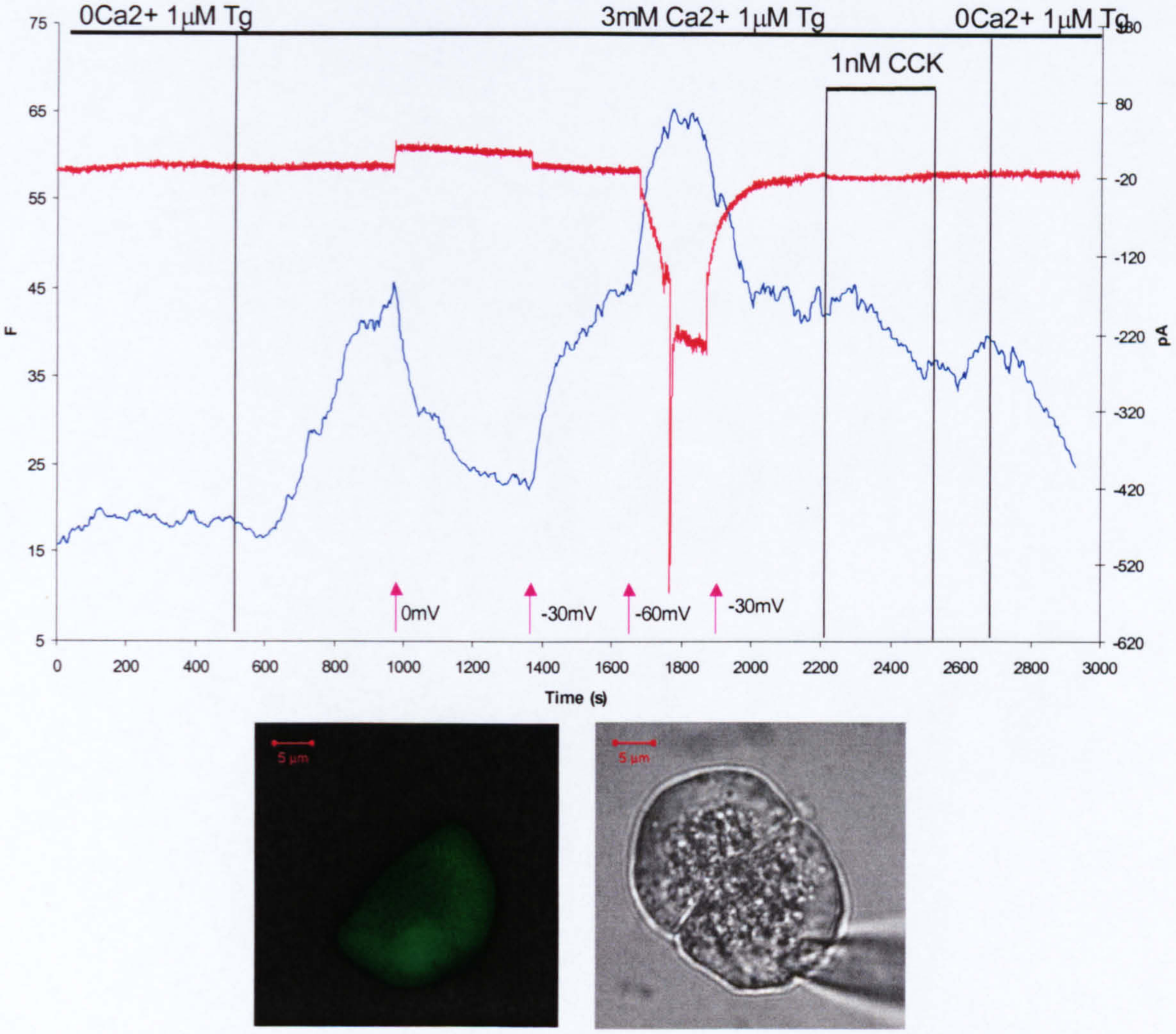

Figure 3.7 **Changes in membrane holding potential alter the level of calcium plateau**. Cells were loaded with fluo-4 via the patch pipette. Fluorescence and transmitted light pictures shown below (scale bar 5μm). The blue trace represents the measurements of calcium changes from fluo-4 and red trace shows the current measurements. The cells have been treated with thapsigargin followed by application of high external calcium (3mM). The changes in membrane holding potential are indicated by the pink arrows at the bottom of the graph, the initial holding potential is –30mV. This followed by application of 1nM CCK on the cytosolic calcium plateau.

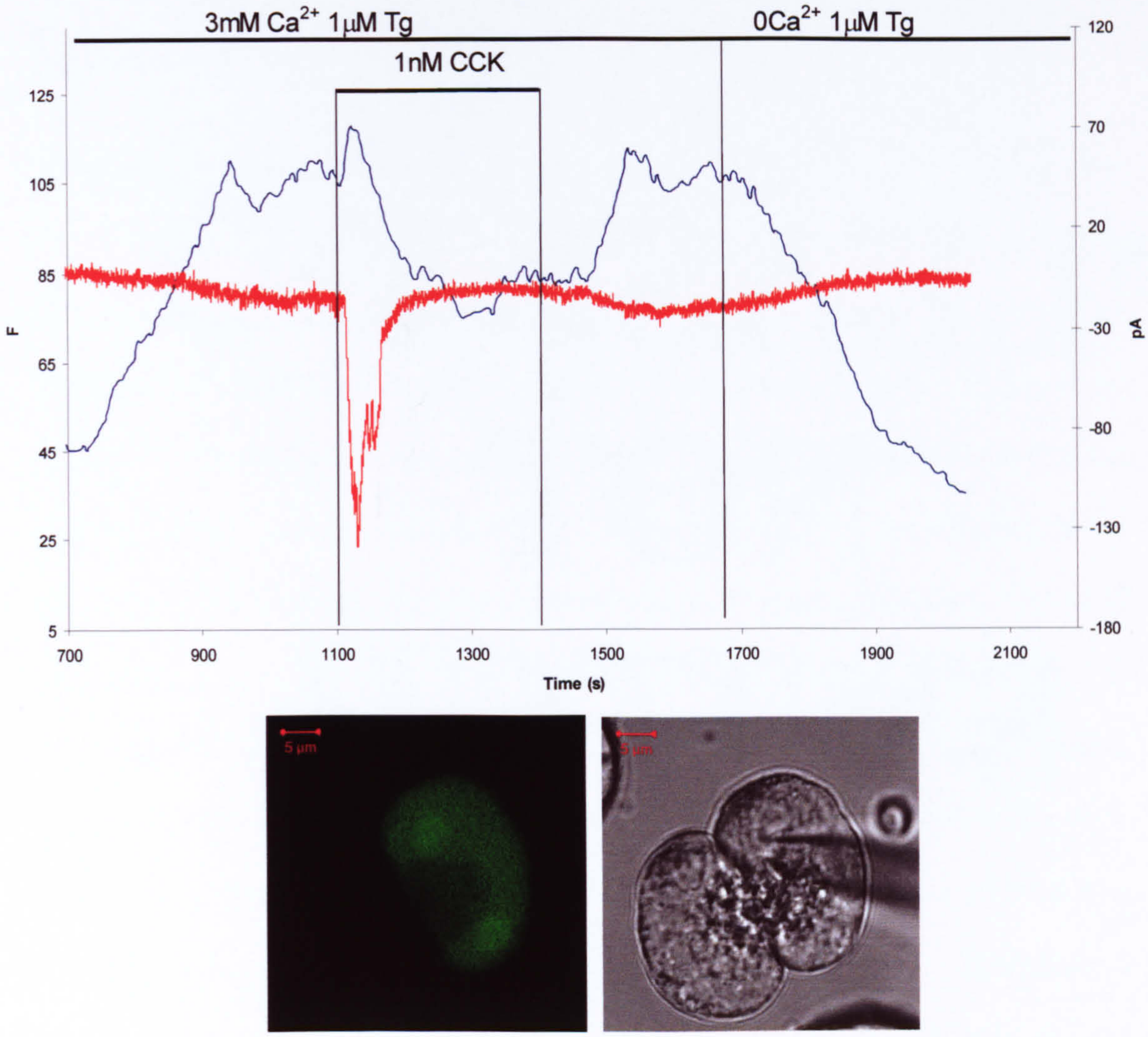

Figure 3.8 **Agonist-induced reduction of the calcium plateau under patch clamp conditions**. Cells were loaded with fluo-4 via the patch pipette. The cells have been treated with thapsigargin followed by application of high external calcium (3mM) to create a cytosolic calcium plateau. 1nM CCK was applied for ~200s as indicated on the graph. The blue trace represents the measurements of calcium changes from fluo-4 and red trace shows the current measurements made at –30mV (the holding potential used in this experiment). Fluorescence(left) and transmitted light (right) pictures shown below (scale bar 5μm).

The effect of CCK on a calcium plateau formed by uncaging of caged calcium within the cell

Thapsigargin treatment and re-admittance of high calcium externally builds a plateau that is a balance of two processes, calcium influx and calcium efflux. Experiments to elucidate whether the effect of the secretagogues was an effect on extrusion or an inhibition of calcium influx were performed using caged calcium. Uncaging of calcium within the cell in zero external calcium created a plateau by a mechanism that was independent of calcium influx. The experiments were performed under patch clamp conditions to allow an unlimited supply of caged compound. Inhibition of the SERCA pumps with thapsigargin was performed in order to deplete the internal stores. Whole cell calcium uncaging was used to create the calcium plateau in zero external calcium. Figure 3.9 shows an experiment performed under these conditions, the pink dotted line at the bottom of the trace indicates the period where the uncaging was performed at regular intervals to create the plateau. The blue trace represents the calcium measured by fluo-4 fluorescence and the red trace currents measured at –30mV. The application of 1nM CCK on the of the uncaged calcium plateau, resulted in a decrease in the plateau level (n=8/9).

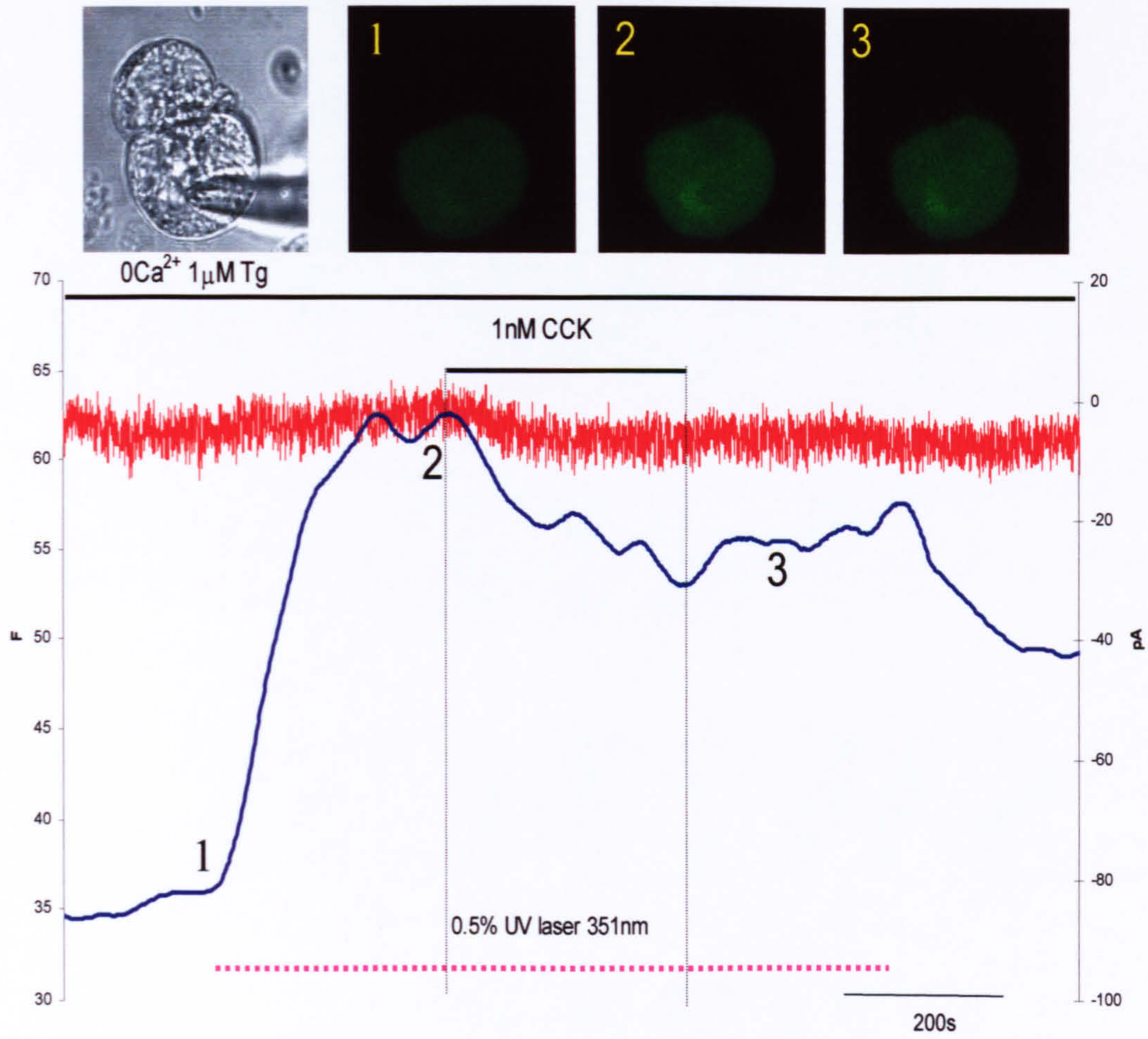

Figure 3.9 **CCK application on a plateau created by uncaged calcium in a cell placed in zero external calcium** An example of a doublet of cells where one cell is in whole cell patch clamp configuration. The calcium sensitive dye and caged calcium (NP-EGTA) have been loaded into the cell via the patch pipette. The pink dotted line indicates the period of time when the cell was exposed to UV laser light (0.5% of the maximal laser power) has been applied for calcium uncaging. This results in the formation of a cytosolic calcium plateau in zero external calcium (blue trace fluo-4 trace) (the cell has previously been treated with 1μM thapsigargin for a minimum of 600s) . The numbers on the trace refer to the numbered images (above) of the cell fluorescence recorded at the corresponding points during the experiment. The red line corresponds to the current measurements (right axis pA) made at –30mV. 1nM CCK is applied on the plateau formed by calcium uncaging.

Identification of the Extrusion Mechanism Involved

There are two prospective mechanisms of extrusion in these cells, the plasma membrane pumps (PMCA) and the sodium/calcium exchanger (Na^{2+}/Ca^{2+}). The replacement of sodium in all external solutions with NMDG, a molecule that carries an equal charge but is unable to go through the Na^{2+}/Ca^{2+} exchanger was performed. The activation of calcium extrusion by 1μM ACh (figure 3.10a)(n=18/18) and 1nM CCK (figure 3.10b)(n=10/12) was unaffected by the replacement of sodium with NMDG.

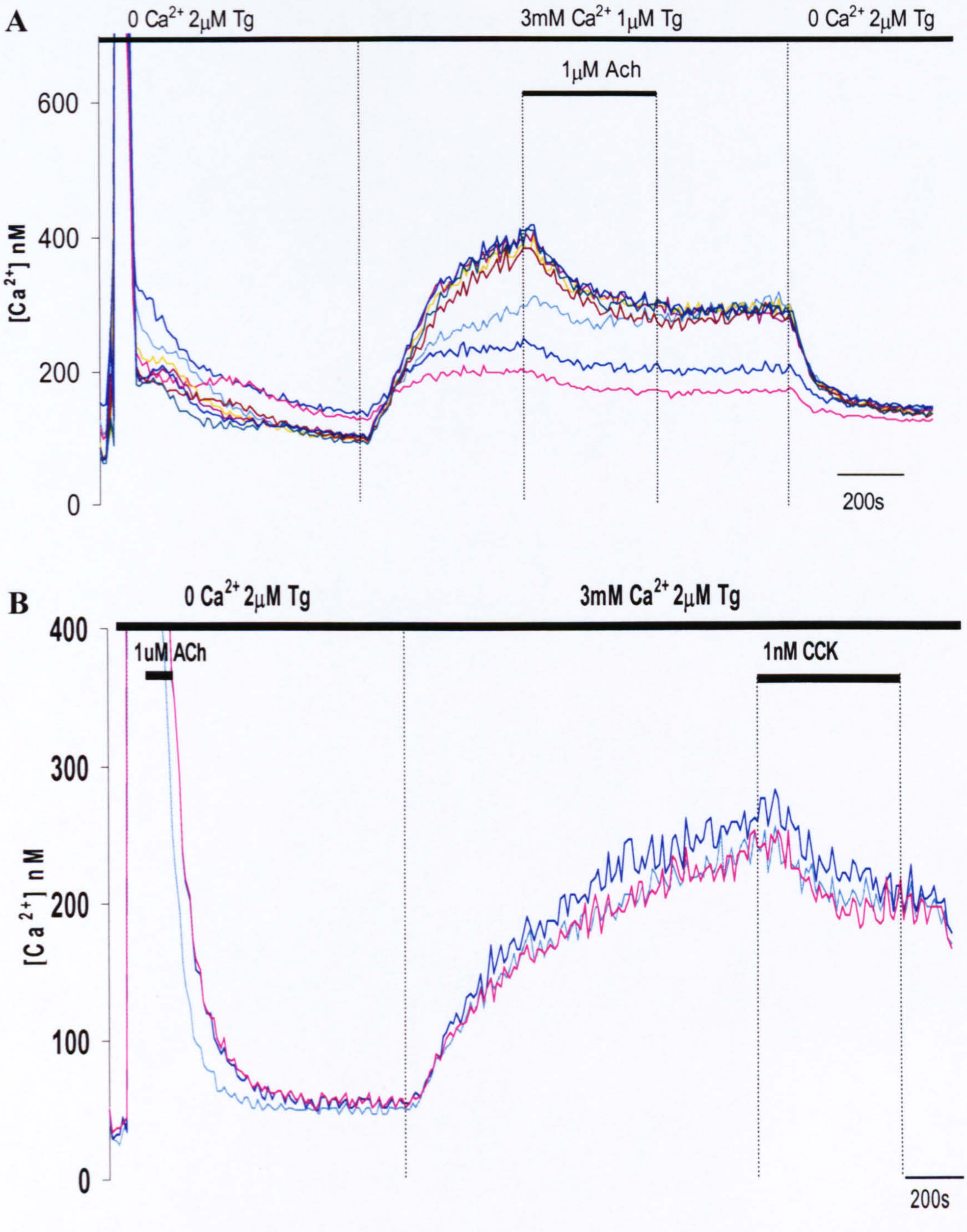

Figure 3.10 **Effects of agonists in Na^+ free conditions** $NMDG^+$ was substituted for Na^+ in all external solutions. The fura-2 loaded cells have then been treated with 1μM Thapsigargin in zero calcium, 3mM external calcium was then applied and 1μM ACh (A) or 1nM CCK (B) applied on the cytosolic calcium plateau. Each line represents an individual cell.

Investigation of the IP_3 Dependency of the Secretagogue Mediated Effect on Calcium Extrusion

The decrease in the calcium plateau level is stimulated by secretagogues ACh and CCK, both of which produce IP_3 as a messenger (Streb *et al.*, 1985;Powers *et al.*, 1985). In order to investigate if IP_3 alone can activate this extrusion cells were loaded via the patch pipette with caged IP_3. Initial experiments were done to establish the efficacy of the uncaging conditions and the functionality of the caged molecule at high calcium concentrations that are present under these conditions. These experiments were performed where the internal calcium stores were intact. Figure 3.11a shows a cell that has been loaded with caged IP_3 and then high external calcium applied without thapsigargin treatment. The pink dotted line at the bottom of the trace indicates the period of uncaging. There is a small increase of calcium level (blue trace) on application of high external calcium, uncaging of IP_3 results in calcium transients (blue trace) and triggered Ca^{2+}-activated currents (red trace). This confirms the functionality of the uncaged molecule and suitability of the uncaging conditions.

The uncaging of IP_3, under identical loading and uncaging conditions (as control experiment discussed above), on a calcium plateau created by the application of high external calcium after depletion of the internal stores, does not result in a decrease in the calcium plateau level, figure 3.11b (n=16). The non-involvement of IP_3 and its receptor in the activation of calcium extrusion by agonists was confirmed by the use of the IP_3 receptor antagonist in mouse pancreatic acinar cells, caffeine (Toescu *et al.*, 1992). The application of caffeine necessitates the use of fura red as a calcium

indicator, which is less sensitive to the quenching effects of caffeine which prevents the utilisation of other fluorescent dyes. The same protocol as previously described was performed; caffeine was applied on the plateau before the application of agonist. There was a small decrease in the plateau level upon caffeine application and there was no inhibition of the calcium plateau reduction in response to agonist 1μM Ach, figure 3.12 (n=12).

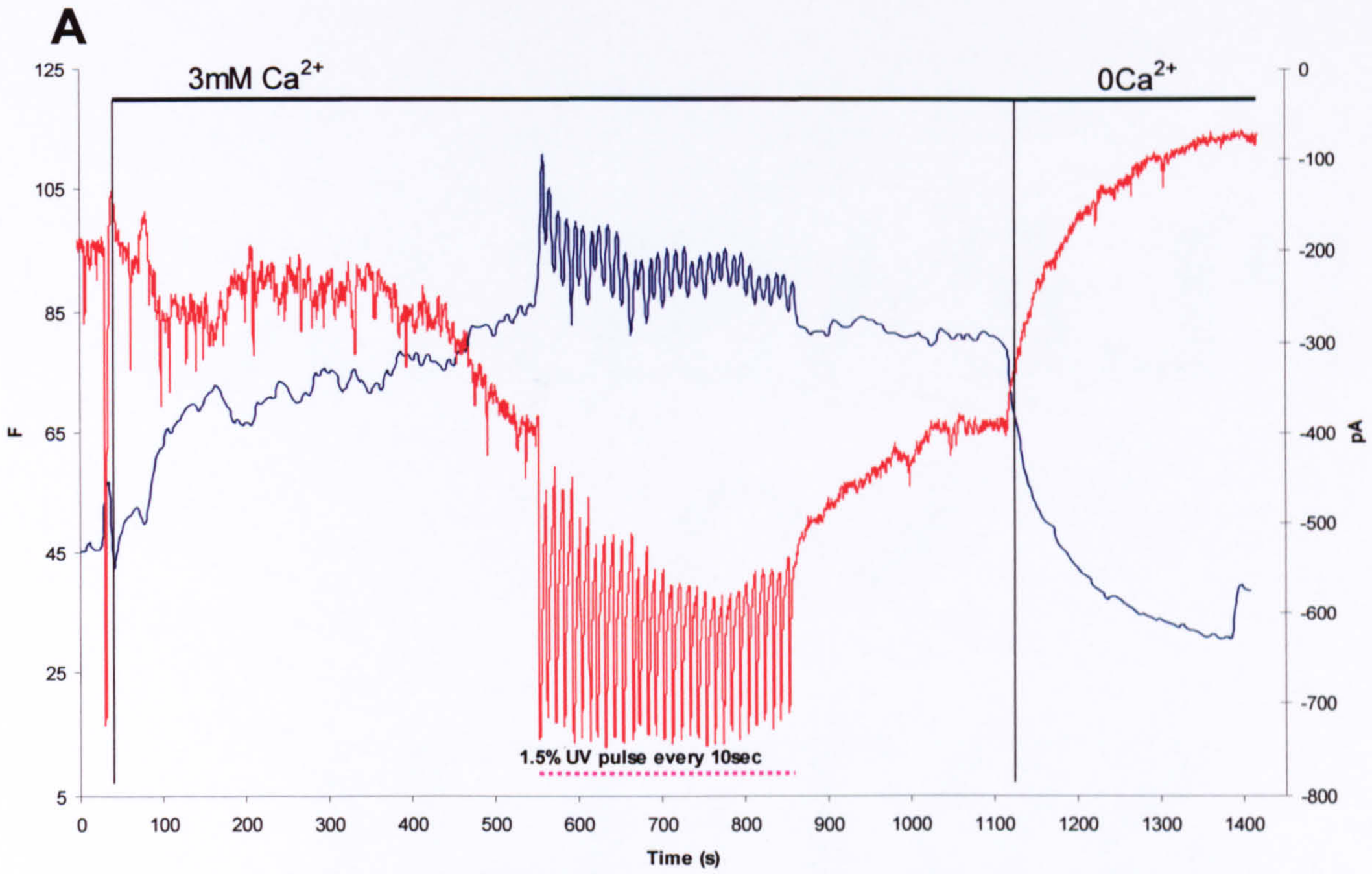

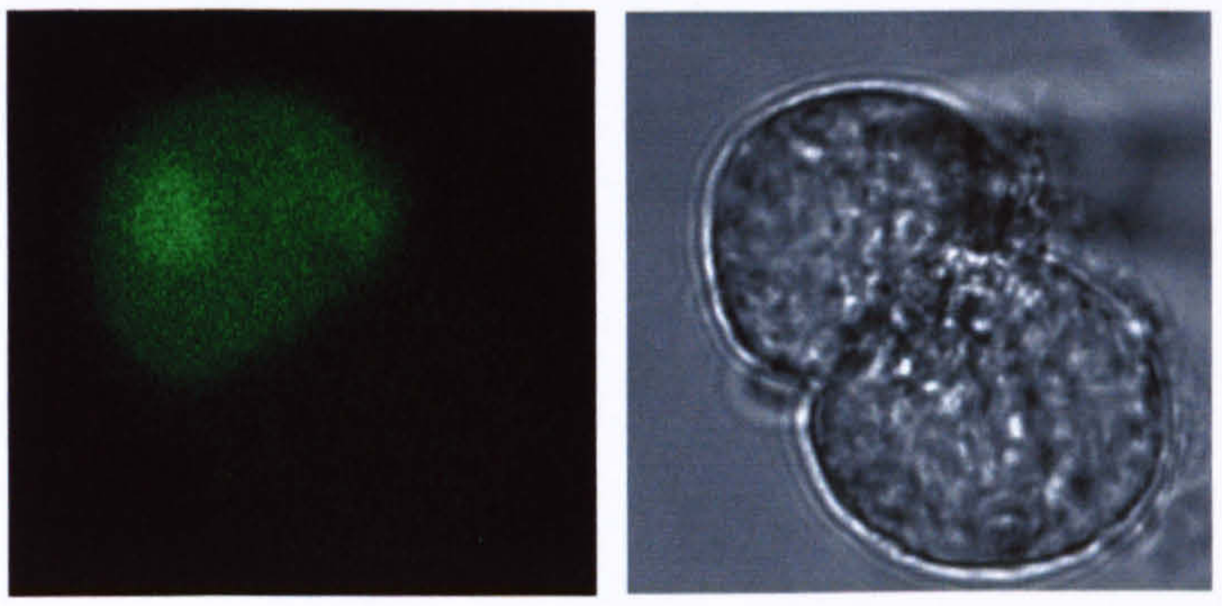

Figure 3.11 **Uncaging of IP_3 in control conditions and after formation of thapsigargin-induced cytosolic calcium platea** . Cells were loaded with fluo-4 and caged IP_3 via the patch pipette. The blue trace represents the measurements of calcium changes from fluo-4 and red trace shows the current measurements made at –30mV the holding potential used. Fluorescence (left) and transmitted light (right) pictures shown below. **(A)** A control experiment to verify the suitability of the uncaging conditions . The cells were exposed to high external calcium (3mM) the uncaging of IP_3 is indicated by the pink dotted line. Part **B** of this figure is shown on the next page.

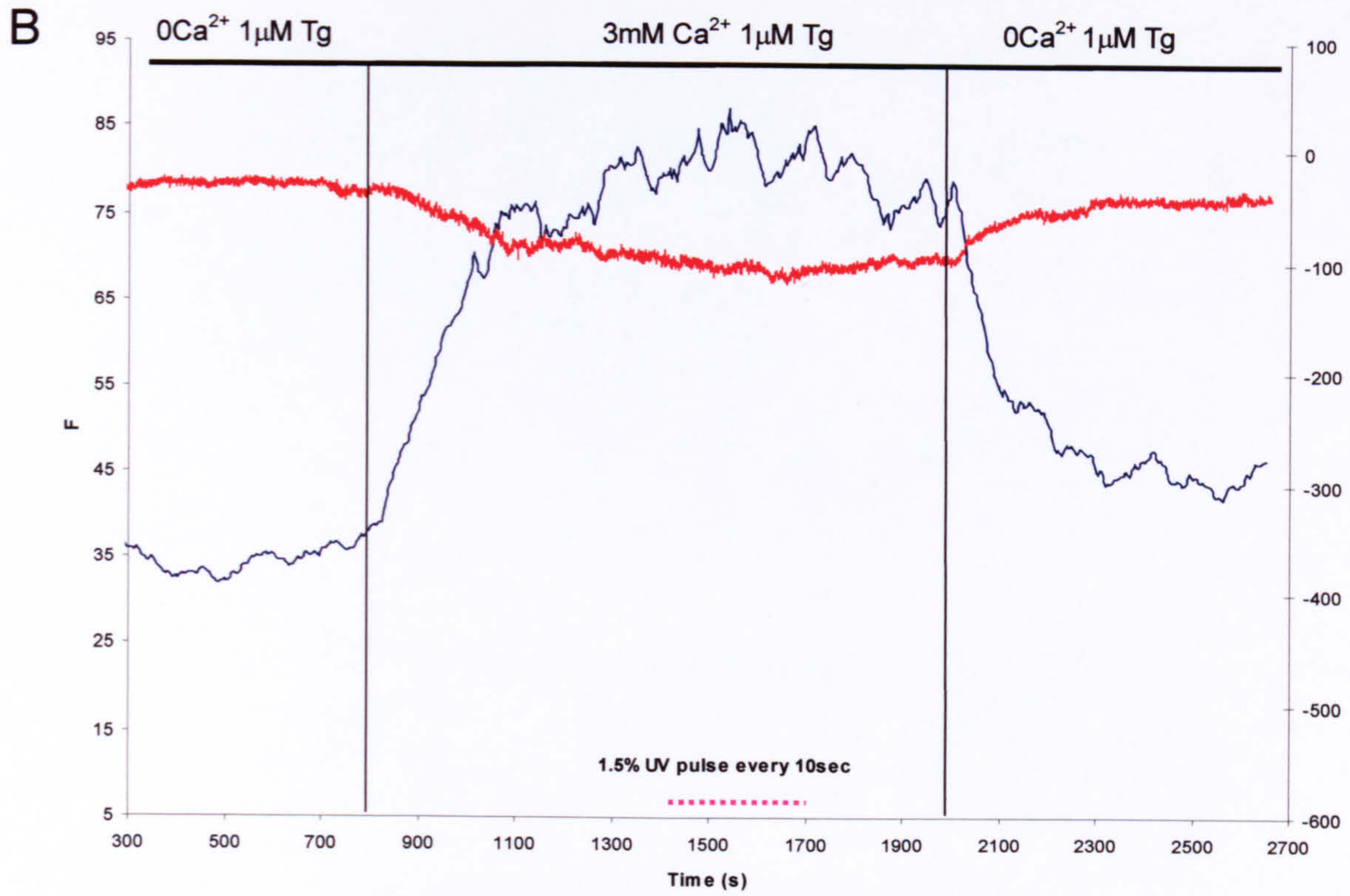

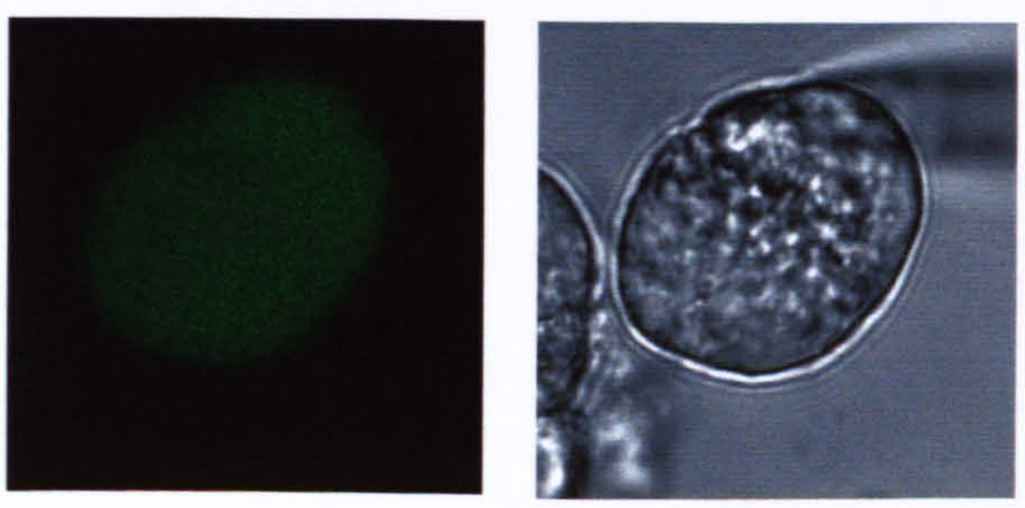

(B) The cells were treated with thapsigargin to deplete the stores followed by application of high external calcium (3mM) to create a cytosolic calcium plateau. the pink dotted line indicates the period where uncaging of IP_3 was performed.

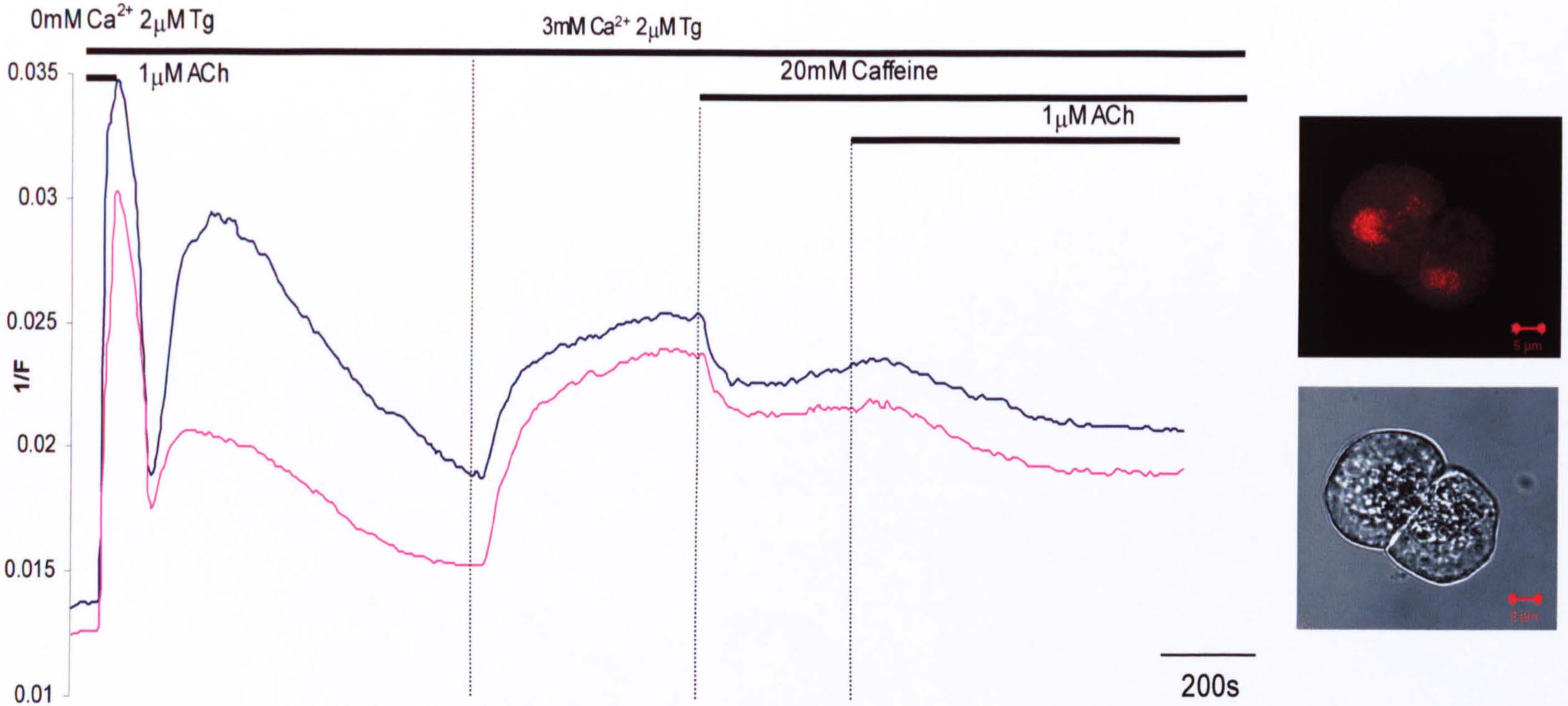

Figure 3.12 **The Effect of 1μM ACh on the thapsigargin-induced cytosolic plateau in the presence of an IP_3R antagonist** An example of a cell doublet of fura red loaded cells (fluorescent and transmitted light pictures on the right, scale bar corresponds to 5μm), thapsigargin depletion followed by formation of cytosolic calcium plateau by application of high external calcium (3mM). Application of caffeine (20mM) on the plateau resulted in a small decrease of fluorescence. Finally 1μM ACh was applied in the continued presence of caffeine. Dark blue line corresponds to measurements from the top cell and the pink line the bottom cell. fura red measurements were inverted (fura red fluorescence decreases upon calcium binding).

Effects of Classical Regulators of PMCA on Calcium Plateau Levels and on Secretagogue-Induced Plateau Reduction

PMCA are reported to be regulated by Protein Kinase C (PKC) (Carafoli, 1994). Investigation of the role PKC may play in the observed activation of PMCA mediated calcium extrusion used a PKC activator, phorbol-12-myristate-13-acetate (PMA) and a diacylglycerol (DAG) analogue DC_{10}. Application of PMA at 1μM on the calcium plateau caused an increase in calcium level in 50% of cells (n=4) and, increasing the concentration to 3μM induced an increase in the calcium plateau in 100% of cells (n=4), figure 3.13. Application of DC_{10} a DAG analogue had no effect on the calcium plateau when applied at two different concentrations (5 and 10μg/ml), subsequent ACh application demonstrated the decrease in plateau level as shown in figure 3.14 (n=19 total, n=10 @5μg/ml and n=9 @10μg/ml).

PMCA are also reported to be regulated by calmodulin (reviewed by (Carafoli, 1994;Monteith *et al.*, 1998)), investigation of the potential role of calmodulin in the agonist-stimulated extrusion utilised the inhibitor Calmidazolium chloride. The application of the calmodulin inhibitor on the plateau at two different concentrations (25μM and 50μM) had no effect on the plateau level, subsequent application of 1μM ACh produced the reduction in plateau level (n=8/9 @ 25μM and 26/27 @ 50μM figure 3.15.

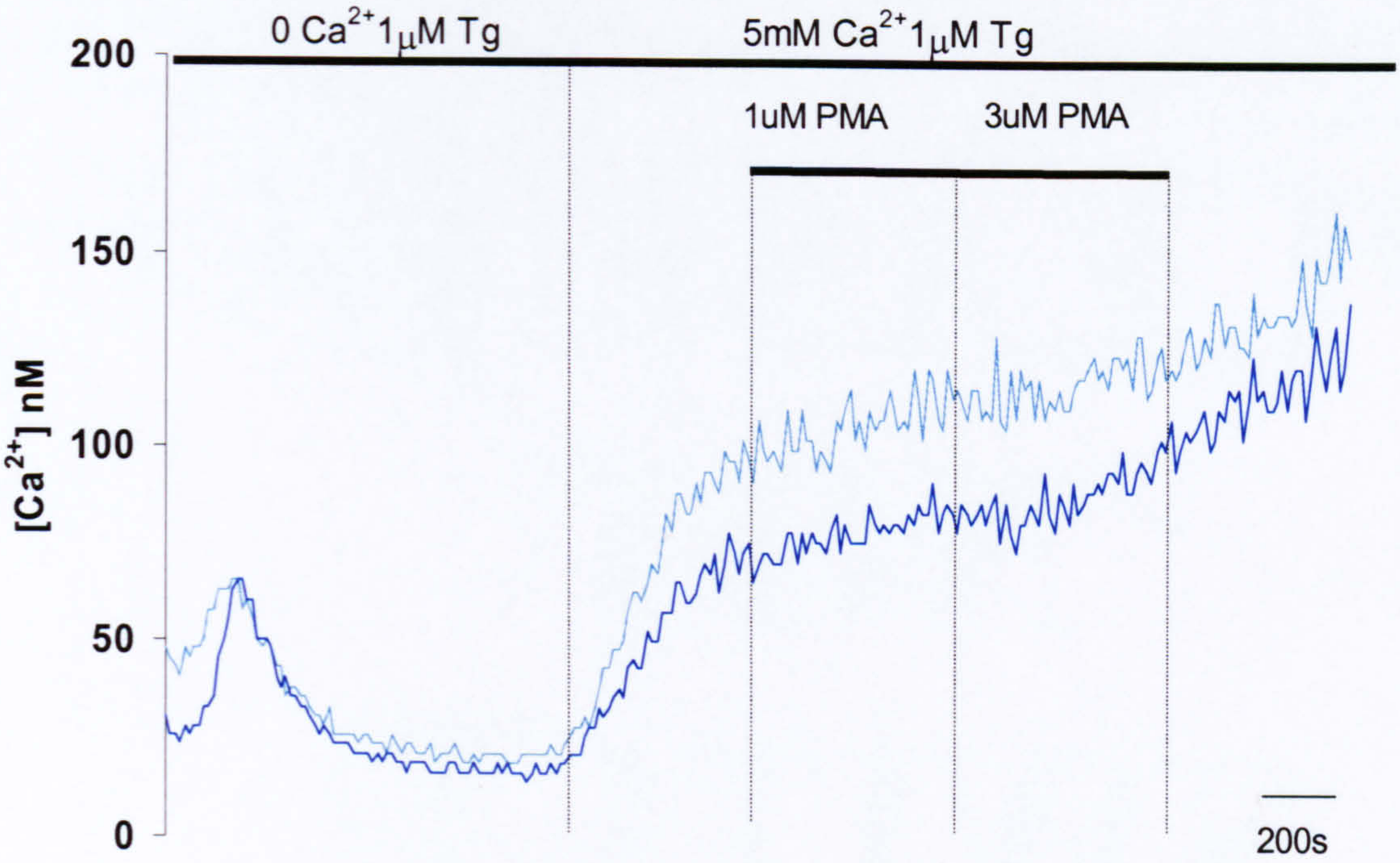

Figure 3.13 **The effect of PMA on the thapsigargin-induced cytosolic calcium plateau** Fura-2 loaded cells were used in this experiment. The periods of application of the substances are shown by bars in the upper part of the figure. Individual cells are represented by each line.

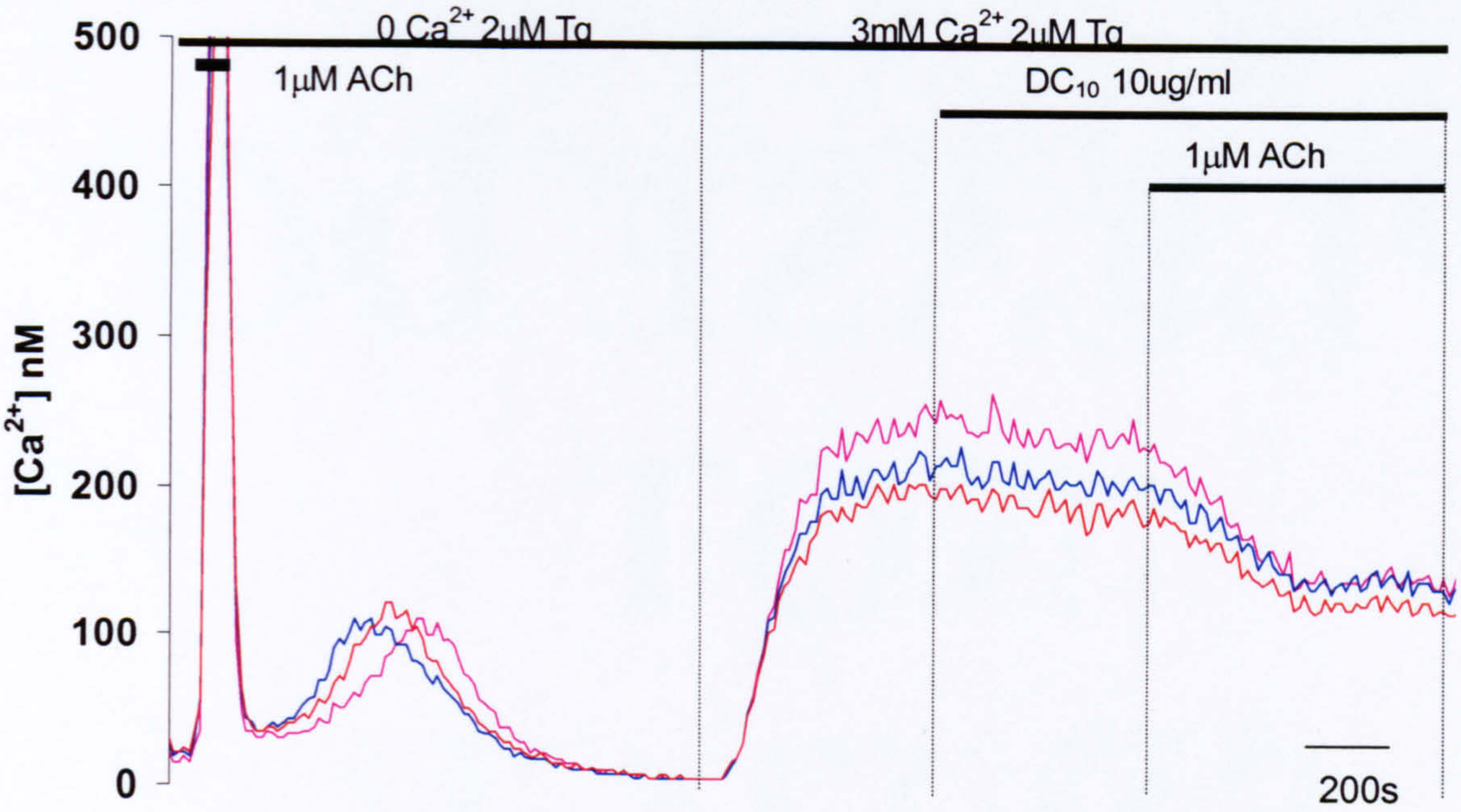

Figure 3.14 **The effect of an analogue of DAG (DC_{10}), on the thapsigargin-induced cytosolic calcium plateau** Fura-2 loaded cells were used in this experiment. The periods of application of the substances are shown by bars in the upper part of the figure. Note that ACh was applied in the continued presence of DC_{10}. Individual cells are represented by each line.

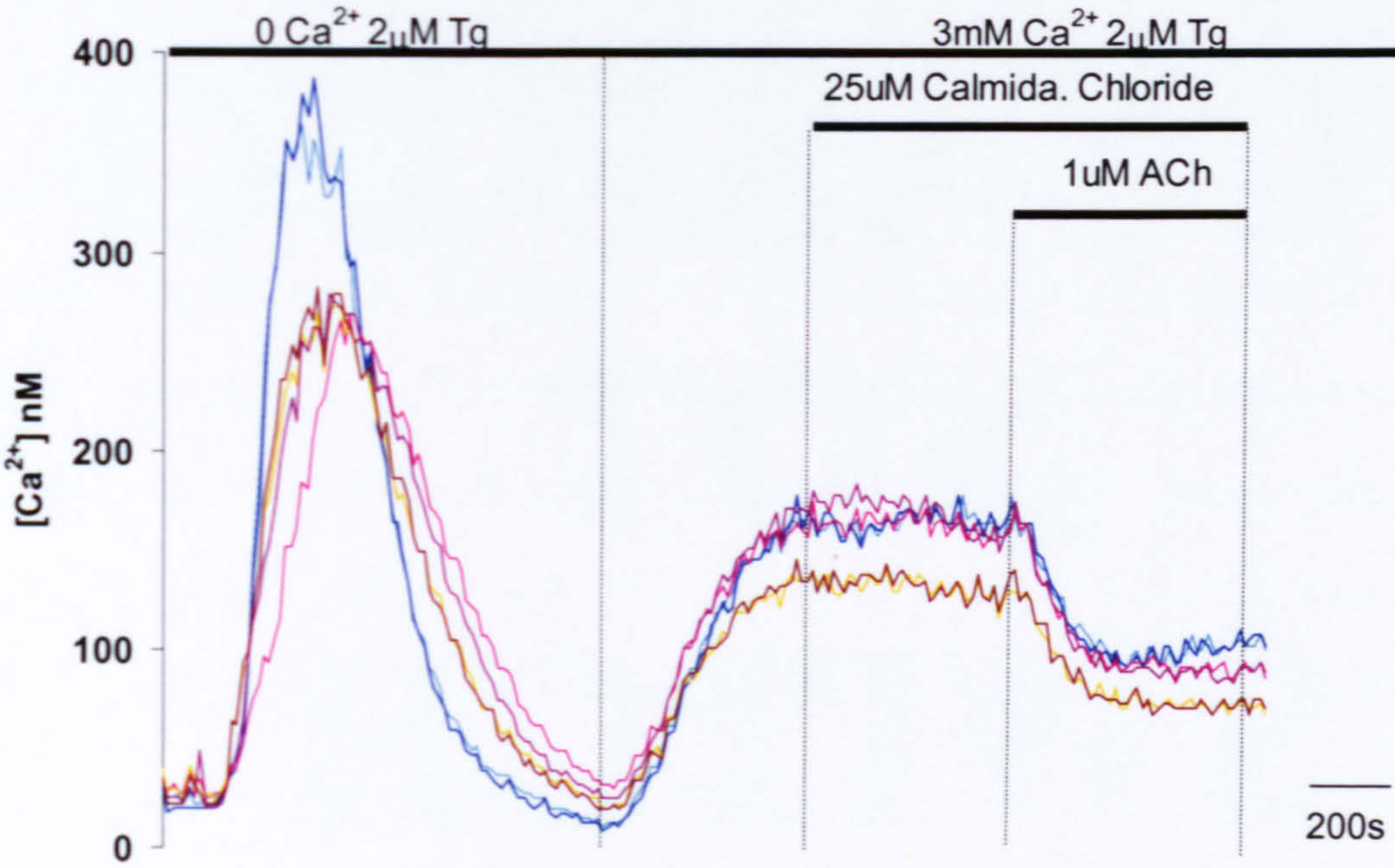

Figure 3.15 **The effect of a calmodulin inhibitor, calmidazolium chloride, on the thapsigargin-induced cytosolic calcium plateau and on ACh-induced plateau reduction** Fura-2 loaded cells were used in this experiment. The periods of application of the substances are shown by bars in the upper part of the figure. Individual cells are represented by each coloured line.

Another cellular messenger that was a potential regulator of the PMCA was cGMP, which has been previously implicated in the regulation of the PMCA activity by activation of the cGMP-dependent protein kinase (Furukawa & Nakamura, 1987). Cell permeant analogues 8-bromo cGMP (1mM) and dibutyryl cGMP (200μM) were used. Application of both analogues on the cytosolic calcium plateau resulted in no change in the plateau level, figures 3.16a (n=12/12) and 3.16b (n=11/12). The following application of 1μM ACh still resulted in the reduction in plateau level and in this example of 8-Bromo-cGMP, recovery to pre-stimulation plateau level after agonist removal (figure 3.16a). The application of 1μM ACh in the continued presence of dibutyryl cGMP also produced the reduction in the plateau linked to activation of calcium extrusion (n=12/12).

Actions of cell permeant analogues of cAMP were also investigated on the calcium plateau. cAMP is known to activate Protein Kinase A (PKA) and may be involved in PMCA activity regulation (Johansson *et al.*, 1992) (James *et al.*, 1989). Figure 3.17a shows the use of 8-bromo-cAMP at two different concentrations 1mM and 200μM. 8-Bromo-cAMP at 1mM in 6/10 showed no effect on the plateau level the other 4 showing a decrease in plateau level. When used at 200μM in 4/5 cells showed no effect on the plateau level, the other 1 cell showed an increase in calcium plateau level. The ensuing application of 1μM ACh after 1mM 8-bromo-cAMP was still able to produce a reduction in the calcium plateau level in 8/10 cells. Figure 3.17b shows dibutyryl cAMP also has no effect on the plateau level (n=8). The application of 1μM ACh in the continued presence of the dibutyryl cAMP displayed the expected reduction in calcium plateau level (n=8).

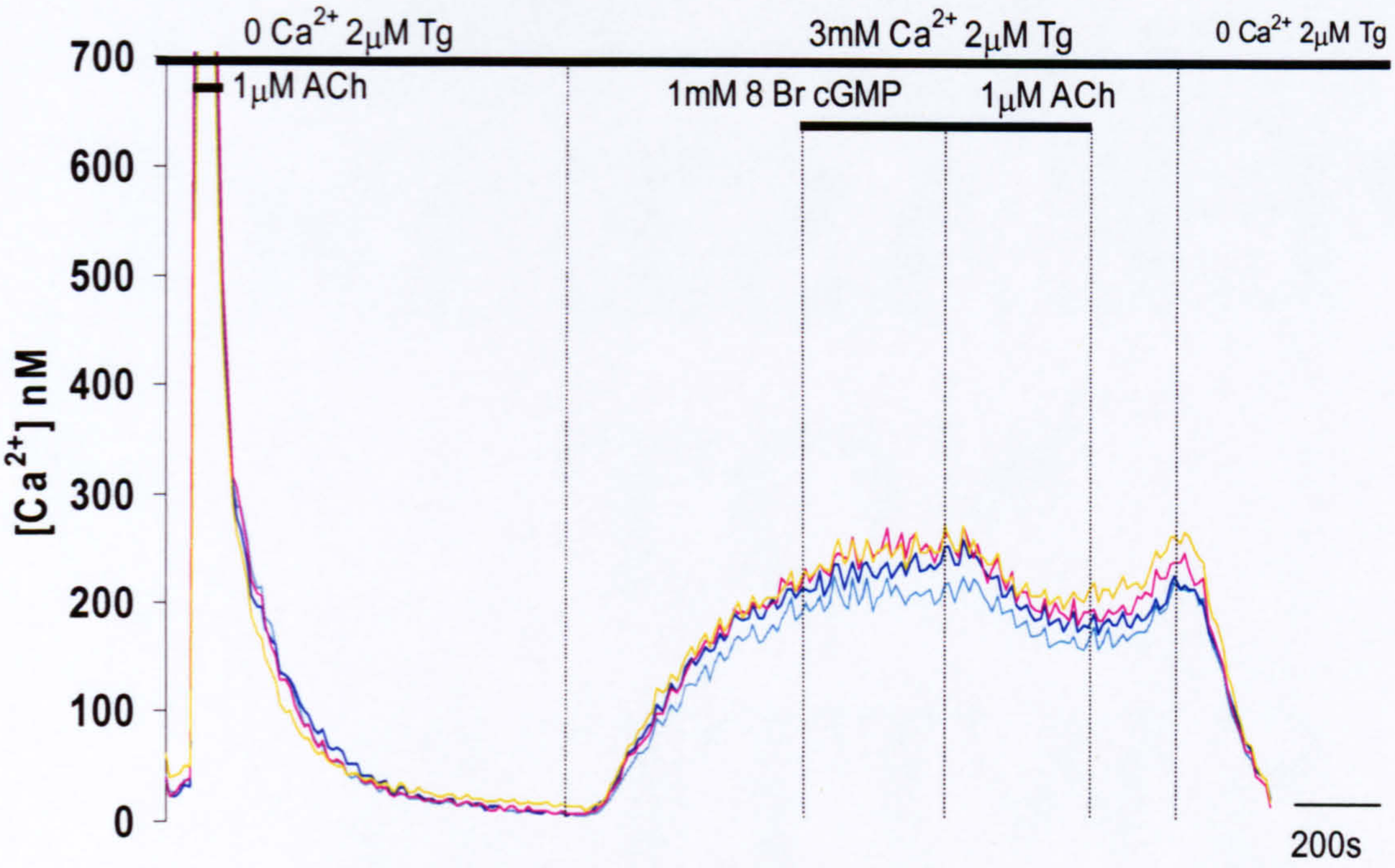

Figure 3.16 **Effect of cGMP on thapsigargin-induced cytosolic calcium plateau and on ACh-induced plateau reduction** Fura-2 loaded cells were used in this experiment. The periods of application of the substances are shown by bars in the upper part of the figure. (**A**) 8-Bromo-cGMP (1mM) was applied after plateau formation and removed before application of 1μM ACh. Part **B** of this figure is shown on the next page. Each line represents an individual cell.

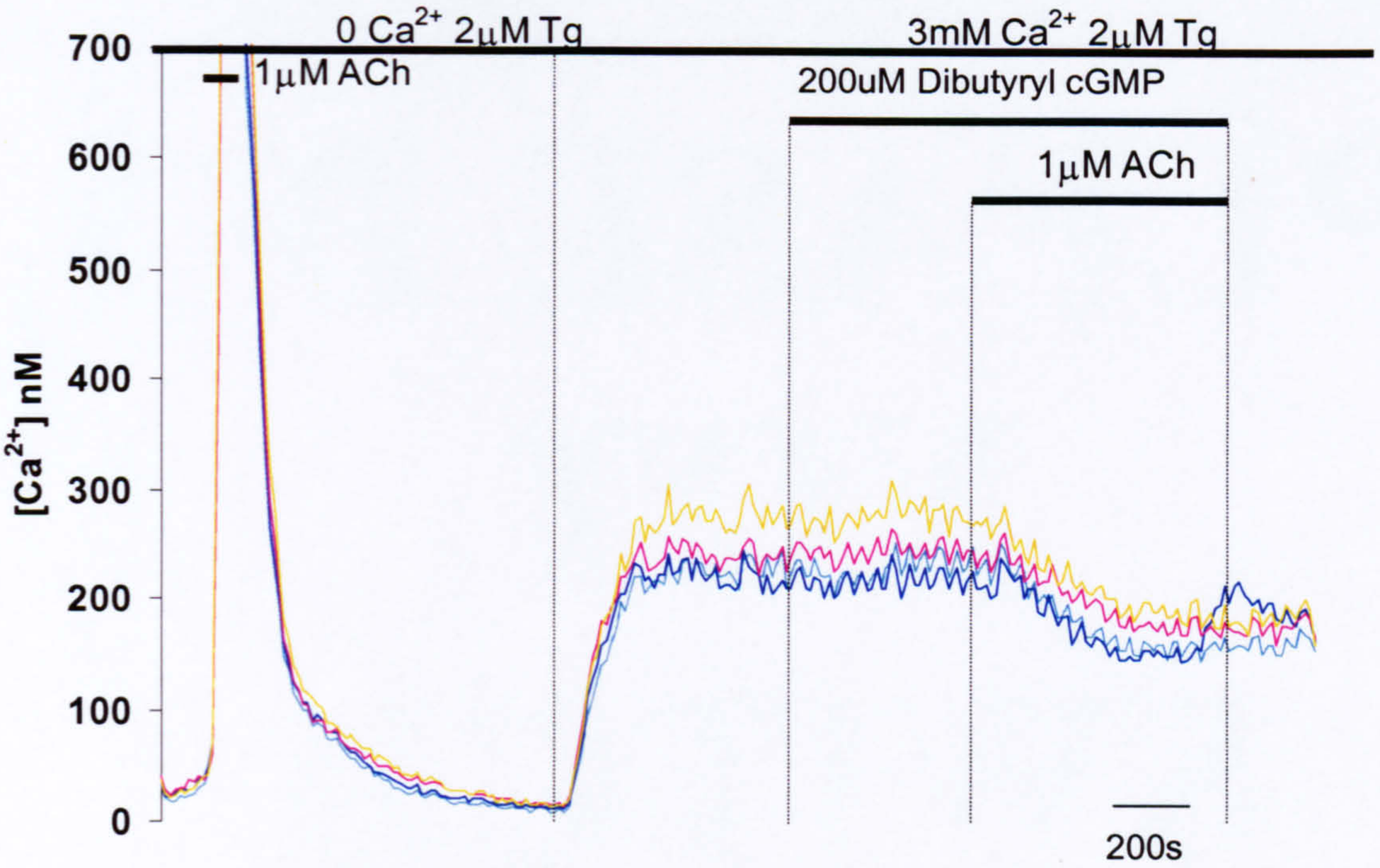

(B) Dibutyryl cGMP (200μM) was applied after the plateau was formed and subsequently, in the continued presence of dibutyryl cGMP, 1μM ACh was applied. Each line represents an individual cell. Part (**A**) of this figure was shown on the previous page.

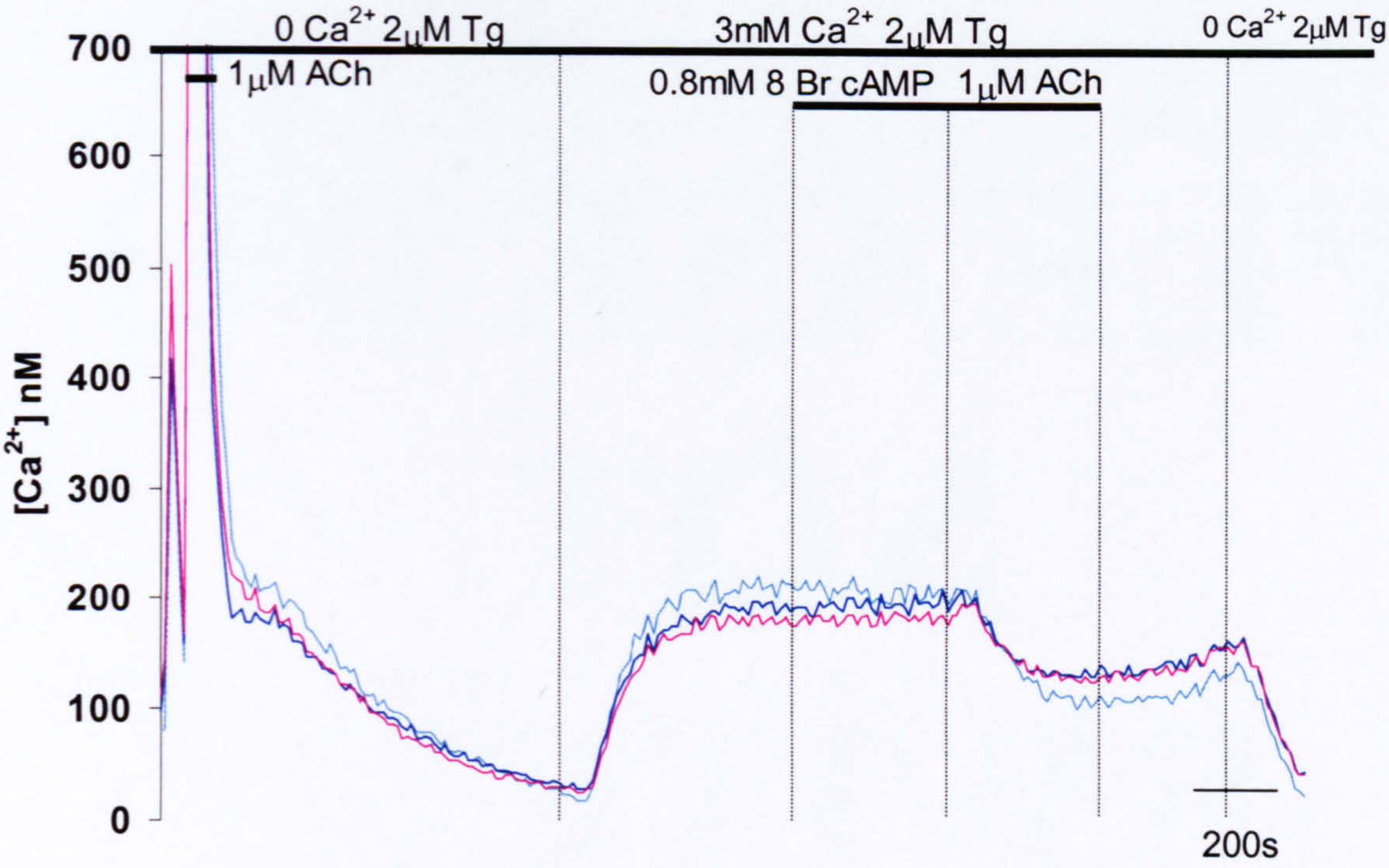

Figure 3.17 **Effects of cAMP on thapsigargin-induced cytosolic calcium plateau and on ACh-induced reduction of the plateau.** Fura-2 loaded cells were used in this experiment. The periods of application of the substances are shown by bars in the upper part of the figure **(A)** 8-Bromo-cAMP (0.8mM) was applied after the plateau was formed. Each line represents an individual cell. Part (**B**) of this figure is shown on the next page.

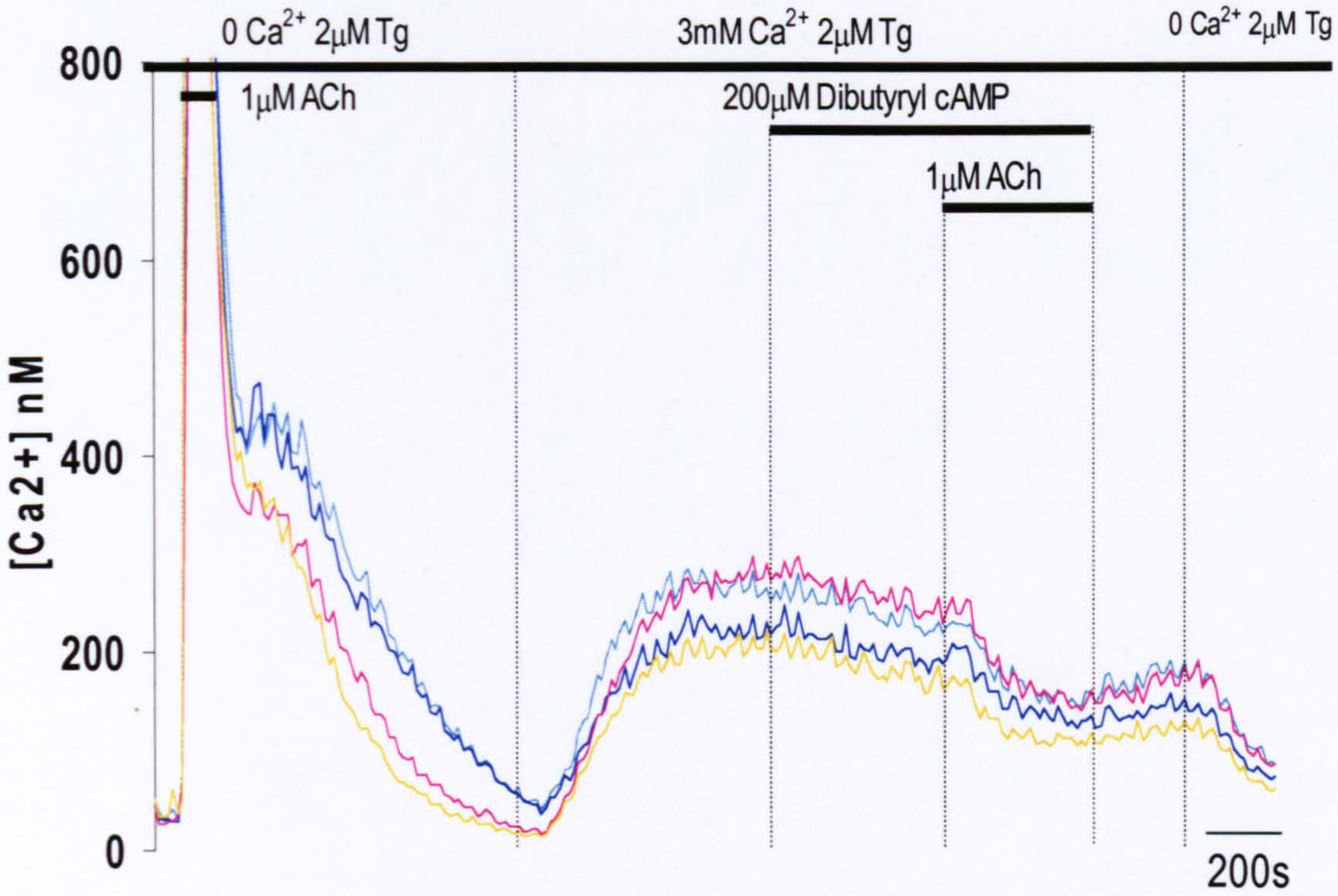

(B) dibutyryl cAMP (200μM) was applied after the cytosolic calcium plateau was formed and subsequent application of 1μM ACh was performed in the continued presence of dibutyryl cAMP. Agonists were then washed and external calcium removed. Each line represents an individual cell. Part (**A**) of this figure was shown on the previous page.

CCK analogue JMV-180 binds to the high affinity site on the CCK_A receptor (Matozaki *et al.*, 1990). This activates the phospholipase A (PLA) pathway (Gonzalez *et al.*, 1999) and PLC pathway (Yule *et al.*, 1999), which results in PKC activation through DAG production and the production of arachidonic acid. As is shown in figure 3.18 application of 1μM JMV 180 after creation of the cytosolic calcium plateau resulted in a reduction of the plateau level (n=23/33). There was a small degree of recovery after removal of the JMV 180 and the following application of 1nM CCK also resulted in a decrease in the plateau level followed by a degree of recovery after removal of the agonist.

$AACOCF_3$ a PLA_2 inhibitor was applied on the plateau, which resulted in a gradual reduction of the plateau level, however subsequent application of 1nM CCK resulted in the characteristic reduction of the calcium plateau at a faster rate than the gradual decline seen with $AACOCF_3$ alone (n=13) as shown in figure 3.19.

Inhibitor of the phospholipase C (PLC) was also used. Both the ACh and the CCK receptor are known to be coupled to this enzyme (Reviewed by (Williams, 2001)). The inhibitor ET-18-$0CH_3$ was applied on the plateau as shown in figure 3.20 and then in the continued presence of the inhibitor 1μM ACh was applied. An increase in the level of the calcium plateau was observed (n=8), the increase begins before application of 1μM ACh begins.

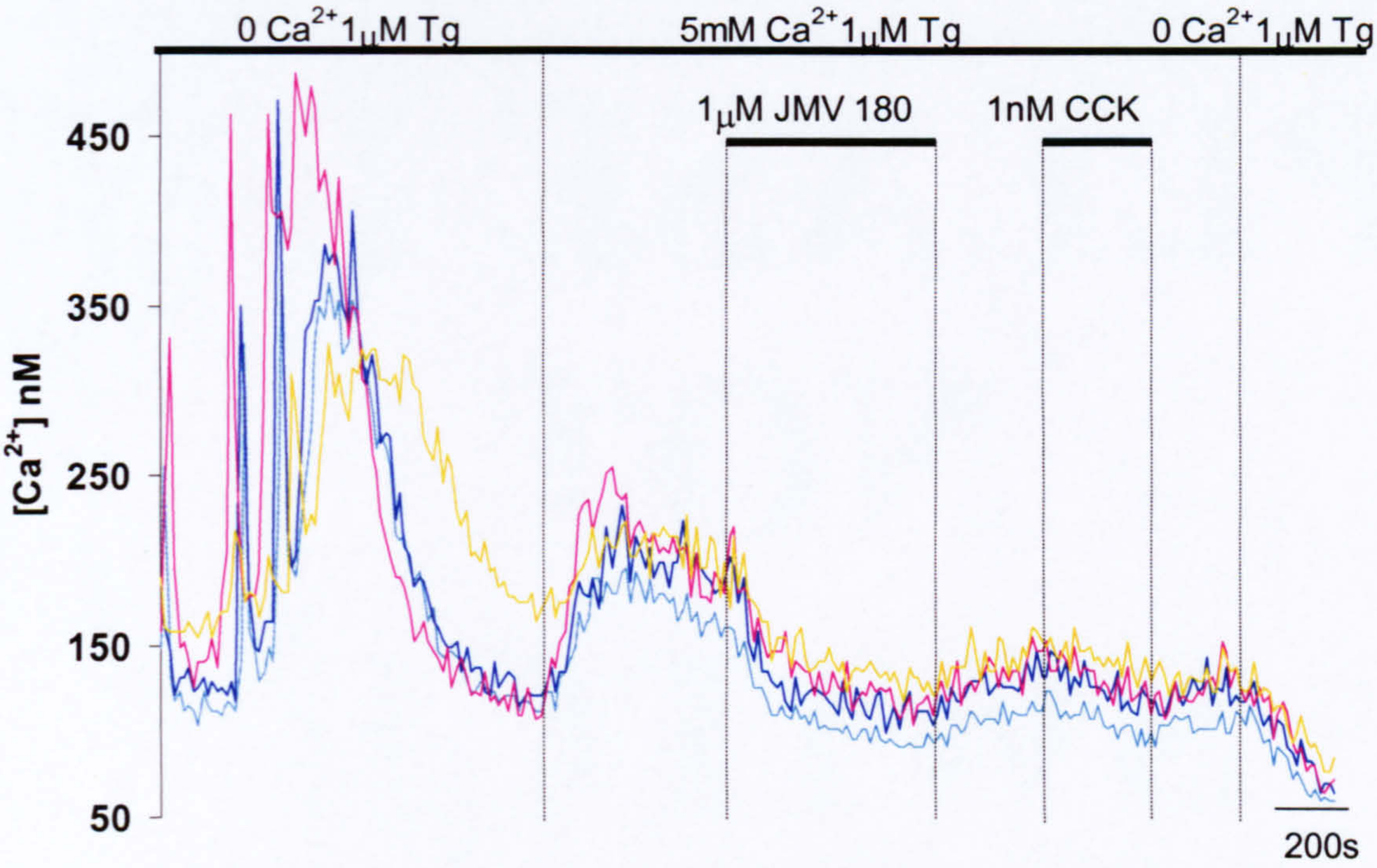

Figure 3.18 **The application of JMV-180 a high affinity site CCK receptor agonist on a thapsigargin-induced cytosolic calcium plateau** An example of a group fura-2 loaded cells (individual cells represented by each line) that have been treated with thapsigargin in zero external calcium, after that 3mM external calcium was reintroduced and a cytosolic calcium plateau built. The application of JMV-180 (1μM) a CCK analogue resulted in a decrease of the plateau level. This was followed by removal of JMV-180. The cell was later challenged with 1nM CCK. At the end of the experiment calcium free extracellular solution was applied.

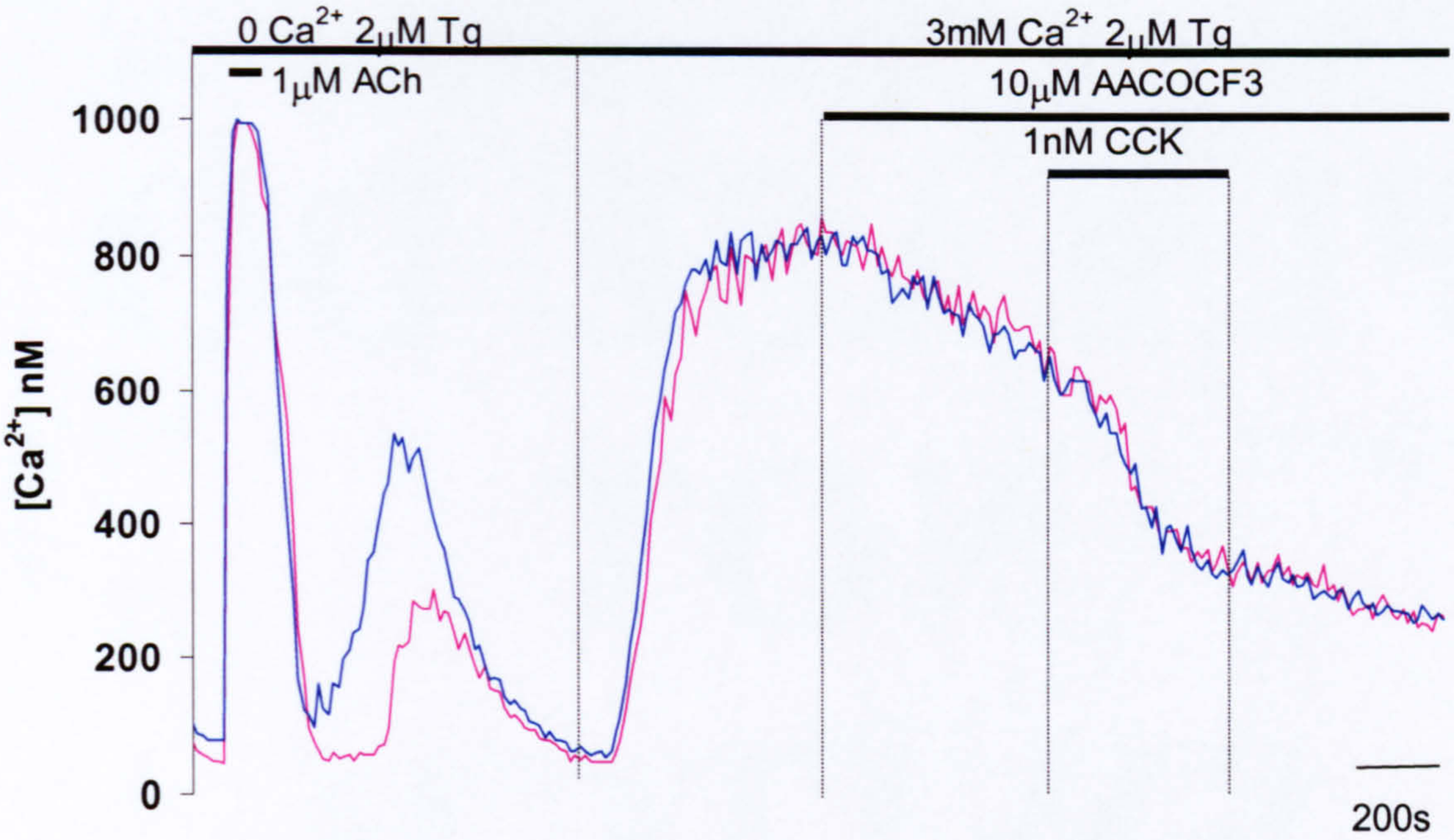

Figure 3.19 **The effect of a PLA_2 inhibitor, $AACOCF_3$, on the thapsigargin-induced calcium plateau and on CCK-induced plateau reduction** These are representative trace of fura-2 loaded cells that have been treated with thapsigargin in zero external calcium. After that 3mM external calcium was reintroduced and a cytosolic calcium plateau built. The PLA_2 inhibitor (10μM) was applied after the plateau was formed. Later 1nM CCK was applied in the continued presence of the inhibitor. Individual cells represented by each line.

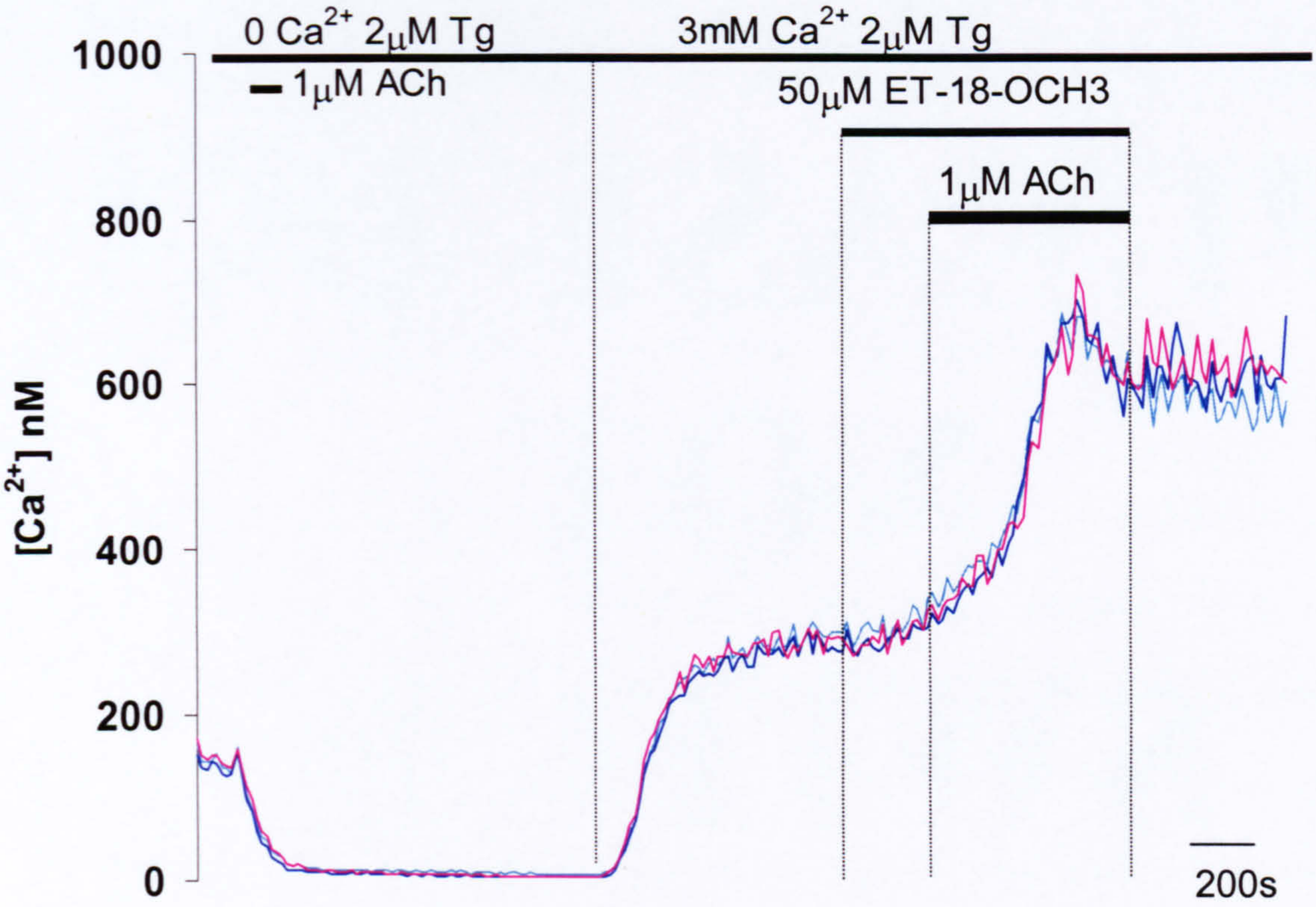

Figure 3.20 **The effect of a PLC inhibitor, ET-18-OCH_3 on the thapsigargin-induced cytosolic calcium plateau and on Ach-induced plateau reduction** The figure shows traces from fura-2 loaded cells that have been treated with thapsigargin in zero external calcium. After that 3mM external calcium was reintroduced and a cytosolic calcium plateau built. 50μM ET-18-OCH_3 was applied after the plateau was formed. Finally 1μM ACh was applied in the continued presence of ET-18-OCH_3. Individual cells represented by each line.

MAP kinase inhibitor PD98059 was used to assess the possible involvement of this pathway in the regulation of PMCA activity. The activation of MAP kinase in response to secretagogues has been shown (Siegel *et al.*, 2001), (Schafer *et al.*, 1998). The application of the MEK inhibitor on the cytosolic calcium plateau showed no effects on the plateau level or the subsequent application of 1μM ACh, which again produced a decrease in the level of the calcium plateau (figure 3.21).

Tyrosine kinase is another pathway whose role in the activation of the PMCA by secretagogues was investigated. Genistein a general tyrosine kinase inhibitor was used. Application on the plateau resulted in a gradual decrease in the plateau level (figure 3.22a), an effect that was absent when the genistein analogue genistin was used at the same concentration (figure 3.22b). This was not unexpected as Yule and colleagues showed that genistein has an inhibitory effect on influx mechanisms (Yule *et al.*, 1994). In the continued presence of the inhibitor genistein, an apparent inhibition of the 1μM ACh activation of calcium extrusion was observed (n=8) (Figure 3.17a). The 1μM ACh effect on plateau level was not inhibited by the genistein analogue, genistin, as seen in figure 3.17b (n=7). However the interpretation of these experiments was difficult due to the initial effect of genistein on the plateau level. Only cells where interpretation was not ambiguous have been considered.

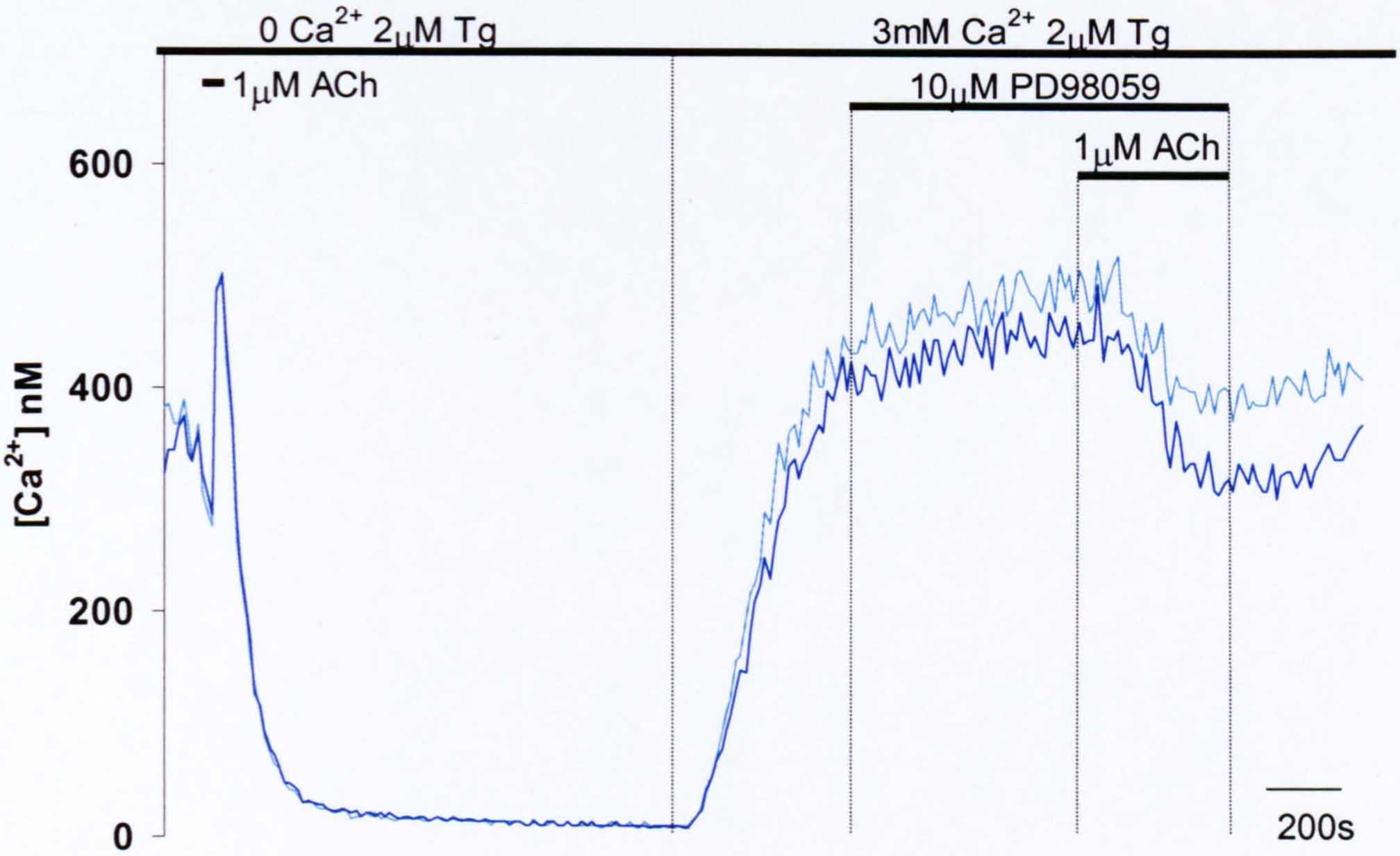

Figure 3.21 **The effect of a MEK kinase inhibitor, PD98059 on the thapsigargin-induced cytosolic calcium plateau and on ACh-induced plateau reduction** these are traces recorded from fura-2 loaded cells that have been treated with thapsigargin in zero external calcium. After that 3mM external calcium was reintroduced and a cytosolic calcium plateau built. 10μM PD98059 was applied after the plateau was formed. Finally 1μM ACh was applied in the continued presence of the inhibitor. Individual cells represented by each line.

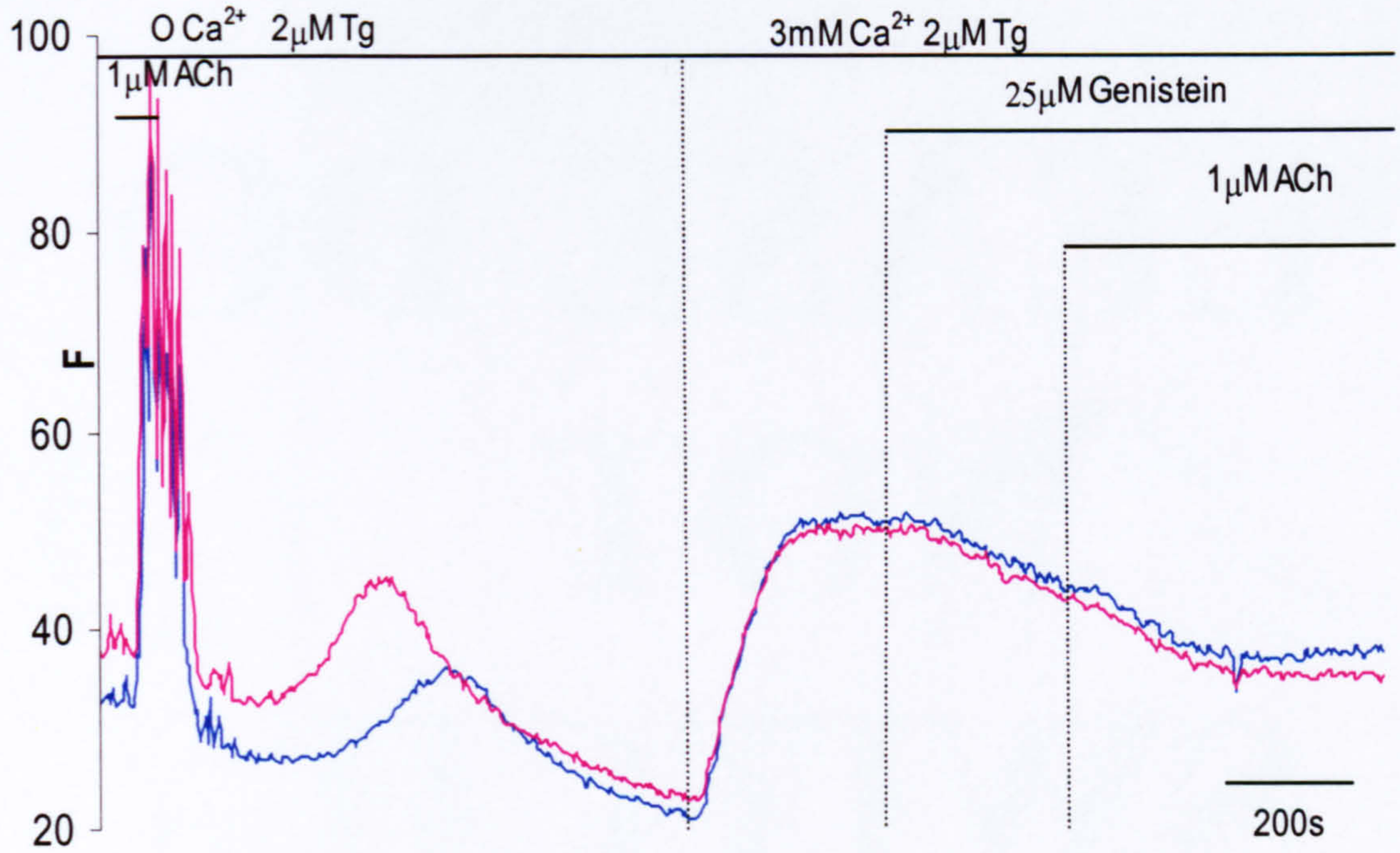

Figure 3.22 **The effect of a tyrosine kinase inhibitor, genistein and its inactive structural analogue genistin on the thapsigargin-induced cytosolic calcium plateau and ACh-induced plateau reduction** Fura-2 loaded cells have been used in this experiment. The cells have been treated with thapsigargin in zero external calcium. After that 3mM external calcium was reintroduced and a cytosolic calcium plateau built. **(A)** 25μM genistein was applied after cytosolic calcium plateau was formed. 1μM ACh was applied in the continued presence of the genistein. Individual cells represented by each line. Part (**B**) of this figure is shown on the next page.

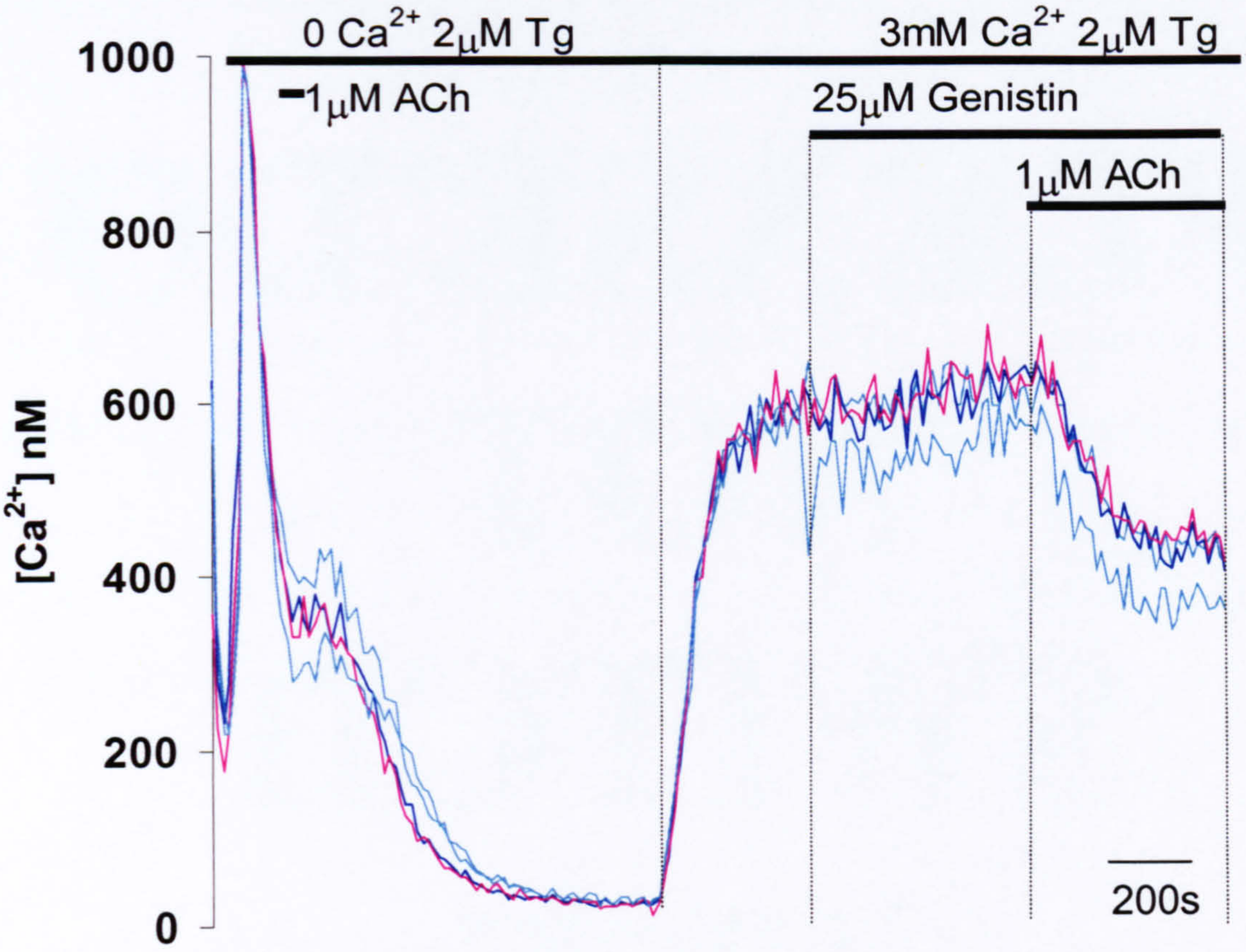

(B) 25μM genistin was applied after the cytosolic calcium plateau was formed. 1μM ACh was applied in the continued presence of the genistin. Individual cells represented by each line. Part (**A**) of this figure was shown on the previous page.

The cytoskeleton has been implicated in the regulation of influx and signalling mechanisms in AR4-2J cells (rat pancreatic acinar tumour cell line)(Bozem *et al.*, 2000). To examine any effects that the cytoskeleton may have on influx and efflux mechanisms involved in building the cytosolic calcium plateau cytochalasin D was applied on the plateau. Cytochalasin D had no effect of the on the level of the plateau shown in figure 3.23. 1μM ACh was applied in the continued presence of cytochalsin D and no inhibition in the activation of calcium efflux by the agonist was seen (n=8). This finding is in agreement with studies that have also found no influence by disruption of the cytoskeleton on PMCA activity (Rosado & Sage, 2000), (Dean *et al.*, 1997).

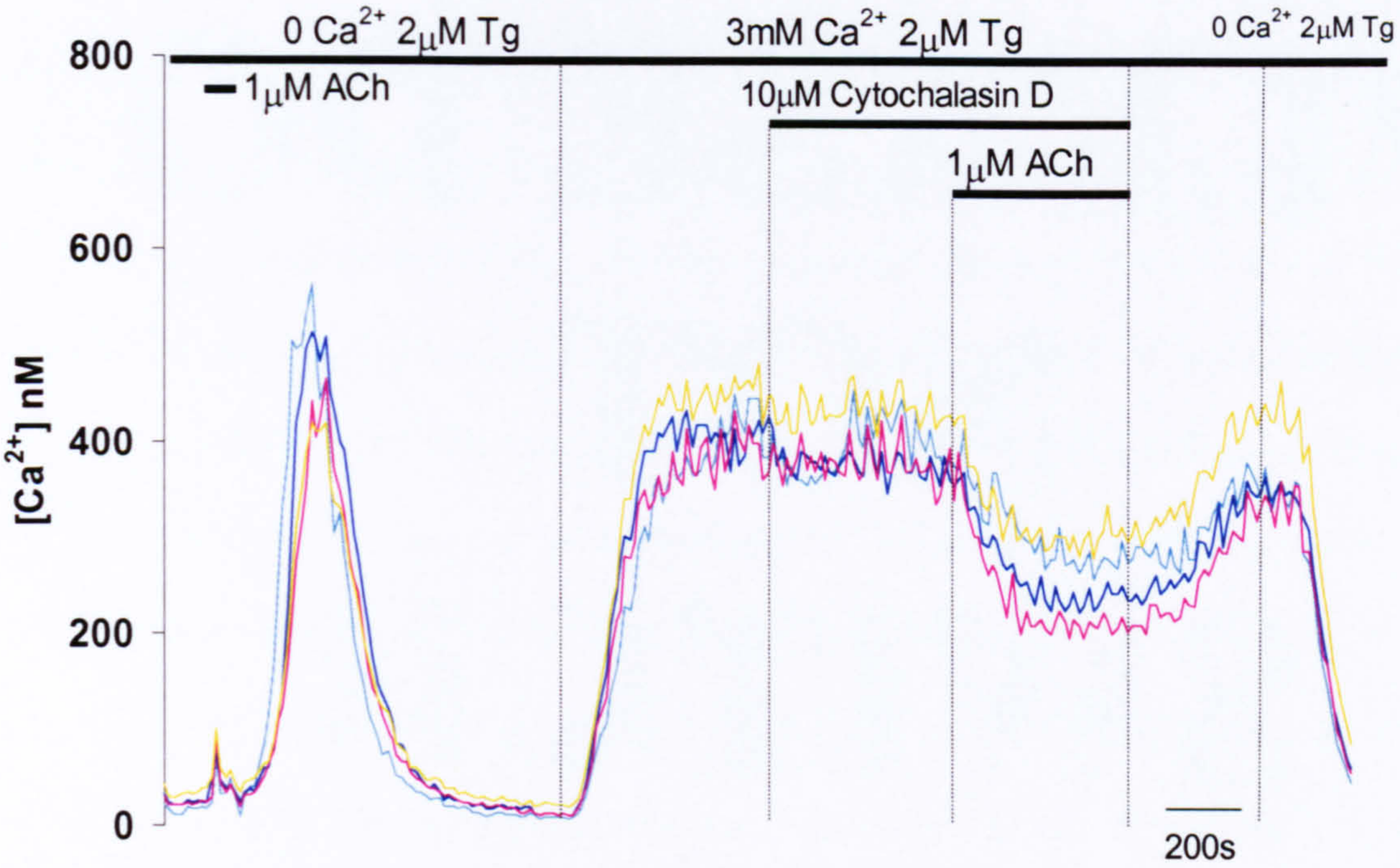

Figure 3.23 **The effect of an inhibitor of actin polymerisation, cytochalsin D, on the thapsigargin-induced cytosolic calcium plateau and on ACh-induced plateau reduction** Fura-2 loaded cells were used in this experiment. The cells have been treated with thapsigargin in zero external calcium. After that 3mM external calcium was reintroduced and a cytosolic calcium plateau built. 10μM Cytochalsin D was applied after the cytosolic calcium plateau was formed. At the end of the experiment 1μM ACh was applied in the continued presence of the inhibitor. Finally Cytochalsin D and ACh were removed followed by removal of the external calcium. Individual cells are represented by each coloured line.

Discussion

The investigation into effects of secretagogues under these conditions is important in terms of understanding potential calcium toxicity in the acinar cell. Raraty *et al.* have showed sustained calcium elevations to be toxic and involved in vacuole formation, analogous to that seen during pancreatitis development (Raraty *et al.*, 2000). The action of secretagogues under these conditions may be fundamental to the progression of conditions such as pancreatitis and these studies are therefore of value in the understanding of such conditions. The application of agonists on a thapsigargin-induced cytosolic calcium plateau allowed examination of the actions on influx and efflux mechanisms. The main finding was that both secretagogues acetylcholine and cholecystokinin activate calcium efflux in the acinar cell at physiological concentrations, demonstrating that there are mechanisms within the cells to limit calcium toxicity as a result of agonist exposure.

It is difficult to estimate the physiological concentration of ACh. However, physiological concentrations of CCK have been measured in the range 5-20pM. Therefore the clear decrease of calcium plateau induced by application of 20pM CCK demonstrates the physiological significance of the phenomenon. The results from this study confirm the findings of Zhang and colleagues (Zhang *et al.*, 1992) and extend the effect to physiological concentrations of agonists. However I had to confirm the action to be due to activation of efflux.

Investigation of mitochondria under these conditions was carried out to confirm that the reduction in calcium plateau was not due to stimulation of calcium uptake into

the mitochondria. The application of oligomycin and rotenone demonstrated that the mitochondria after formation of cytosolic calcium plateau, already (before agonist application) hold some calcium. Mitochondrial NADH is the important source of high-energy electrons necessary for transfer through the electron cascade and formation of mitochondrial membrane potential. The concentration of NADH also reflects intramitochondrial calcium concentrations (Voronina *et al.*, 2002). The results demonstrated a decrease in NADH autofluorescence in 15/17 cells (figures 3.4, 3.5, 3.6) where a response to the agonist was measurable. This indicates that the mitochondria are not taking up calcium, if that were the case a rise would be expected. The drop in NADH autofluorescence could indicate an increase in energy utilisation by agonist activated PMCA. It could also be due to a drop in mitochondrial calcium, as the drop in cytosolic calcium would reduce the driving force for calcium uptake into mitochondria. Simultaneous cytosolic calcium and NADH autofluorescence measurements (figure 3.6) confirmed that the agonist induced reduction in plateau level correlated to the reduction in NADH autofluorescence.

Experiments were conducted under electrophysiological patch clamp conditions to investigate whether the effect of secretagogues is due to changes in the membrane potential and hence driving force for calcium ion movement and permeability of the calcium channels (figures 3.3 and 3.4). The conclusion was that the agonist-induced reduction in cytosolic calcium plateau was not related to any changes in membrane potential or permeability. The decrease in calcium plateau level in response to secretagogues was intact under voltage clamp conditions.

The activation of secretion could account for the calcium reduction observed in response to ACh and CCK application by loss of dye from secreted granules. However, the recovery of calcium to pre-stimulation levels after agonist removal does not support the calcium loss being via an activation secretion causing a loss of calcium sensitive dye. The application of Cytochalasin D (figure 3.23) had no effect on the agonist induced calcium reduction; Cytochalasin D application has been shown to inhibit amylase secretion in pancreatic cells (Valentijn *et al.*, 1999). This again suggests that the loss of calcium is not due to an activation of secretion. The efficiency of secretion at room temperature (the temperature in which all my experiments have been conducted) is unlikely to account for the speed of calcium reduction seen in response to agonist application.

The reduction in the level of the calcium plateau was an effect of the agonist on one of two mechanisms. The plateau was created as a balance of two processes, influx and efflux of calcium; therefore it was thought to be either an inhibition of influx or an activation of calcium efflux. The latter had already been proposed to be the case for high concentrations of ACh by Zhang and colleagues (Zhang *et al.*, 1992). Calcium mobilising hormones in hepatocytes had also been reported to stimulate calcium efflux (Duddy *et al.*, 1989).

In order to verify that this phenomenon was due to efflux regulation a situation where only efflux was active was used in order to study effects purely on the efflux mechanisms. Uncaging of calcium was used to create the plateau, where the caged calcium was loaded into the cytoplasm through the patch pipette. Cells were placed in zero external calcium solution. Under this condition there was no element of

influx involved and subsequent application of agonist showed a reduction in the calcium level of the plateau, figure 3.5. This confirmed that the effect was due to an activation of efflux.

The next challenge was identification of the pathway involved in this regulation of calcium extrusion. Firstly the target of the agonist regulation had to be identified; previously the relevance of the Na^+/Ca^{2+} exchanger in calcium extrusion in the acinar had been studied and found not to contribute significantly (Tepikin *et al.*, 1992;Muallem, 1989;Belan *et al.*, 1996). In experiments where Na^+ was substituted with NMDG in all external solutions, application of both agonists resulted in the reduction of calcium plateau level, figure 3.6. Implicating the PMCAs as the target molecule of secretagogue regulated extrusion.

Identification of the pathway involved in agonist regulation of the PMCA mediated extrusion began with examination of IP_3 as a potential modulator. The use of caged IP_3 allowed manipulation of the IP_3 levels at a specific time of the protocol, as there are no cell permeant analogues of IP_3 available. This allowed the equivalent of addition of IP_3 on the plateau. There was no effect on the thapsigargin-induced calcium plateau level by IP_3 uncaging alone. The control experiments performed alongside demonstrated the functionality of the uncaging and the effect of the IP_3 in circumstances where the stores were intact (figure 3.7a). The inhibition of the IP_3 receptor by caffeine application on the calcium plateau (figure 3.8) confirmed that IP_3 is not involved in the regulation of PMCA mediated calcium extrusion under these conditions.

The next strategy was to investigate molecules that had previously been implicated in the regulation of the PMCA activity. PKC was the first candidate investigated, the rationale being that DAG is produced by occupancy of the CCK receptor at both the high and low affinity sites. JMV-180 also successfully induced a reduction in the calcium plateau (figure 3.18) and this is shown to only occupy the high affinity site that is reported to produce DAG (Matozaki *et al.*, 1990). DAG activates PKC, as does phorbol-12-myristate-13-acetate (Sienaert *et al.*, 1996;Nishizuka, 1984). It has previously been demonstrated that PKC phosphorylation stimulates PMCA activity in erythrocytes, jurkat T cells and neutrophils (Pollock *et al.*, 1987;Rickard & Sheterline, 1985;Balasubramanyam & Gardner, 1995). It has also been shown that PKC can phosphorylate the PMCA within the calmodulin-binding domain. This did not affect basal activity but this may remove the potential regulation of PMCA activity by calmodulin once the cell is stimulated (Enyedi *et al.*, 1996;Enyedi *et al.*, 1997). This would not be the case for agonist-mediated activation of extrusion in the pancreatic acinar cell, as the findings of my studies demonstrate activation as a direct result of cell stimulation. However the effect of PKC has also been shown to depend on the isoform of PMCA expressed. In the current studies, the treatment with PMA causes an increase rather than a decrease in the plateau level. This is in agreement with results published by Camello and colleagues who also saw an increase in plateau level using a similar protocol. In their experiments the PMA effect was blocked by the PKC inhibitor GF109203X in pancreatic acinar cells (Camello *et al.*, 1999). This effect of PKC activation could be due to an inhibition of calcium extrusion or an activation of calcium influx. Rosado and Sage report that PKC activates calcium entry in human platelets (Rosado & Sage, 2000), PKC has also been reported to activate SOC entry in human glomerular mesangial cells (Ma *et al.*,

2001). My studies have not investigated this in detail; further experiments would be necessary to elucidate the mechanism of PMA modulation of the plateau.

PKC and its potential role as mediator of the secretagogue stimulation of the PMCA calcium extrusion were further investigated using a DAG analogue DC_{10}. Investigations using a DAG analogue DC_{10} showed no effect on the plateau level. This is contradictory to the results with PMA, and questions whether the effect of PMA is due to activation of PKC. No effect of $DC_{10}$was seen on the subsequent ACh stimulation of extrusion. This indicates that PKC activation is not the pathway through which agonists stimulate calcium extrusion.

The modulation of interaction between calmodulin and the PMCA is proposed to be the target of kinase-mediated regulation. Indeed in vivo experiments using peptides from the calmodulin-binding domain of the PMCA observed an attenuation of calmodulin mediated PMCA activity upon phosphorylation (Hofmann *et al.*, 1994). It was therefore prudent to investigate calmodulin as the prospective mediator of agonist stimulated PMCA activity. In my experiments the calmodulin inhibitor, calmidazolium chloride was applied on the plateau with no effect. This suggests that non-stimulated activity of the PMCA in the pancreatic acinar cell is not regulated by calmodulin (In agreement with unpublished data by Julie Gardener from this lab). The subsequent activation of extrusion by ACh was intact in the presence of the calmodulin inhibitor. This suggests that calmodulin is also not involved in the agonist activation of PMCA. This also implies that any modulation of PMCA activity by signal transduction pathways in the acinar cell is not due to modulation of PMCA/calmodulin interactions. It has been shown that some splice variants of the

PMCA have a low affinity for calmodulin (Filoteo *et al.*, 2000;Ba-Thein *et al.*, 2001); therefore the absence of calmodulin regulation of calcium extrusion is not unsupported (Strehler *et al.*, 1989). Cleavage by calpain of the C terminus that includes the calmodulin-binding domain has demonstrated an activation of the PMCA (James *et al.*, 1989). The physiological relevance of the calpain action on the PMCA in its regulation is questionable.

cAMP-dependent protein kinases have been reported to regulate the activity of the PMCA. They are reported to change the affinity of the PMCA for Ca^{2+}, changing the K_m to 1μM from 10μM on *in vitro* experiments with purified PMCA protein (James *et al.*, 1989). cAMP and its role in the regulation of the PMCA and hence calcium extrusion in platelets was also examined by Johansson and colleagues. An approximate two-fold increase in the rate of calcium extrusion was observed on treatment of human platelets with a cell permeable analogue of cAMP or forskolin treatment in agreement with James and colleagues. However they reported an absence of an effect on the affinity of the PMCA for calcium (Johansson *et al.*, 1992). Variation of the isoforms expression patterns of those that possess the consensus sequence for cAMP-dependent protein kinase mediated phosphorylation may explain some of the discrepancies (Carafoli, 1994). However it has been reported that the cAMP-mediated regulation is due to phosphorylation near the calmodulin-binding domain of the PMCA (James *et al.*, 1989). Therefore my finding that cell permeant analogues of cAMP generally had no effect on the calcium plateau level or the agonist mediated activation of the calcium extrusion in the pancreatic acinar cell was consistent with the absence of calmodulin regulation of the PMCA under these conditions. The activation of efflux in hepatocytes by hormones

vasopressin and angiotensin II reported by Duddy and colleagues in 1989 was not mediated by cAMP, PKC activation or affected by calmodulin inhibitors (Duddy *et al.*, 1989). This concurs with the results from my studies.

Furukawa and Nakamura studied cGMP-dependent protein kinase involvement in the regulation of the calcium extrusion on PMCA purified from aortic smooth muscle. They found that treatment with cGMP and a cGMP-dependent protein kinase result in an increase in calcium affinity and an enhancement of the rate of the pump (Furukawa & Nakamura, 1987). In my experiments there was no effect of the application of cell permeant analogues of cGMP on the plateau level. This indicates no effect of cGMP on either efflux or influx mechanisms. This is surprising; as it has been previously reported in rat pancreatic acinar cell that cGMP activates calcium influx mechanisms (Pandol & Schoeffield-Payne, 1990;Bahnson *et al.*, 1993). This was possibly due to the level of activation at which the influx was already functioning under these conditions. Though influx was not saturated as exposure to higher concentrations of external calcium resulted in higher plateau levels (data not shown). Studies in vascular endothelial cells show a cGMP-dependent inhibition of the calcium extrusion mechanisms, thought to be due to modulation of the PMCA. That is shown to be one mechanism through which NO modulates calcium homeostasis (Dedkova & Blatter, 2002). Contradictory to this cGMP was found to lower basal calcium levels by activation of the PMCA in the same cell type (Chen *et al.*, 2000). Dedkova and colleagues attempted to explain this as a dose dependency of the Nitric oxide (NO) actions.

The investigation utilising the phospholipase A_2 (PLA_2) inhibitor $AACOCF_3$ was undertaken primarily owing to the ability of JMV-180 and 20pM CCK to induce the reduction in the calcium plateau level. The efficacy of the low physiological concentrations of agonists and the ability of a CCK analogue, which only activates the high affinity site on the CCKa receptor, to induce the response, implies that only the activation of the signal transduction associated with occupancy of the high affinity site is required. The signal transduction pathway linked to the high affinity site is that involving PLA_2. The application of the inhibitor, $AACOCF_3$, caused a slow decline in the plateau level. However activation of extrusion was still produced by agonist application on the plateau in the presence of the inhibitor. This suggested the agonist-induced activation of the PMCA did not require the PLA_2 enzyme. The effect of the inhibitor alone on the plateau is most likely to be an inhibitory effect on the influx pathway, though further investigation is required to confirm this.

ACh and CCK (at the low affinity site) receptors are coupled to PLC. To investigate the requirement of the PLC enzyme in secretagogue-induced activation of the PMCA the PLC inhibitor ET-18-0CH_3 was used. In all cases an increase in the calcium was observed as a result of addition of ET-18-OCH_3 itself before application of the agonist. Any effect of the agonist-induced response was impossible to interpret. The reduction in the plateau may have been inhibited or just masked by the inhibitor-induced calcium increase.

MAPK pathway was briefly investigated using the general MEK inhibitor PD98059. The cells treated with this inhibitor displayed an intact agonist-induced activation of calcium extrusion. MAPK pathway had not previously been shown to regulate the

PMCA. Tyrosine phosphorylation had already been shown to have a probable role in PMCA regulation (Dean *et al.*, 1997) and further investigations concentrated on this area. Tyrosine phosphorylation of the PMCA has been demonstrated in human platelets by Dean and colleagues (Dean *et al.*, 1997). Tyrosine phosphorylation of the PMCA inhibited the PMCA activity measured by ATP hydrolysed mg/min/mg or protein in purified membrane fractions. The same study showed a complete reversal of tyrosine kinase inhibition of PMCA activity by genistein. The interpretation of the results from the present study is that genistein inhibits the secretagogue activation of the PMCA and therefore agonist modulation is mediated by tyrosine kinase action. This contradicts the results from Dean and colleagues who propose that tyrosine kinase activity inhibits the PMCA activity almost fully. Genistein application on the calcium plateau in the pancreatic acinar cell resulted in a reduction of the plateau level. This is in support of findings by Yule and colleagues that inhibition of the tyrosine kinases attenuates calcium influx (Yule *et al.*, 1994). CCK and carbachol effects on tyrosine phosphorylation state in the pancreatic acinar cell have been reported despite there being no intrinsic tyrosine kinase activity. A reduction of agonist stimulated enzyme secretion in rat pancreatic acinar has also been suggested by after tyrosine kinase inhibition (Lutz *et al.*, 1993). The activation of PMCA activity proposed by the results of this study could account for this finding, as an increase in the rate of removal of calcium would decrease the calcium signal that is required for secretion in the apical region. This notion is further supported by the primary site of extrusion being the apical pole (Belan *et al.*, 1996;Belan *et al.*, 1997), the region from which secretion occurs. The location of Src-related protein tyrosine kinases on the cytoplasmic side of the plasma membrane (Tsunoda *et al.*, 1996)and therefore the location of subsequent activation is ideal for a potential role in the

regulation of the PMCA in the apical region and influx at the basal lateral membranes.

It was proposed that the tyrosine phosphorylation site could alter the affinity of the PMCA protein for calmodulin. However the inhibition by tyrosine phosphorylation could not be overcome with a 60-fold increase in calmodulin, suggesting that there is no interference of calmodulin binding to the PMCA (Dean *et al.*, 1997). Dean at al., reported a 2-fold increase in PMCA activity upon addition of calmodulin in control conditions. The lack of an effect on the plateau by the calmodulin inhibitor, calmidazolium chloride, and on the subsequent secretagogue-induced activation of the PMCA activity (figure 3.15) in these studies would support this finding and confirm that there is little involvement of calmodulin in the PMCA activity. However the discrepancy of calmodulin effects between Dean et al., and current studies, is possibly explained by being below the detection limit or that calmodulin is not involved in the regulation of PMCA activity in the pancreatic acinar cell. The isoform expressed in the pancreatic acinar cell is unknown. However it is well described that different calmodulin sensitivities exist between the isoforms (Carafoli, 1994).

These studies indicate that the ability of the agonists to activate the PMCAs, be it through a tyrosine kinase pathway or another mediator could have a dramatic effect on the temporal aspects of calcium signalling in the pancreatic acinar cell. Studies that have examined the effect of the over expression of the PMCA, have shown dramatic changes in calcium homeostasis within those cells (Brini *et al.*, 2000).

Indeed these same studies showed that cells over expressing the PMCA, in the continued presence of agonist, displayed more effective calcium clearance than if the agonist was rapidly washed. This lends support to the idea of the agonist-activated extrusion. As there is an increase in the amount of PMCA protein, there is an increase in the target molecule for agonist-activated extrusion and the effect of the agonist on extrusion is more readily observed under these conditions.

The importance of calcium extrusion in cell calcium signals and hence cell function is verified by knockout studies in mice. Studies in knockout mice have demonstrated the involvement of the PMCA2 in hearing and balance function. Knockout of the PMCA2 gave rise to mice with severe hearing (deaf) and mobility deficits. Mice that carried point mutations in PMCA2 had less severe deficits (Shull, 2000). Calcium homeostasis is a dynamic process that has auto-regulatory feedback in controlling the abundance of the proteins involved in calcium signalling. Expression of the proteins involved in calcium homeostasis within the cell including the PMCA are thought to be regulated by the calcium load of the endoplasmic reticulm (Kuo *et al.*, 1997). The calcium load of the ER governs the amount of calcium released by agonists and consequently the processes governed by calcium release. In the case of pancreatic acinar cell, the major function is secretion of digestive enzymes that requires a calcium signal. However other cell functions such as protein synthesis and gene expression are also proposed to be calcium-regulated processes (Paschen, 2001)(Dolmetsch *et al.*, 1998). Activation of calcium extrusion by agonists maybe an additional mechanism of regulating the temporal and spatial aspects of such fundamental physiological reactions.

The pathophysiological calcium signals described as a sustained calcium plateau, which have been implicated in the development of pancreatitis, may perhaps be limited by this agonist-induce activation of extrusion. The activation of extrusion by agonists seems to provide a protective mechanism to limit exposure to high toxic levels of calcium. Further understanding of this phenomenon and clarification of the pathway that mediates this activation could lead to development of therapies aiming to limit toxic calcium levels.

Chapter 4

The effects of a bile salt, taurolithocholic acid 3-sulfate, on calcium signalling in the pancreatic acinar cell

Introduction

Among the proteins secreted by the exocrine pancreas are the inactive precursors (zymogens) of digestive enzymes. Normally these inactive precursors are activated upon cleavage by enterokinases (enteropeptidase) found in the brushborder of the small intestine. They therefore remain inactive until after secretion and transit through the pancreatic and common ducts. However, when the premature activation of these enzymes occurs, auto-digestion of the pancreas can result, the underlying mechanism of the disease acute pancreatitis. The mechanism by which premature intracellular activation of these enzymes has been the subject of extended research. Recently it has been shown that abnormal elevations of intracellular calcium are required for the activation of intracellular trypsin and subsequent formation of vacuoles (Raraty *et al.*, 2000). This study suggests that it is the abnormal elevation of calcium which is solely required for premature activation of the zymogens. Kruger and colleagues however, present evidence to suggest that it is the specific type of calcium signals in response to a secretagogue not those induced by ionomycin or SERCA inhibition, which initiates the intracellular activation of the zymogens (Kruger *et al.*, 2000). Overall both studies propose that it is a prolonged or sustained rise in calcium that is required for the activation of the zymogens.

Entry of bile into the pancreas by reflux has been implicated in the pathology of acute pancreatitis. Eugene Opie proposed that a blockage of the ampoule of Vater by a gallstone could cause bile to permeate the pancreas and elicit the onset of acute pancreatitis; this was termed the "common duct theory" (Opie, 1901). Bile acids were confirmed to have the ability to induce acute pancreatitis (Niederau *et al.*,

1990;Senninger, 1992). However the cellular mechanisms were undetermined. The actions of Bile acids have been studied in hepatocytes, where it has been found that some bile acids can induce the release of calcium from internal calcium stores (Combettes *et al.*, 1988;Combettes *et al.*, 1990). The effects of some of the bile acids in the pancreatic acinar cell are now being studied. The initial studies showed that acinar cells exhibited a calcium response upon application of bile acid taurolithocholic acid 3-sulfate (TLC-S) (Voronina *et al.*, 2002). The responses were heterogeneous, some cells exhibiting an oscillatory pattern and others responding with an initial large transient followed by a plateau of raised cytosolic calcium. The responses were found to be dependent upon IP_3 receptors owing to their sensitivity to caffeine. The plateau phase of the response was found to be dependent upon external calcium, therefore due to calcium influx. Oscillations in the absence of external calcium were found to run down, and this is thought to be due to an exhaustion of internal calcium stores.

TLC-S dose response in the pancreatic acinar cell

Examples of calcium responses in pancreatic acinar cells to different concentrations of TLC-S are shown in figure 4.1. The range of TLC-S studied was 25μM to 500μM (25μM to 100μM my work, 200μM, 300μM and 500μM from S. Voronina work shown for reference only). The proportion of cells responding increased with increasing concentration of TLC-S (figure 4.2, blue bars). A higher sensitivity to TLC-S (micro molar) was seen when compared to other bile acids where calcium responses were only seen at much higher concentrations (milli molar) in pancreatic acinar cells (Voronina *et al.*, 2002). Higher concentrations of TLC-S produced a

higher proportion of cells responding with a sustained plateau phase (see figure 4.2, maroon bars). This is summarised in figure 4.2, the higher concentrations show a higher proportion of the cells responses involving the formation of a plateau. 50% of responding cells at 25μM displayed a sustained plateau phase, increasing to 65% at 100μM and 100% at 500μM.

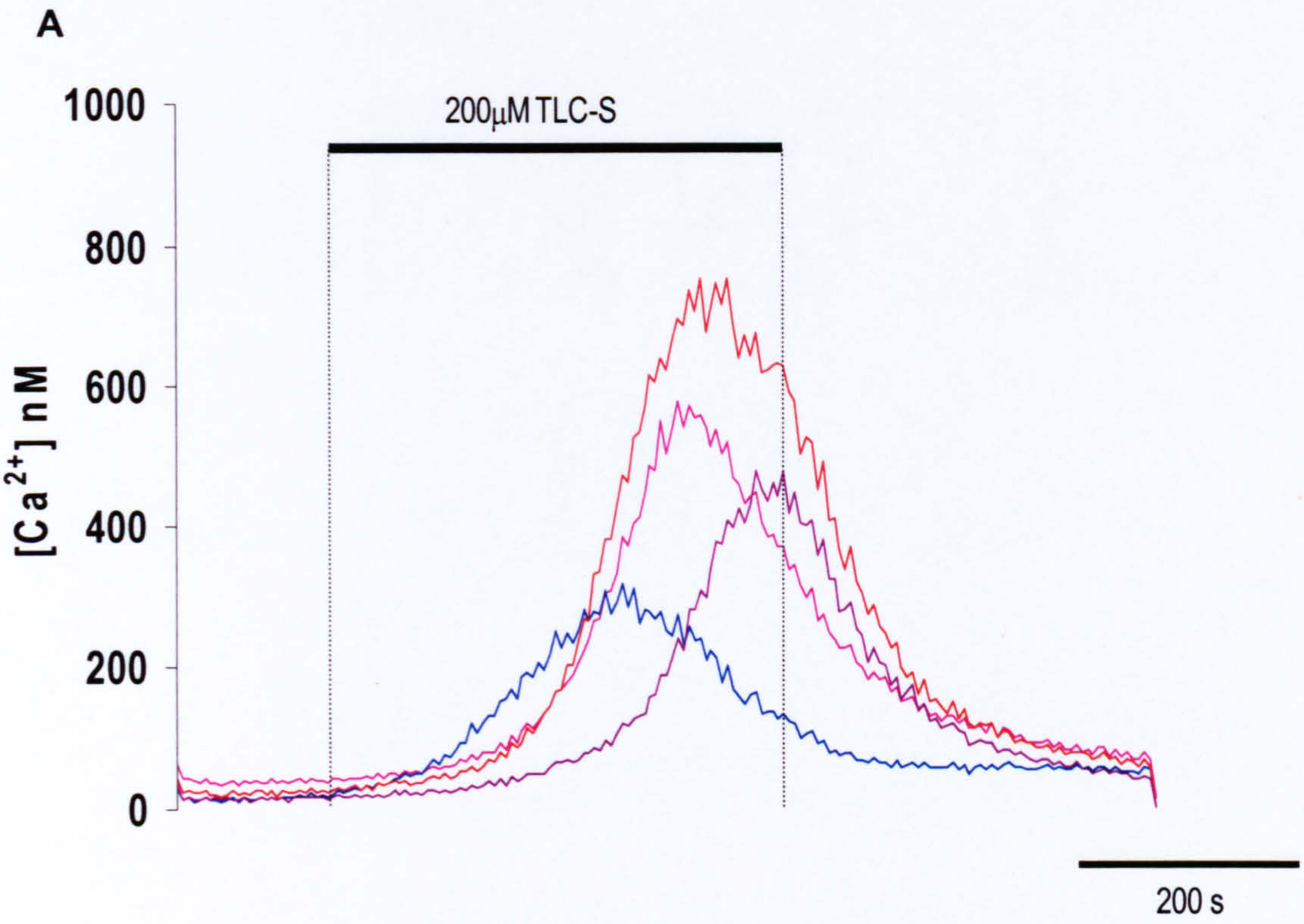

Figure 4.1 **TLC-S-induced calcium responses in mouse pancreatic acinar cells** The parts of the figure show effects of different concentrations of TLC-S. Examples of responses to TLC-S in cells loaded with fura-2 (**A**) shows effects of 200μM TLC-S. (Parts (**B**) and (**C**) of this figure are shown on the next page). (**B**) shows calcium changes triggered by 25μM TLC-S. (**C**) Shows calcium responses to additions of first 50μM TLC-S and then 100μM TLC-S. The period of TLC-S application is indicated by the black bar above the trace. The different coloured traces correspond to individual cells.

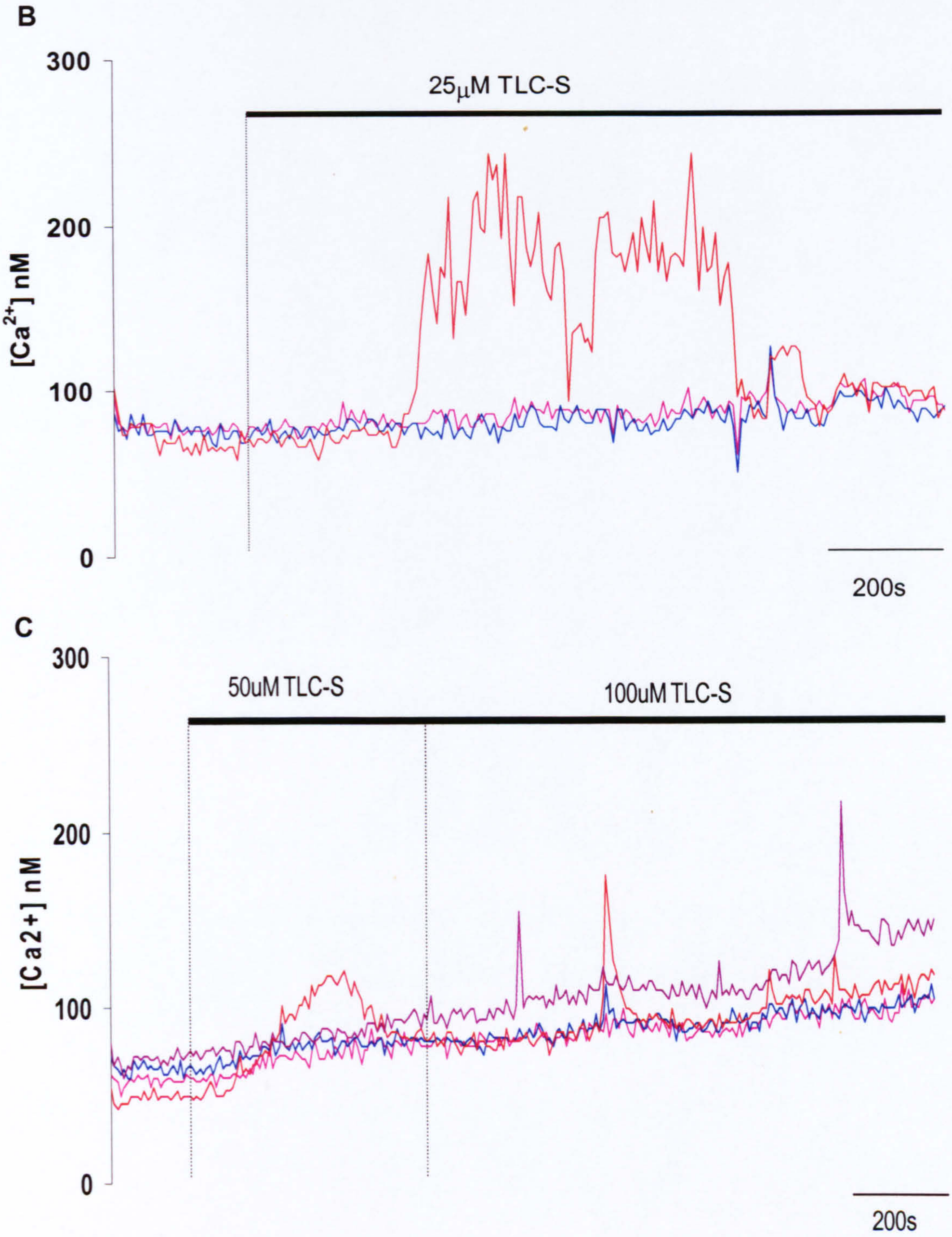
B
300
200
100
0
[Ca2+] nM
25μM TLC-S
200s
C
300
200
100
0
[Ca2+] nM
50uM TLC-S
100uM TLC-S
200s

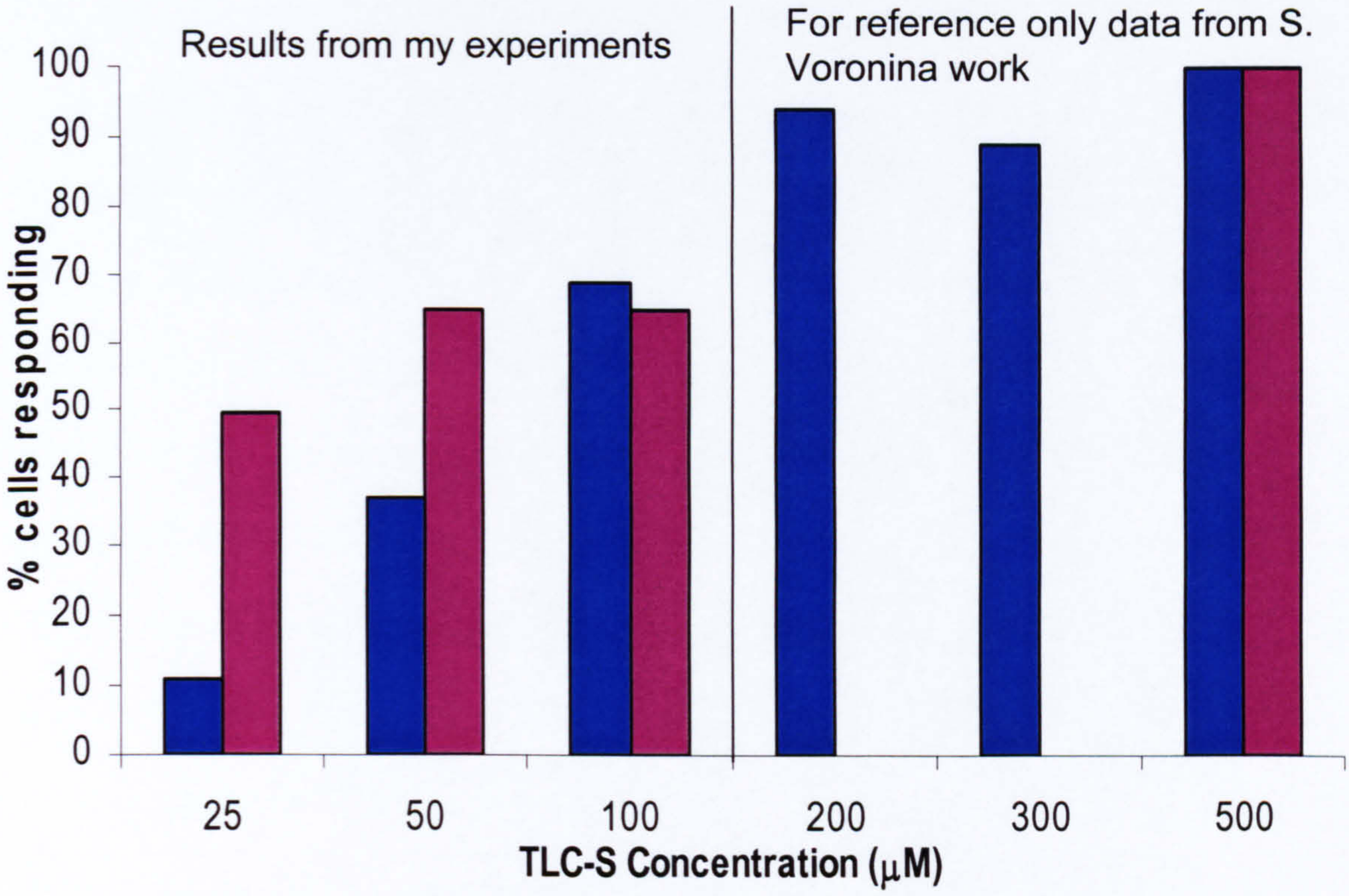

Figure 4.2 **The TLC-S-induced calcium responses in mouse pancreatic acinar cells** A summary of the percentage of cells demonstrating a calcium response to different concentrations of TLC-S shown in blue ■ . The percentage of responding cells that involve a sustained plateau phase in the response are shown in maroon ■ for each concentration.

Action of bile acid TLC-S on a thapsigargin-induced calcium plateau

The action of bile acids on a sustained cytosolic calcium plateau was of particular interest, (The effects of secretagogues on such a plateau are discussed in chapter 3) in light of the work done by Raraty and colleagues, and Kruger and colleagues on the role of calcium in the pathophysiology of acute pancreatitis (Raraty *et al.*, 2000;Kruger *et al.*, 2000). Both studies found sustained elevation of calcium was found to be of importance in intracellular activation of trypsin. It was therefore of interest to study the possible effects of bile acids during elevated cytosolic calcium. The classical protocol of plateau formation by depletion of the endoplasmic reticulm stored calcium using the SERCA pump inhibitor thapsigargin was employed. This allowed manipulation of the cytosolic calcium concentrations through alterations of the external calcium concentrations, due to the activation of store operated calcium (SOC) influx. The experiments usually started with depletion of internal calcium stores in calcium free external solution. Thereafter a plateau of cytosolic calcium was built by increasing the external calcium concentration. The level of the plateau was dictated by two processes, the rate of influx through SOC channels (SOCC) and the rate of calcium efflux from the cytosol. TLC-S at a concentration of 200μM was applied upon an established calcium plateau. The responses were again heterogeneous. However there were two main types of calcium responses observed, some cells exhibiting a mixture of both types. One response is a further transient increase of cytosolic calcium, a typical example is shown in figure 4.3 (top trace), the other being a drop in the level of the calcium plateau, figure 4.3 (bottom trace, turquoise and red lines). TLC-S at a concentration of 200μM induced responses in 89.8% of cells; of those responding cells 30.5% demonstrated a transient increase in

calcium on top of the calcium plateau; 30.5% exhibited a drop in the level of the calcium plateau (figure 4.3, turquoise and red lines) and 29.8% produced both a release and a drop. These results are summarised in figure 4.4. The average decrease of calcium in those cells displaying a reduction from the plateau level was, 147±11nM (S.E.)(n=85)(inclusive of all cells, including those with an initial increase) that corresponded to 30% of the original plateau level. The average height (at peak) of increase in calcium response to TLC-S was 195±17nM (S.E.)(n=85) (inclusive of all cells, including those that show a subsequent decrease), corresponding to 63% of the original plateau level.

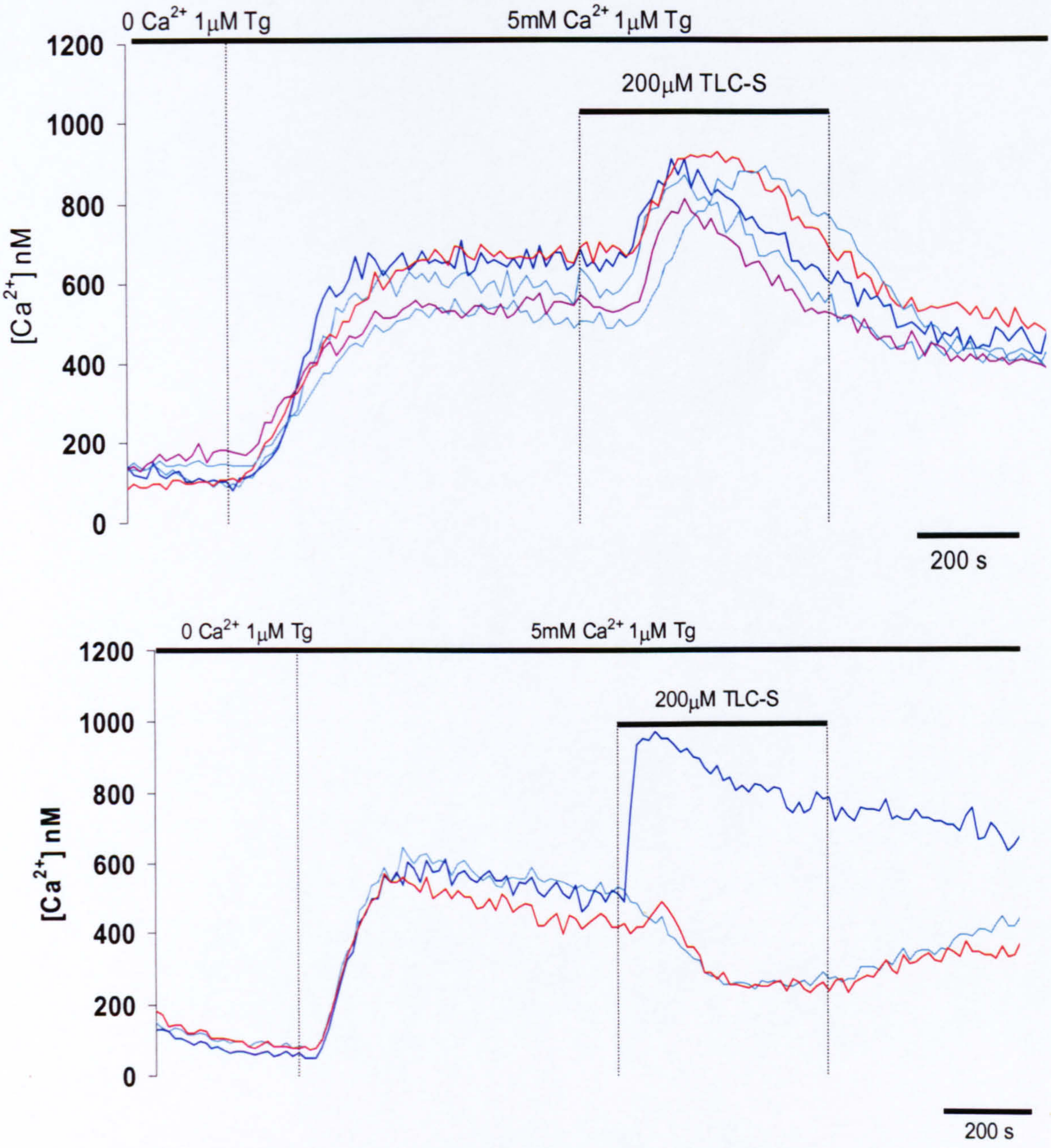

Figure 4.3 **Effects of TLC-S calcium responses on a thapsigargin-induced cytosolic calcium plateau** Top trace shows a representative trace of a cluster of cells (each line represents individual cells) that exhibit an increase in calcium on top of the thapsigargin-induced plateau in response to 200μM TLC-S. The bottom trace shows a representative trace of two cells (red and turquoise lines) that demonstrate a decrease in calcium and one cell (blue line) that shows an increase in response to 200μM TLC-S.

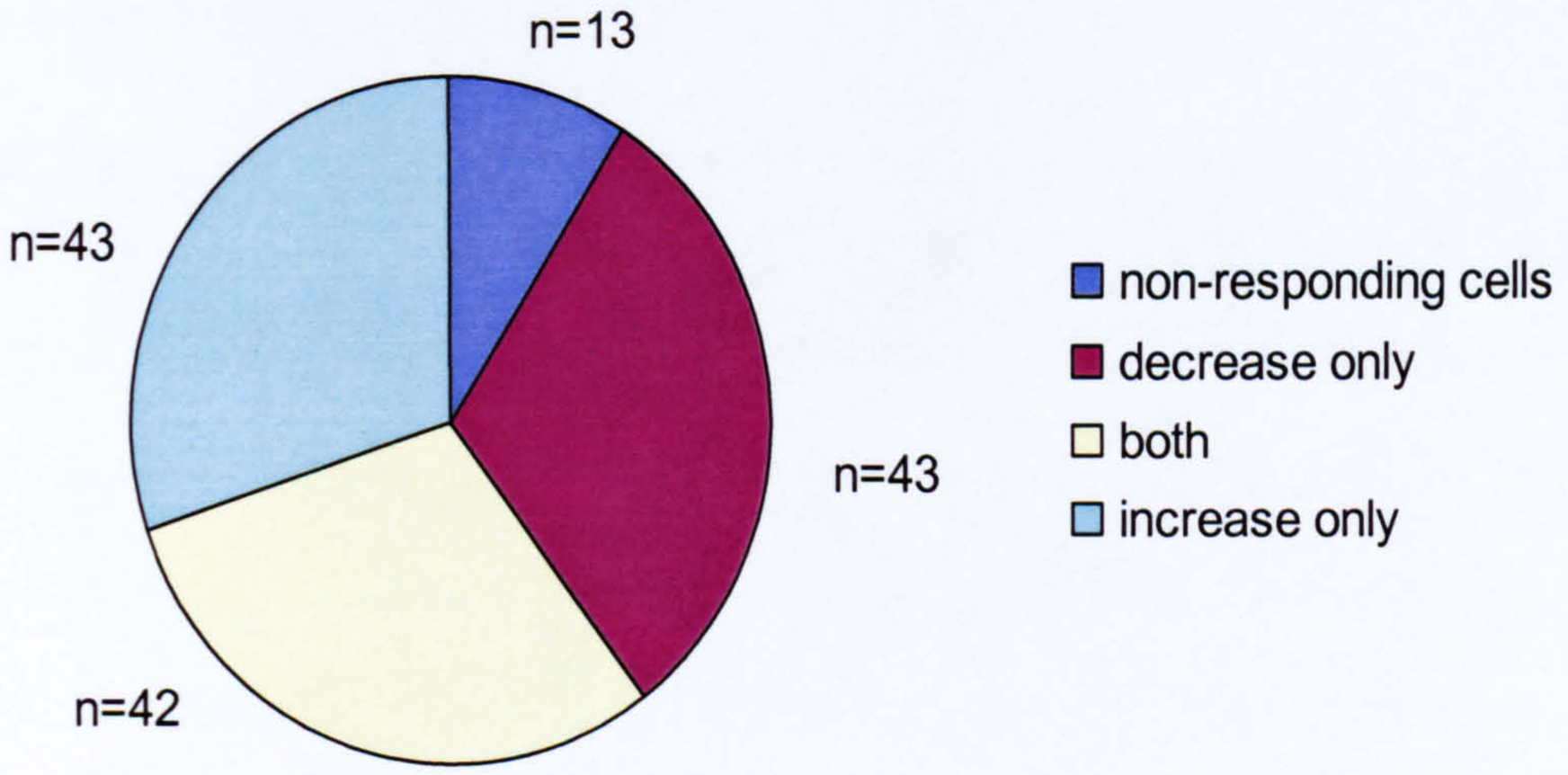

Figure 4.4 **Summary of the effects of TLC-S on a thapsigargin-induced cytosolic calcium plateau** A summary of the effects of 200μM TLC-S on the thapsigargin-induced cytosolic calcium plateau. The maroon section represents cells that exhibit a decrease in plateau level only. The turquoise section represents the cells that exhibit an increase of calcium on the thapsigargin-induced cytosolic calcium plateau only. Some cells exhibit both responses an increase followed by a decrease represented by the yellow section. The blue section shows non-responding cells.

Calcium stores in the TLC-S induced calcium response on a thapsigargin-induced calcium plateau

Secretagogue-releasable Calcium store and the TLC-S induced calcium response

Thapsigargin, a SERCA pump inhibitor, was applied for at least 15mins in the absence of external calcium. This should result in complete depletion of the ER calcium stores; some thapsigargin insensitive stored calcium may remain (Missiaen *et al.*, 2002b). Application of supramaximal (1nM) concentration of secretagogue cholecystokinin (CCK) on top of the calcium plateau demonstrated no further increase in calcium, a drop in the level of the plateau was however evident. This effect was further discussed in Chapter 3. Subsequent application of TLC-S still displayed a transient increase in cytosolic calcium (n=25) (fig 4.5). The possible role of IP_3 receptors in this response was tested using the antagonist caffeine. The IP_3 receptor under normal store calcium conditions has been implicated in calcium release in response to TLC-S (Voronina *et al.*, 2002). Owing to complications of dye quenching by caffeine these experiments were done using the fluorescent indicator Fura Red, which is less affected by caffeine quenching than other calcium indicators. Cells were then exposed to thapsigargin for 15mins and then external calcium increased and a cytosolic calcium plateau built. Caffeine was then applied on the plateau, resulting in a small reduction of the plateau level. TLC-S was then applied in the presence of caffeine 100% of cells (n=15) showed an increase in calcium as shown in figure 4.6.

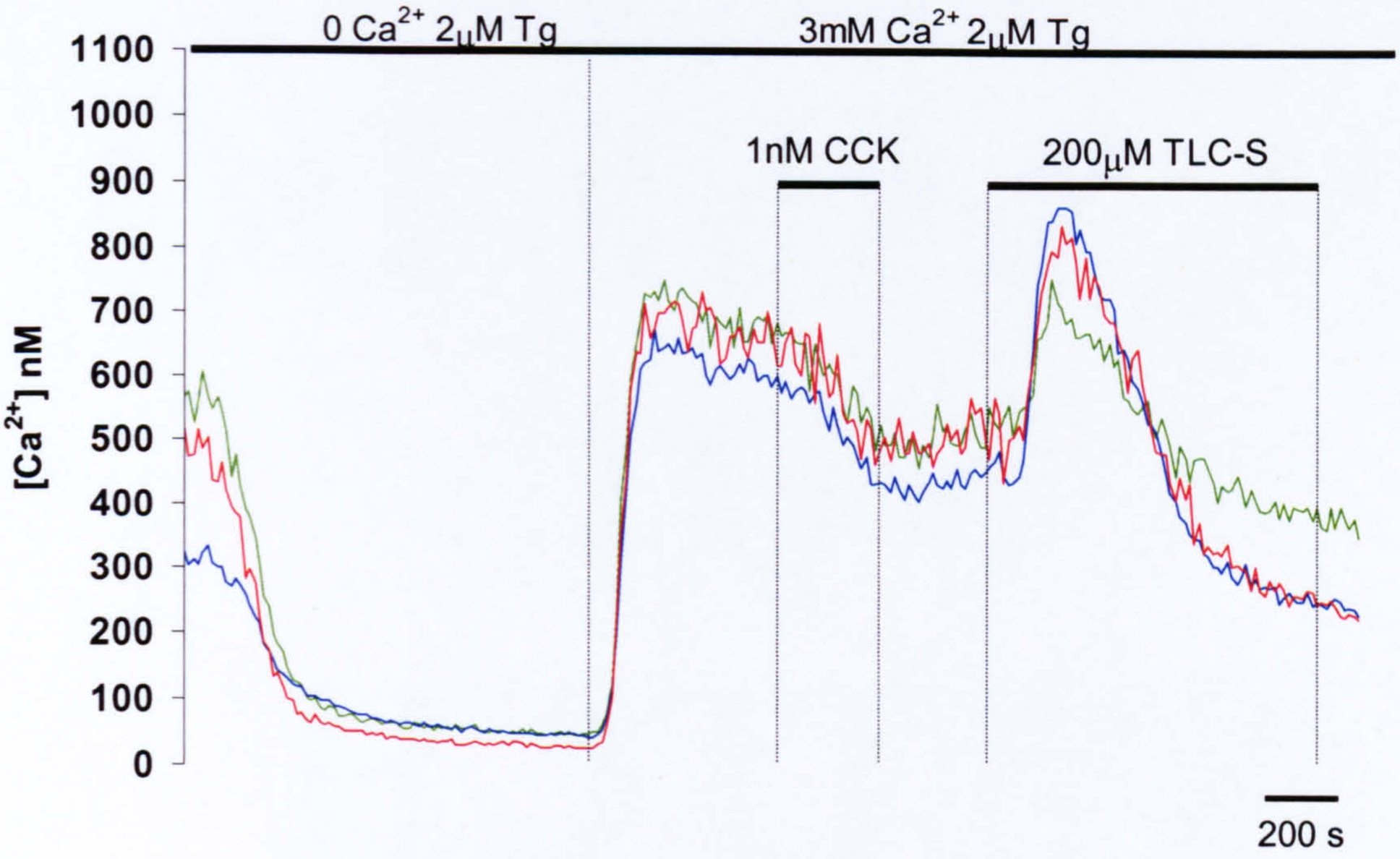

Figure 4.5 **TLC-S induced calcium increase on a thapsigargin-induced calcium plateau after the application of the secretagogue CCK** Three cells (individual lines represent 3 different cells) showing the response to 200μM TLC-S on the thapsigargin-induced cytosolic calcium plateau following an application of 1nM CCK. Cells were loaded with fura-2.

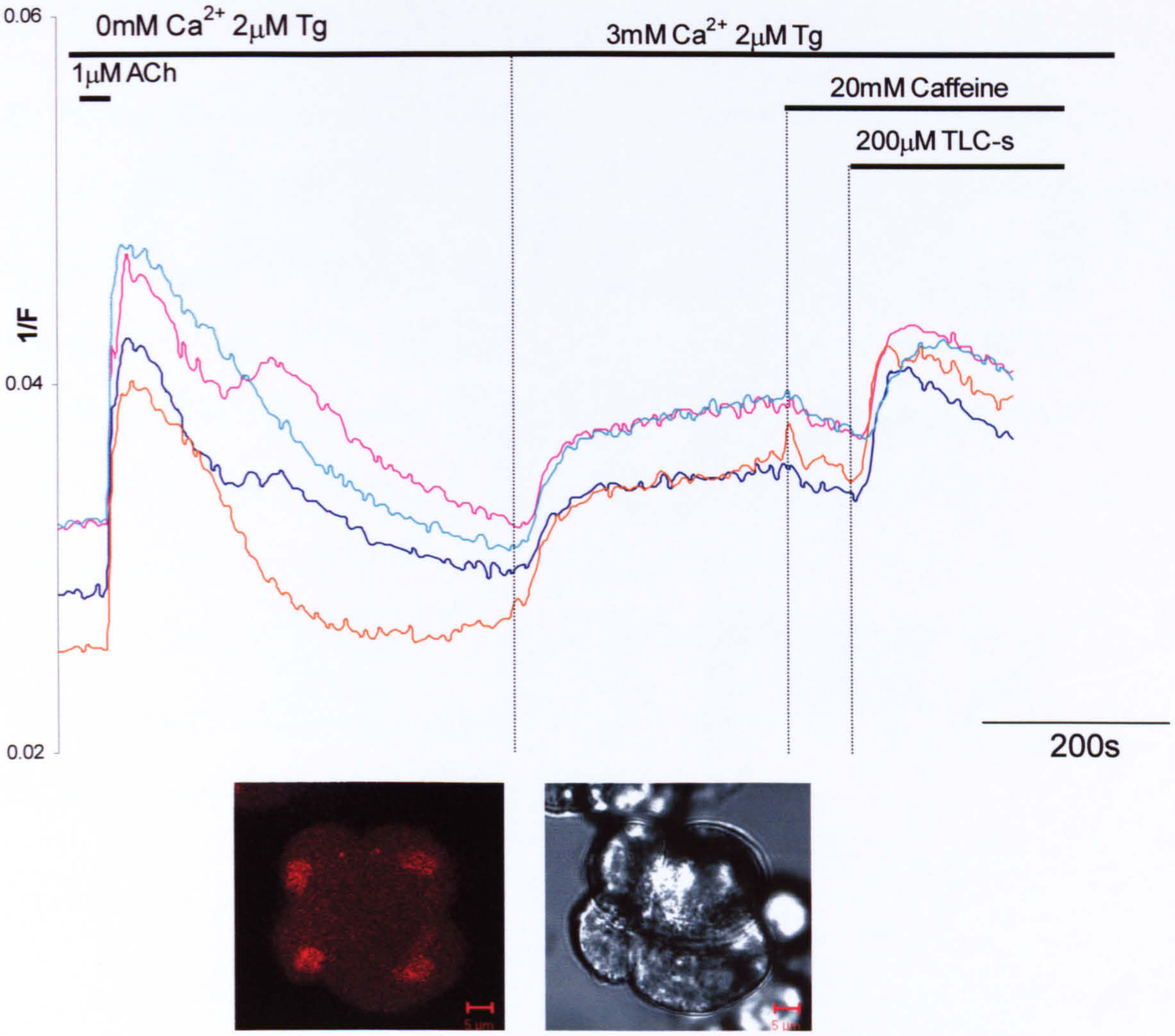

Figure 4.6 **Effect of TLC-S on a calcium plateau in the presence of caffeine** Cells were loaded with Fura-red and treated with ACh and thapsigargin in zero external calcium. After that 3mM external calcium was reintroduced and a cytosolic calcium plateau built. The application of 20mM caffeine resulted in a small decrease of fluorescence. Finally TLC-S was applied in the presence caffeine. Each colour line represents an individual cell, the fluorescence and transmitted light images are shown below (scale bar 5μm). Fura red measurements are inverted (fura red fluorescence decreases upon binding calcium).

The effect of TLC-S on Mag fluo-4 loaded stores

Monitoring calcium in internal stores using a fluorescent indicator with a high K_d for calcium, allows detection of calcium in compartments with high concentrations such as those typically seen in internal stores. In an attempt to identify any store which loses calcium upon TLC-S application and hence the source of the calcium, cells were loaded AM with Mag Fluo-4. The same protocol was followed as for cytosolic measurements; regions of interest were drawn using the transmitted light images. However under this protocol no change in any of the regions was consistently observed during the response to TLC-S (n=8). The reason for lack of responses has not been further investigated. Contamination of the signal by cytosolic dye may mask any changes in internal calcium store levels.

Spatial characteristics of the TLC-S induced calcium response

In an attempt to localise the site of the increase in calcium induced by TLC-S, high-speed confocal imaging was performed. The response under normal calcium conditions was shown to develop in a specific pattern, always originating in the apical region (Voronina *et al.*, 2002). Cells were loaded with fluo-4 as a calcium indicator compatible with the laser lines of excitation available on the confocal. The same depletion and plateau building protocol was applied; high speed scanning (395ms per scan) was performed for the period of TLC-S application on the plateau. Different regions of the cells were analysed in order to try and identify any site of preferential calcium increase. The response to TLC-S is a slow building response and no differential increase of calcium was identified in any discreet region within the cell. These experiments (n=16) demonstrate that the calcium increases with the same time course in all regions across the cell, fig 4.7.

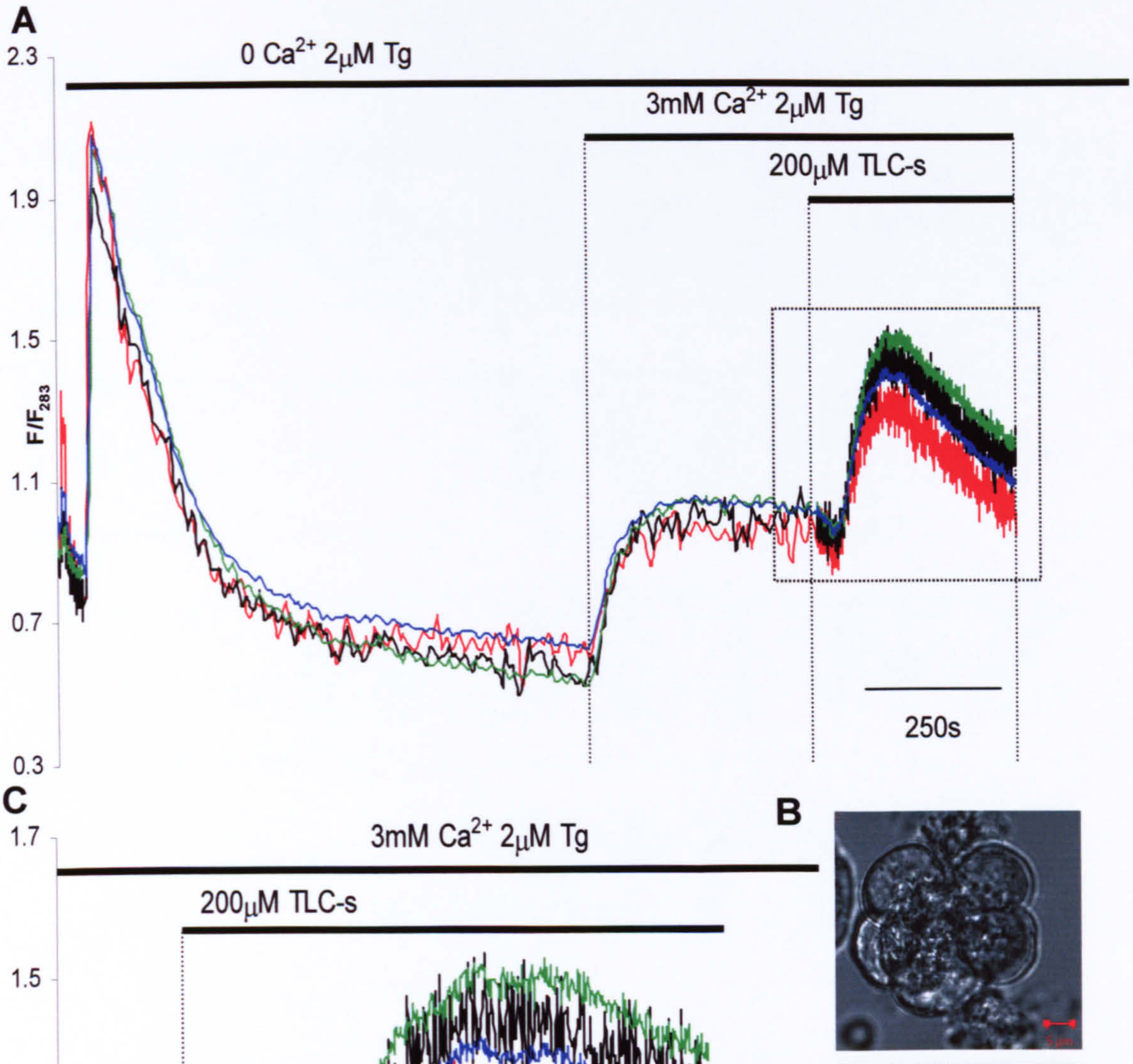
A
0 Ca2+ 2μM Tg
3mM Ca2+ 2μM Tg
200μM TLC-s
2.3
1.9
1.5
1.1
0.7
0.3
F/F283
250s
C
3mM Ca2+ 2μM Tg
200μM TLC-s
1.7
1.5
1.3
1.1
0.9
0.7
F/F283
apical
belt
basal
whole cell
50s
B
5 μm
5 μm

Figure 4.7 **High spatial and temporal resolution of the TLC-S-induced calcium increase** Cells were loaded with fluo-4, images were recorded using the confocal system The fluorescence changes during thapsigargin-induced depletion of calcium stores and cytosolic calcium plateau formation were recorded at an acquisition rate of 1 frame per 3 seconds. Before the application of 200μM TLC-S the acquisition rate was increased to approximately 2.5 frames per second (395ms per frame). This allows detailed analysis of the onset of the TLC-S-induced response within a single cell. The fluorescence changes were recorded from the regions of interest shown in **B** (bottom right). The colour of the traces correspond to the colour of the outlines of the regions of interest. (**B**) shows transmitted light (upper) and fluorescence (middle) images of the cluster (scale bar corresponds to 5μm). (**B**) also shows (lower image) the cell from which fluorescence was recorded and the selection of the regions of interest. (**C**) shows details of the part of the graph **A** outlined by the box. (**A**) shows the whole experiment. A single cell from a cluster has been analysed in 3 regions of the cell apical (red), belt region (black), basal (green) and the cell as a whole (blue)

CCCP sensitive organelles (thapsigargin or IP_3 insensitive) and their role in the TLC-S calcium response

Carbonyl cyanide 3-chlorophenylhydrazone (CCCP) is a protonophore, and collapses all proton gradients within the cell. Treatment with CCCP was one of the protocols used for testing the contribution of mitochondrial calcium to the TLC-S activated calcium increase. Short application of CCCP (400-500s) caused a release of calcium on top of the plateau recovering back to the level of the original plateau. However the subsequent increase by TLC-S was unaffected (figure 4.8 upper trace), 69% of cells (n=36) released calcium. But a longer exposure to CCCP >600s before application of the bile acid resulted in a further reduction of the number of cells showing an increase in calcium after TLC-S treatment to 27% of cells displaying an increase in calcium (n=22) (Fig 4.8 lower trace).

Another cellular structure of pancreatic acinar cells, which would be affected by a proton gradient collapse, are the secretory granules. They are known to hold a large amount of calcium. However the amount of calcium bound to proteins within the granule and the quantity that is free, remains unclear (Yoo & Albanesi, 1990;Gerasimenko *et al.*, 1996;Yoo & Jeon, 2000). CCCP application was shown to collapse the proton gradient in the granules as shown in figure 4.9 where the cells are loaded with lysotracker green. Lysotracker loads preferentially into acidic compartments such as the secretory granules. The regions of punctate high fluorescence shown in the images at the top of figure 4.9, localise to the apical pole

consistent with lysotracker loading of the secretory granules. Upon CCCP application the fluorescence drops demonstrating the collapse of the proton gradient, causing diffusion of the lysotracker which is no longer retained in the granules. The regions of interest corresponding to the granules (blue and pink traces) have a higher starting fluorescence in comparison to whole cell values (green and red traces) and demonstrate a steeper loss of fluorescence upon CCCP application. Therefore CCCP application should also prevent granule calcium storage. This suggests that the granules are not involved in the TLC-S activated calcium increase.

A more specific blocker of the granule proton gradient and hence calcium storage within the granules is bafilomycin. Bafilomycin is a specific V type H^+ATPase inhibitor, the type functional on the membranes of the secretory granules (Goncalves, 1998). Treatment of the cells with 100nM bafilomycin did not abolish the TLC-S activated calcium increase, 46% of cells (n=26) showed a subsequent calcium increase. 66% of cells (n= 9) treated with 300nM bafilomycin also showed a subsequent calcium increase in response to TLC-s application, Fig 4.10.

The possibility of mitochondria specifically, being the source of the TLC-S sensitive additional calcium released under these conditions, was addressed using rotenone and oligomycin. Rotenone an electron transport inhibitor and oligomycin an ATP synthase inhibitor, cause the proton gradient in the mitochondria matrix to decay, preventing the uptake of calcium and causing release of any calcium stored in the mitochondria (reviewed by (Duchen, 1999;Duchen, 2000)). Application of rotenone and oligomycin 400-500s prior to the application of TLC-S resulted in a small

increase of calcium on the plateau in 9 of 42 cases (due to release of calcium from within the mitochondria upon collapse of the proton gradient.). However rotenone and oligomycin treatment did not prevent the subsequent increase in calcium in 72% of cells (n=46) figure 4.11. Interestingly the drop in calcium plateau level seen in cells after TLC-S was not observed. Recovery after the increase was to the level of the original plateau (n=14) where the experiments ran long enough to make this assessment.

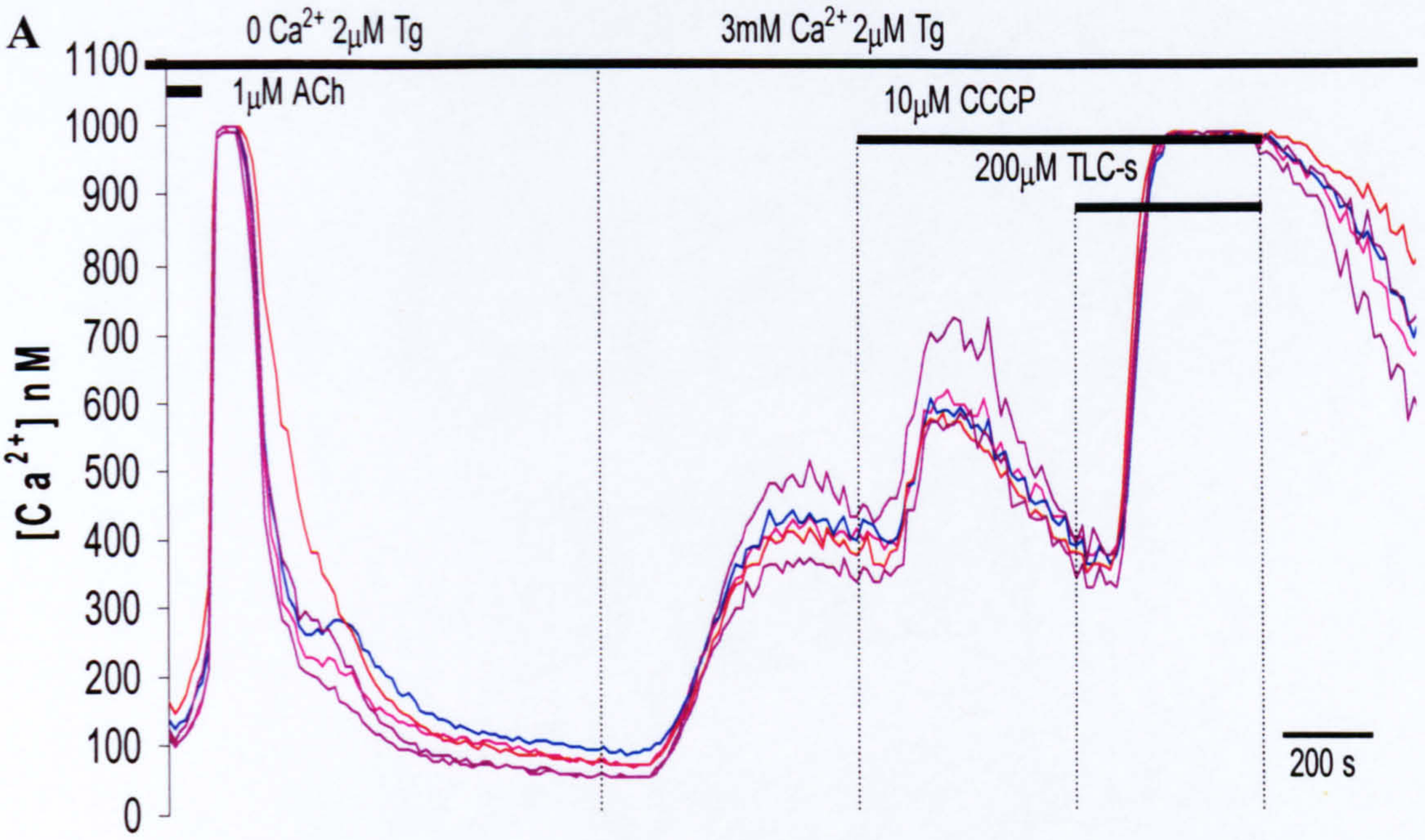

Figure 4.8 **The effect of CCCP application on the TLC-S induced rise of cytosolic calcium plateau**. **(A)** shows traces from an experiment where the cells have been exposed to CCCP after the formation of the thapsigargin-induced plateau. This was followed by TLC-S application in the continued presence of CCCP. Each line represents an individual cell. Part **B** of this figure is sown on the next page.

B

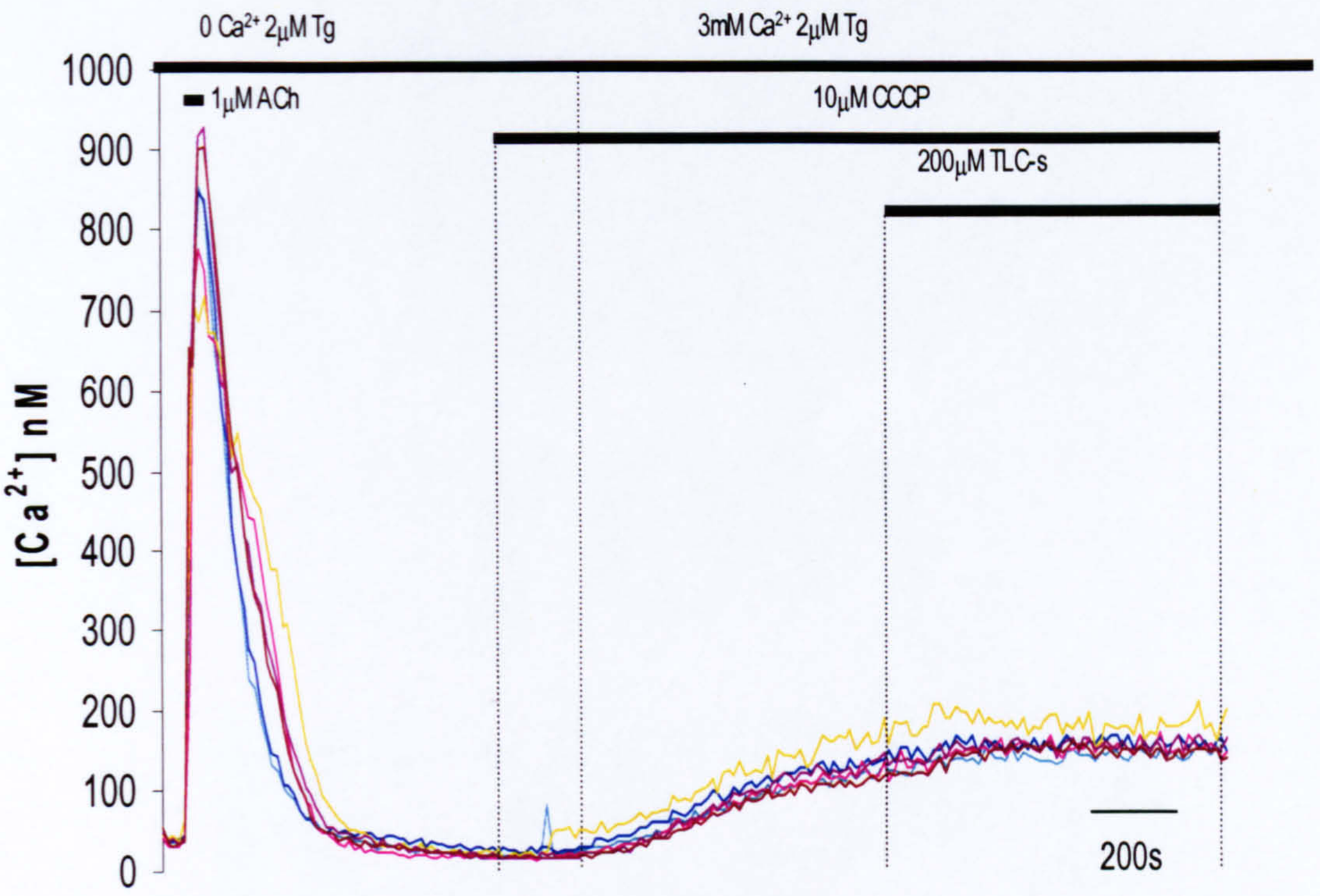

(B) shows an experiment in which CCCP was applied before readmission of calcium to external solution and maintained for the rest of the experiment. Subsequent application of TLC-S occurred in continued presence of CCCP. Each line represents a single cell. Part **A** of this experiment is shown on the previous page.

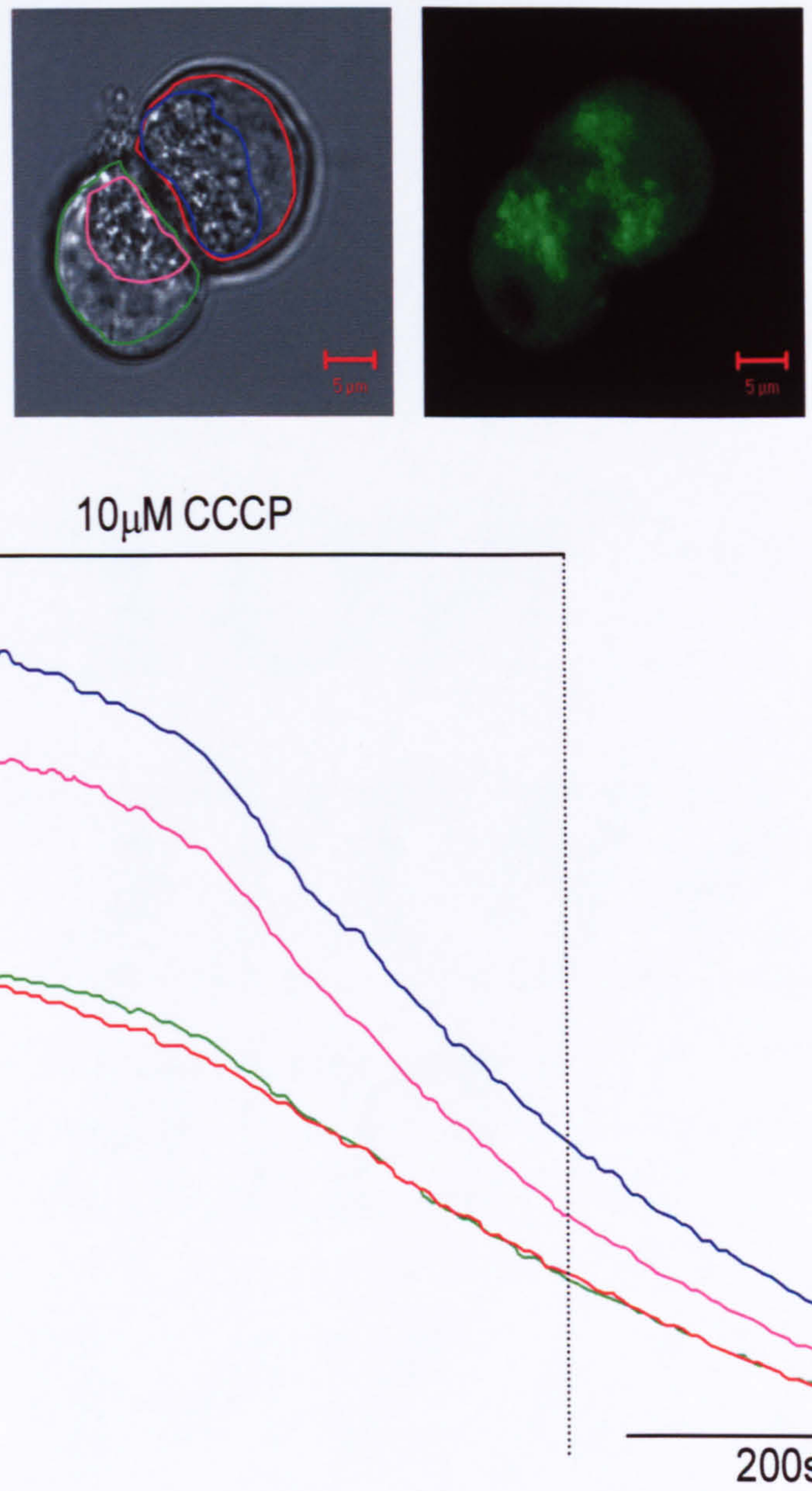

Figure 4.9 **The effect of CCCP application on Lysotracker fluorescence of cells and granular regions.** An example of a doublet that has been loaded with a dye that preferentially loads acidic compartments, lysotracker green. The transmitted and fluorescence pictures show the dye localised to the apical pole in the secretory granules. The fluorescence traces were taken from both cells (from regions shown on the transmitted light image). The bar shows the time of application of 10µM CCCP. The line colours correspond to the colours of regions of interest shown on the transmitted light image above (scale bar 5µm).

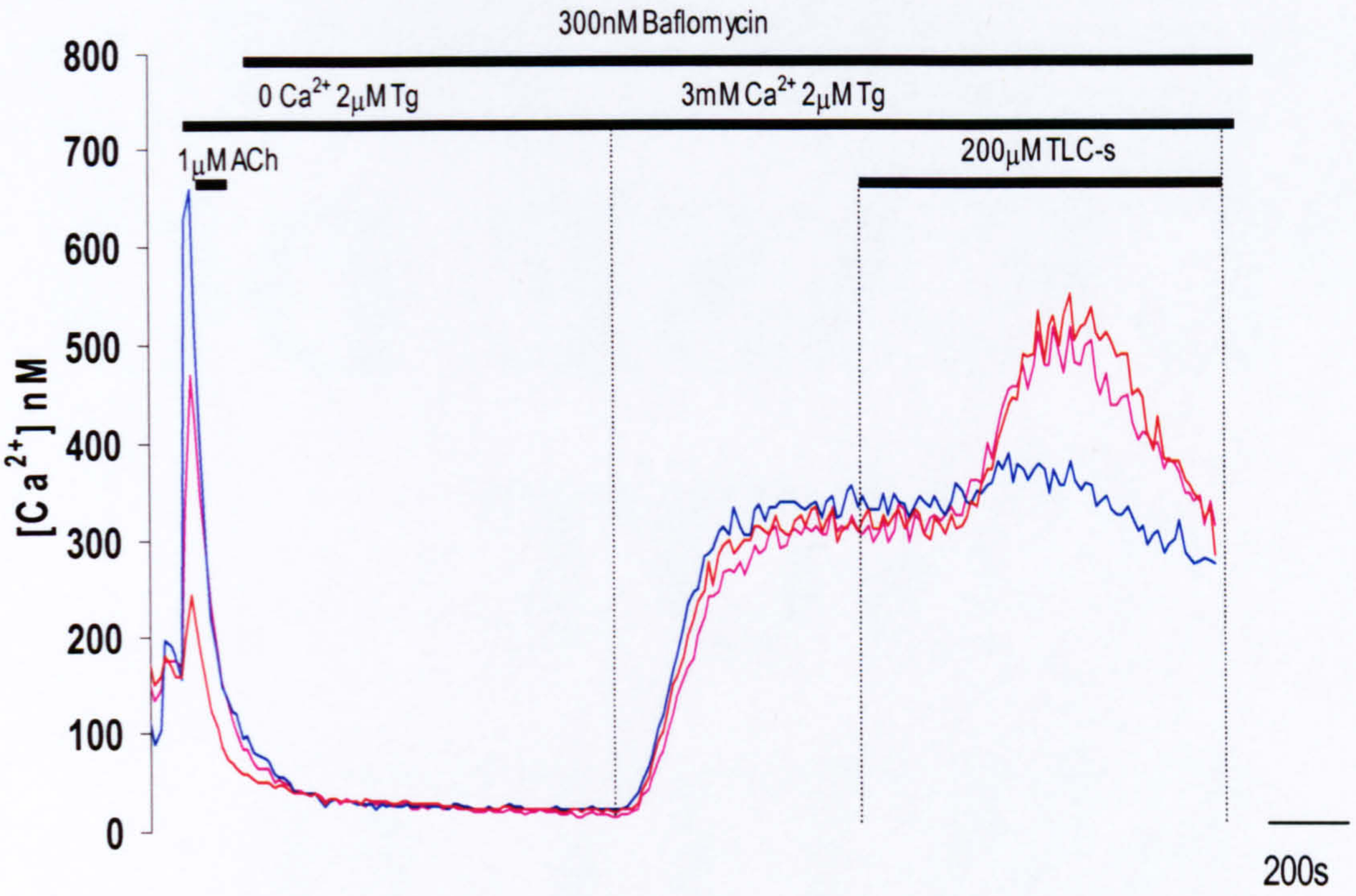

Figure 4.10 **The effect of bafilomycin on a TLC-S-induced rise of the cytosolic calcium plateau** Fluorescence was recorded from fura-2 loaded cells. The depletion of the calcium stores was followed by application of bafilomycin. The readministration of calcium to external solution and the application of TLC-S were done in the continuous presence of bafilomycin. Each trace represents a single cell.

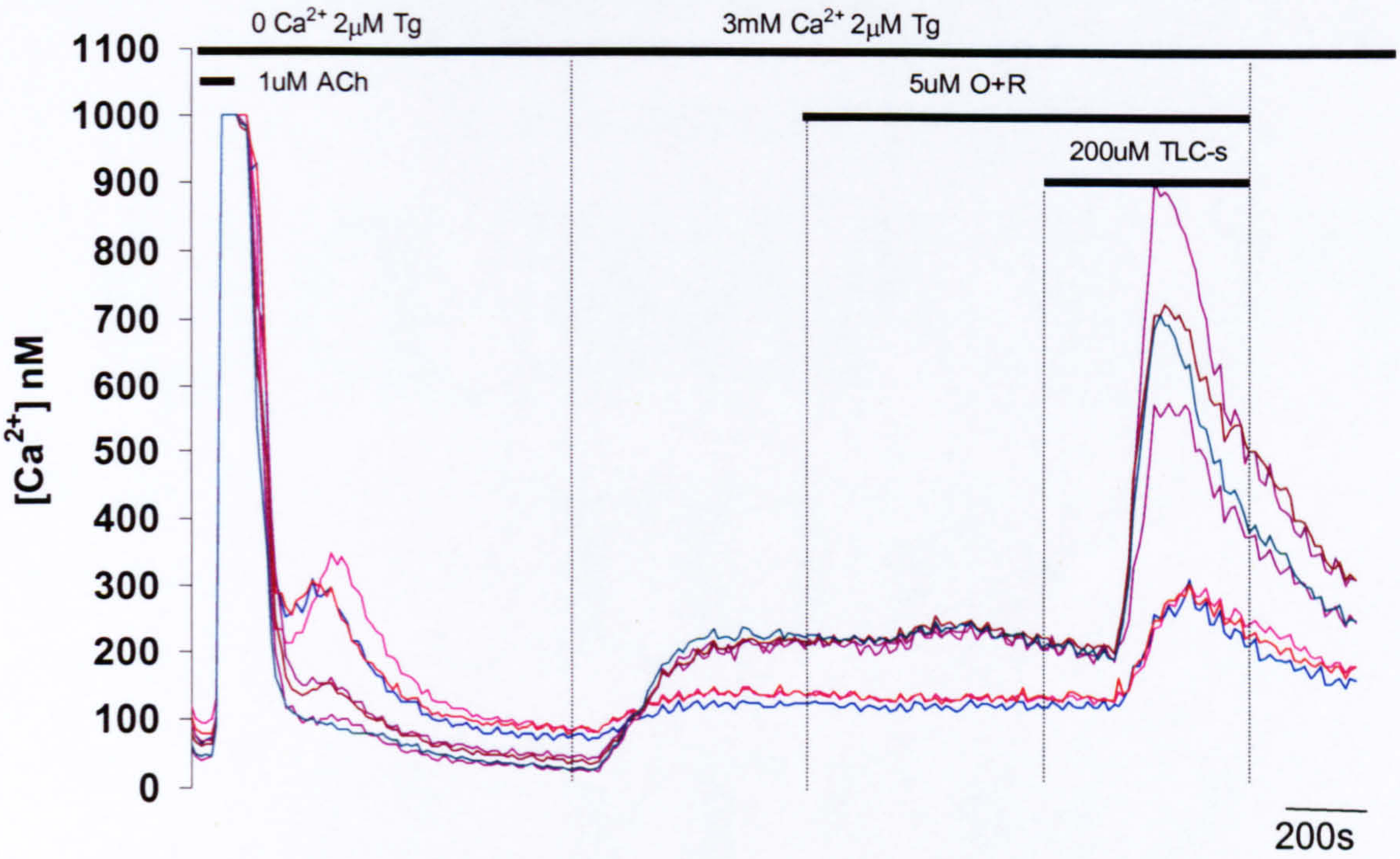

Figure 4.11 **Effect of oligomycin and rotenone on TLC-S induced rise of cytosolic calcium plateau**. Fura-2 loaded cells were used in this experiment. Oligomycin (5μM) and rotenone (5μM) were applied simultaneously after the plateau was formed. TLC-s was applied in the continued presence of the mitochondrial inhibitors. Each line represents a single cell.

Involvement of the Golgi apparatus in the TLC-S induced calcium response

An organelle whose role in intracellular calcium signalling is poorly understood is that of the Golgi apparatus. Recent investigation in other cell types, examining the role of the Golgi specific calcium pump pmr1 indicated that the Golgi had the ability to store and release calcium (Missiaen *et al.*, 2002a). These studies also suggested that there was a portion of Golgi stored calcium which was not released by application of IP_3 (Missiaen *et al.*, 2002a). A compound brefeldin A, inhibits membrane trafficking from the ER to the Golgi apparatus, causing Golgi disassembly and swelling of the ER. This has been shown to inhibit early events in the exocytic pathways, protein transport between the ER and Golgi (Hendricks *et al.*, 1992). Kömhoff and colleagues previously demonstrated that this compound efficiently disassociates the Golgi in rat pancreatic acinar cells at 10μg/ml after 1hr incubation (Komhoff *et al.*, 1994). It has been recently shown in work by N. Dolman that this is also the case in acutely isolated mouse pancreatic acinar cells (poster presentation). In my experiments, incubation of the cells with 10μg/ml Brefeldin A for at least 1hr at 37°C, conditions previously shown to allow disassociation of the Golgi was then followed by loading with calcium indicator, fura-2. The same protocol was followed as previously described, and TLC-S was applied after depletion of the stores and subsequent formation of calcium plateau, figure 4.12 (All solutions contained 10μg/ml Brefeldin A). The further increase of calcium upon TLC-S application occurred in 71% of cells (n=14), a frequency comparable to that observed without treatment with Brefeldin A.

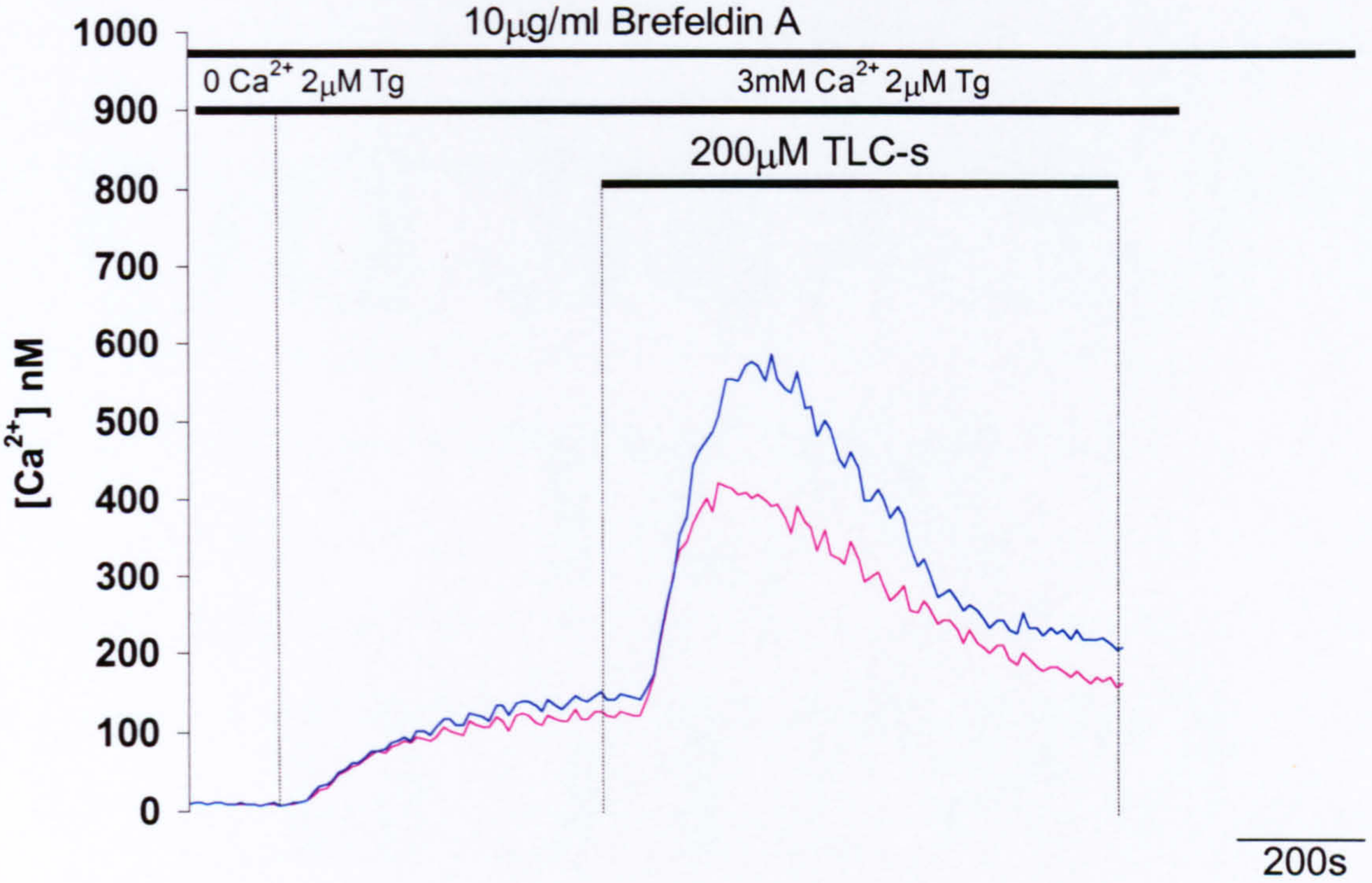

Figure 4.12 **The Effect of Brefeldin A on the TLC-S –induced calcium rise of cytosolic calcium plateau**. these experiments were performed after 1.5Hrs pre-incubation with brefeldin A at 37°C. During the experiment the formation of plateau and subsequent application of TLC-S were also performed in the continuous presence of brefeldin A. Each trace represents a single cell. Fura-2 loaded cells were used in this experiment.

TLC-S induced calcium responses after short-term calcium elevations

The TLC-S induced increase in calcium after thapsigargin treatment was dependent upon the exposure to high external calcium. No increase in calcium was detected if there had been no previous increase in external calcium (n=23) figure 4.13. The exposure to high external calcium under these conditions is to simplify the study of influx and efflux mechanisms. It is not however a physiological relevant condition. During physiological calcium signalling the calcium would be at high levels, such as the levels of the plateau, for short periods of time only. In order to examine the TLC-S induced responses under more physiological conditions, a protocol that involved the depletion of the thapsigargin sensitive store and then mimicry of a global calcium wave such as those induced by high concentrations of secretagogue was applied. In order to achieve high levels of cytosolic calcium quickly, thapsigargin treated cells were exposed to external solution containing 10mM calcium for a short period of time. Then the external calcium concentration was reduced to 0mM or 3mM to mimic the downward recovery phase of a physiological response. Shortly after reducing the external calcium concentration to 0mM (figure 4.14A), TLC-S was applied and 20% of cells demonstrated a further small increase of calcium. TLC-S-induced calcium rise was detected in 79% of cells when external calcium drops to 3mM (figure 4.14B), demonstrating further calcium increase of a magnitude comparable to that seen for a normal plateau protocol.

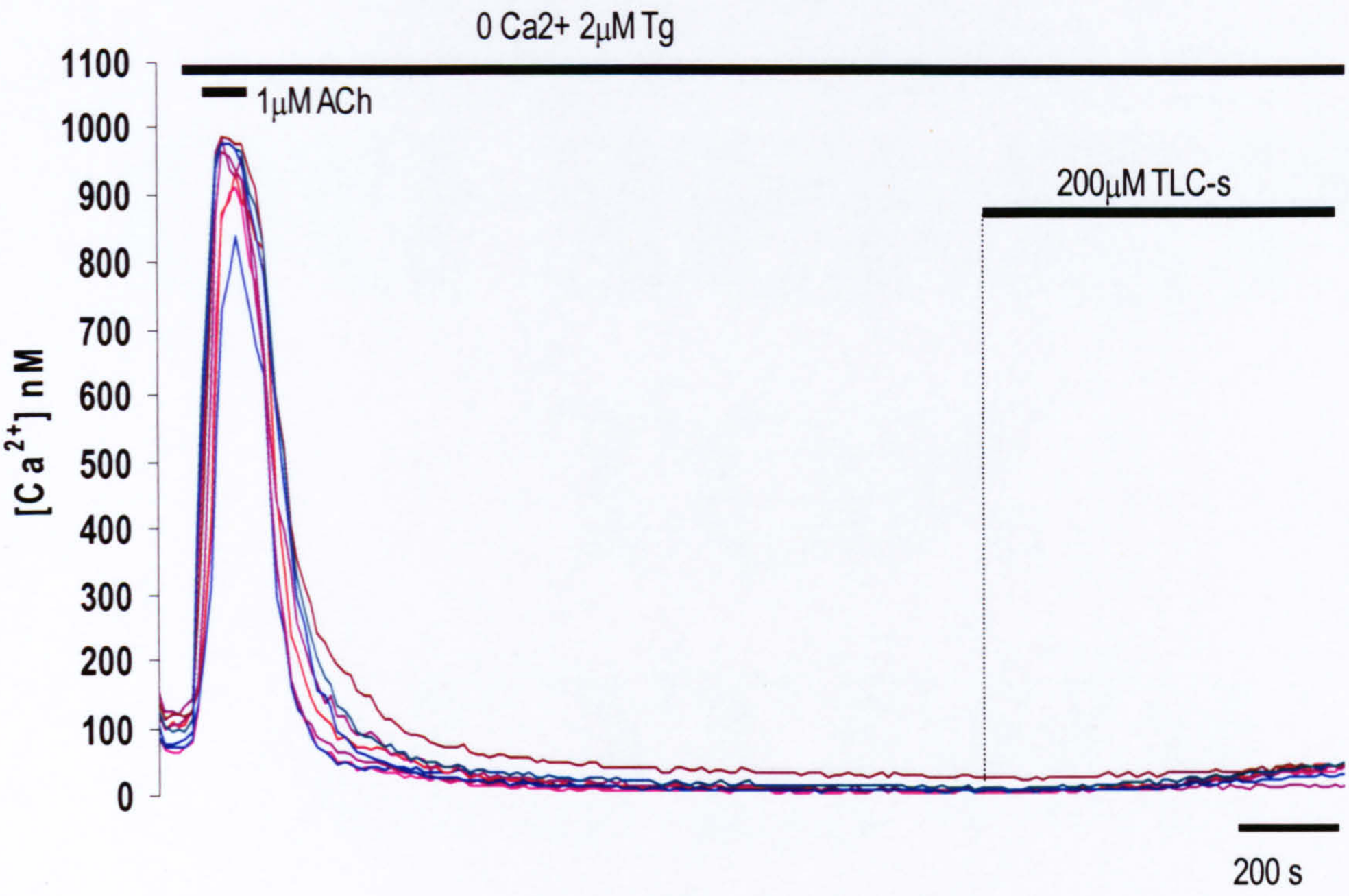

Figure 4.13 **In thapsigargin treated cells TLC-s does not induce a calcium rise when applied at low cytosolic calcium.** Fura-2 cells were used in this experiment. There was no readmission of external calcium before TLC-S application. Each line represents an individual cell.

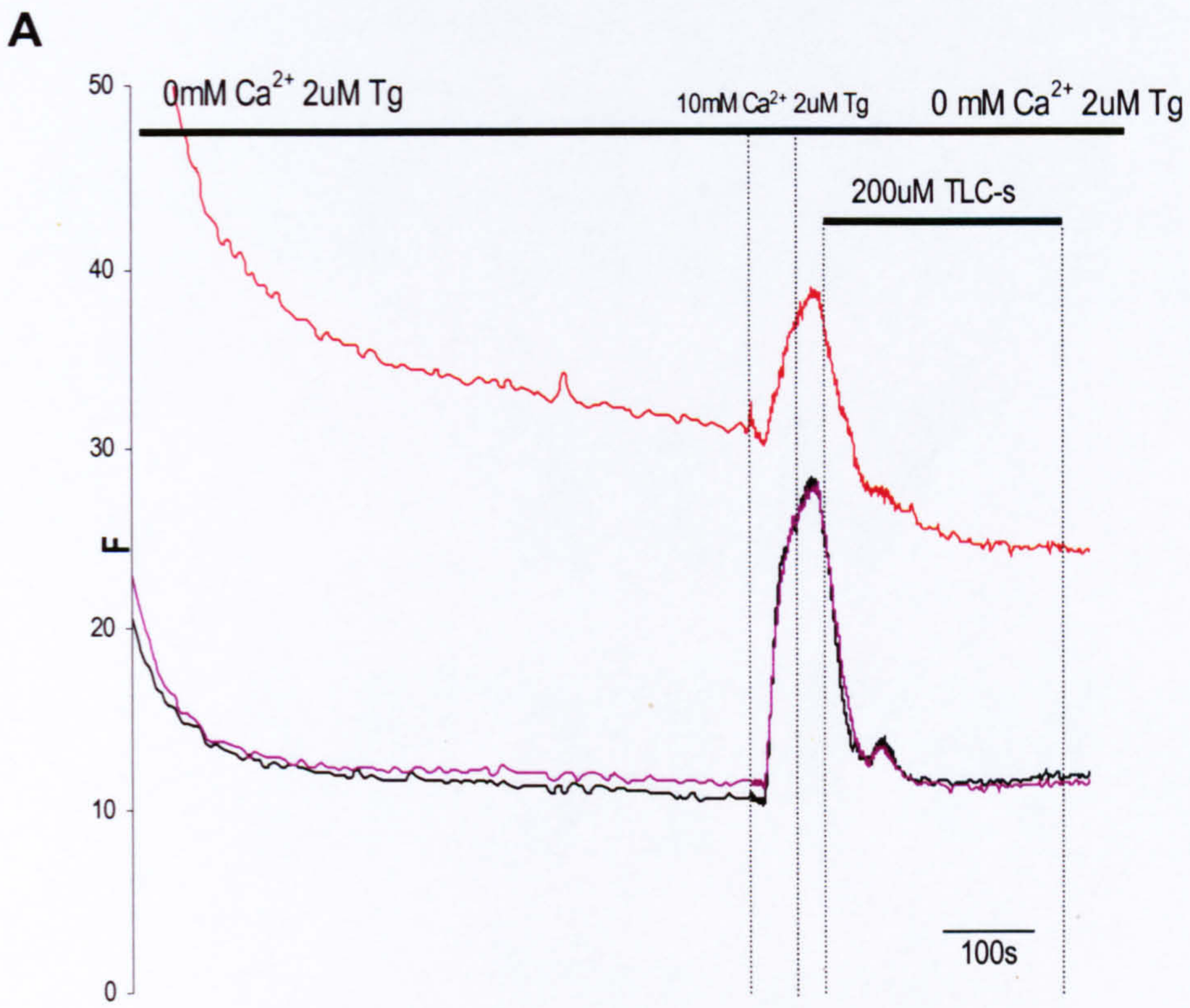

Figure 4.14 **TLC-S-induced responses after short term calcium elevations** Fluo-4 loaded cells were used in this experiment. (**A**) Cells were treated with thapsigargin to deplete internal stores followed by a short application (50s) of 10mM external calcium. TLC-S was applied ~30secs after returning to zero external calcium. Each trace represents a single cell. Part B of this figure is shown on the following page.

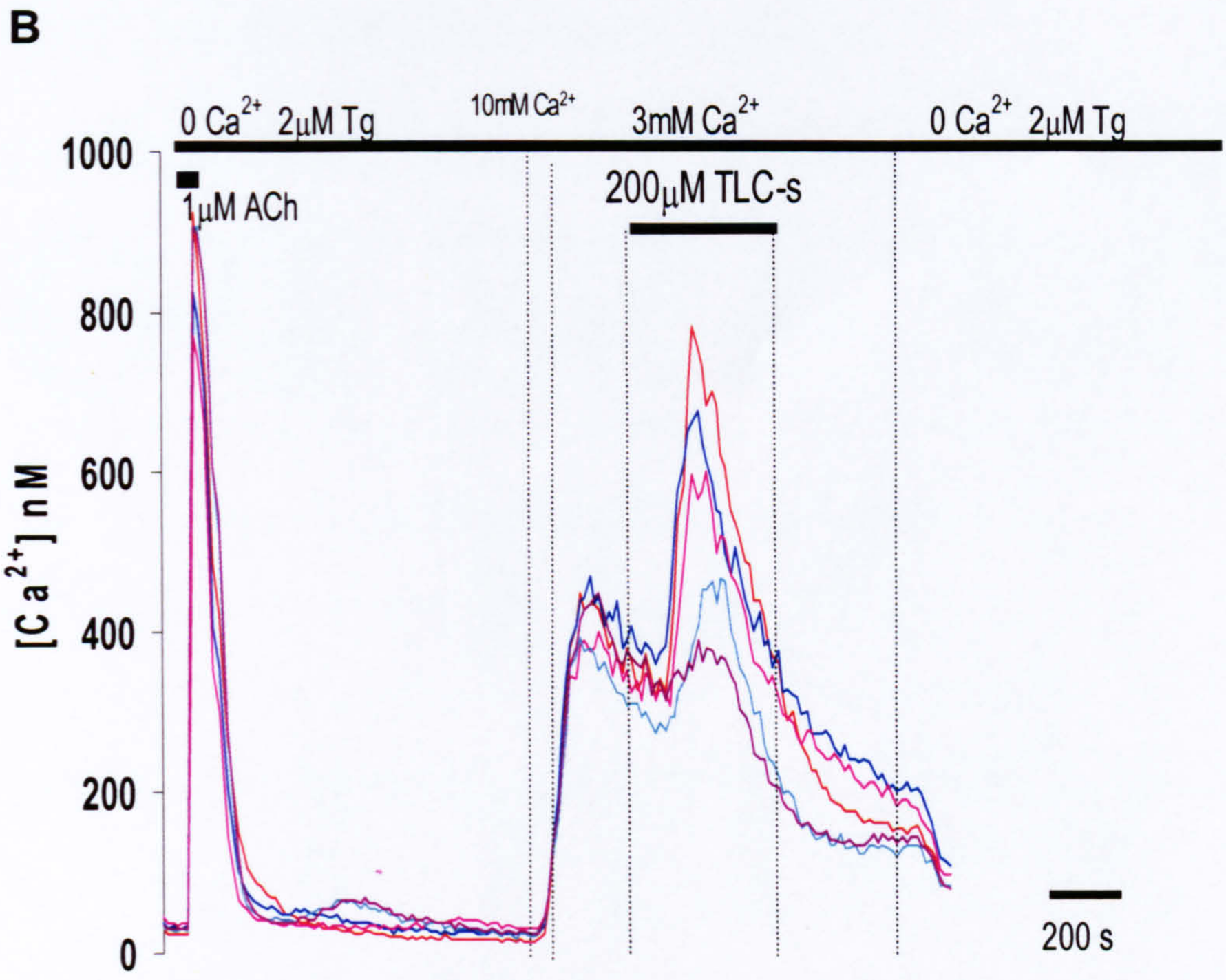

(**B**) shows responses recorded from cells that are loaded with Fura-2. In this experiment short exposure to 10mM external calcium was followed by perfusion with 3mM external calcium The period of TLC-S application is shown by the bar. External calcium was removed at the end of the experiment. Individual cells are represented by different coloured lines. Part **A** of this figure is shown on the previous page.

TLC-S responses following global uncaging of calcium

A different protocol using uncaging of calcium within the cell to mimic a physiological calcium signal was also performed. Caged calcium was AM loaded into the cells simultaneously with the fluorescent calcium indicator fluo-4. Depletion of internal stores using thapsigargin was followed as previously described. Whole cell calcium uncaging, as indicated by the pink arrow in figure 4.15, was achieved using a UV flash in zero external calcium, and a subsequent increase in calcium was observed. TLC-S was then applied on the downward phase of the calcium transient induced by uncaging. No further increase was observed after the calcium transient produced by uncaging (n=12).

TLC-S response following fast removal of external calcium

The transient nature of the increase in response to TLC-S argues against a permeablisation effect of TLC-S, however the actions of TLC-S on calcium influx mechanisms within the cell are unknown. Experiments were done to investigate the role of external calcium during the bile acid evoked transient. The depletion protocol followed by calcium plateau formation was used as before. However external calcium was removed rapidly before application of the bile acid, utilising a fast perfusion system where the perfusion chamber was fully exchanged in 4 sec (calibration done by S. Voronina). No significant further increases in calcium due to TLC-S application (n=10) were detected whereas the control response (without the removal of external calcium) remained intact (figure 4.16). There was in a few cases (3 out of 10) a very small rise of calcium upon application of the TLC-S. However the effect is most significantly attenuated.

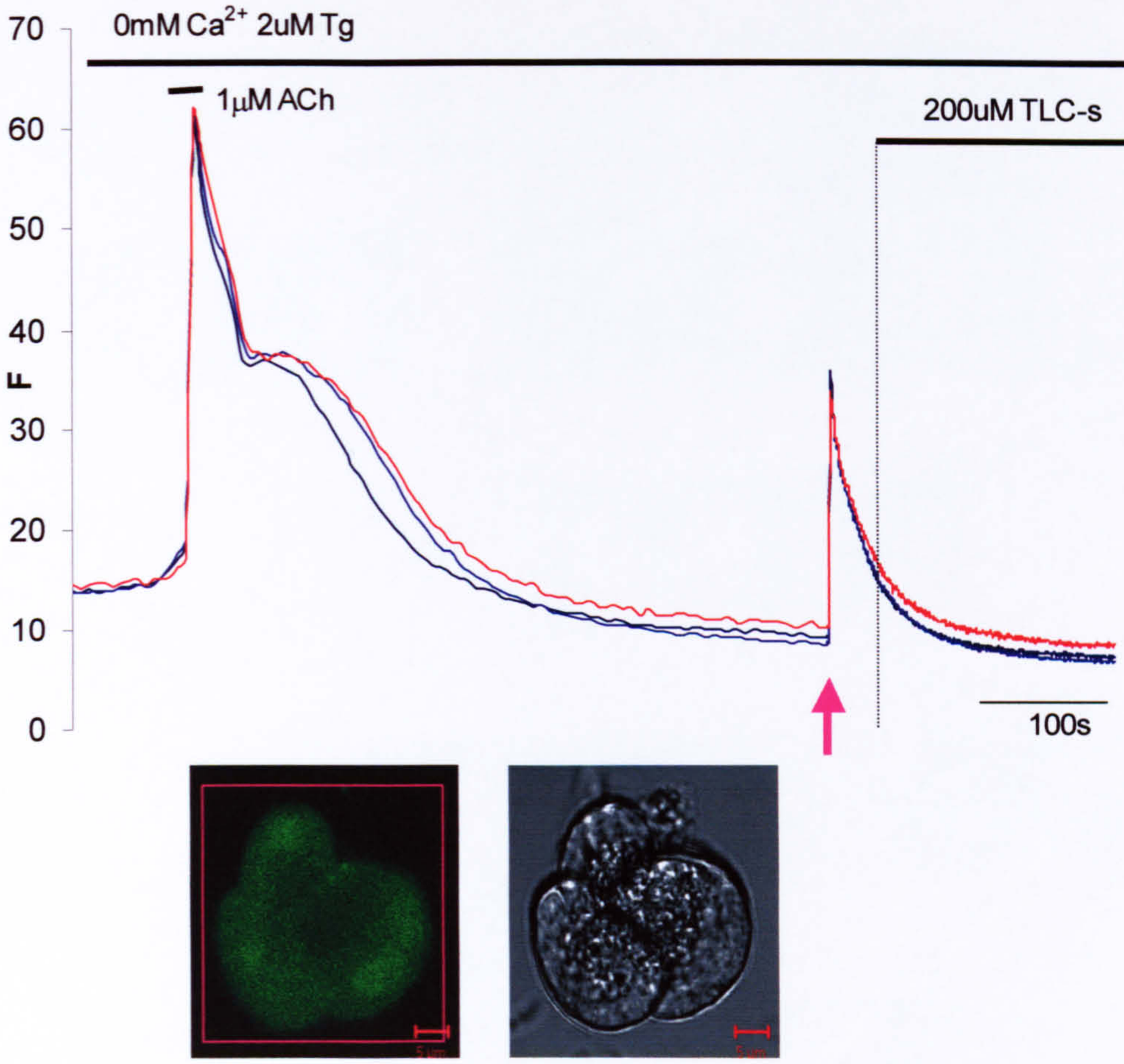

Figure 4.15 **TLC-S application after global calcium uncaging**. Three cells are shown in the fluorescent (left) and transmitted light (right) images below (scale bar 5μm). Cells were loaded with fluo-4 and NP-EGTA. The thapsigargin/Ach depletion of internal stores was performed followed by a global uncaging of calcium by UV illumination (at the moment indicated by the pink arrow). The pink box on the fluorescent image corresponds to the region of uncaging. TLC-S was applied during the downward phase of the calcium recovery, the period of TLC-S application is shown by the bar in the upper part of the figure. Each line represents a single cell.

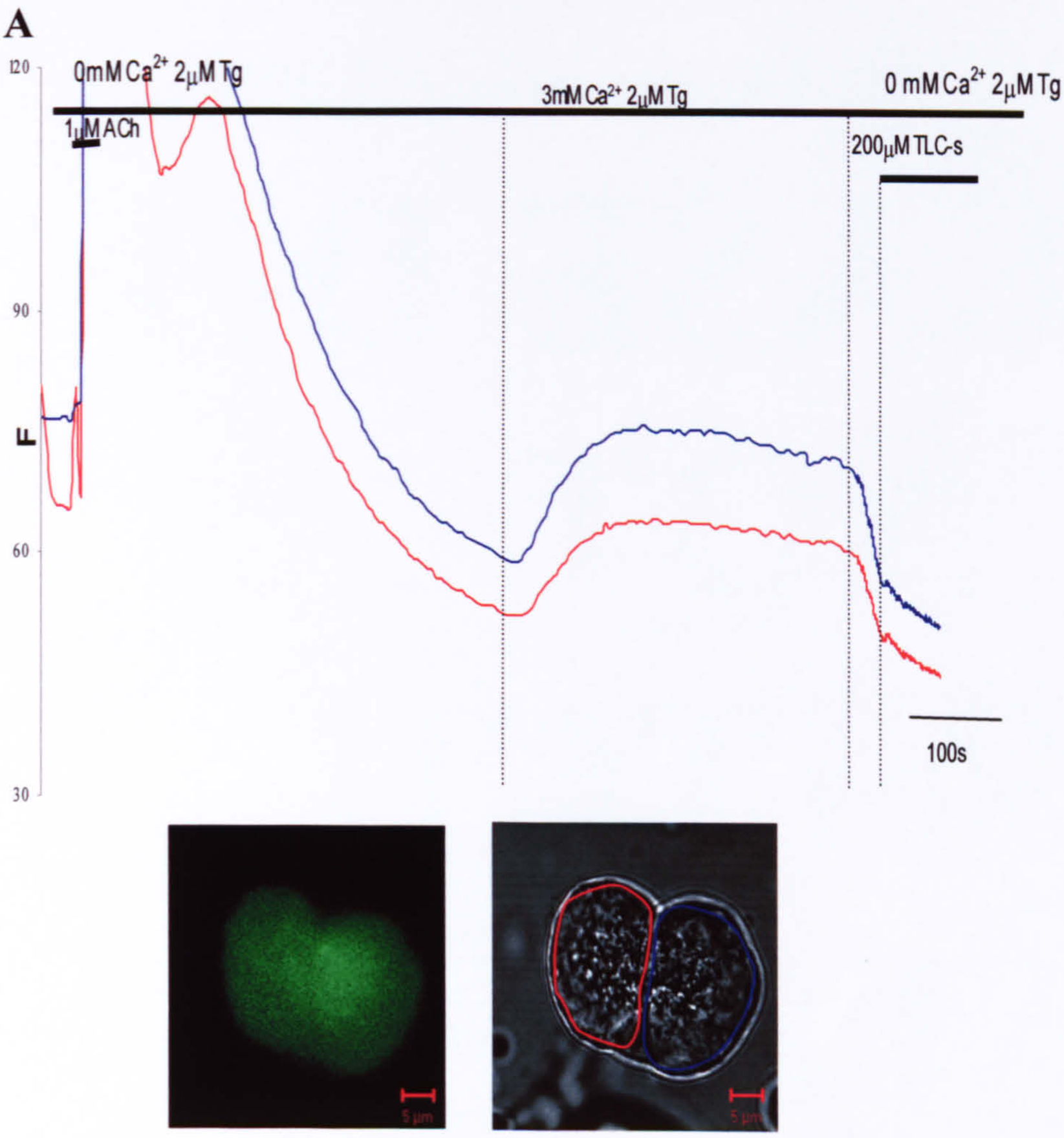

Figure 4.16 **The fast removal of external calcium following formation of a cytosolic calcium plateau and the effect of this procedure on the TLC-S-induced calcium response** (**A**) Shows an experiment where after establishing a cytosolic calcium plateau external calcium was rapidly removed by a very fast perfusion system and TLC-S applied (30s after calcium removal). The colour of the traces correspond to the colour of the outlines of the regions of interest (see transmitted light image- bottom right) cells were laded with fluo-4, the fluorescence image is shown on the bottom left part of the figure. Part **B** of this figure (control experiment) is shown on the next page.

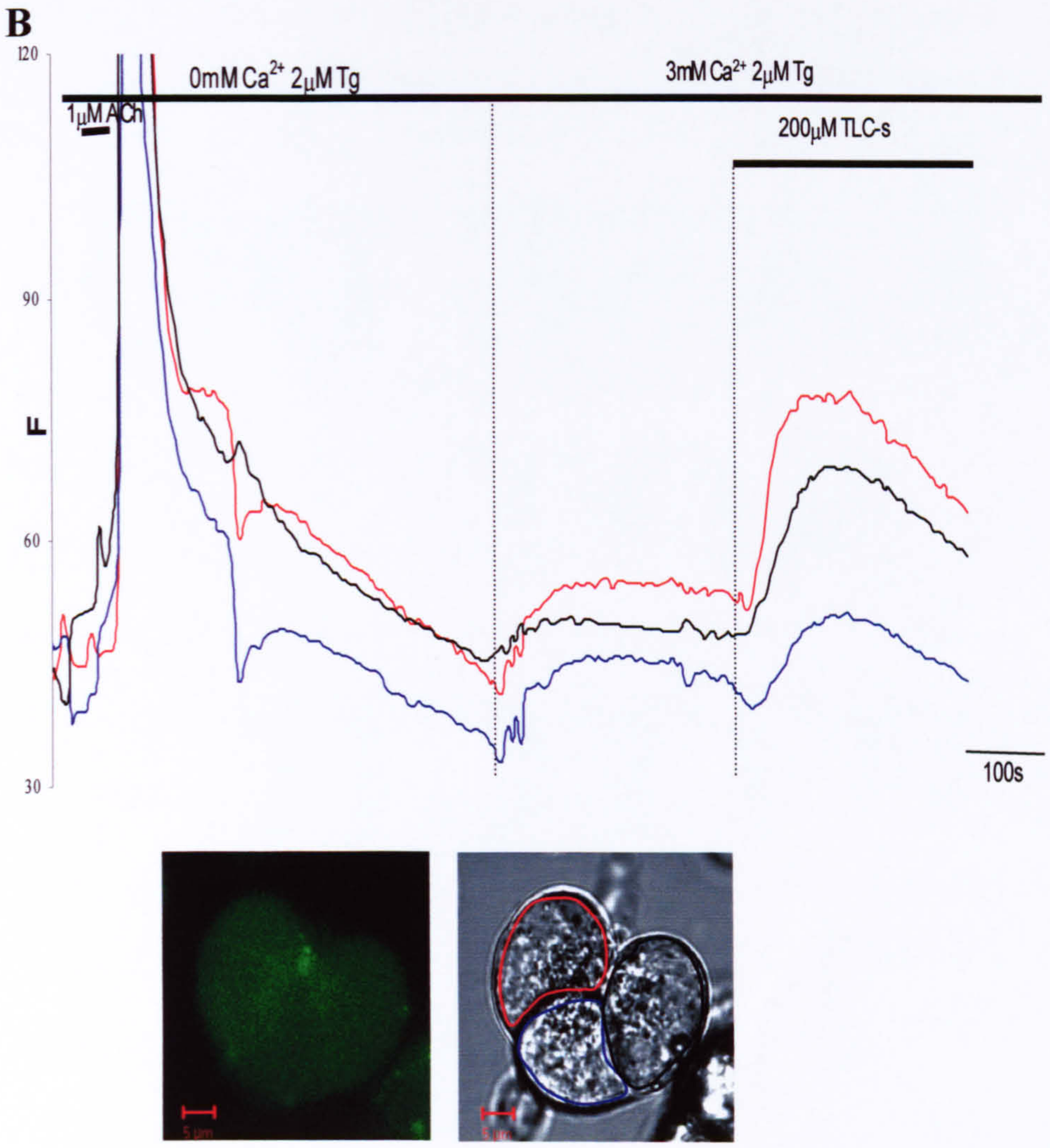

(**B**) Shows a control response to the application of TLC-S after formation of calcium plateau (recorded from the same cell preparation as **A**). Each trace represents a single cell. The colour of the traces correspond to the colour of the outlines of the regions of interest shown on transmitted image (bottom right). The fluorescence image of fluo-4 loaded cells is shown in the bottom left part of the figure. Part **A** of this figure is shown on the previous page.

TLC-S induced Calcium rise in the presence of Lanthanum ions

The experiments that involved the application of TLC-S after fast removal of external calcium suggest the participation of calcium influx in the TLC-S response. I used Lanthanum ions (La^{3+}), which have been shown to block influx via calcium-release-activated calcium channel (CRAC)(Hoth & Penner, 1992), to further investigate calcium influx contribution to the TLC-S response. A concentration of 30μM La^{3+} was used to avoid compromise of the PMCA activity (Toescu & Petersen, 1995). 30μM La^{3+} was applied in the presence of high external calcium after formation of the cytosolic calcium plateau. A gradual reduction in the plateau was observed as expected, confirming the action of La^{3+} on the influx mechanisms. TLC-S was then applied (60-100s after beginning La^{3+} exposure). The transient increase of calcium in response to TLC-S was not blocked by La^{3+} in 20 out of 25 cells (80%) as is shown in figure 4.17, where two of the three cells (blue and purple lines) show a small increase in calcium as a result of TLC-S application. The third cell (red line) does not show any calcium response to the TLC-S application. Overall there seems to be an attenuation of the TLC-S induced increase of calcium after La^{3+} treatment. The amplitude of TLC-S response was 24.4 ± 12.5 (S.E.) (n=20) % of the plateau in the presence of La^{3+} in comparison to 62.6 ± 7.7 (S.E.)(n=85) with no La^{3+} treatment.

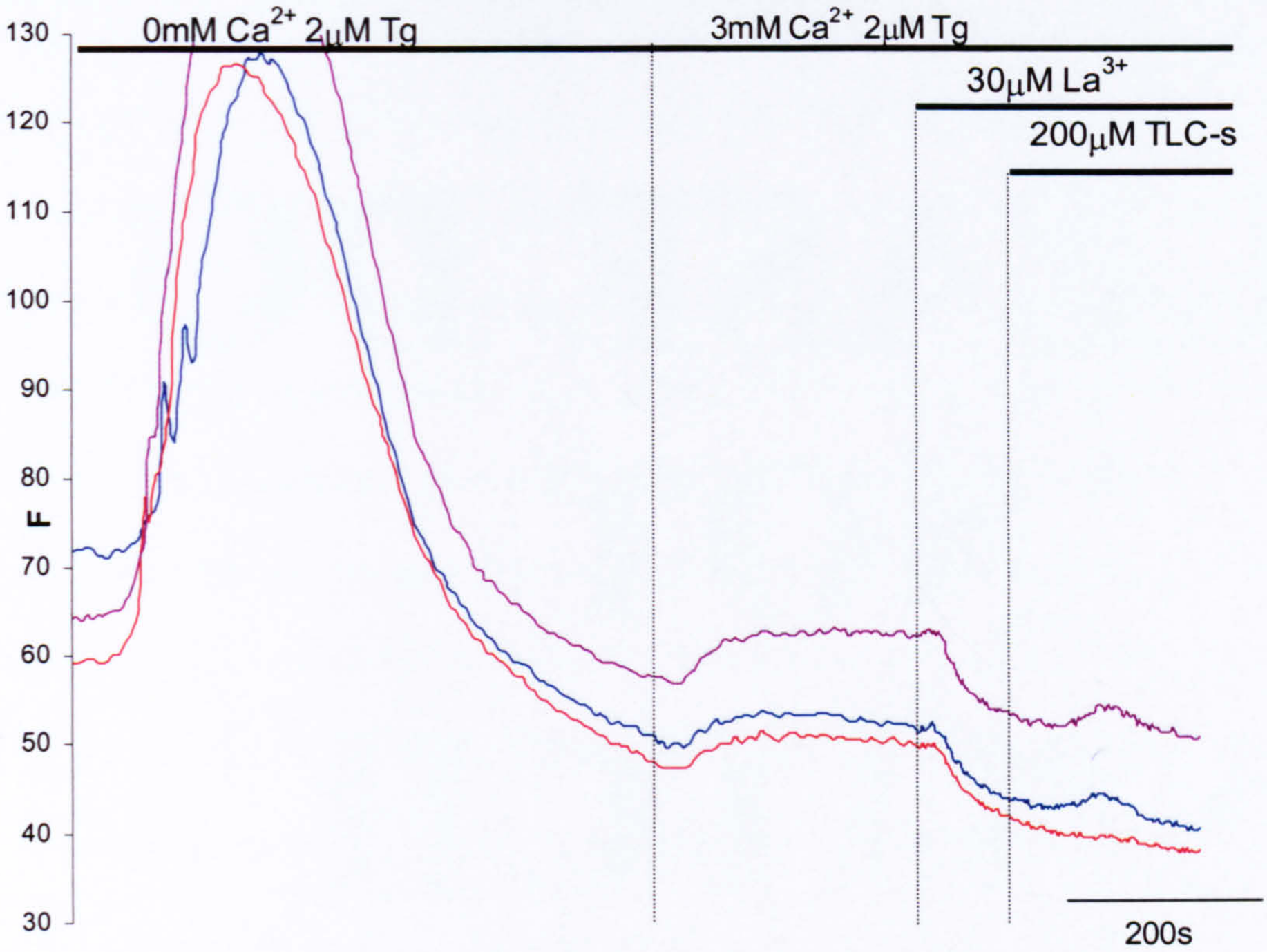

Figure 4.17 **Inhibition of calcium influx by La^{3+} and the effect of La^{3+} on the TLC-S induced calcium increase** After the usual procedure of formation of a cytosolic calcium plateau La^{3+} was applied to inhibit calcium influx (note decrease of cytosolic calcium following La^{3+} application). TLC-s was applied in continued presence of La^{3+}. Each trace represents a single cell.

TLC-s effects on acutely isolated pancreatic acinar cell morphology

Bile acid pancreatic infusion is used as an *in vivo* model of pancreatitis (Steer, 1999). In the study by Raraty and colleagues examining the role of calcium elevation in pancreatitis, vacuole formation in acutely isolated cells was used as a measure of pancreatic cell damage (Raraty *et al.*, 2000). This is comparable with cell damage observed in pancreatitis animal models. The examination of vacuole formation following exposure to concentrations of TLC-S known to induce calcium elevations was performed on acutely isolated cells. This analysis would lead to an indication of the degree of cell damage induced by bile acids on the pancreatic acinar cell. Treatment of the acutely isolated cells with 200μM and 500μM TLC-S was carried out at 37°C for 50mins. The cells were then fixed and processed for electron microscopy (EM) examination. Mrs J Henry of the veterinary faculty performed the processing and preparation of the cells for EM. A measurement of the area of the apical pole of the cell occupied by vacuoles and granules was carried out on images taken by EM. An example of an image from the EM studies is shown in figure 4.18. The cellular structures are labelled, and the dashed line indicates the area typically considered as the apical region. The values were expressed as a fraction area of the apical pole (a more detailed description of how these values were obtained is described in chapter 2 materials and methods). Figure 4.19 is a summary of 2 independent experiments, where the control cells were taken from the same preparations. Blue bars represent granule measurements and pink represent vacuole measurements. Treatment of cells with 200μM TLC-S made no statistically significant change (student ttest) to the fraction area occupied by granules in the apical pole or the fraction area occupied by vacuoles between control (n=13) and

treated cells (n=13). Treatment with 500μM TLC-S also made no statistically significant changes (student ttest) in the fraction area occupied by granules in the apical pole or fraction area occupied by the vacuoles in the apical pole between control (n=9) and treated (n=8) cells. These are preliminary results representing only one experimental preparation at each concentration; further work is required to clarify the effect of TLC-S on the granular and vacuole areas.

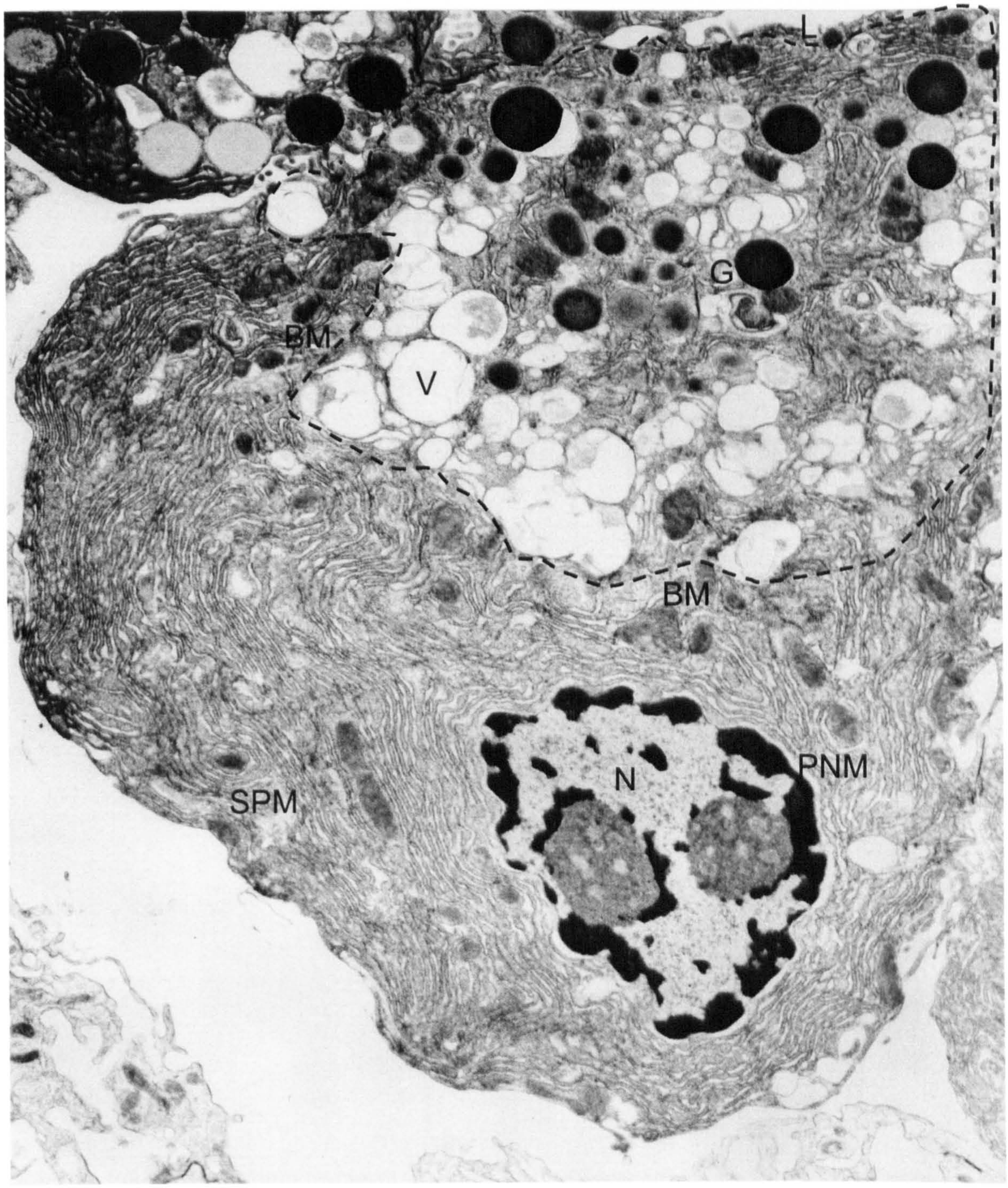

Figure 4.18 **Electron microscopy image of an pancreatic acinar cell**. The structures within the cell are labelled as: N=nucleus, SPM= subplasmalemmal mitochondria, PNM=perinuclear mitochondria, BM= belt mitochondria, G=granules, V=vacuoles, L=lumen and the dashed line indicates the region that is referred to as the apical pole for fraction area calculation.

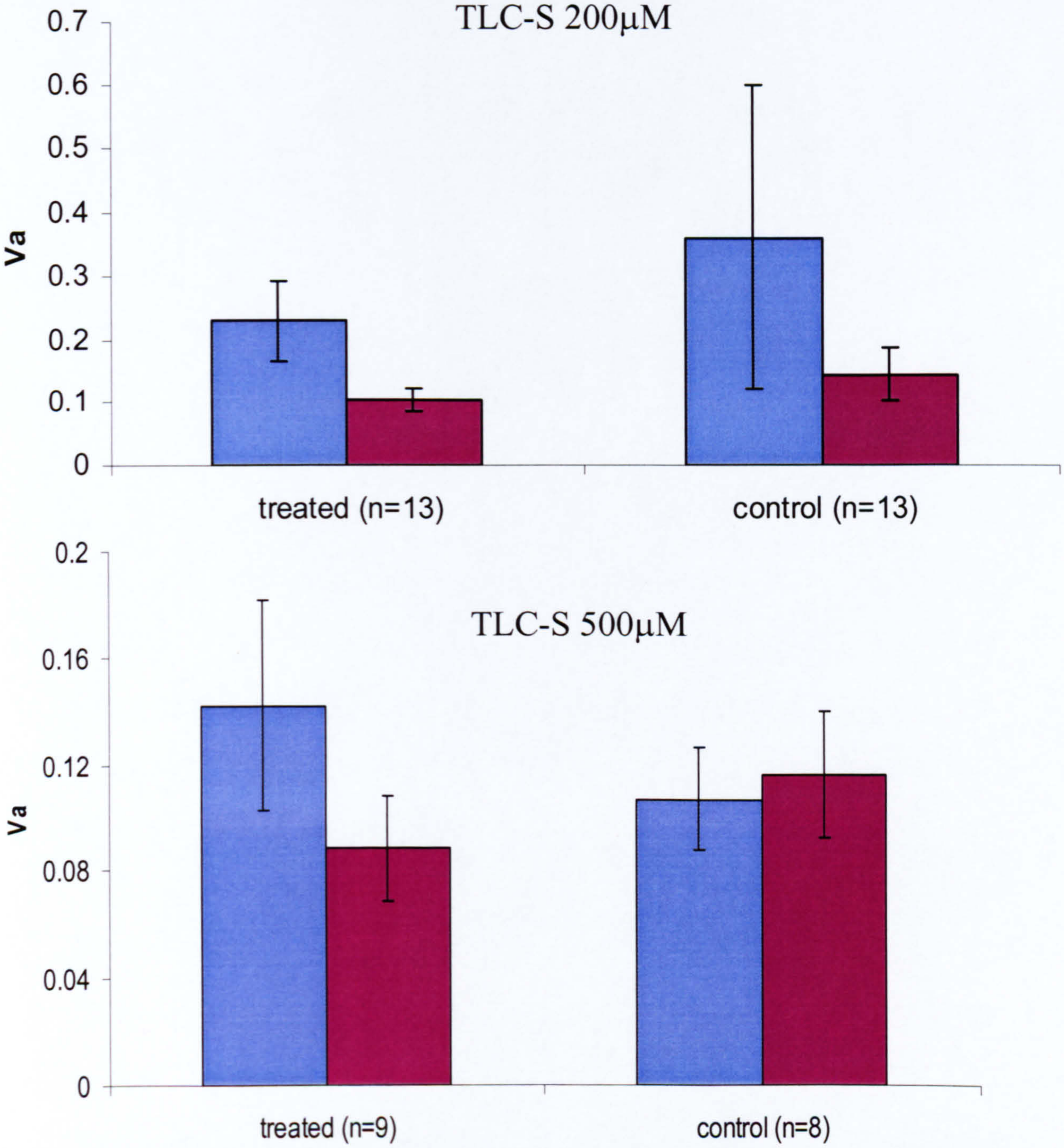

Figure 4.19 **Analysis of granule and vacuole fraction areas by Electron Microscopy examination** Summary of the analysis of vacuole and granule fraction areas of the apical pole in acinar cell preparations incubated with TLC-S at 37°C for 50minutes. One preparation was treated with 200μM TLC-S (TOP) and the other preparation was treated with 500μM TLC-S (BOTTOM). The Maroon bars represent the area of vacuoles ■ and the blue bars represent the area of granules ■. The standard (errors) are indicated on all graphs.

Discussion

The calcium plateaux in this series of experiments are formed by a dynamic equilibrium between influx mechanisms stimulated by the depletion of internal stores and efflux mechanisms. The response to TLC-S is of 2 types which result in 2 different effects. The first is an increase in calcium on top of the calcium plateau. The second TLC-S effect is a reduction of the calcium level of the plateau.

The first effect, an increase in calcium is a transient effect. The average increase is of ~200nM calcium measured by fura-2 fluorescent changes. The development of the calcium increase is a slow process, which means that discreet spatial identification of the source of calcium was impossible. Changes in internal store calcium measured by loading with Mag fluo-4, a dye suitable for measurements at higher concentrations as seen in the endoplasmic reticulum again revealed nothing of the source of this calcium increase.

Owing to the transient nature of the TLC-S responses it was initially considered that the responses were due to release of calcium from an intracellular organelle. Therefore elimination of intracellular organelles, potential sources of calcium within the cell, was performed using various pharmacological agents. The results from the oligomycin and rotenone experiments suggest TLC-S effects on the mitochondria are not responsible for the further increases on the calcium plateau. This was further supported by the results from the protonophore, CCCP applications. The short applications of CCCP on top of the plateau resulted in an increase of calcium recovering back to the level of the original plateau. Subsequent TLC-S application

resulted in an increase in calcium as seen previously. The longer applications of CCCP, where the building of the cytosolic calcium plateau was difficult, were more complicated to interpret. The ATP production, in the cells treated with agents that collapse the mitochondria, is unavoidably altered. The longer applications of CCCP will have a greater impact on the ATP state of the cell, due to the increased exposure times, the cell must function on a finite source of ATP for longer. The reduction to 27% of cells responding to TLC-S by an increase in calcium may purely be a symptom of the ATP depletion rather than an attenuation of the TLC-S calcium increase.

CCCP at concentrations used in these experiments in addition to collapse of the mitochondria will also affect the proton gradients within the secretory granules. This was confirmed by the reduction of lysotracker green fluorescence upon CCCP application (figure 4.9). CCCP treatment should therefore also result in the depletion of calcium from the granules in addition to the calcium lost from mitochondria. This would account for the consistently larger increase of calcium upon application of CCCP in comparison to that seen with oligomycin and rotenone treatment. The more specific targeting of the secretory granules calcium stores without compromising the ATP state of the cells was done using Bafilomycin. This again failed to block the subsequent calcium increase in response to TLC-S. Both these results suggest that the secretory granules are not the source of the calcium increase.

Investigation of the Golgi apparatus's role in the TLC-S employed the use of a compound Brefeldin A to dissociate the Golgi as discussed earlier. However no studies have examined the effects of Brefeldin A on calcium signalling within the

cell. The role of the Golgi apparatus in calcium signalling is difficult to study. Loading of the lumen of the Golgi with calcium sensitive dyes would be required to confirm the action of brefeldin A. Accurate reporting of intra-golgi calcium is difficult due to the lack of a Golgi specific calcium sensitive dye. Golgi loading may occur when using dye with a high calcium affinity like those used to monitor ER calcium. Though discrimination between loading in other organelles in the same region of the cell and the Golgi is impossible. In the experiments where internal store calcium measurements were performed, cells were loaded with Mag fluo-4, thought to load primarily into the ER. However after depletion of the ER using thapsigargin there was evidence of a compartment in the apical/basal boundary region that was still calcium loaded, due to the fluorescence of the trapped dye. This is the region where the Golgi apparatus has been shown to be located. The presence of mitochondria within the same region (Tinel *et al.*, 1999;Park *et al.*, 2001) however makes the identification of this compartment based on location alone difficult. Pinton and colleagues have also shown the thapsigargin sensitivity of the Golgi apparatus, where treatment with thapsigargin and 2,5-di-(*tert*-butyl)-1,4-benzohydroquinone (tBuBHQ) depleted the Golgi calcium store by 50%, measured using a Golgi targeted aequorin probe (Pinton *et al.*, 1998). This again makes the identification and study of the Golgi calcium stores difficult using available dyes, as it will be partially depleted after inhibition of the SERCA pumps. This also may suggest a contamination of present dye based ER measurements from the Golgi calcium.

Another matter that complicates the use of calcium sensitive dyes within the Golgi is the behaviour of the dye within the lumen, where the pH is more acidic than that of

the ER. In cultured cells the use of Golgi targeted chameleon proteins has proven to be a more precise method of localising the sensor to the correct region (Greisbeck, 2001). The interpretation of the Brefeldin A data would benefit from further investigation of Golgi calcium signals. The action of Brefeldin A on the calcium within the organelle also needs confirmation before ruling out the Golgi as the source of calcium in the TLC-S response.

The use of a fast perfusion system to evaluate the role of external calcium in the TLC-S induced calcium increase, implicated a dependence on the presence of external calcium. However, interpretation of the figure 4.16 is complicated. The gradient of calcium decrease is altered upon the application of TLC-S. This could be due to a small amount of calcium influx from remaining external calcium. This however is unlikely considering that the bath exchange rate would mean an almost 10-fold exchange of bath solution occurring before the application of TLC-S. The change in gradient could also be accounted for by release of calcium from within the cell. The amount of calcium released is not sufficient to show above the rate of calcium decrease, which is revealed by the use of a fast perfusion system (4sec bath exchange). The calcium store being targeted by the TLC-S, if such an additional store exists, requires high levels of cytosolic calcium to become charged with calcium. This suggests a low affinity for calcium, it also releases its calcium relatively quickly. So the absence of a substantial increase in calcium in response to TLC-S, in conditions of zero external calcium as seen in figure 4.13 does not completely rule out an alternative internal store. The absence of an increase on the downward phase after a global uncaging (figure 4.15) and only a small proportion of the cells, 20%, showing a small increase in calcium under an alternative protocol

depicted in figure 4.14b, also supports the idea that the store, if it exists, loses its calcium very easily.

If such a store exists the physiological relevance is debatable. The cytosolic calcium concentrations experienced during physiological responses within the cell are only transiently high during global responses. Micro-domains of high calcium have been described in discreet locations, explaining the ability of mitochondria to participate in calcium signalling despite their low affinity for calcium (Rizzuto *et al.*, 1993). This argument could also be applied to such a store that may be the target of TLC-S actions.

However the association of the TLC-S induced calcium increase to high external calcium could also implicate an activation of influx mechanisms. The identification of which influx mechanism maybe being modulated was the aim of the experiments using La^{3+} to block the calcium release-activated calcium (CRAC) channels, first described in mast cells by Hoth and Penner in 1992. La^{3+} did not completely prevent the TLC-S induced calcium increase as can be seen in figure 4.17. However this does not rule out activation of a calcium influx, as there are studies that suggest there are different forms of calcium influx. Tsunoda and Tashiro report the presence of two different influx mechanisms in rat pancreatic acinar cell; the first, termed receptor-operated calcium influx (ROCI), responsible for the plateau seen after the initial large transient in the continued presence of agonist; the second being responsible for the refilling of depleted stores (Tsunoda & Tashiro, 1999). They demonstrate the differential permeability to Mn^{2+} with the refilling influx being impermeable to Mn^{2+} and ROCI being permeable to Mn^{2+}, as detected by Mn^{2+}

quenching of the fura-2. Camello and colleagues (Camello *et al.*, 1999) also describe two different forms of influx in the mouse pancreatic acinar cell. One mediated by a non-selective cation channel and the other being a more Ca^{2+} selective channel, possibly CRAC. Krause and colleagues have also described a calcium influx that is carried by a non-specific cation channel in mouse pancreatic acinar cells, sensitive to genistein and flufenamic acid (Krause *et al.*, 1996). So the absence of a complete inhibition by La^{3+} on the TLC-S induced calcium increase suggests that if indeed an influx pathway is being modulated, it is not that of CRAC. In light of the Camello and Krause studies it would be of interest to study effects of genistein and flufenamic acid on the TLC-S induced calcium increase, to test the potential role of the non-specific cation channel in the response.

The second type of response to TLC-S is that of a drop in the plateau level. In 42 cells both an increase and a subsequent drop is observed. However in 43 cells no increase is seen, only a drop in the plateau level. The average drop in calcium from the plateau level is 147nM±11 (S.E.), suggesting a possible activation of efflux mechanisms or an inhibition on influx mechanisms. The latter would be difficult to reconcile with the increase of calcium mechanisms discussed previously, unless TLC-S had potentially dual effects on influx mechanisms with an initial activation followed by inhibition. Another explanation for the two types of responses to TLC-S observed in some cells is an increase followed by activation of calcium efflux mechanisms. The calcium dependency of calcium extrusion mechanism in pancreatic acinar cells has been previously reported (Tepikin *et al.*, 1992). However a reduction is seen in some cells where no previous increase in calcium in response to TLC-S has occurred. Results from chapter 3 suggest a calcium independent

mechanism of secretagogue mediated PMC regulation. The TLC-S may also activate this pathway of PMCA regulation, resulting in a decrease in calcium plateau level.

The work concentrated mainly on the increase of calcium caused by TLC-S. However, examination of the experiments where oligomycin and rotenone treatment was performed showed no cells that displayed a decrease in plateau level in response to TLC-S. There were also no cells displaying a decrease in response to TLC-S in the cells treated with CCCP. The identification of cells that were displaying both an increase and a drop in response to TLC-S was difficult under these conditions. This was owing to the time of exposure to TLC-S and removal before the drop phase may have started. Recovery to plateau level was evident in some experiments, and no further drop was evident. This again may have been due to ATP depletion of the cells after mitochondrial collapse. This may implicate TLC-S stimulation of an efflux mechanism that is ATP dependent i.e. the PMCA, again supporting the notion of a calcium independent regulation of the PMCA suggested in chapter 3.

The decrease in calcium below the level of the plateau was evident in experiments where a secretagogue was applied to the plateau before TLC-S (fig 4.5). In order to examine the potential modulation by TLC-S of the efflux mechanisms, the use of the fast perfusion system protocol where high external calcium is removed and then TLC-S would be prudent. If the TLC-S were modulating the efflux mechanisms, you would expect an increase in the rate of calcium decrease upon application of TLC-S. In the experiment shown in figure 4.16 the rate is actually slowed down upon application of TLC-S. As discussed earlier, this could be due to the release from an internal store or an increase in influx. Any latency of the potential effect of TLC-S

on efflux will make it difficult to study. The absence of an increase in calcium extrusion rate under this protocol does not rule out a TLC-S mediated modulation of extrusion mechanisms. Application of TLC-S earlier in the calcium-decreasing phase mediated by calcium extrusion, visualised after removal of external calcium, may allow any effects of TLC-S on efflux mechanisms to become evident after any latency period.

The potential regulation of calcium extrusion mechanisms within the pancreatic acinar cell by TLC-S is relevant to the role of Bile acids in the development of pancreatitis and pathophysiological calcium elevations implicated in the disease process. An experimental protocol allowing investigation of the efflux mechanisms in isolation from calcium influx was already utilised to study the effects of secretagogues on a plateau created by uncaging calcium (chapter 3). Utilisation of this protocol would be interesting with regard to both aspects of the TLC-S induced calcium responses on the plateau. The transient increase in calcium in response to TLC-S, if dependent upon extracellular calcium, would be absent. It has recently been described that pancreatic acinar cells express a bile acid transporter. It is also report that the uptake of bile into the cells activates SOC through inhibition of the SERCA pumps (Kim *et al.*, 2002). In the conditions of the cytosolic plateau in my experiments the SERCA pumps are already inhibited by thapsigargin. Subsequent application of agonists in these conditions do not induce a calcium increase (figure 4.5) suggesting a complete inhibition of SERCAs and depletion of the store. Therefore this cannot explain the further transient increase in calcium observed.

The preliminary experiments performed examining the effects of TLC-S on the fraction volume of the apical pole occupied by granules and vacuoles showed no observations of any change in vacuole or granular fraction volumes after TLC-S exposure. An extension of the time course of TLC-S exposure would be valuable in furthering these investigations. A longer exposure to TLC-S maybe necessary to observe the formation of vacuoles that is expected, as exposure to bile is reported to induce pancreatitis (Niederau *et al.*, 1990;Senninger, 1992). A study that examined the effects of bile salts, at a similar concentration to that which we used, on the structural integrity of the acinar cell has recently been reported. An increase in vacuolisation after 20mins incubation which was most prominent at 2hrs was shown (Kim *et al.*, 2002). This suggests that a longer incubation may reveal similar signs of cell damage. The difference in time scale could be explained by the composition of the bile mix they used in comparison to the single TLC-S type that I investigated.

Chapter 5

Measuring NFκB activation in HeLa and pancreatic acinar cells.

Chapter 5:Measuring NFκB activation in HeLa and pancreatic acinar cells.

Introduction

Nuclear factor (NF) κB is a transcription factor that is known to be involved in the cellular regulation of the inflammatory mediators such as cytokines and chemokines (Baldwin, Jr., 1996). Such molecules have been shown to be up-regulated in human and experimental pancreatitis (Grady *et al.*, 1997;Dunn *et al.*, 1997). The inhibition by pharmacological agents, has demonstrated their role in the disease (Grady *et al.*, 1997). The inhibition of NFκB itself by pyrrolidine dithiocarbamate (PDTC) during the induction of experimental, taurocholate (TCA)-induced pancreatitis in rats, improved the survival from 12% to 56% (Satoh *et al.*, 1999). Treatments with antioxidants (Grady *et al.*, 1997) and antibodies neutralising TNFα (Gukovskaya *et al.*, 1997) have also resulted in improvements in measures of pancreatitis, suggesting involvement of NFκB in disease development. In contrast, Steinle and colleagues found that inhibition of NFκB activation by two different inhibitors, NAC and PDTC both antioxidants, exacerbate the symptoms of pancreatitis. Implicating NFκB in a damage limitation role during pancreatitis development (Steinle *et al.*, 1999). Steinle and colleagues postulate that this is through anti-apoptotic effects of NFκB (Steinle *et al.*, 1999). The same inhibitors have however been shown to reduce intracellular trypsinogen activation (Han *et al.*, 2001). Attempts to explain the discrepancies between these studies pointed to the different concentrations of inhibitors used. The times, at which these observations were made also differ, protective effects are noted early in the pancreatitis development and the increased severity of the condition at a later time point.

Chapter 5:Measuring NFκB activation in HeLa and pancreatic acinar cells.

Supramaximal concentrations of secretagogue CCK or its analogue caerulin have both been used to induce experimental pancreatitis, termed hormone-induced pancreatitis. The role of NFκB in hormone-induced pancreatitis has been studied and the rapid activation of NFκB has been linked to subsequent cell damage (Gukovsky *et al.*, 1998). Studies performed looking at the pathways involved in hormone activation of NFκB found a requirement for protein kinase C (PKC) and elevated calcium (Han & Logsdon, 1999;Han & Logsdon, 2000;Tando *et al.*, 1999). The measurement of NFκB activation was done by a number of different procedures including DNA binding of nuclear extracts, western blotting to monitor levels of inhibitor proteins IκBα and IκBβ and the quantification of mRNA of an NFκB target gene, *mob-1*.

NFκB is anchored in the cytoplasm by its inhibitor proteins IkBα and IkBβ, only translocating to the nucleus to activate transcription upon disassociation from the inhibitor proteins. This disassociation occurs when the inhibitor protein is phosphorylated in a manner that targets it for degradation, unmasking a nuclear localisation signal in the NFκB protein. NFκB exists in the cytoplasm as a homo- or heterodimer. There are currently 5 known members of the family which make up these dimers, one of which p65 (also known as RELA) was the subunit investigated by the previous studies of the pancreas using western blotting (Han & Logsdon, 1999).

The aim of this section of my PhD work was to develop a method that would allow measurement of NFκB activation or IκB degradation in living pancreatic acinar cells. This would potentially allow us to study in more detail the spatial and temporal roles

of calcium in the process of NFκB activation. The previous studies examining the activation of NFκB by CCK all showed an effect of supramaximal CCK concentrations, the actions of physiological concentrations have not been described. I hoped that this method would provide a more sensitive way of measuring NFκB activation and would allow detection of the effects of physiological concentrations of secretagogues.

The GFP-p65 construct used for the measurement of NFκB activation was kindly donated by Dr M. White. The construct was shown to be functional in HeLa cells by G. Nelson (Nelson *et al.*, 2002) and Z. Seymour. My studies in HeLa cells have been conducted to show that it is possible to measure calcium signals using Fura Red calcium indicator and follow translocation of the GFP labelled NFκB to the nucleus (in collaboration with Zöe Seymour). The translocation can be quantified by taking measurements of GFP fluorescence in the cytoplasm and nucleus, and then a ratio of the nucleus/cytoplasm can be calculated.

An IκBα-GFP construct was to be used to measure the degradation of the IκBα, the construct was also kindly donated by Dr Mike White. The IκBα-GFP levels decreased upon activation; again studies have been previously conducted in HeLa cells using this method (Nelson *et al.*, 2002). In both constructs the GFP conjugated protein expression was under the control of the CMV promoter.

Investigation of the NFκB cascade in HeLa cells

The eventual aim of these experiments was to investigate the role of calcium in the activation of NFκB by measurement of the p65-GFP translocation in pancreatic acinar cells. The initial series of results are from experiments performed in HeLa cells in collaboration with Zöe Seymour in Dr M. Whites group in order to familiarise myself with the quantification of p65-GFP expressing cells.

p65-GFP transfected HeLa cells were stimulated with TNFα (10ng/ml) to induce activation of NFκB. The images and traces shown in this dissertation were achieved as a result of my own experiments. Figure 5.1 shows an example of a control TNFα induction of NFκB translocation experiment; the top figure shows the cells expressing p65-GFP before stimulation and the lower panel 30minutes after TNFα application. The GFP translocation can be measured as a ratio of nuclear:cytoplasmic fluorescence. The increase in this ratio indicates an increase in the amount of nuclear p65-GFP. These measurements can be made over a period of time to produce a more dynamic picture of the translocation (figure 5.2). The translocation can also be observed from the fluorescence pictures shown in figures 5.2 where before and after stimulation images are shown. There is clearly visible nuclear accumulation of the GFP in some cells.

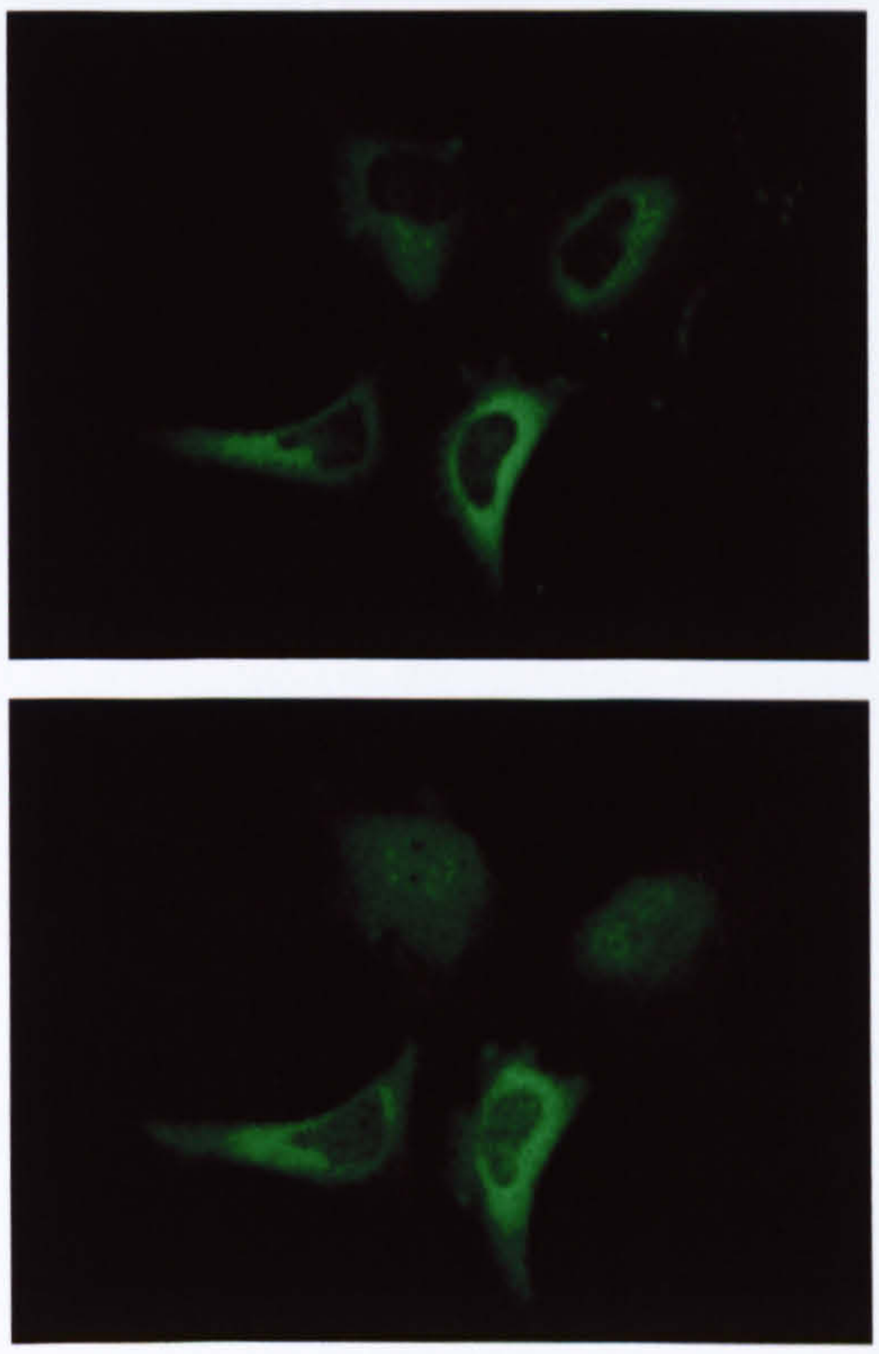

Figure 5.1 **Changes of p65-GFP distribution in HeLa cells induced by TNFα** The upper image shows fluorescence of HeLa cells expressing p65-GFP before stimulation. The lower image shows these cells 30min after exposure to TNFα (10ng/ml final concentration).

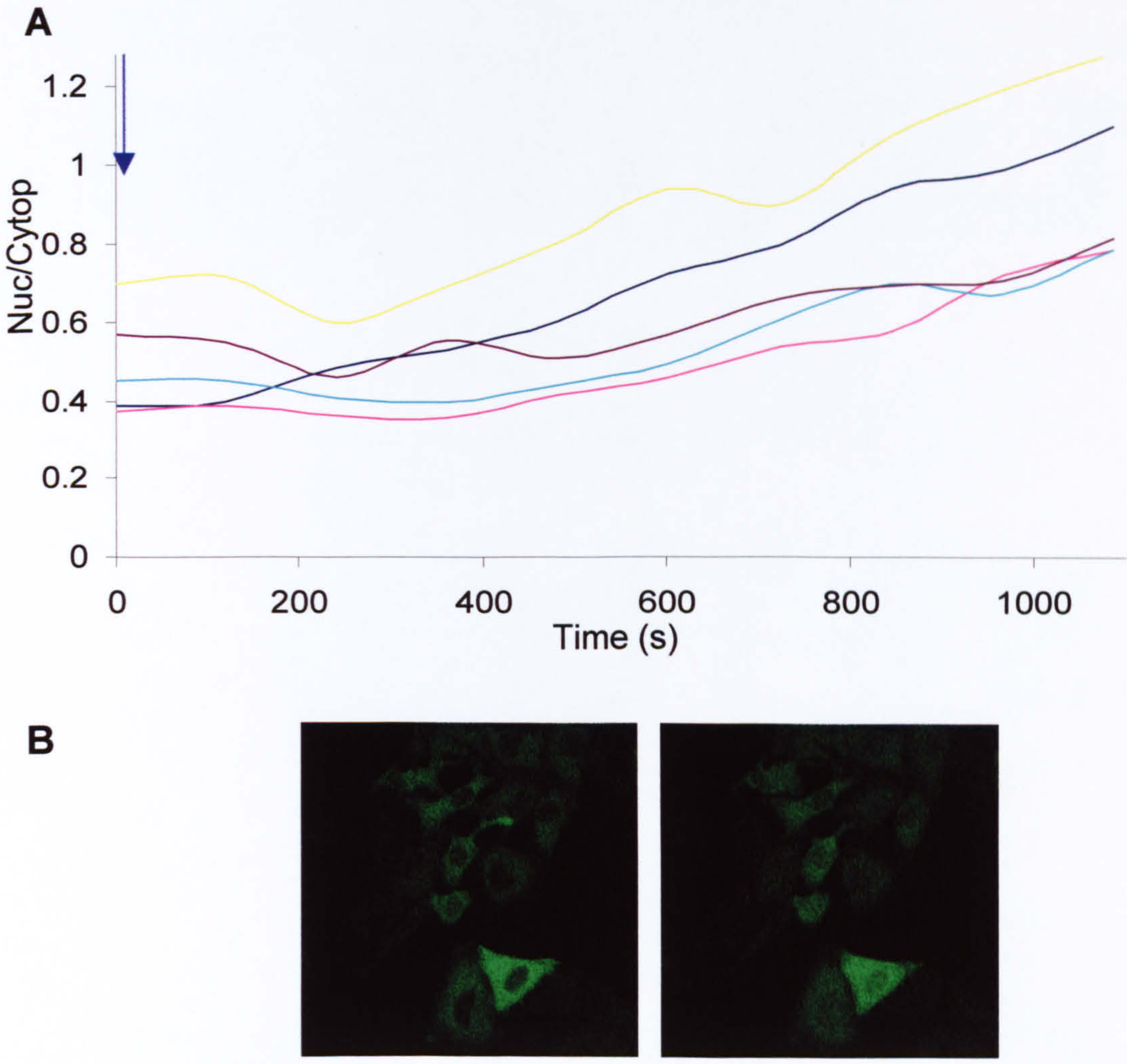

Figure 5.2 **An example of TNFα–induced translocation of p65-GFP in HeLa cells** The graph in (**A**) shows the translocation of p65-GFP measured by nuclear:cytoplasmic GFP fluorescence intensity ratio in 5 cells. The addition of TNFα addition is shown by arrow. The images in (**B**) show GFP fluorescence localisation, before (left) and 30min after (right) TNFa application.

Loading of HeLa cells expressing p65-GFP with fura red

Figure 5.3 shows HeLa cells expressing p65-GFP loaded with fura red, a calcium sensitive probe. The simultaneous monitoring of calcium changes via fura red fluorescence changes and NFκB activation via p65-GFP localisation should therefore be possible.

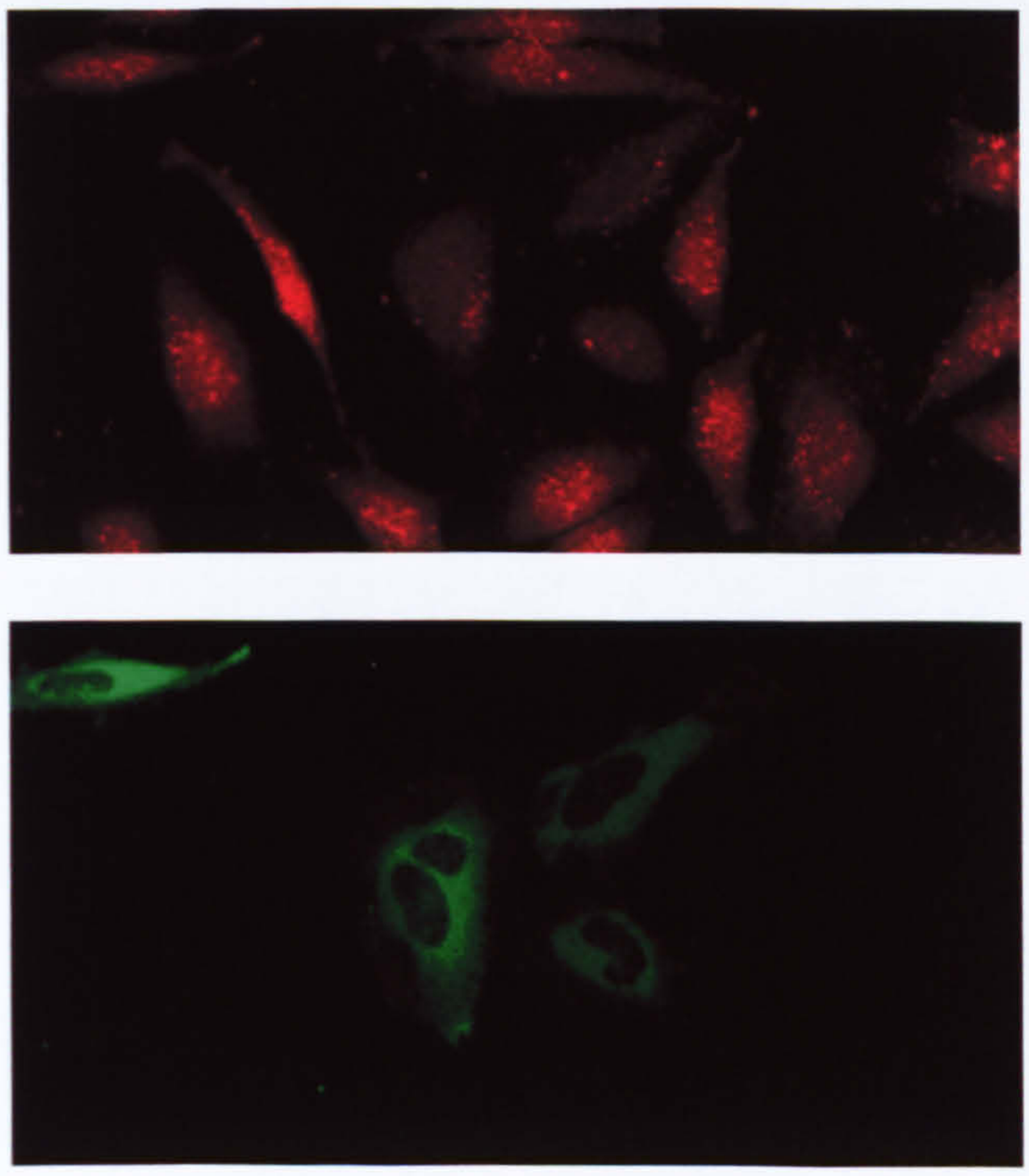

Figure 5.3 **Fura red loading of HeLa cells expressing p65-GFP.** The upper image shows the distribution of fura-red. The lower image shows the distribution of p65-GFP. Note the nuclear exclusion of p65-GFP

Analysis of NFκB distribution after an increase in calcium induced by uncaging of NP-EGTA (simple uncaging)

Uncaging of caged calcium (loaded into the cells in AM form) as is shown in figure 5.4 can induce a calcium transient measured by fura red. The uncaging was performed in cells expressing the p65-GFP as shown in the images alongside the charts. Fura-red calcium trace is shown in 5.4a illustrating the calcium changes during the first 200s of the protocol that includes the uncaging. The images of the fura red loaded cells are shown on the right (5.4a) (numbered cells correspond to p65-GFP expressing cells, where subsequent translocation was measured). The top image (5.4a) represents before and the bottom image (5.4a) after uncaging of calcium. The ratio of nuclear:cytoplasmic p65-GFP fluorescence is shown in 5.4b. This quantifies the degree of nuclear translocation of the p65-GFP molecule. The same line colours in graphs 5.4a and 5.4b correspond to the same cell. In one cell (no. 4, figure 5.4b) there appears to be a large increase in the nuclear:cytoplasmic ratio that is not as evident in the other cells (numbers match with the numbered cells in the images on the right hand side). The slow slight upward trend in all the other cells may be due to a gradual change in the focal plane.

Overall data from 4 different experimental plates (3 independent cultures) shows that 16 cells underwent calcium increases through UV flash mediated uncaging of calcium. Only 1 cell demonstrated a large increase in the nuclear: cytoplasmic ratio indicative of nuclear accumulation of p65-GFP. 15 control cells where no uncaging had been performed from the same experimental plates showed no increase in the nuclear: cytoplasmic ratio.

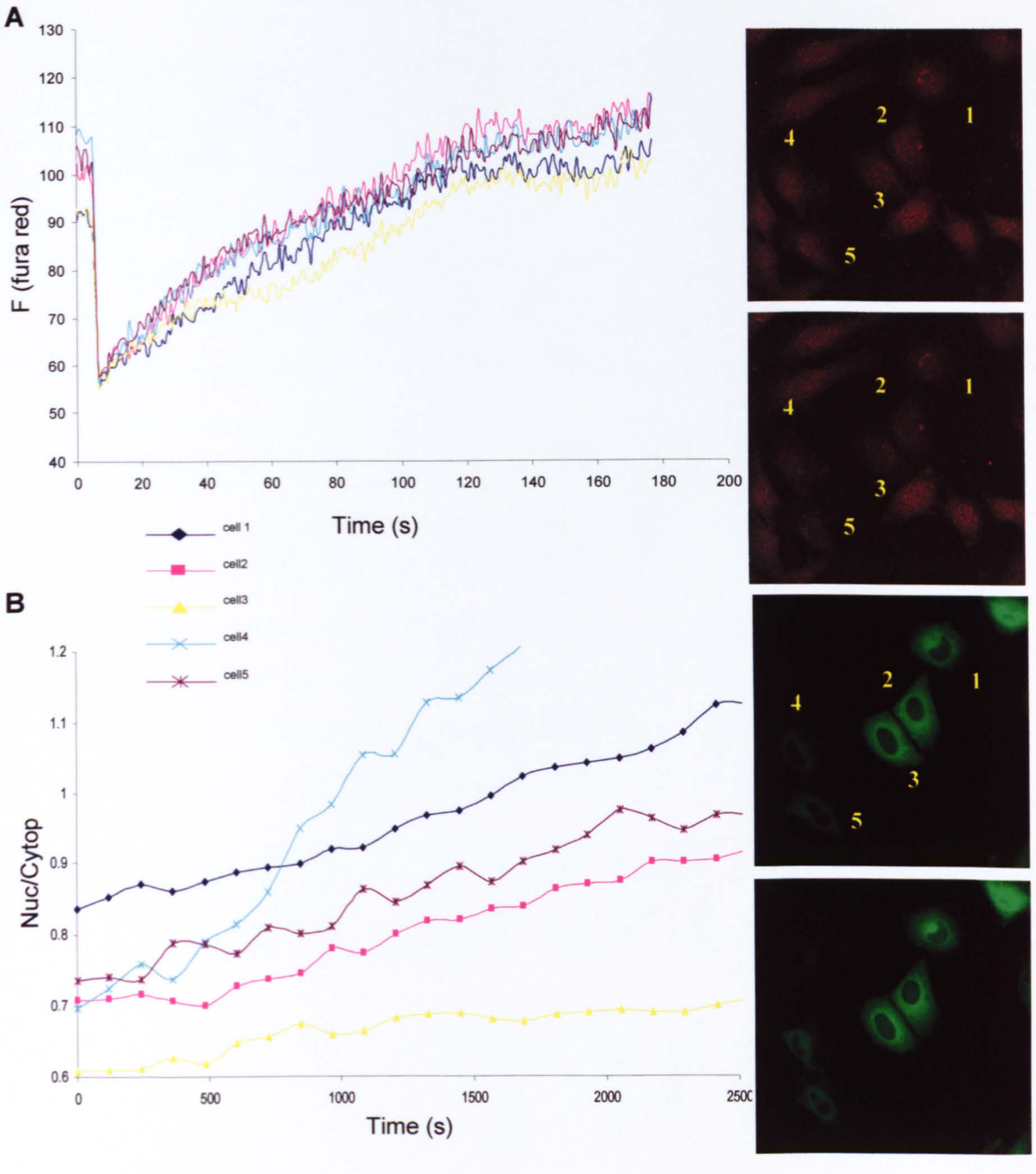
A
F (fura red)
Time (s)
cell 1
cell2
cell3
cell4
cell5
B
Nuc/Cytop
Time (s)
1
2
3
4
5

Figure 5.4 **Analysis of NFκB redistribution after an increase in calcium induced by uncaging of NP-EGTA (simple uncaging)** HeLa cells that had been transfected with p65-GFP plasmid 24hrs earlier, were loaded with caged calcium (NP-EGTA) and fura-red. (**A**)The cells expressing the p65-GFP protein were then flashed with UV light to uncage the calcium in those cells. The calcium was monitored by fura-red fluorescence, uncaging regions were drawn to exclude the nucleus from UV illumination. The images on the right of the graph show the fura red image before (top) and after (bottom) calcium uncaging (**B**) The traces represent the nuclear/cytoplasmic ratios of GFP fluorescence over 2500s following the uncaging by the UV flash. The images to the right show the GFP distribution before (top) and 2500s after (bottom) the calcium uncaging. The line colours in the calcium trace match to the same cell same colour trace in the GFP translocation measurements. The cells are numbered on the images to indicate which cell corresponds to each trace.

Analysis of NFκB distribution after an increase in calcium induced by uncaging of NP-EGTA (a ramp protocol)

Another protocol used for elevating the calcium through uncaging was termed a ramp protocol. In these experiments the cells were again loaded with fura red and NP-EGTA (caged calcium). The microscope scan region for the calcium uncaging was reduced to include only one of the GFP expressing cells; the scan region used is shown in the middle image of 5.5c (fura red loading only). The full field of view is shown in the first image (left 5.5c), which includes the ramped cell and the two control cells labelled 1 and 2 that correspond to the traces (labelled) of p65-GFP nuclear:cytoplasmic ratio in 5.5b. Figure 5.5a shows changes of calcium indictor fura red from the single cell that underwent the ramp protocol. The illumination by the UV laser (black line figure 5.5a) whilst scanning causes additional excitation of the calcium indicator (fura-red). This explains the immediate sharp increase in fura red fluorescence at the beginning of the UV illumination and sharp drop in fura red fluorescence at the end of UV illumination. However this additional excitation is constant. The relative starting level of fura red fluorescence (before UV illumination) and finishing level (after UV illumination) indicates the increase in calcium as a result of calcium uncaging indicated by a decrease in fura red fluorescence.

The gradual recovery to resting calcium levels is then seen over ~70s. The GFP translocation was measured as a nuclear:cytoplasmic ratio. There is no significant translocation either in the control cells (no uncaging) or treated cell (ramped) in comparison to changes of ratio seen with TNFα treated control cells. There appears to be a difference between the ramped cell and the controls, though the difference is

small. In this particular experiment the change in ratio in the ramped cell is more than double that seen in the control (non-ramped) cells. However from 3 experimental plates (2 different cultures) 9 cells underwent a ramp protocol and only one cell showed any degree of translocation. 8 control cells that were not subject to ramping protocol from the same experimental plates show no increase in the nuclear: cytoplasmic ratio.

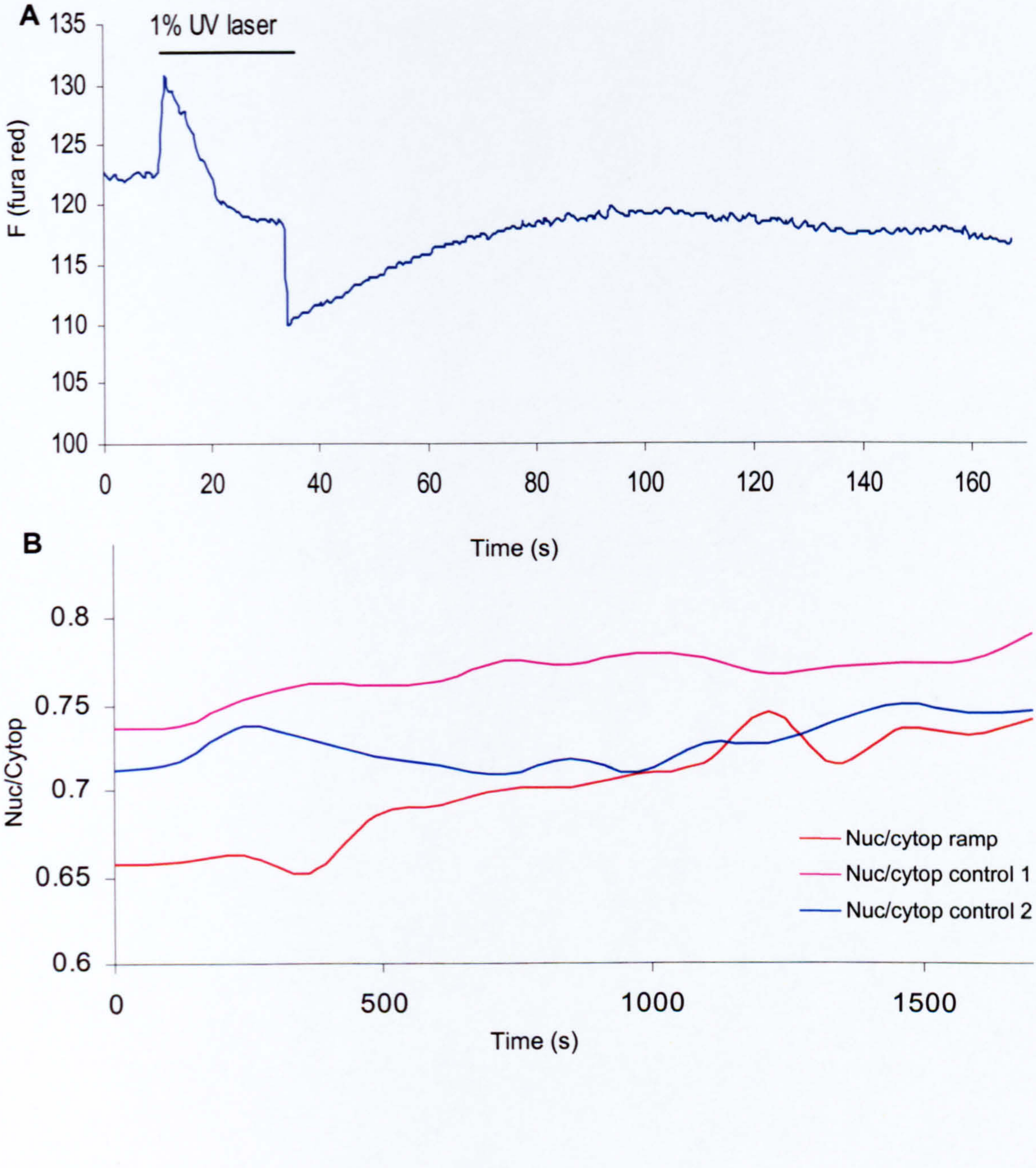
A
1% UV laser
F (fura red)
135
130
125
120
115
110
105
100
0
20
40
60
80
100
120
140
160
Time (s)
B
Nuc/Cytop
0.8
0.75
0.7
0.65
0.6
0
500
1000
1500
Time (s)
Nuc/cytop ramp
Nuc/cytop control 1
Nuc/cytop control 2

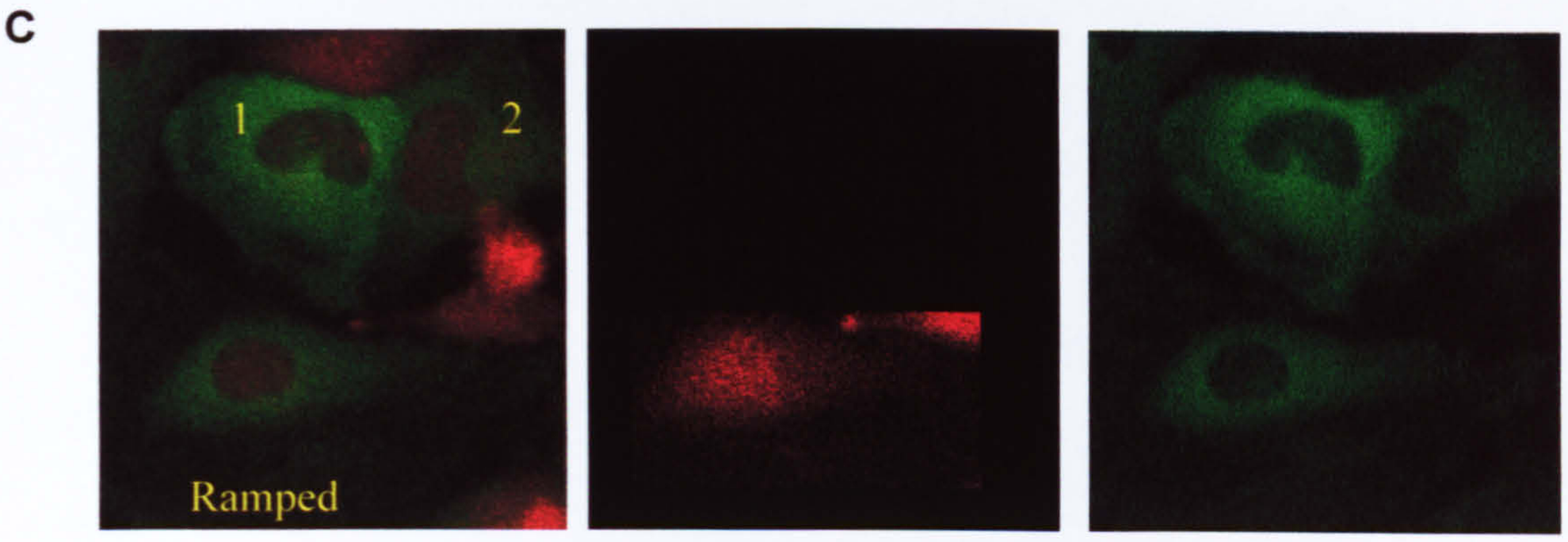

Figure 5.5 **Analysis of NFκB distribution after an increase in calcium induced by uncaging of NP-EGTA (Ramp protocol)** HeLa cells that had been transfected with p65-GFP plasmid 24hrs earlier, were loaded with caged calcium (NP-EGTA) and fura-red. (**A**)One of the cells expressing the GFP protein (labelled ramped in part **C**) was exposed to low levels of UV illumination over a period of time indicated by the black line in (**A**) to uncage calcium in that cell. The calcium changes in this cell were monitored by fura-red fluorescence, (**B**) The trace represents the nuclear/cytoplasmic ratio of GFP fluorescence over 1700s following the uncaging by the UV illumination. The pink trace corresponds to the cell that underwent the ramp protocol, red and blue traces correspond to p65-GFP expressing cells in the field that did not undergo a ramp protocol. The cells are numbered on the images to indicate which cell corresponds to which trace. The Left image in (C) shows all three cells with the fura red and GFP fluorescence overlaid. The middle image shows the ramped cell only (fura red signal) and the right image shows the GFP localisation in all three cells.

The aim of these experiments was to investigate the role of calcium in NFκB activation within the pancreatic acinar cells. An area of interest due the possible involvement of NFκB cascade in pancreatitis development discussed earlier. I now moved on to attempting similar experiments of NFκB activation measurements in pancreatic acinar cells.

Short term culture of acutely isolated pancreatic acinar cells: culturing conditions and tests for agonist sensitivity

Initial experiments investigated the longer-term survival of the acutely isolated acinar cells. This was with the rationale that to allow expression of the conjugated protein, the cells would require long-term incubation at 37°C. There is little experience of pancreatic acinar cell culturing in our laboratory; as in the majority of experiments, cells are used within 4hrs of isolation. The culture conditions as described in section 2.2 were adapted from Brannon *et al.*, 1985 (Brannon *et al.*, 1985). The morphology of the cells and responses to secretagogues ACh and CCK were the means of evaluating the condition of the cells after a period in culture. The responses to different concentrations of secretagogues are well characterised for acutely isolated cells (Petersen *et al.*, 1991). Secretagogues were applied to the cells cultured for 18-24hrs and which had then been loaded with fura-2, figure 5.6a. Responses to these concentrations of the secretagogues were similar to those demonstrated in acutely isolated cells. Low concentrations, 20pM CCK and 50nM ACh demonstrated an oscillatory pattern and in the case of ACh oscillations were superimposed on an elevated baseline plateau. Higher concentrations, 1nM CCK and 1μM ACh produced much larger single long-lasting calcium transients.

Morphologically the cells, which survived, exhibited the polarisation familiar to the pancreatic acinar cell, distinct basal and apical (granule containing) poles. The surviving and subsequently studied cells were mainly in medium sized clusters (10-40 cells). These cells often possessed a better morphology than the cells in the smaller clusters (~5 cells). Single cells never survived in these culture conditions. Occasionally doublets were seen, however they were not as healthy (judged on their morphology) as cells in larger clusters. Examples of a small cluster and a medium sized cluster after 23hrs in culture are shown in figure 5.6b. In summary cells cultured between 20-24hrs from 3 independent cultures showed the following sensitivity: 25% (8/33) of cells responded to 20pM CCK, 88% (29/33) of cells responded to 50nM ACh, 100% of cells responded to 1nM CCK (23/23), 500nM ACh (10/10) and 1μM ACh (25/25).

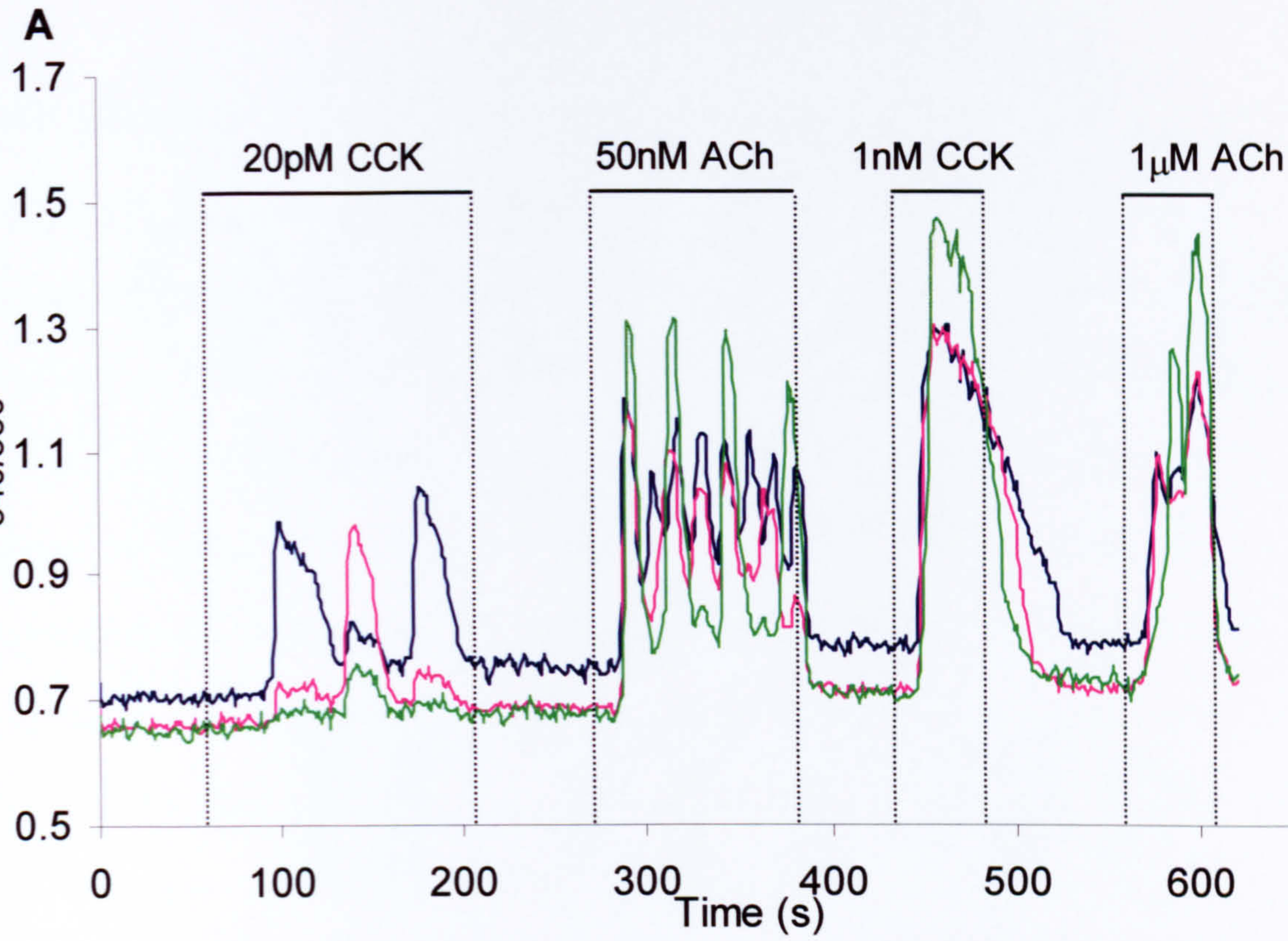

Figure 5.6 **Calcium responses of cultured pancreatic acinar cells** (**A**) Shows calcium responses in cells cultured for 23hrs and then loaded with fura-2. (**B**) Transmitted light pictures of two different clusters of acinar cells cultured for 23hrs.

Expression of the NFκB p65-GFP conjugated protein in pancreatic acinar cells

Microinjection of p65-GFP constructs in medium to large clusters of pancreatic acinar cells followed by incubation at 37°C (5-14hrs) resulted in expression of the protein, detectable by the appearance of GFP fluorescence. Zeiss LSM 510 system was used to monitor expression of p65-GFP. Results of successful microinjection of the plasmid p65-GFP followed by expression of the GFP detected 5 hours later, is shown in figure 5.7. In figure 5.7a there are two cells in the cluster that are expressing the GFP conjugated protein. As is evident the GFP already has a significant degree of nuclear localisation. Figure 5.7b shows one of the cells at a higher magnification before (top) and after (bottom) 40minutes exposure to supramaximal concentration of CCK. A total of 4 cells from 3 independent experiments showed no further measurable accumulation of GFP in the nucleus after cell stimulation. In this and other similar experiments the cluster shape has changed during the exposure to supramaximal concentration of agonist, changing the focal plane of the image, making quantification difficult. However no significant differences in nuclear intensity were observed (data not shown). The majority of cells expressing the GFP protein showed a significant amount of protein already in the nucleus. The only one cell (out of 10 cells, 6 independent experiments which includes experiments with the use of inhibitor described below) that did not show a nuclear distribution immediately upon detection of expression also showed no increase of nuclear accumulation during exposure to 1nM CCK though owing to movement of the cells conclusive quantification was not possible (figure 5.8).

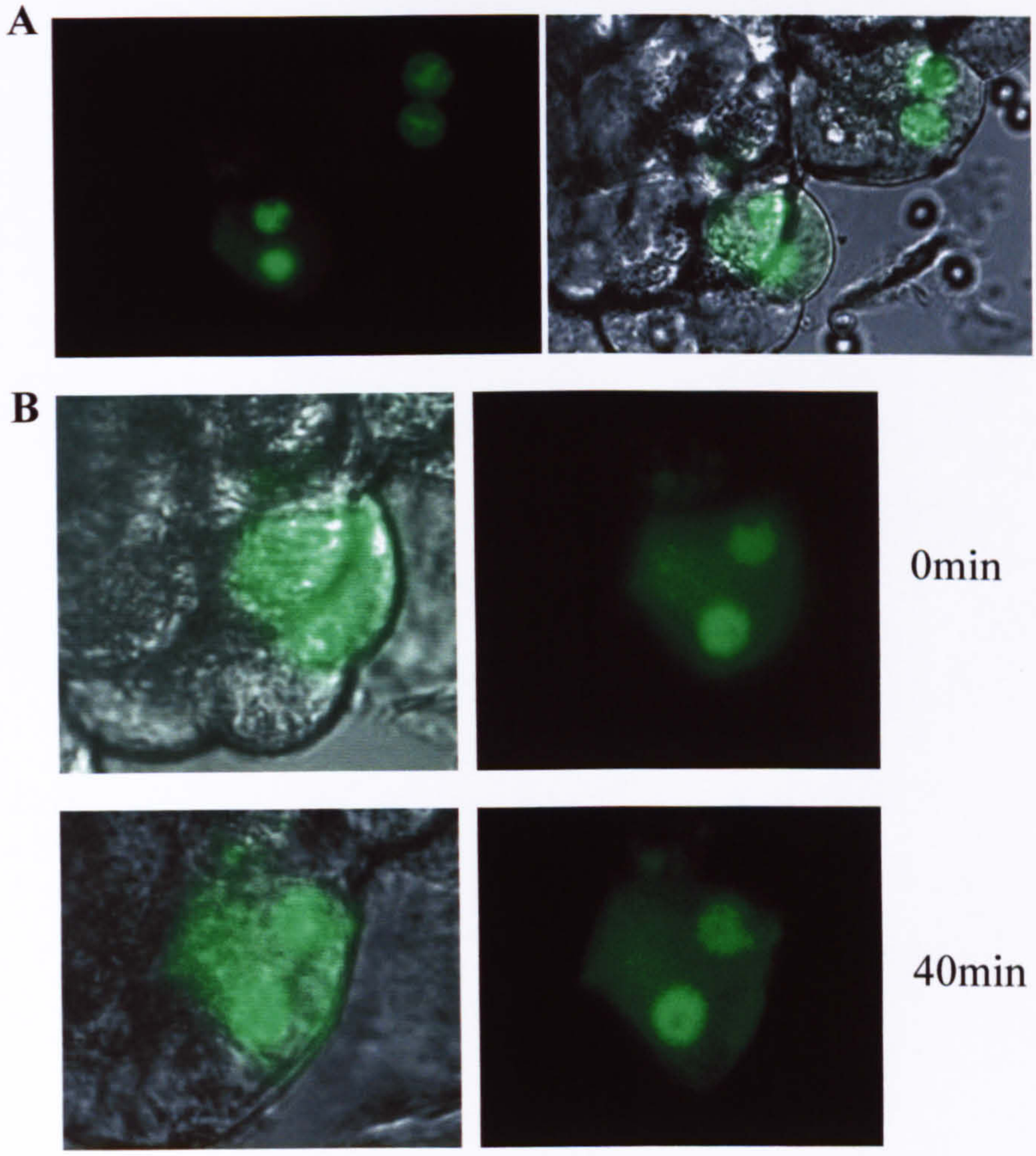

Figure 5.7 **The expression of p65-GFP in pancreatic acinar cells** (**A**) Shows the expression pattern of p65-GFP in cells 5 hours after microinjection of the p65-GFP construct (GFP fluorescence on the left and transmitted light and GFP fluorescence superimposed on the right). (**B**) One cell expressing the p65-GFP construct before application of secretagogue (top) and the same cell after 40mins exposure to 1nM CCK (bottom) (transmitted light and GFP fluorescence superimposed on the the left and GFP fluorescence on right). There is some change in cluster shape during stimulation which causes an alteration in the focal plane.

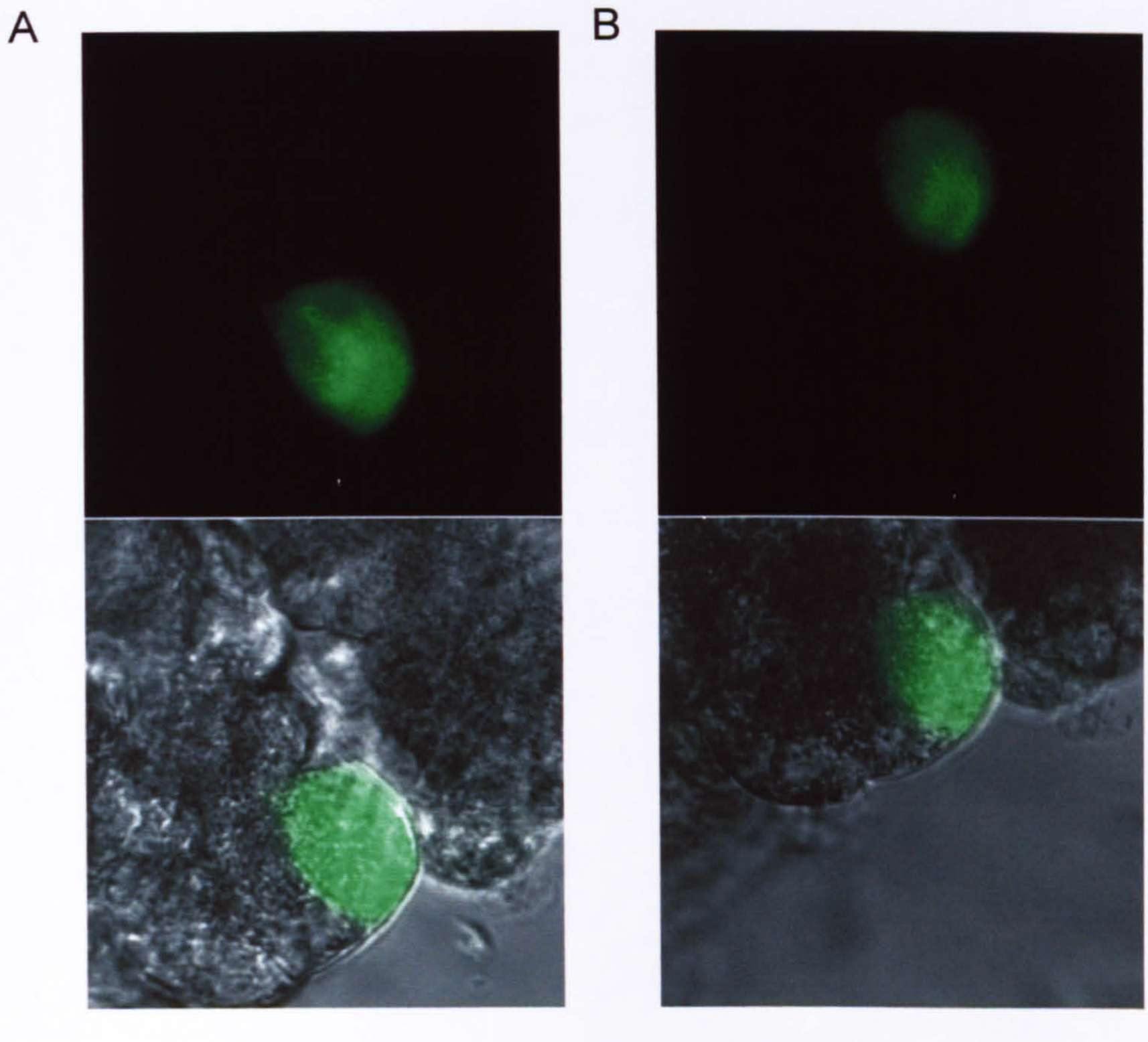

Figure 5.8 **The only cell that was not already expressing p65-GFP with a predominate nuclear distribution and the effect of 1nM CCK application** (**A**)The cell before treatment with 1nM CCK (**B**) The same cell after 40mins treatment of 1nM CCK (Top image is GFP fluorescence and the bottom image is the transmitted light and GFP fluorescence images overlaid).

The use of PKC inhibitors to reduce the nuclear localisation of p65-GFP

In an attempt to reduce the amount of nuclear localised GFP protein, cells confirmed to be expressing the GFP were incubated with 1μM GF109203X. GF109203X is a PKC inhibitor that Han and colleagues (Han & Logsdon, 1999;Han & Logsdon, 2000) have shown to inhibit NFκB dependent transcription of *mob-1* and reduce the amount of p65 protein detected in the nucleus after 30minutes incubation. Figure 5.9a depicts cells that are expressing the p65-GFP protein detected preferentially within the nuclear compartment, and the same cells after addition of 1μM GF109203X at 3 time points 20,40 and 90minutes after addition. Values of the nuclear intensity measured are shown under each image. There is no sustained significant change in intensity between time points. The drop in intensity in the top nuclei at the 40minute time point is not carried through to the 90minute time point and is likely to be owing to a cell movement. There is evidence of changes in the focal plane at which the cells are situated, note changes in the shape of the cells and the distance between the two nuclei. The nuclear localisation of the GFP was confirmed by co-staining with Hoechst a dye that stains DNA. The yellow signal in the overlay (figure 5.9b) of the GFP and Hoechst images indicates co-localisation.

A higher concentration of GF109203X, 10μM, was used and the cells expressing the p65-GFP were left in the presence of the inhibitor overnight (21hrs). In these experiments the first 45minutes of incubation with GF109203X produced no change in nuclear intensity. After that cells were removed from the stage of the microscope and placed into an incubator for overnight culturing. The movement of the cells after being left overnight makes quantification impossible, as the same focal plane cannot be re-analysed. However it is possible to see that the p65-GFP is still localised within

the nucleus, as shown in figure 5.10. The inhibitor GF109203X had no effect on the nuclear localisation of the p65-GFP protein in 4 cells from 2 independent cultures.

A

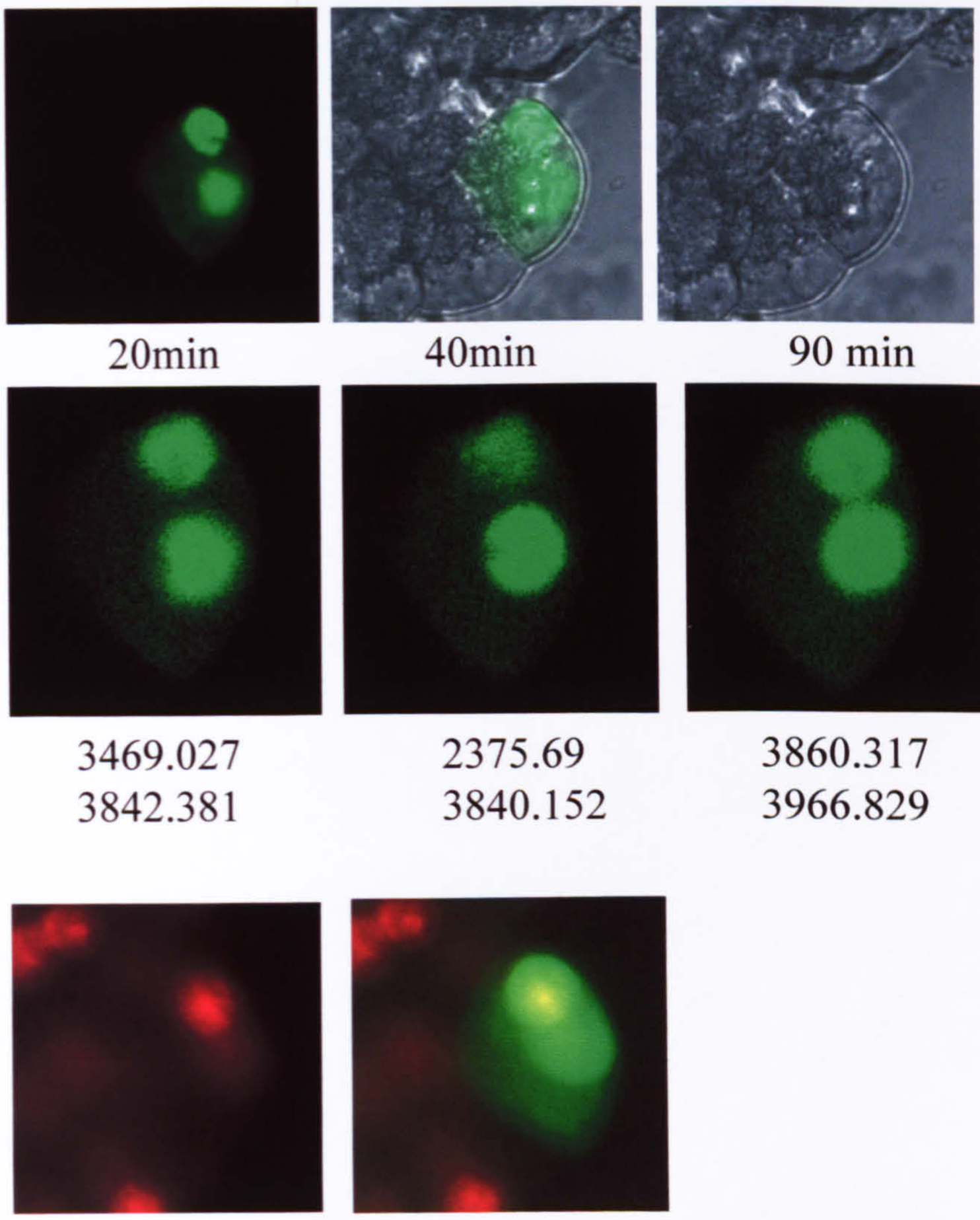

B

Figure 5.9 **Expression of p65-GFP in acinar cells before and after treatment with PKC inhibitor GF109203X (A)** The upper row shows fluorescent image of a cell expressing p65-GFP, an overlay of fluorescent and transmitted light images and transmitted image of the cluster. The lower row shows p65-GFP distribution after 20, 40, and 90 minutes incubation with the PKC inhibitor GF 109203X (1μM). The average nuclear intensities are displayed under each time point. The upper number corresponding to measurements from the upper nucleus and the lower number corresponds to the measurements from the lower nucleus. The is no significant change in intensity during the incubation. (**B**). Co-staining the cells expressing p65-GFP with the nuclear stain Hoechst.

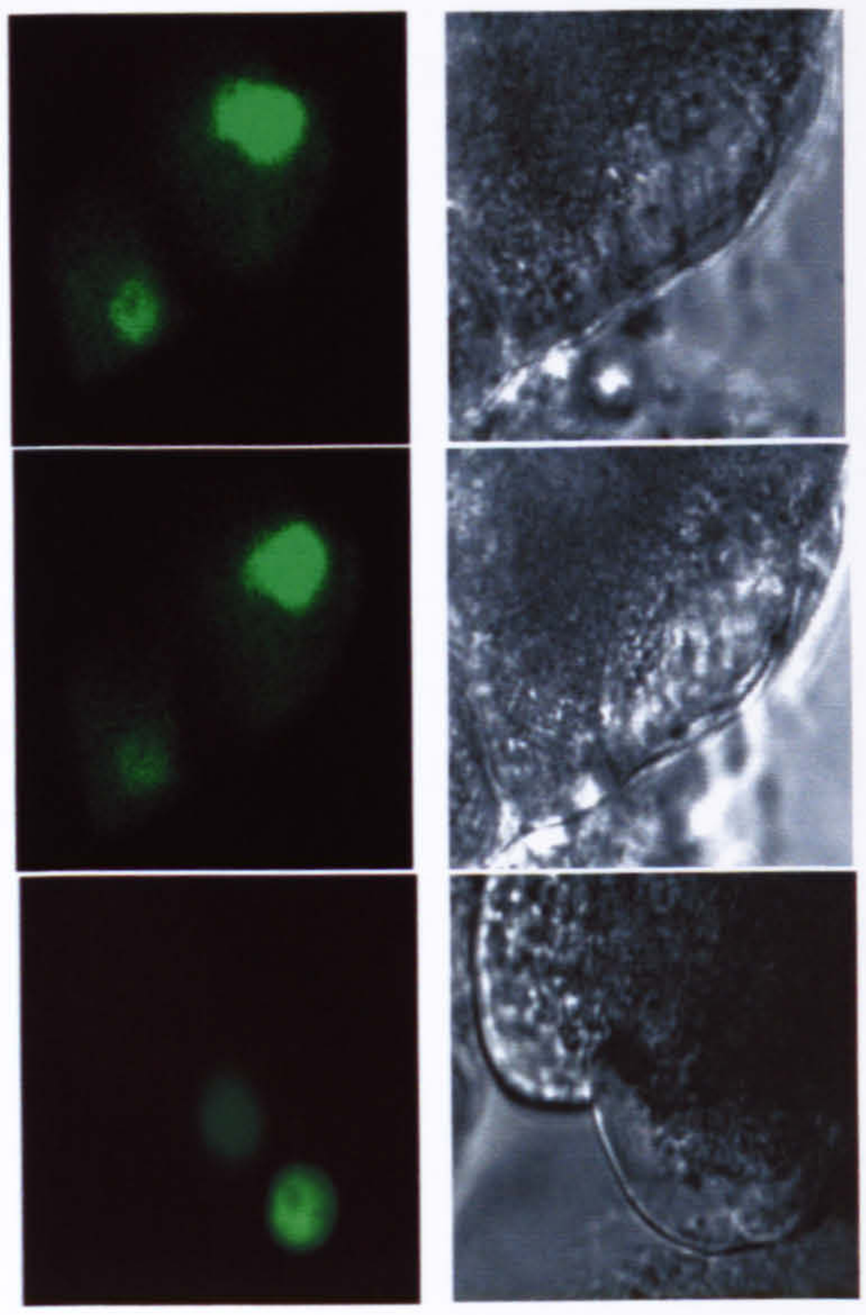

Figure 5.10 **Images of cells expressing p65-GFP in the absence and the presence of PKC inhibitor GF109203X**. p65-GFP expression before application of the inhibitor and after 45min and 21hrs incubation with GF109203X (10μM). The cells were moved overnight back to the incubator, therefore the exact same focal plane could not be achieved.

Attempts to reduce the p65-GFP nuclear localisation using photobleaching

An alternative approach was to destroy the fluorescence in nucleus, hoping that further accumulation of p65-GFP in response to agonist would become measurable. The destruction of the GFP conjugated protein was achieved by bleaching with the excitation light, in this case the 488nm laser line. Figure 5.11 shows a cell expressing p65-GFP with preferential nuclear localisation (Strehler *et al.*, 1989). During the experiment the bottom nucleus is completely bleached and the drop in fluorescence is demonstrated in the blue trace of the chart below. The other nucleus is split into two regions, one that is bleached (pink) and the other half that is not (green). As can be seen in the pictures the fluorescence of the lower nucleus decreases during the bleaching and does not recover. The fluorescence in the second (upper) nucleus where only part of the area is bleached is seen to drop very rapidly in the area of bleaching, followed by partial recovery. The fluorescence from the other non-bleached part drops more slowly. This is possibly due to the diffusion of the protein into the bleached half of the nucleus resulting in recovery of fluorescence in the bleached half and a compensatory gradual drop in the non-bleached half.

The protocol of bleaching the nucleus prior to stimulation with supra maximal concentration of agonist was performed; however no further increase in nuclear fluorescence was seen upon application of agonist (1 experiment). Movement artefacts again made a quantifiable analysis impossible. Images from this experiment are shown in 5.12, the shift in the position of the clusters and change in shape make the analysis difficult.

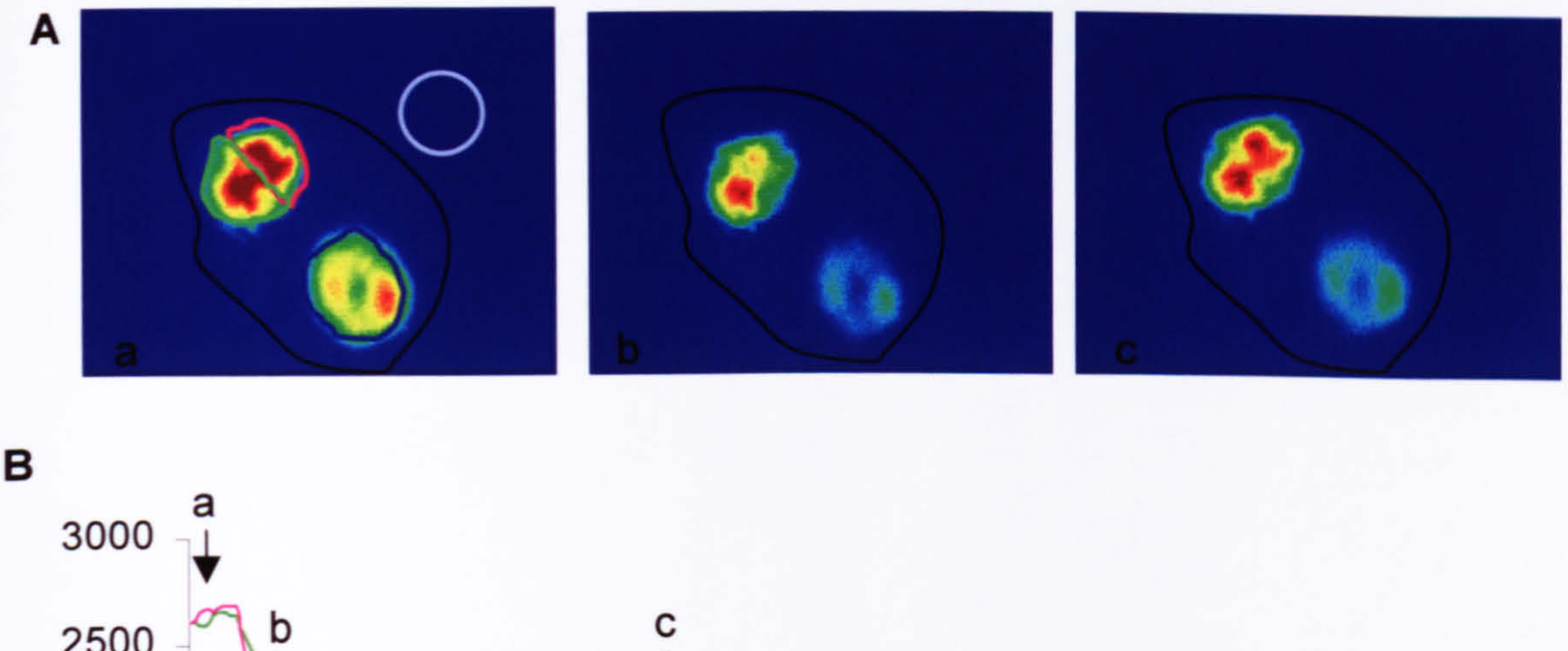

Figure 5.11 **Bleaching of p65-GFP in a nuclear regions in a cell** The cell outline indicated by the black line in (**A**) is bi-nucleated and expressing the p65-GFP in a predominate nuclear localisation. (**A**) The top nucleus is divided in two regions (as indicated in the top left image) the pink region is subjected to a bleaching the green half is not bleached. The second nuclear region is encompassed entirely in the bleached region (indicated by the blue region). The graph in (**B**) where the lines correspond to the regions indicated in the images in (**A**) demonstrate the changes in fluorescence during and after the bleaching(pink line on the bottom of the trace). Arrows in **(B)** indicate the time points at which the images shown in **(A)** were taken.

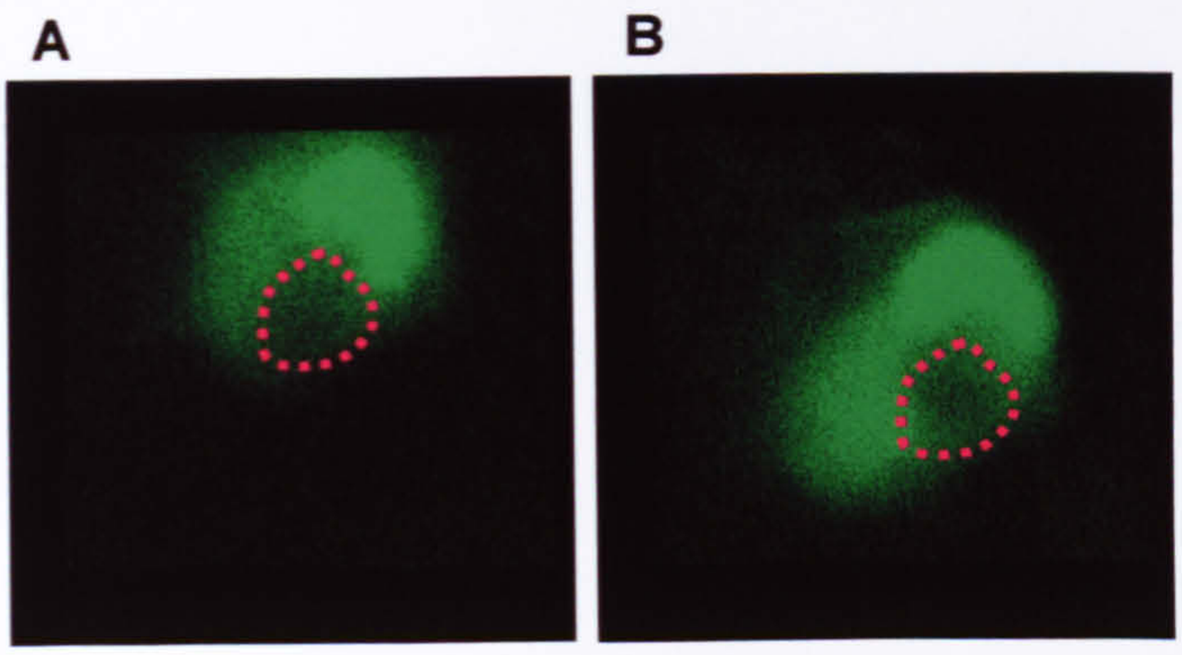

Figure 5.12 **Bleaching of a nuclear region followed by application of 1nM CCK** The cell with one bleached nucleus was stimulated with 1nM CCK. (**A**) Shows the cell before stimulation and (**B**) 75 min after CCK application. The large degrees of movement during CCK application made quantification impossible due to the changes in focal plane and hence the region of cell being analysed.

Expression of IκBα-GFP conjugated protein in pancreatic acinar cells

Another molecule involved in the activation NFκB is the inhibitor protein IκBα. The conjugated IκBα-GFP was also available; the measurement of its degradation has been demonstrated in HeLa cells to be an accurate measurement of NFkB activation, with a similar time course to endogenous protein degradation. This was done by monitoring simultaneously the p65-DsRed translocation, IκBα-GFP degradation and then transcription activation through a reporter gene (Nelson *et al.*, 2002). In my experiments the IκBα-GFP construct was microinjected into pancreatic acinar cells, which were then incubated at 37°C to allow expression of the GFP conjugated protein. As can be seen in figures 5.13i-iii the expression of the IκBα-GFP is bright with a significant amount of nuclear localisation (10 cells from 6 independent experiments). It was expected that a reduction in the fluorescence would occur upon stimulation of NFκB cascade with secretagogue CCK. Different concentrations of CCK were used 50pM (5.13i)(n=3), 1nM (n=2) (data not shown), 10nM (5.13ii) (n=3) and 100nM (5.13iii) (n=2). The toxic effects of the supramaximal concentrations 10 and 100nM are illustrated by the formation of blebs on the cells surface (figure 5.14). The changes of cell shape associated with the bleb formation make quantification of the fluorescence signal difficult. In figure 5.13i in response to 50pM CCK there seems to be a reduction in the fluorescence in the nuclear region. This however is not accompanied by an expected reduction in the cytoplasm. The drop in nuclear fluorescence and hence the nuclear: cytoplasm ratio was potentially due to a movement artefact. The high concentration of 10nM CCK shown to activate NFkB in other studies (Tando *et al.*, 1999;Han & Logsdon, 1999) showed an overall reduction of fluorescence as measured over the whole cell,

accompanied by a smaller reduction of the cytoplasmic signal (figure 5.13ii); this maybe indicative of an increase in IκBα-GFP degradation. However the transmitted light pictures show the blebs formed around the edge of the cell and the resulting change in shape and position. These could be producing the drop in fluorescence seen in the cytoplasm. The highest concentration of CCK used was 100nM. This again was shown to cause the formation of blebs, which contained IκBα-GFP indicated by the increase in fluorescence in that region (figure 5.13iii pink trace). However no significant reduction in the cytoplasmic signal was observed though there was an increase in the nuclear signal. Again this was probably due to changes in the cells shape and position increasing the fluorescence in the nuclear region of interest.

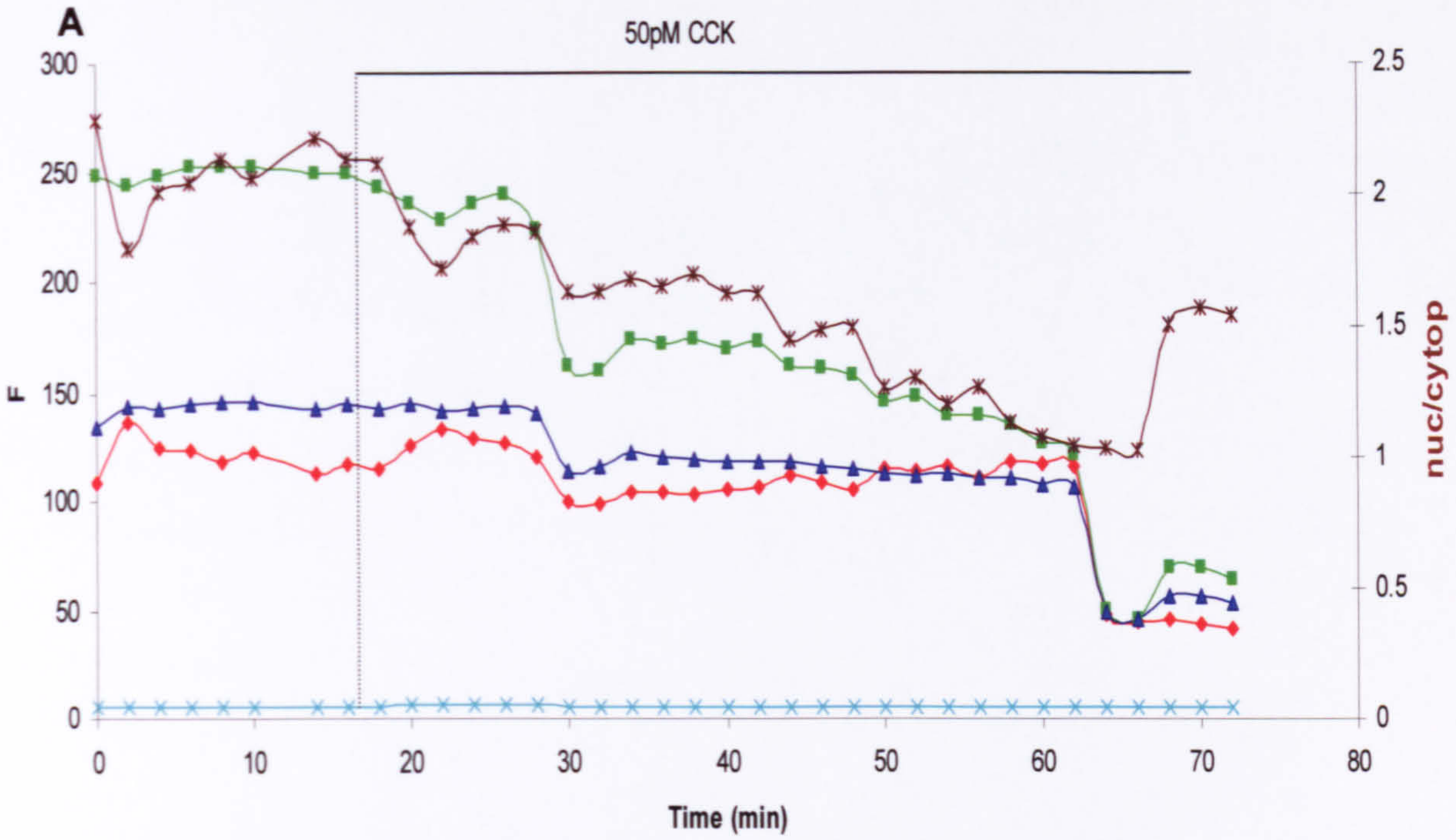

Red – Cytoplasm
Green- Nucleus
Blue- Whole Cell
Turquoise – Background
Brown – Nucleus/Cytoplasm

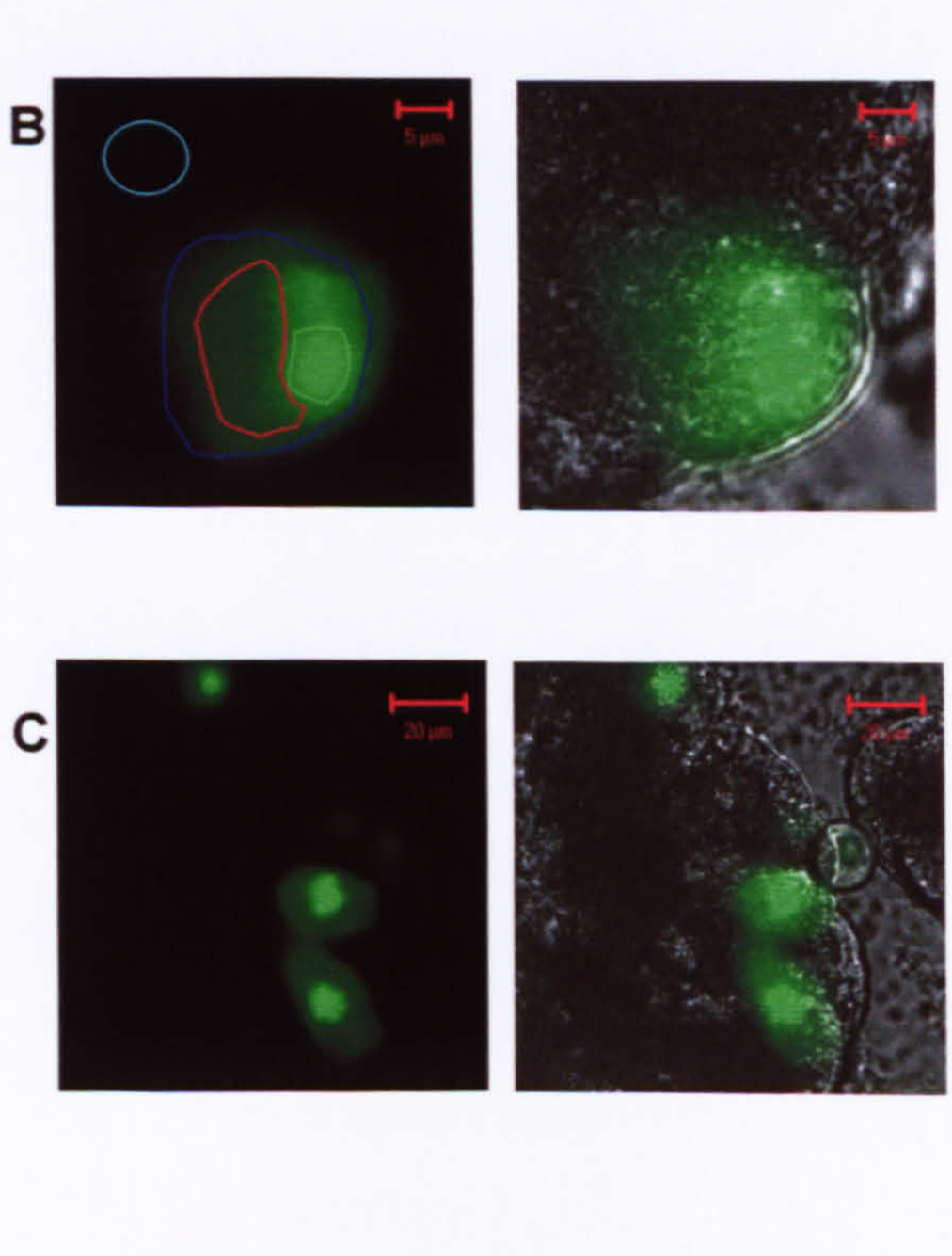

Figure 5.13i IκBα-GFP distribution before and after application of 50pM CCK (A) The graph shows the measurements of GFP fluorescence from the regions of the cell shown in (B). The brown trace in (A) corresponds to the ratio (see right axis) of nuclear:cytoplasmic measurements. **(B)** Left image shows fluorescence of IκBα-GFP expressing cell and the selected regions of interest. Right image shows overlay of fluorescence and transmitted images(scale bar equals 5μm). **(C)** Shows a wider field of view that contains other cells that are also expressing IκBα-GFP. Image was taken after 50pM CCK treatment. (scale bar equals 20μm)

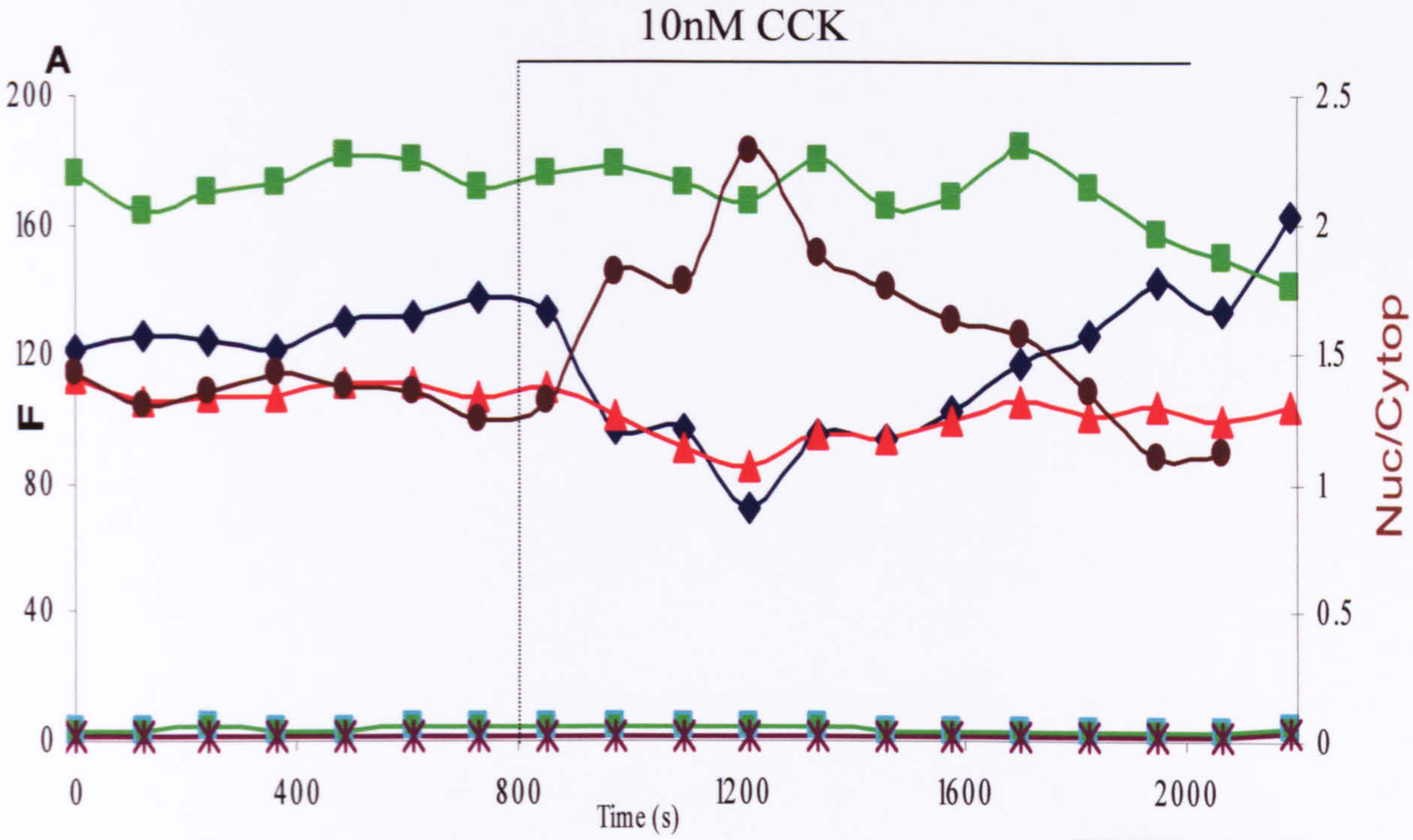

Green- nucleus,
Red- cytoplasm,
Blue- whole cell
Yellow- neighbouring non-expressing cell
Turquoise- background
Nucleus/Cytoplasm-Brown

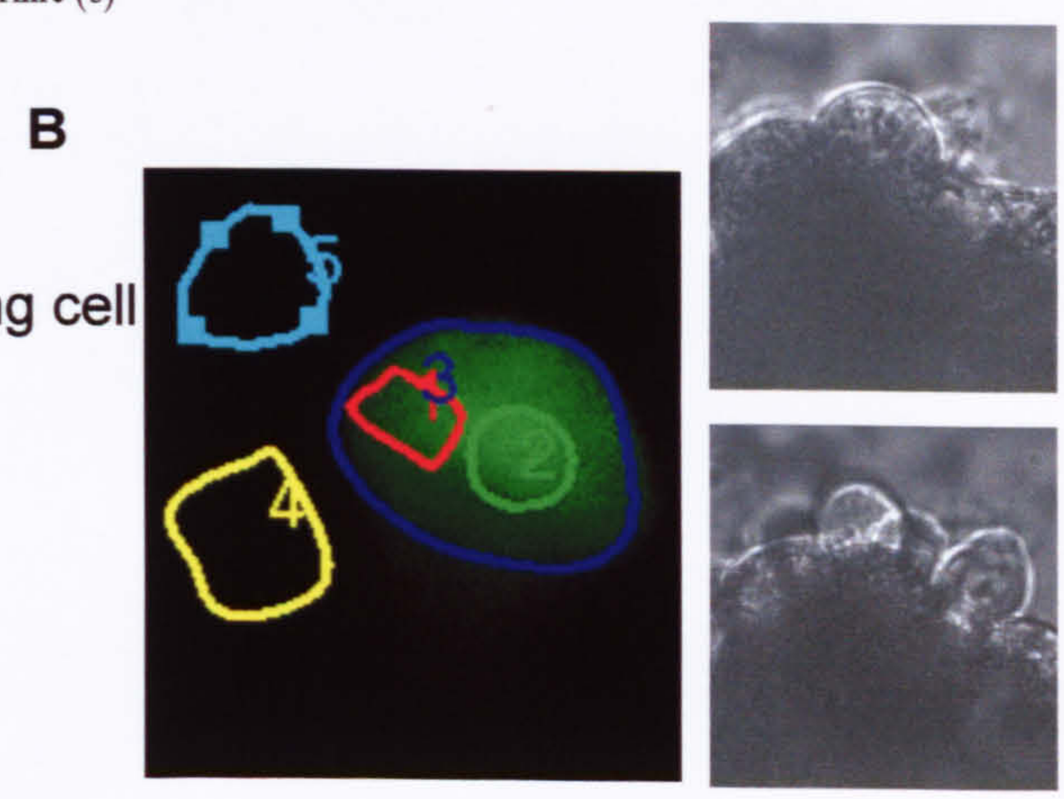

Figure 5.13ii **IκBα-GFP distribution before and after application of 10nM CCK** (**A**)The graph shows the measurements of GFP fluorescence from the regions of the cell shown in (**B**). The brown trace in (**A**) corresponds to the ratio of nuclear:cytoplasmic measurements (see right axis). Transmitted light pictures are shown in (**B**) the top was recorded before and the bottom image was recorded after treatment with 10nM CCK. The right image in (**B**) shows the fluorescence of the cell and the selected regions of interest.

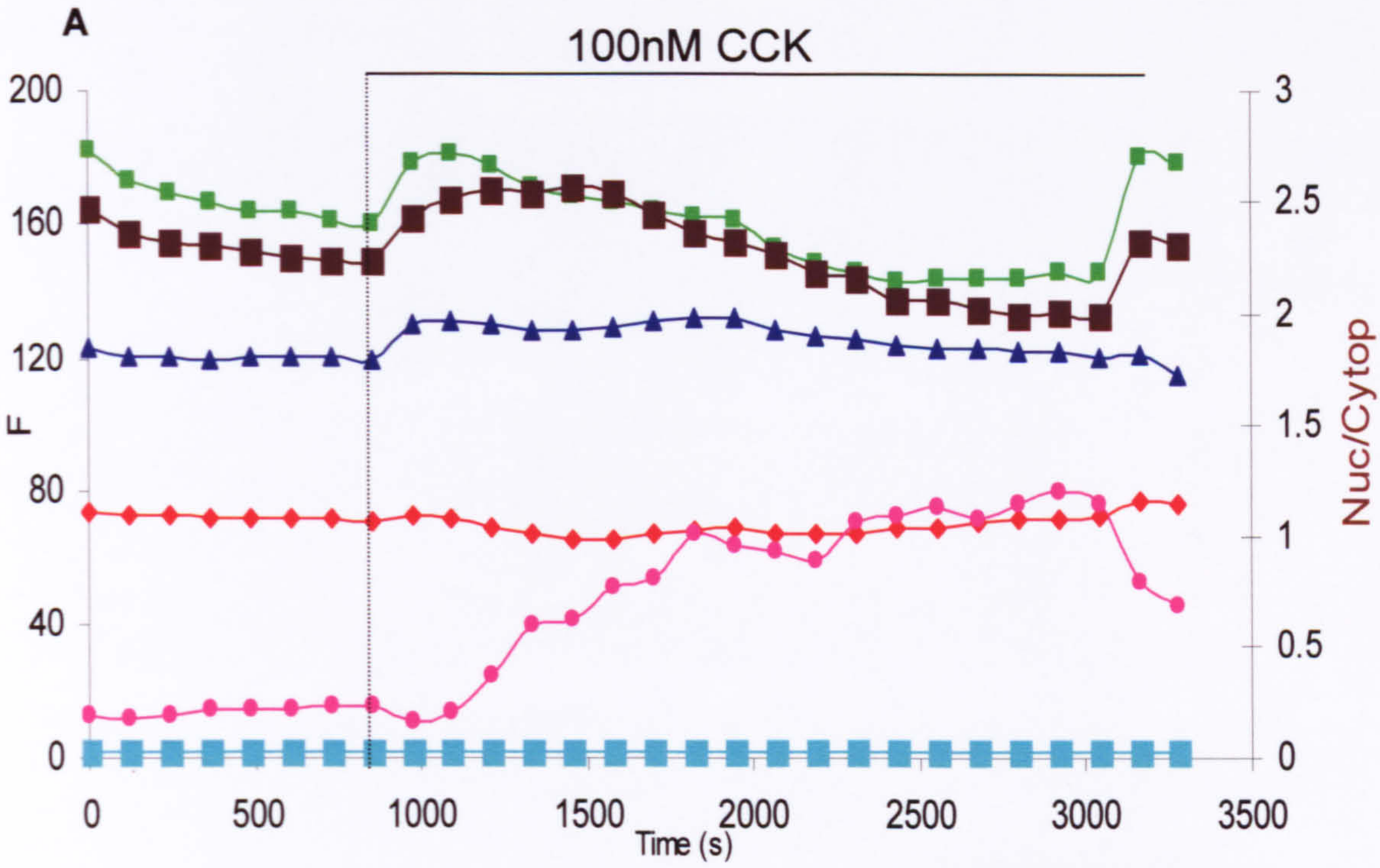

Green- nucleus
Red- cytoplasm
Blue- whole cell
Yellow- background
Turquoise- neighbouring non-expressing cell
Nucleus/Cytoplasm-Brown

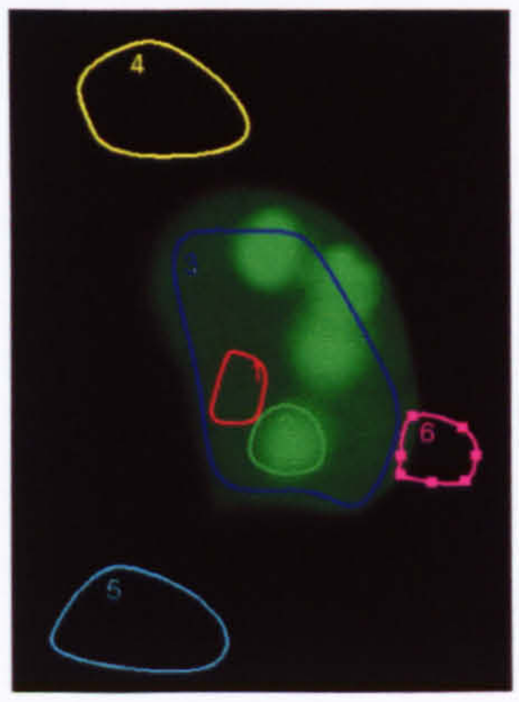

Figure 5.13iii **IκBα-GFP distribution before and after application of 100nM CCK** (**A**)The graph shows the measurements of GFP fluorescence from the regions of the cell shown in (**B**). The brown trace in (**A**)corresponds to the ratio of nuclear:cytoplasmic measurements. (B) shows fluorescent image and the selected regions of interest.

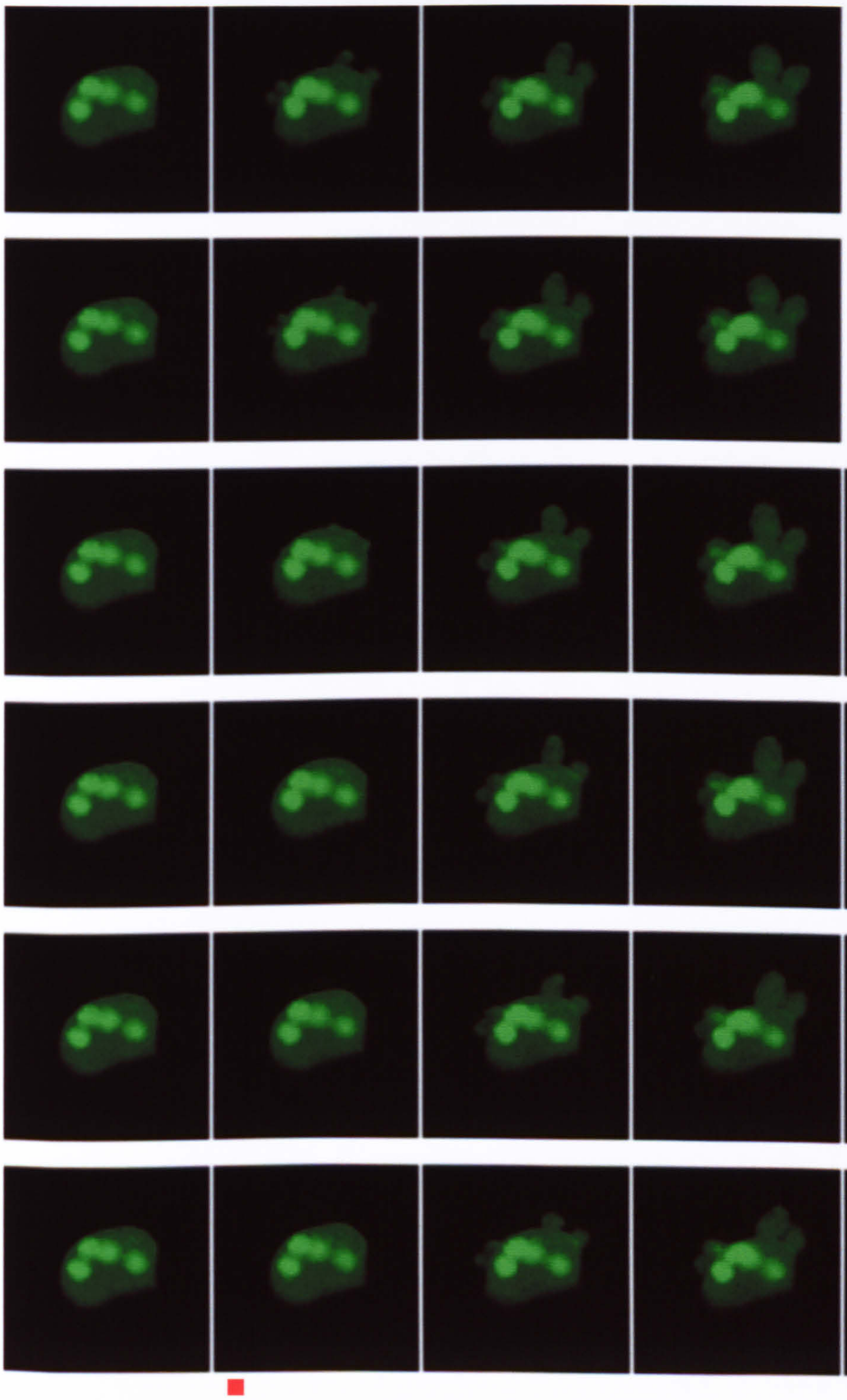

Figure 5.14 **Application of 100nM CCK induces blebbing** A series of images taken over 40mins the red square indicates the addition of 100nM CCK. The fluorescence is due to expression of IκBα-GFP.

Treatment of the cells with a p38 MAPK and proteasomal inhibitor before attempts to measure IκBα degradation

In an attempt to increase the induction of the IκBα-GFP degradation, cell isolation, injection and subsequent expression was done in the presence of SB203580, a p38 MAPK inhibitor and MG132, a proteasomal inhibitor. These inhibitors were used to successfully prevent the activation of cytokine expression due to inhibition of NFkB activation in rat pancreatic acinar cells (Blinman *et al.*, 2000). The stimulation of the cells expressing IκBα-GFP was preceded by removal of the inhibitors and extended washing of the cells; both inhibitors are reported to be reversible. Figure 5.15 shows the IκBα-GFP expressing cell and the traces of changes in the fluorescence in response to 100nM CCK. Two large cell movement artefacts occurred during the experiment. These artefacts may mask any induction of IκBα-GFP degradation; there was no clear evidence of any decrease in fluorescence in the cytoplasm or in the nuclear region (8 cells from 2 independent preparations, 3 experiments). The isolation, injection and expression of p65-GFP construct was also performed in the presence of the inhibitors SB203580 and MG132. There was no change in the distribution of GFP fluorescence, but there was still a significant amount of GFP in the nuclei, as shown in figure 5.16 (1 experiment). The removal of chick embryo extract from the culture medium was also done in one p65-GFP injection experiment, the GFP fluorescence was still localised to the nucleus (data not shown, 1 experiment).

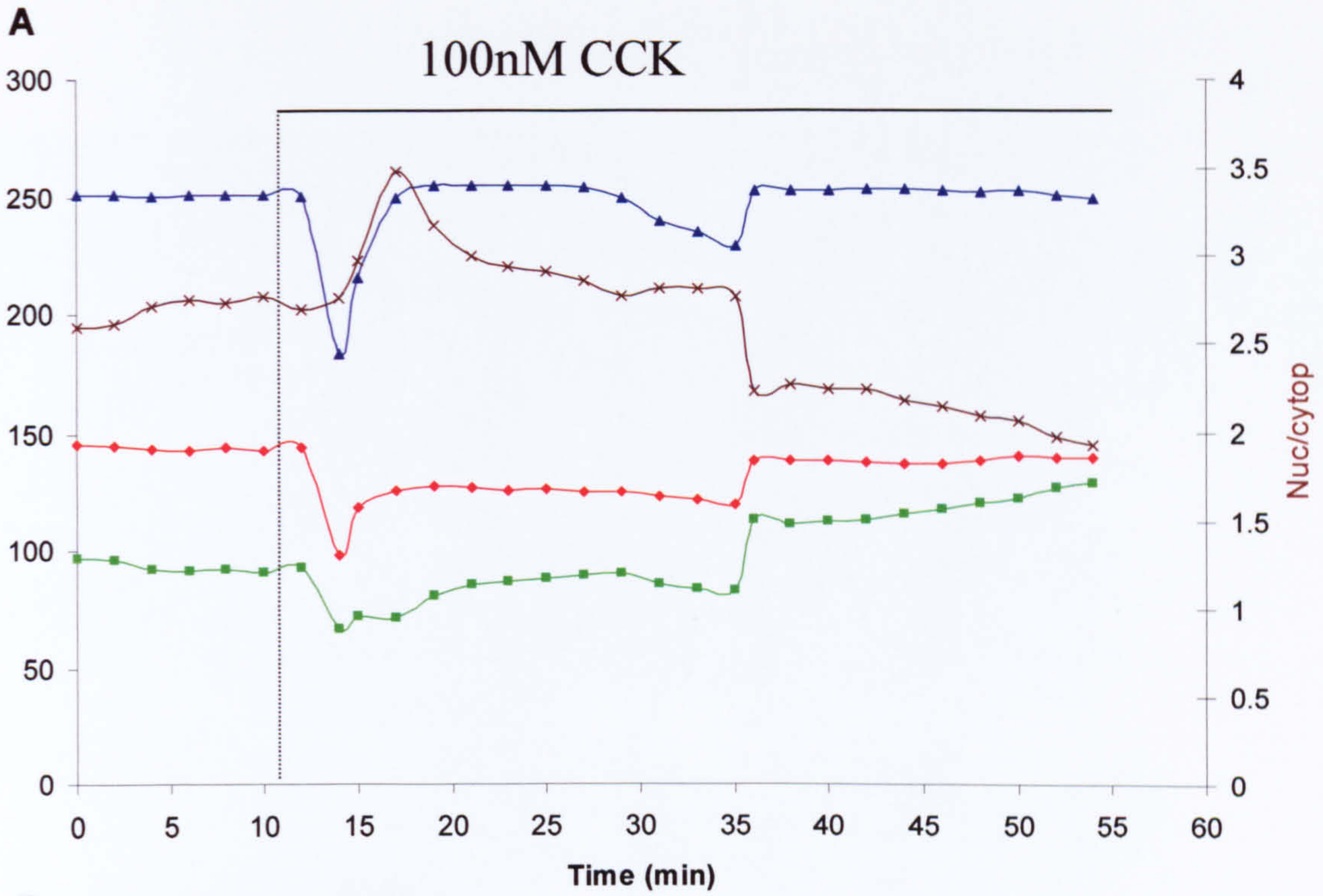

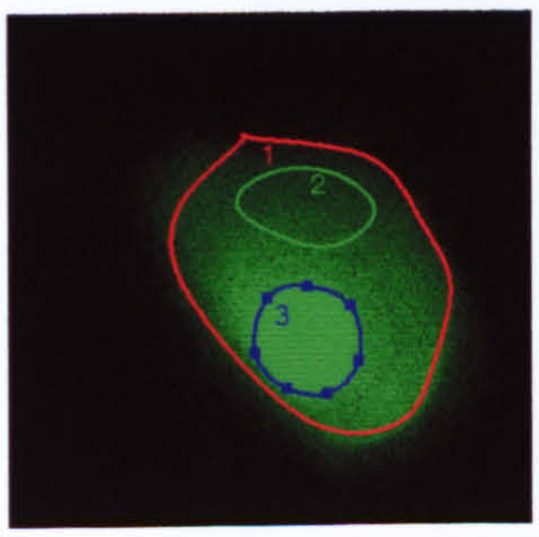

Red- Whole cell
Green – Cytoplasm
Blue – Nucleus
Brown Nucleus/cytoplasm

Figure 5.15 **IκBα-GFP distribution in the presence of SB203580, a p38 inhibitor and MG 132, a proteasome inhibitor and the effect of subsequent CCK application**. The expression of IκBα-GFP development in the presence of inhibitors SB203580 (20μM) and MG 132 (10μM) which were then washed off before the beginning of the experiment. (**A**) Graph in A shows the fluorescence recorded from the regions of the cell shown in (**B**). The brown trace in (**A**) represents the nucleus:cytoplasmic ratio (see right axis). There was a strong movement artefact during the recording. (**B**) Shows the fluorescent images and the selected regions of interest.

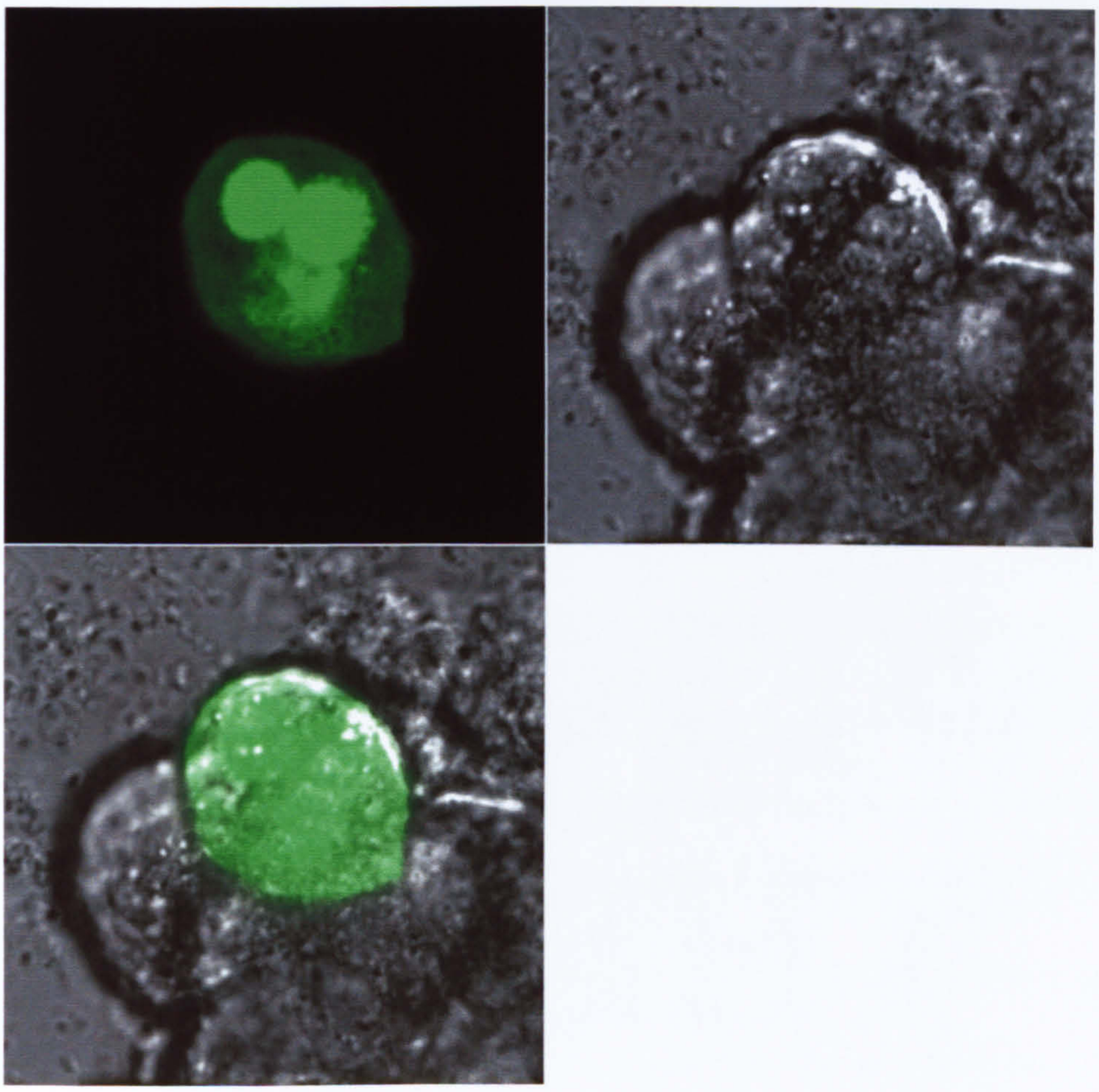

Figure 5.16 **The expression pattern of p65-GFP in the presence of p38 inhibitor, SB203580 and proteasome inhibitor MG 132**. The cells were incubated with SB203580 (20μM) and MG 132 (10μM). Fluorescence image is shown on the left, transmitted on the right. The bottom image shows the overlay of fluorescence and transmitted images.

Discussion

Initial experiments in HeLa cells demonstrated the ability to measure the NFκB activation via changes in p65-GFP distribution as an end point measurement and from a dynamic situation (time course)(figures 5.1 and 5.2). The studies in HeLa cells also allowed me to demonstrate the functionality of simultaneous calcium and translocation measurements. This was firstly shown by successful loading of p65-GFP expressing cells (figure 5.3), followed by experiments where changes in calcium could be monitored in response to uncaging of NP-EGTA measured through changes in fura red fluorescence and subsequent translocation via nuclear:cytoplasmic GFP ratios (figures 5.4 and 5.5). Interestingly a degree of translocation was observed in some experiments in response to calcium uncaging events in some HeLa cells. The temporal characteristics of the calcium increase seem to be very varied in the TNFα responses under normal conditions. It is known that such aspects of calcium signals are important in the regulation of downstream effects of calcium. Dolmetsch and colleagues showed that the frequency of calcium oscillations influence the activation of different transcription factors (Dolmetsch *et al.*, 1998). Calcium oscillation frequency has also been linked to activation of NFκB. Reduction of the oscillation frequency relative to the frequency induced by histamine in human aortic endothelial cells decreased the degree of NFκB activation measured by reporter gene activation (Hu *et al.*, 2002;Hu *et al.*, 1999).

The uncaging of calcium experiments may not have emulated the temporal characteristics of the calcium signals successfully and therefore we saw only two cells that may have exhibited some nuclear translocation of the p65-GFP, though not

to the same degree as that seen in cells treated with TNFα. However this only occurred in one experiment and it may be an artefact. The other conclusion is that the calcium increase alone is not enough to activate translocation of the p65-GFP molecules. This is supported by findings that calcium was required but was not sufficient enough to activate NFκB in pancreatic acinar cells (Han & Logsdon, 2000;Tando *et al.*, 1999). Both groups confirmed the requirement for PKC activity in addition to calcium elevation.

The effect of the calcium may be to modulate the actions of NFκB rather than to activate the translocation. Effects of calcium on the permeability of nuclear pores has been reported (Lee *et al.*, 1998;Perez-Terzic *et al.*, 1996;Stehno-Bittel *et al.*, 1995). This may be involved in the time the active subunit remains in the nucleus. Limiting or facilitating the access of the inhibitor subunit to the transcriptionally active subunit in the nucleus could be the means of calcium modulation. The calcium may also change the affinity of the NFκB active subunit for the promoter sequence or for other factors involved in transcription. This could be via the actions of calcium-activated kinases or calcium-calmodulin regulated kinases. Phosphorylation of the transcriptionally active subunit or the inhibitor protein may alter the activity of the pathway.

The main aim of these experiments was to monitor the degree of NFκB activation in pancreatic acinar cells. The experiments then transferred to measurements made in acinar cells.

The experiments investigating the agonist sensitivity of the cultured pancreatic acinar cells showed a concentration sensitivity consistent with those observed in acutely isolated cells (5 hours post isolation). This suggests that the cells, which are cultured for up to 24hrs under these conditions, are similar to the acutely isolated cells in their receptor profiles and affinities for the secretagogues. Therefore applications of agonists in the subsequent experiments are sufficient to induce the calcium responses as desired.

The injection of constructs encoding p65-GFP resulted in successful expression of the GFP conjugated protein, as detected by GFP fluorescence. The protein however already displayed a significantly higher fluorescence in the nucleus, in 9 out of 10 cells. Stimulation with agonists, which have previously been confirmed to activate NFκB in this cell type, produced no measurable increase of nuclear p65-GFP levels. It was suspected that the NFκB pathway was already fully activated in these cells. Attempts were made to reverse this nuclear NFκB accumulation by treatment with a PKC inhibitor GF109203X, which was reported by Han and colleagues to prevent the activation of NFkB pathways in rat pancreatic acinar cells (Han & Logsdon, 2000). This was unsuccessful; the application of the inhibitor had no measurable effect on the nuclear fluorescence of the p65-GFP protein.

The reduction of p65-GFP levels by photobleaching of the protein was possible. The first bleaching experiment also demonstrated the motility of the GFP molecule within the nucleus. The experiment where half of the projection area of the nucleus was subjected to photobleaching and the other half was not, showed a compensatory drop in the non-bleached half concurrent to the recovery in the bleached half. Almost no

recovery was observed in the nucleus which had been entirely bleached. Application of CCK after bleaching of the nuclear region of a cell produced no further measurable accumulation of p65-GFP (figure 5.12). The changes in cluster position and shape made the analysis difficult. Application of such powerful light to the nucleus could compromise the cell owing to possible DNA damage, which would induce stress pathways such as the NFκB cascades or p53.

The ability of the p65-GFP protein to freely move within the nuclear compartment (experiments with bleaching half of the nucleus) indicates that the p65-GFP is not all bound to the target sequence on the DNA. It would be of interest to analyse transcriptional activity in cells under these conditions (although practicalities of transcriptional activity measurements are complicated). Analysis of transcriptional activity may indicate the reason for nuclear accumulation of p65-GFP. If the nuclear accumulation is a symptom of over expression of the p65 subunit, which floods the endogenous inhibitor proteins capabilities to anchor the p65 subunit in the cytoplasm, then one might not expect a high level of transcription activation, indicating that the location within the nucleus may not be the only requirement for transcription activation. Alternatively a real induction of the NFkB cascade may induce a much higher level of transcriptional activity than any induced by overflow of the p65 protein owing to increased protein levels. Nuclear accumulation of p65 due to the application of LMB, an inhibitor of nuclear export, (p65 accumulates owing to cycling of the protein between the two compartments) in HeLa cells is not enough to induce transcriptional activity (Nelson *et al.*, 2002). However these experiments also demonstrated nuclear accumulation of the IκBα, which could have still been inhibiting the interaction of the p65 subunit and its target DNA sequences.

However what may be a more relevant finding is that the termination of transcription activity was the same as in cells not LMB treated, indicating that the inhibition can occur without nuclear export of the transcriptionally active subunit. An additional factor other than the location of the p65 protein is required for transcriptional activity.

The injection of the construct and expression of IκBα-GFP protein were successfully performed in the pancreatic acinar cell. Unexpectedly the IκBα-GFP also localised to the nucleus in the majority of experiments. This can be attributed to the lack of membrane bound organelles in the nucleoplasm and consequently larger volume accessible for diffusion fluid. This explanation was offered to account for the preferential nuclear distribution of other fluorescence molecules introduced into the cells (Connor, 1993;al Mohanna *et al.*, 1994). The aim was to measure the degradation of the protein; the site of IκBα degradation is the proteasome. The proteasome has been localised in both the cytoplasm and the nuclear compartments. Degradation of the native protein has also been measured in both the nuclear and cytoplasmic compartments (Renard *et al.*, 2000). Stimulation of the cells by different concentrations of CCK did not induce any measurable changes in the levels of IκBα–GFP, as artefacts from cell movement made analysis difficult. It is important to note however that a small degree of degradation may have been masked. The same concentrations of CCK have been used previously to activate the NFκB pathway (Han & Logsdon, 1999) and reasons for the discrepancy are not clear. The use of reversible inhibitors to block IκBα–GFP degradation before CCK addition was in order to maximise the potential change in IκBαGFP levels. There was still no measurable decrease in the IκBα-GFP fluorescence.

The absence of any measurable activation of NFκB cascade by either p65-GFP translocation to the nucleus, or degradation of IκBα–GFP in response to concentrations of CCK previously shown to activate the pathway in similar preparations could be attributed to a number of reasons. It is possible that the NFκB pathway was already saturated in this cell preparation; hence further activation was impossible to induce and measure. Pandol and colleagues have demonstrated the activation of the NFκB stress pathway as a result of cell isolation procedure (Blinman *et al.*; 2000). However others have used the similar isolation procedures and measured a subsequent induction of the NFkB cascade. Interestingly in experiments of Han and colleagues cells were allowed to rest for 2hrs after isolation (Han & Logsdon, 2000).

In the present studies the cells were microinjected to introduce the DNA constructs, due to an absence of expression with transfection techniques. The invasive procedure of microinjection is unavoidably going to induce the stress responses in injected cells. This could be a further explanation of the high background stress levels. However, the incubation time required for the expression of the GFP conjugated proteins is 5-14 hours, which varies with each experiment. This may allow time for the recovery of and down regulation of such microinjection-induced stress pathways.

Expression of the GFP conjugated proteins is driven by the CMV (Cyclomegalovirus) promoter, a very strong constitutively active promoter. Such high levels of expression may in itself stress the cells. The resources and energy of the cell will be redirected from other cellular processes to sustain the expression of

the GFP conjugated proteins. Compensatory increases in resource levels and reallocation may alter the resting cell conditions. The responses to CCK are thought to be intact owing to the rearrangement of the cytoskeleton in response to the agonist application detected through bleb formation (figure 5.14). The alterations of the cytoskeleton in response to high concentrations of agonists have been previously reported (Torgerson & McNiven, 2000).

The main difficulty in these experiments was the very low survival rate of cells after pressure injection and the impossibility of accurate analysis of small fluorescence changes due to cell movement artefacts.

Chapter 6

Final Discussion

Final Discussion

This thesis presents an examination of the actions of agonists, ACh and CCK, and bile acid, TLC-S, on a sustained cytosolic calcium plateau. It has been demonstrated that the agonists induced a reduction in calcium level, most likely via an activation of calcium efflux, whilst TLC-S induces three types of responses including, an increase in calcium level, an increase followed by a reduction, and a reduction in calcium.

The actions of ACh, CCK and TLC-S under conditions of sustained elevated cytosolic calcium are of interest with regard to the onset and development of pancreatitis. The action of secretagogues is probably due to acceleration of calcium efflux, most likely via the PMCA (see figures 3.9 and 3.10). The effect was revealed in "analytical" experiments using a calcium plateau formed by exposure of thapsigargin treated cells to high external calcium. The secretagogue-dependent acceleration of calcium extrusion should also have an effect on more physiological patterns of calcium signalling. The activation of calcium removal will affect the temporal properties of calcium transients and frequency of calcium oscillations.

In the experiment described in figure 3.9, the plateau was created by uncaging calcium within the cell in zero external calcium conditions. A reduction of the calcium plateau level in response to the agonist was observed. These experiments strongly support the idea that ACh and CCK reduce the calcium plateau level by enhancing the calcium extrusion rate.

This is in line with findings from S. Muallems' group who reported an acceleration of calcium extrusion by very high supramaximal concentrations of secretagogues

(Zhang *et al.*, 1992). My study suggests that much lower "physiological" concentrations of secretagogues are able to stimulate calcium efflux in pancreatic acinar cells. In other cell types similar effects of hormones on calcium efflux have been reported. Duddy and colleagues found that hormone vasopressin accelerates the calcium extrusion rate in hepatocytes (Duddy *et al.*, 1989) and Usachev and colleagues demonstrated an increase in calcium extrusion rate induced by bradykinin and ATP in neurons (Usachev *et al.*, 2002).

The observation by Campos-Toimil and colleagues that the plateau phase of responses to ACh in rat pancreatic acinar cells are at lower levels for 10μM ACh than at 1μM ACh, also support the idea of agonist stimulation of calcium extrusion (Campos-Toimil *et al.*, 2002). The degree of plateau reduction for 20pM CCK was less than that seen for 1nM and 10nM CCK, as was the case for 100nM and 1μM ACh (Table 1 chapter 3). This is also in agreement with observations of Campos-Toimil and colleagues.

The condition associated with elevated calcium in the acinar cells, acute pancreatitis, was proposed by Opie to be triggered by exposure to bile caused by reflux of bile due to blockage at the Ampulla of Vater. The effects of bile acid, TLC-S on calcium mobilisation in the pancreatic acinar cell have recently been investigated (Voronina *et al.*, 2002). The ability of TLC-S to induce release from internal calcium stores in oscillatory patterns and single transients with an elevated plateau was described in these experiments. The application of TLC-S, to cells treated with thapsigargin in presence of 3-10mM of external calcium to form an elevated calcium plateau, allowed examination of the effects of TLC-S on efflux and influx mechanisms.

In a proportion of the cells the effect of the TLC-S was opposite to that of ACh and CCK, an increase and not a decrease of the plateau level. This should make TLC-S a particularly dangerous activator of calcium toxicity. Some studies have suggested that calcium increases in response to TLC-S are due to its actions on the SERCA pumps in the ER membrane. My experiments indicate that this is not the only and probably not the main mechanism of TLC-S action. TLC-S clearly stimulates calcium release from internal stores of intact cells and its effect could be abolished by caffeine, an IP_3 receptor inhibitor (Voronina, *et al.*, 2001). The other action of TLC-S was discovered in experiments on cells with stores depleted by thapsigargin. I found that in considerable proportion of such cells exposed to elevated external calcium TLC-S increase calcium levels. TLC-S may influence the calcium influx mechanisms in the pancreatic acinar cell, as La^{3+} application and removal of external calcium attenuated the peak of TLC-S-induced calcium release. The application of La^{3+} did not completely abolish the calcium increase in response to TLC-S application, indicating that the increase is not purely influx through La^{3+} sensitive channels. The remaining increase in the presence of La^{3+} could be calcium influx through a La^{3+} insensitive channels or release from cellular organelles.

The involvement of organelle stored calcium in the TLC-S mediated calcium increase was investigated. The involvement of mitochondria and the granules was eliminated by results of experiments utilising inhibitors of these organelles; protonophore CCCP, a combination of rotenone and oligomycin and bafilomycin (see figures 4.8, 4.10 and 4.11). The involvement of the Golgi apparatus is still questionable, although the compound brefeldin A (reported to disassemble the Golgi

apparatus) had no effect on the TLC-S-induced calcium increase. This experiment however, cannot completely exclude that calcium release from Golgi contributes to TLC-S-induced by calcium response. The direct studies of Golgi involvement should ideally include intragolgi calcium measurements. This is however complicated and could not be done within the framework of the project. Presently we cannot exclude that part of the TLC-S-induced calcium rise is due to calcium release from an intracellular calcium store. This store could be the Golgi apparatus or an as yet unidentified thapsigargin insensitive intracellular store or calcium binding proteins.

The drop in calcium plateau level in response to TLC-S, sometimes observed after a calcium increase and sometimes in isolation, could be attributed to an increase in efflux. This type of response to TLC-S was not studied in detail; nonetheless there are some indications from the experiments examining the role of mitochondria in the TLC-S responses, that this type of TLC-S response is eliminated when mitochondria participation is prevented. The reduction of calcium plateau level after a TLC-S induced increase in calcium could be also attributed to an increase in extrusion. In this case action of TLC-S would be similar to ACh and CCK and conceivably could be mediated by the same mechanism.

The findings from chapters 3 and 4 and the effects of ACh, CCK and TLC-S on the machinery involved in calcium homeostasis are summarised in the figure 6.1. The red dashed lines indicate the findings from my studies. In particular the figure outlines the secretagogue mediated stimulation of the PMCA (possibly by tyrosine kinase action), the TLC-S actions on calcium influx mechanism, TLC-S mediated

release from ER and possible TLC-S induce calcium releases from an as yet unknown non-thapsigargin sensitive calcium store.

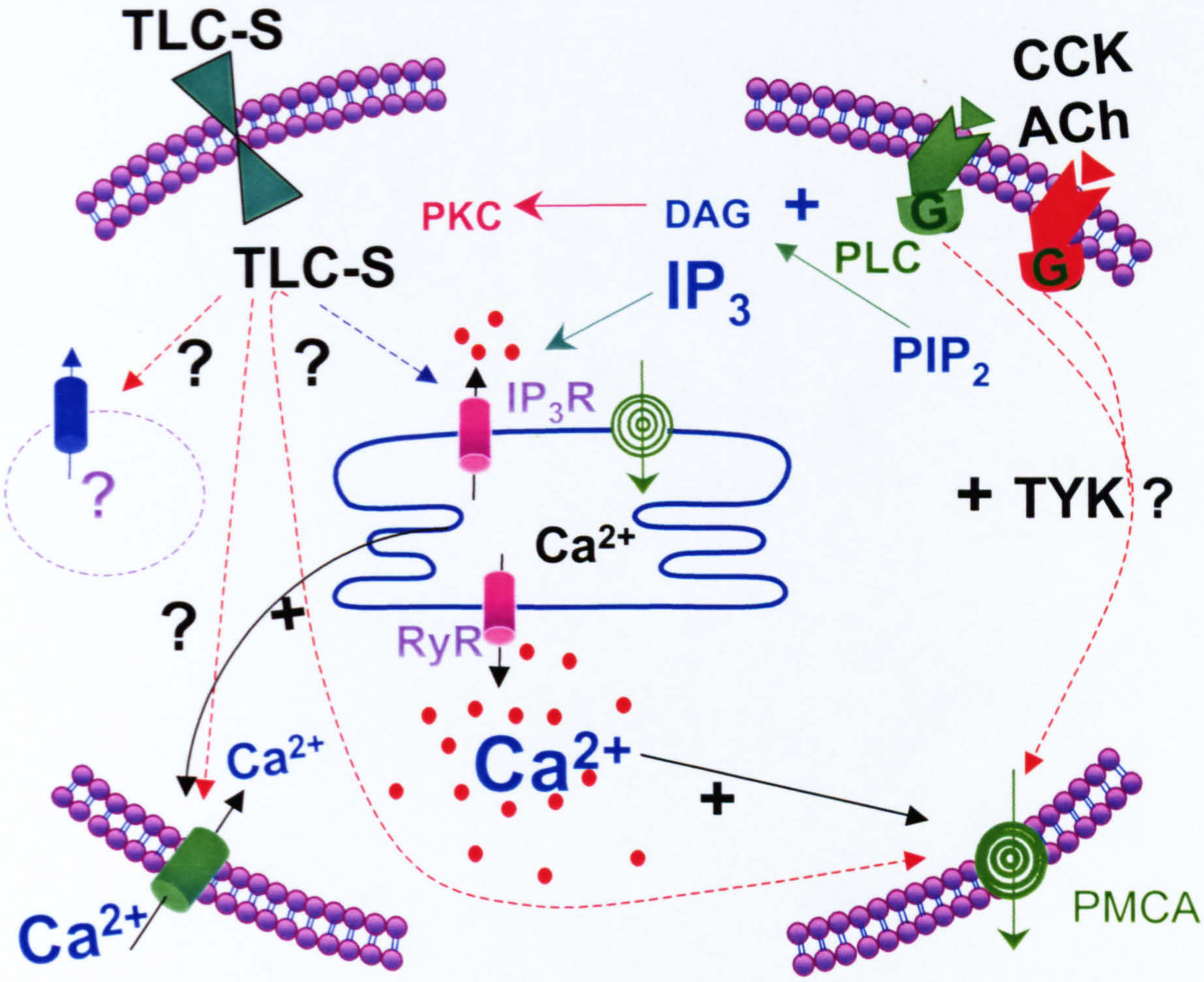

Figure 6.1 **A summary of the pathways examined in my thesis**. The TLC-S is probably imported into the pancreatic acinar cell via a transporter (Kim *et al.*, 2002), the dashed lines indicate the actions of TLC-S on the calcium homeostasis machinery within the cell proposed so far. The action on the ER is via the IP_3R (blue dashed line)(Voronina *et al.*, 2002), the actions indicated in chapter 4 of this thesis on influx and possibly release from an thapsigargin insensitive internal calcium store and the effect on calcium efflux through the plasma membrane are shown by red dashed lines. The important action of secretagogues ACh and CCK on the appropriate receptor is to activate the PLC mediated calcium mobilisation pathway. My results indicate (chapter 3) that these secretagogues also stimulate plasma membrane calcium pumps (red dashed line).

The trigger for development of acute pancreatitis is still unknown though associations with gallstones or micro crystals, high levels of secretagogues and high levels of alcohol intake exist. The trigger may actually be a combination of effects, of these and other factors. The action of bile may therefore be enhanced by secretagogue exposure. It is also important to note that patterns of calcium signalling change during progression of pancreatitis (Ward *et al.*, 1996).

Understanding of the regulation of PMCA by hormones and neurotransmitters may lead to the development of therapies to help control the problems related to acute calcium toxicity and deficiencies of calcium homeostasis related to ageing (Michaelis *et al.*, 1996;Griffith *et al.*, 2000;Thibault *et al.*, 2001). However the mechanisms of calcium clearance via the PMCA is common across all cell types. Therefore treatment could require targeting the effected cell type.

NFκB is considered as a mediator of acute pancreatitis (Grady *et al.*, 1997;Dunn *et al.*, 1997;Steinle *et al.*, 1999;Gukovsky *et al.*, 1998;Demols *et al.*, 2000). The participation of calcium in the activation of NFκB in pancreatic acinar cells has been observed at high supramaximal concentrations. Though the calcium increase is not absolutely necessary it appears to work synergistically with PKC activation (Han & Logsdon, 2000;Tando *et al.*, 1999). The aim of my experiments was to develop a method that would allow the simultaneous fast measurement of calcium and NFκB activation in the pancreatic acinar cell. Unfortunately the NFκB cascade appeared to be already fully activated in this cell preparation after introduction of the fusion protein encoding vectors. Attempts to reverse or inhibit the activation of the cascade

failed. No further activation could be measured upon stimulation with concentrations of agonist already reported to activate the pathway. The difficulty in quantifying the activation due to cell movement artefacts coupled with the apparent significant activation of NFκB before stimulation made this method of NFκB activation measurement unsuccessful. The reasons for the significant NFκB activation could be attributed to; the isolation procedure, the microinjection procedure of vector introduction, the toxicity of high levels of GFP (Liu *et al.*, 1999), or the high levels of expression driven by the CMV promoter or a combination of these. The reason for the observed NFκB activation has not been further investigated. I also had a low probability of expression of constructs after pressure injection and low survival rate of injected cells. Different transfection approach is clearly required to further develop this line of research.

This thesis extends the knowledge of secretagogue-induced regulation of calcium extrusion in the pancreatic acinar cell. The examination of TLC-S induced calcium signalling in the pancreatic acinar cell may lead to a greater understanding of the possible causes of onset and progression of acute pancreatitis.

Chapter 7

Bibliography

Bibliography

Abramcheck, C. W. & Best, P. M. (1989). Physiological role and selectivity of the in situ potassium channel of the sarcoplasmic reticulum in skinned frog skeletal muscle fibers. *J.Gen.Physiol* 93, 1-21.

Adams, S. R. & Tsien, R. Y. (1993). Controlling cell chemistry with caged compounds. *Annu.Rev.Physiol* 55, 755-784.

Adkins, C. E., Wissing, F., Potter, B. V., & Taylor, C. W. (2000). Rapid activation and partial inactivation of inositol trisphosphate receptors by adenophostin A. *Biochem.J.* 352 Pt 3, 929-933.

al Mohanna, F. A., Caddy, K. W., & Bolsover, S. R. (1994). The nucleus is insulated from large cytosolic calcium ion changes. *Nature* 367, 745-750.

Alderton, J. M., Ahmed, S. A., Smith, L. A., & Steinhardt, R. A. (2000). Evidence for a vesicle-mediated maintenance of store-operated calcium channels in a human embryonic kidney cell line. *Cell Calcium* 28, 161-169.

Algul, H., Tando, Y., Beil, M., Weber, C. K., Von Weyhern, C., Schneider, G., Adler, G., & Schmid, R. M. (2002). Different modes of NF-kappaB/Rel activation in pancreatic lobules. *Am.J.Physiol Gastrointest.Liver Physiol* 283, G270-G281.

Allbritton, N. L., Meyer, T., & Stryer, L. (1992). Range of messenger action of calcium ion and inositol 1,4,5- trisphosphate. *Science* 258, 1812-1815.

Anwer, M. S., Engelking, L. R., Nolan, K., Sullivan, D., Zimniak, P., & Lester, R. (1988). Hepatotoxic bile acids increase cytosolic Ca^{2+} activity of isolated rat hepatocytes. *Hepatology* 8, 887-891.

Ashby, M. C., Craske, M., Park, M. K., Gerasimenko, O. V., Burgoyne, R. D., Petersen, O. H., & Tepikin, A. V. (2002). Localized Ca^{2+} uncaging reveals polarized distribution of Ca^{2+}- sensitive Ca^{2+} release sites: mechanism of unidirectional Ca^{2+} waves. *J.Cell Biol.* 158, 283-292.

Ba-Thein, W., Caride, A. J., Enyedi, A., Paszty, K., Croy, C. L., Filoteo, A. G., & Penniston, J. T. (2001). Chimaeras reveal the role of the catalytic core in the activation of the plasma membrane Ca^{2+} pump. *Biochem.J.* 356, 241-245.

Bahnson, T. D., Pandol, S. J., & Dionne, V. E. (1993). Cyclic GMP modulates depletion-activated Ca^{2+} entry in pancreatic acinar cells. *J.Biol.Chem.* 268, 10808-10812.

Bakowski, D. & Parekh, A. B. (2001). Sarcoplasmic/endoplasmic-reticulum-Ca^{2+}-ATPase-mediated Ca^{2+} reuptake, and not $Ins(1,4,5)P_3$ receptor inactivation, prevents the activation of macroscopic Ca^{2+} release-activated Ca^{2+} current in the presence of physiological Ca^{2+} buffer in rat basophilic leukaemia-1 cells. *Biochem.J.* 353, 561-567.

Balasubramanyam, M. & Gardner, J. P. (1995). Protein kinase C modulates cytosolic free calcium by stimulating calcium pump activity in Jurkat T cells. *Cell Calcium* 18, 526-541.

Baldwin, A. S., Jr. (1996). The NF-kappa B and I kappa B proteins: new discoveries and insights. *Annu.Rev.Immunol.* 14, 649-683.

Barritt, G. J. (1999). Receptor-activated Ca^{2+} inflow in animal cells: a variety of pathways tailored to meet different intracellular Ca^{2+} signalling requirements. *Biochem.J.* 337 (Pt 2), 153-169.

Belan, P., Gerasimenko, O., Petersen, O. H., & Tepikin, A. V. (1997). Distribution of Ca^{2+} extrusion sites on the mouse pancreatic acinar cell surface. *Cell Calcium* 22, 5-10.

Belan, P. V., Gerasimenko, O. V., Tepikin, A. V., & Petersen, O. H. (1996). Localization of Ca^{2+} extrusion sites in pancreatic acinar cells. *J.Biol.Chem.* 271, 7615-7619.

Berridge, M. J. (1981). Phosphatidylinositol hydrolysis and calcium signaling. *Adv.Cyclic.Nucleotide.Res.* 14, 289-299.

Berridge, M. J. (1995). Capacitative calcium entry. *Biochem.J.* 312 (Pt 1), 1-11.

Bezprozvanny, I., Watras, J., & Ehrlich, B. E. (1991). Bell-shaped calcium-response curves of $Ins(1,4,5)P_3$- and calcium-gated channels from endoplasmic reticulum of cerebellum. *Nature* 351, 751-754.

Bhatia, M., Brady, M., Shokuhi, S., Christmas, S., Neoptolemos, J. P., & Slavin, J. (2000). Inflammatory mediators in acute pancreatitis. *J.Pathol.* 190, 117-125.

Blinman, T. A., Gukovsky, I., Mouria, M., Zaninovic, V., Livingston, E., Pandol, S. J., & Gukovskaya, A. S. (2000). Activation of pancreatic acinar cells on isolation from tissue: cytokine upregulation via p38 MAP kinase. *Am.J.Physiol Cell Physiol* 279, C1993-C2003.

Blondel, O., Moody, M. M., Depaoli, A. M., Sharp, A. H., Ross, C. A., Swift, H., & Bell, G. I. (1994). Localization of inositol trisphosphate receptor subtype 3 to insulin and somatostatin secretory granules and regulation of expression in islets and insulinoma cells. *Proc.Natl.Acad.Sci.U.S.A* **91**, 7777-7781.

Bockman, D. E., Schiller, W. R., Suriyapa, C., Mutchler, J. H., & Anderson, M. C. (1973). Fine structure of early experimental acute pancreatitis in dogs. *Lab Invest* **28**, 584-592.

Boitano, S., Dirksen, E. R., & Sanderson, M. J. (1992). Intercellular propagation of calcium waves mediated by inositol trisphosphate. *Science* **258**, 292-295.

Boulay, G., Brown, D. M., Qin, N., Jiang, M., Dietrich, A., Zhu, M. X., Chen, Z., Birnbaumer, M., Mikoshiba, K., & Birnbaumer, L. (1999). Modulation of Ca^{2+} entry by polypeptides of the inositol 1,4, 5- trisphosphate receptor (IP_3R) that bind transient receptor potential (TRP): evidence for roles of TRP and IP_3R in store depletion-activated Ca^{2+} entry. *Proc.Natl.Acad.Sci.U.S.A* **96**, 14955-14960.

Bouscarel, B., Kroll, S. D., & Fromm, H. (1999). Signal transduction and hepatocellular bile acid transport: cross talk between bile acids and second messengers. *Gastroenterology* **117**, 433-452.

Bozem, M., Kuhlmann, S., Blum, R., Feick, P., & Schulz, I. (2000). Hormone-stimulated calcium release is inhibited by cytoskeleton- disrupting toxins in AR4-2J cells. *Cell Calcium* **28**, 73-82.

Brannon, P. M., Orrison, B. M., & Kretchmer, N. (1985). Primary cultures of rat pancreatic acinar cells in serum-free medium. *In Vitro Cell Dev.Biol.* **21**, 6-14.

Brini, M., Bano, D., Manni, S., Rizzuto, R., & Carafoli, E. (2000). Effects of PMCA and SERCA pump overexpression on the kinetics of cell Ca^{2+} signalling. *EMBO J.* **19**, 4926-4935.

Broad, L. M., Armstrong, D. L., & Putney, J. W., Jr. (1999). Role of the inositol 1,4,5-trisphosphate receptor in Ca^{2+} feedback inhibition of calcium release-activated calcium current ($I_{(crac)}$). *J.Biol.Chem.* **274**, 32881-32888.

Camello, C., Pariente, J. A., Salido, G. M., & Camello, P. J. (1999). Sequential activation of different Ca^{2+} entry pathways upon cholinergic stimulation in mouse pancreatic acinar cells. *J.Physiol* **516 (Pt 2)**, 399-408.

Camello, P., Gardner, J., Petersen, O. H., & Tepikin, A. V. (1996). Calcium dependence of calcium extrusion and calcium uptake in mouse pancreatic acinar cells. *J.Physiol* 490 (Pt 3), 585-593.

Campos-Toimil, M., Bagrij, T., Edwardson, J. M., & Thomas, P. (2002). Two modes of secretion in pancreatic acinar cells: involvement of phosphatidylinositol 3-kinase and regulation by capacitative Ca^{2+} entry. *Curr.Biol.* 12, 211-215.

Cancela, J. M., Gerasimenko, O. V., Gerasimenko, J. V., Tepikin, A. V., & Petersen, O. H. (2000). Two different but converging messenger pathways to intracellular Ca^{2+} release: the roles of nicotinic acid adenine dinucleotide phosphate, cyclic ADP-ribose and inositol trisphosphate. *EMBO J.* 19, 2549-2557.

Cancela, J. M. & Petersen, O. H. (1998). The cyclic ADP ribose antagonist 8-NH2-cADP-ribose blocks cholecystokinin-evoked cytosolic Ca^{2+} spiking in pancreatic acinar cells. *Pflugers Arch.* 435, 746-748.

Capiod, T., Combettes, L., Noel, J., & Claret, M. (1991). Evidence for bile acid-evoked oscillations of Ca^{2+}-dependent K^+ permeability unrelated to a D-myo-inositol 1,4,5-trisphosphate effect in isolated guinea pig liver cells. *J.Biol.Chem.* 266, 268-273.

Carafoli, E. (1994). Biogenesis: plasma membrane calcium ATPase: 15 years of work on the purified enzyme. *FASEB J.* 8, 993-1002.

Chen, J., Wang, Y., Nakajima, T., Iwasawa, K., Hikiji, H., Sunamoto, M., Choi, D. K., Yoshida, Y., Sakaki, Y., & Toyo-Oka, T. (2000). Autocrine action and its underlying mechanism of nitric oxide on intracellular Ca^{2+} homeostasis in vascular endothelial cells. *J.Biol.Chem.* 275, 28739-28749.

Chen, X., Ji, B., Han, B., Ernst, S. A., Simeone, D., & Logsdon, C. D. (2002). NF-kappaB activation in pancreas induces pancreatic and systemic inflammatory response. *Gastroenterology* 122, 448-457.

Chiari, H. (1896). Über die selbstverdauung des menschlichen PanKreas. *Z Heilkunde* 17, 69-96.

Ching, T. T., Hsu, A. L., Johnson, A. J., & Chen, C. S. (2001). Phosphoinositide 3-kinase facilitates antigen-stimulated Ca^{2+} influx in RBL-2H3 mast cells via a phosphatidylinositol 3,4,5-trisphosphate-sensitive Ca^{2+} entry mechanism. *J.Biol.Chem.* 276, 14814-14820.

Chini, E. N., Beers, K. W., & Dousa, T. P. (1995). Nicotinate adenine dinucleotide phosphate (NAADP) triggers a specific calcium release system in sea urchin eggs. *J.Biol.Chem.* **270, 3216-3223.**

Combettes, L., Berthon, B., Doucet, E., Erlinger, S., & Claret, M. (1990). Bile acids mobilise internal Ca^{2+} independently of external Ca^{2+} in rat hepatocytes. *Eur.J.Biochem.* **190 , 619-623.**

Combettes, L., Dumont, M., Berthon, B., Erlinger, S., & Claret, M. (1988). Release of calcium from the endoplasmic reticulum by bile acids in rat liver cells. *J.Biol.Chem.* **263, 2299-2303.**

Connor, J. A. (1993). Intracellular calcium mobilization by inositol 1,4,5-trisphosphate: intracellular movements and compartmentalization. *Cell Calcium* **14,** 185-200.

Dean, W. L., Chen, D., Brandt, P. C., & Vanaman, T. C. (1997). Regulation of platelet plasma membrane Ca^{2+}-ATPase by cAMP-dependent and tyrosine phosphorylation. *J.Biol.Chem.* **272 ,** 15113-15119.

Dedkova, E. N. & Blatter, L. A. (2002). Nitric oxide inhibits capacitative Ca2+ entry and enhances endoplasmic reticulum Ca^{2+} uptake in bovine vascular endothelial cells. *J.Physiol* **539, 77-91.**

Demols, A., Van Laethem, J. L., Quertinmont, E., Legros, F., Louis, H., Le Moine, O., & Devicre, J. (2000). N-acetylcysteine decreases severity of acute pancreatitis in mice. *Pancreas* **20, 161-169.**

Dolmetsch, R. E., Xu, K., & Lewis, R. S. (1998). Calcium oscillations increase the efficiency and specificity of gene expression. *Nature* **392,** 933-936.

Duan, R. D. & Erlanson-Albertsson, C. (1988). Calcium fluxes caused by bile salts in rat pancreatic acini. *Scand.J.Gastroenterol.* **23,** 891-896.

Duchen, M. R. (2000). Mitochondria and calcium: from cell signalling to cell death. *J.Physiol* **529 Pt 1,** 57-68.

Duchen, M. R. (1999). Contributions of mitochondria to animal physiology: from homeostatic sensor to calcium signalling and cell death. *J.Physiol* **516 (Pt 1),** 1-17.

Duddy, S. K., Kass, G. E., & Orrenius, S. (1989). Ca^{2+}-mobilizing hormones stimulate Ca^{2+} efflux from hepatocytes. *J.Biol.Chem.* **264,** 20863-20866.

Dunn, J. A., Li, C., Ha, T., Kao, R. L., & Browder, W. (1997). Therapeutic modification of nuclear factor kappa B binding activity and tumor necrosis factor-alpha gene expression during acute biliary pancreatitis. *Am.Surg.* **63**, 1036-1043.

Eimerl, S., Savion, N., Heichal, O., & Selinger, Z. (1974). Induction of enzyme secretion in rat pancreatic slices using the ionophore A-23187 and calcium. An experimental bypass of the hormone receptor pathway. *J.Biol.Chem.* **249**, 3991-3993.

Elliott, A. C. (2001). Recent developments in non-excitable cell calcium entry. *Cell Calcium* **30**, 73-93.

Elwess, N. L., Filoteo, A. G., Enyedi, A., & Penniston, J. T. (1997). Plasma membrane Ca^{2+} pump isoforms 2a and 2b are unusually responsive to calmodulin and Ca^{2+}. *J.Biol.Chem.* **272**, 17981-17986.

Emmanouilidou, E., Teschemacher, A. G., Pouli, A. E., Nicholls, L. I., Seward, E. P., & Rutter, G. A. (1999). Imaging Ca^{2+} concentration changes at the secretory vesicle surface with a recombinant targeted cameleon. *Curr.Biol.* **9**, 915-918.

Enyedi, A., Elwess, N. L., Filoteo, A. G., Verma, A. K., Paszty, K., & Penniston, J. T. (1997). Protein kinase C phosphorylates the "a" forms of plasma membrane Ca^{2+} pump isoforms 2 and 3 and prevents binding of calmodulin. *J.Biol.Chem.* **272**, 27525-27528.

Enyedi, A., Verma, A. K., Filoteo, A. G., & Penniston, J. T. (1996). Protein kinase C activates the plasma membrane Ca^{2+} pump isoform 4b by phosphorylation of an inhibitory region downstream of the calmodulin- binding domain. *J.Biol.Chem.* **271**, 32461-32467.

Enyedi, A., Vorherr, T., James, P., McCormick, D. J., Filoteo, A. G., Carafoli, E., & Penniston, J. T. (1989). The calmodulin binding domain of the plasma membrane Ca^{2+} pump interacts both with calmodulin and with another part of the pump. *J.Biol.Chem.* **264**, 12313-12321.

Falchetto, R., Vorherr, T., Brunner, J., & Carafoli, E. (1991). The plasma membrane Ca^{2+} pump contains a site that interacts with its calmodulin-binding domain. *J.Biol.Chem.* **266**, 2930-2936.

Filoteo, A. G., Elwess, N. L., Enyedi, A., Caride, A., Aung, H. H., & Penniston, J. T. (1997). Plasma membrane Ca^{2+} pump in rat brain. Patterns of alternative splices seen by isoform-specific antibodies. *J.Biol.Chem.* **272**, 23741-23747.

Filoteo, A. G., Enyedi, A., Verma, A. K., Elwess, N. L., & Penniston, J. T. (2000). Plasma membrane Ca^{2+} pump isoform 3f is weakly stimulated by calmodulin. *J.Biol.Chem.* **275**, 4323-4328.

Findlay, I. & Petersen, O. H. (1982). Acetylcholine-evoked uncoupling restricts the passage of Lucifer Yellow between pancreatic acinar cells. *Cell Tissue Res.* **225**, 633-638.

Findlay, I. & Petersen, O. H. (1983). The extent of dye-coupling between exocrine acinar cells of the mouse pancreas. The dye-coupled acinar unit. *Cell Tissue Res.* **232**, 121-127.

Fitz, R. H. (1889). Acute pancreatitis; a consideration of pancreatic hemorrhage, hemorrhagic suppurative, and gangrenous pancreatitis, and of disseminated fat-necrosis. *Boston Medical and Surgical Journal* **120**, 181-187.

Fitzsimmons, T. J., Gukovsky, I., McRoberts, J. A., Rodriguez, E., Lai, F. A., & Pandol, S. J. (2000). Multiple isoforms of the ryanodine receptor are expressed in rat pancreatic acinar cells. *Biochem.J.* **351**, 265-271.

Frick, T. W., Fernandez-del Castillo, C., Bimmler, D., & Warshaw, A. L. (1997). Elevated calcium and activation of trypsinogen in rat pancreatic acini. *Gut* **41**, 339-343.

Furukawa, K. & Nakamura, H. (1987). Cyclic GMP regulation of the plasma membrane Ca^{2+}-Mg^{2+}ATPase in vascular smooth muscle. *J.Biochem.(Tokyo)* **101**, 287-290.

Gaisano, H. Y., Lutz, M. P., Leser, J., Sheu, L., Lynch, G., Tang, L., Tamori, Y., Trimble, W. S., & Salapatek, A. M. (2001). Supramaximal cholecystokinin displaces Munc18c from the pancreatic acinar basal surface, redirecting apical exocytosis to the basal membrane. *J.Clin.Invest* **108**, 1597-1611.

Gaisano, H. Y., Sheu, L., Wong, P. P., Klip, A., & Trimble, W. S. (1997). SNAP-23 is located in the basolateral plasma membrane of rat pancreatic acinar cells. *FEBS Lett.* **414**, 298-302.

Gardner, J. D. & Jensen, R. T. (1986). Receptors and cell activation associated with pancreatic enzyme secretion. *Annu.Rev.Physiol* **48**, 103-117.

Gerasimenko, O. V., Gerasimenko, J. V., Belan, P. V., & Petersen, O. H. (1996). Inositol trisphosphate and cyclic ADP-ribose-mediated release of Ca^{2+} from single isolated pancreatic zymogen granules. *Cell* **84**, 473-480.

Gerasimenko, O. V., Gerasimenko, J. V., Tepikin, A. V., & Petersen, O. H. (1995). ATP-dependent accumulation and inositol trisphosphate- or cyclic ADP- ribose-mediated release of Ca^{2+} from the nuclear envelope. *Cell* **80**, 439-444.

Ghosh, S. & Karin, M. (2002). Missing pieces in the NF-kappaB puzzle. *Cell* **109 Suppl**, S81-S96.

Gilabert, J. A., Bakowski, D., & Parekh, A. B. (2001). Energized mitochondria increase the dynamic range over which inositol 1,4,5-trisphosphate activates store-operated calcium influx. *EMBO J.* **20**, 2672-2679.

Gilabert, J. A. & Parekh, A. B. (2000). Respiring mitochondria determine the pattern of activation and inactivation of the store-operated Ca^{2+} current I_{CRAC}. *EMBO J.* **19**, 6401-6407.

Gobel, A., Krause, E., Feick, P., & Schulz, I. (2001). IP_3 and cyclic ADP-ribose induced Ca^{2+} release from intracellular stores of pancreatic acinar cells from rat in primary culture. *Cell Calcium* **29**, 29-37.

Gonzalez, A., Schmid, A., Sternfeld, L., Krause, E., Salido, G. M., & Schulz, I. (1999). Cholecystokinin-evoked Ca^{2+} waves in isolated mouse pancreatic acinar cells are modulated by activation of cytosolic phospholipase A_2, phospholipase D, and protein kinase C. *Biochem.Biophys.Res.Commun.* **261**, 726-733.

Gorelick, F. S. & Jamieson, J. D. (1994). The pancreatic acinar cell:structure-function relationships. In *Physiology of the Gastrointestinal Tract*, ed. Johnson, L. R., pp. 1353-1376. Raven Press, New York.

Grady, T., Liang, P., Ernst, S. A., & Logsdon, C. D. (1997). Chemokine gene expression in rat pancreatic acinar cells is an early event associated with acute pancreatitis. *Gastroenterology* **113**, 1966-1975.

Grady, T., Saluja, A., Kaiser, A., & Steer, M. (1996). Edema and intrapancreatic trypsinogen activation precede glutathione depletion during caerulein pancreatitis. *Am.J.Physiol* **271**, G20-G26.

Griffith, W. H., Jasek, M. C., Bain, S. H., & Murchison, D. (2000). Modification of ion channels and calcium homeostasis of basal forebrain neurons during aging. *Behav.Brain Res.* **115**, 219-233.

Grynkiewicz, G., Poenie, M., & Tsien, R. Y. (1985). A new generation of Ca^{2+} indicators with greatly improved fluorescence properties. *J.Biol.Chem.* **260**, 3440-3450.

Gukovskaya, A. S., Gukovsky, I., Zaninovic, V., Song, M., Sandoval, D., Gukovsky, S., & Pandol, S. J. (1997). Pancreatic acinar cells produce, release, and respond to tumor necrosis factor-alpha. Role in regulating cell death and pancreatitis. *J.Clin.Invest* **100**, 1853-1862.

Gukovsky, I., Gukovskaya, A. S., Blinman, T. A., Zaninovic, V., & Pandol, S. J. (1998). Early NF-kappaB activation is associated with hormone-induced pancreatitis. *Am.J.Physiol* **275**, G1402-G1414.

Gyorke, S. (1999). Ca^{2+} spark termination: inactivation and adaptation may be manifestations of the same mechanism. *J.Gen.Physiol* **114**, 163-166.

Han, B., Ji, B., & Logsdon, C. D. (2001). CCK independently activates intracellular trypsinogen and NF-kappaB in rat pancreatic acinar cells. *Am.J.Physiol Cell Physiol* **280**, C465-C472.

Han, B. & Logsdon, C. D. (1999). Cholecystokinin induction of mob-1 chemokine expression in pancreatic acinar cells requires NF-kappaB activation. *Am.J.Physiol* **277**, C74-C82.

Han, B. & Logsdon, C. D. (2000). CCK stimulates mob-1 expression and NF-kappaB activation via protein kinase C and intracellular Ca^{2+}. *Am.J.Physiol Cell Physiol* **278**, C344-C351.

Hardingham, G. E., Arnold, F. J., & Bading, H. (2001). Nuclear calcium signaling controls CREB-mediated gene expression triggered by synaptic activity. *Nat.Neurosci.* **4**, 261-267.

Harteneck, C., Plant, T. D., & Schultz, G. (2000). From worm to man: three subfamilies of TRP channels. *Trends Neurosci.* **23**, 159-166.

Hendricks, L. C., McClanahan, S. L., Palade, G. E., & Farquhar, M. G. (1992). Brefeldin A affects early events but does not affect late events along the exocytic pathway in pancreatic acinar cells. *Proc.Natl.Acad.Sci.U.S.A* **89**, 7242-7246.

Hennager, D. J., Welsh, M. J., & DeLisle, S. (1995). Changes in either cytosolic or nucleoplasmic inositol 1,4,5- trisphosphate levels can control nuclear Ca^{2+} concentration. *J.Biol.Chem.* **270**, 4959-4962.

Hermosura, M. C., Takeuchi, H., Fleig, A., Riley, A. M., Potter, B. V., Hirata, M., & Penner, R. (2000). $InsP_4$ facilitates store-operated calcium influx by inhibition of $InsP_3$ 5-phosphatase. *Nature* **408**, 735-740.

Hirano, F., Kobayashi, A., Hirano, Y., Nomura, Y., Fukawa, E., & Makino, I. (2001). Bile acids regulate RANTES gene expression through its cognate NF- kappaB binding sites. *Biochem.Biophys.Res.Commun.* **288**, 1095-1101.

Hirohata, Y., Fujii, M., Okabayashi, Y., Nagashio, Y., Tashiro, M., Imoto, I., Akiyama, T., & Otsuki, M. (2002). Stimulatory effects of bilirubin on amylase release from isolated rat pancreatic acini. *Am.J.Physiol Gastrointest.Liver Physiol* **282**, G249-G256.

Hoenderop, J. G., van der Kemp, A. W., Hartog, A., van Os, C. H., Willems, P. H., & Bindels, R. J. (1999). The epithelial calcium channel, ECaC, is activated by hyperpolarization and regulated by cytosolic calcium. *Biochem.Biophys.Res.Commun.* **261**, 488-492.

Hoenderop, J. G., Vennekens, R., Muller, D., Prenen, J., Droogmans, G., Bindels, R. J., & Nilius, B. (2001). Function and expression of the epithelial Ca^{2+} channel family: comparison of mammalian ECaC1 and 2. *J.Physiol* **537**, 747-761.

Hofer, A. M., Fasolato, C., & Pozzan, T. (1998). Capacitative Ca^{2+} entry is closely linked to the filling state of internal Ca^{2+} stores: a study using simultaneous measurements of ICRAC and intraluminal $[Ca^{2+}]$. *J.Cell Biol.* **140**, 325-334.

Hofmann (1994a). Biliary Secretion and Excretion. In *Physiology of the Gastrointestinal Tract*, ed. Johnson, L. R., pp. 1555-1576. Raven press, New York.

Hofmann, F., Anagli, J., Carafoli, E., & Vorherr, T. (1994). Phosphorylation of the calmodulin binding domain of the plasma membrane Ca^{2+} pump by protein kinase C reduces its interaction with calmodulin and with its pump receptor site. *J.Biol.Chem.* **269**, 24298-24303.

Hokin, M. R. & Hokin, L. E. (1953). Enzyme secretion and the incorporation of P^{32} into phospholipids of pancreas slices. *The Journal of Biological Chemistry* **203**, 967-77.

Hoth, M. & Penner, R. (1992). Depletion of intracellular calcium stores activates a calcium current in mast cells. *Nature* 355, 353-356.

Hu, Q., Deshpande, S., Irani, K., & Ziegelstein, R. C. (1999). $[Ca^{2+}]_i$ oscillation frequency regulates agonist-stimulated NF- kappaB transcriptional activity. *J.Biol.Chem.* 274, 33995-33998.

Hu, Q., Natarajan, V., & Ziegelstein, R. C. (2002). Phospholipase D regulates calcium oscillation frequency and nuclear factor-kappaB activity in histamine- stimulated human endothelial cells. *Biochem.Biophys.Res.Commun.* 292, 325-332.

Humbert, J. P., Matter, N., Artault, J. C., Koppler, P., & Malviya, A. N. (1996). Inositol 1,4,5-trisphosphate receptor is located to the inner nuclear membrane vindicating regulation of nuclear calcium signaling by inositol 1,4,5-trisphosphate. Discrete distribution of inositol phosphate receptors to inner and outer nuclear membranes. *J.Biol.Chem.* 271, 478-485.

Imbert, V., Rupec, R. A., Livolsi, A., Pahl, H. L., Traenckner, E. B., Mueller-Dieckmann, C., Farahifar, D., Rossi, B., Auberger, P., Baeuerle, P. A., & Peyron, J. F. (1996). Tyrosine phosphorylation of I kappa B-alpha activates NF-kappa B without proteolytic degradation of I kappa B-alpha. *Cell* 86, 787-798.

Irvine, R. F. (1990). 'Quantal' Ca^{2+} release and the control of Ca^{2+} entry by inositol phosphates--a possible mechanism. *FEBS Lett.* 263, 5-9.

Iwatsuki, N. & Petersen, O. H. (1978). Electrical coupling and uncoupling of exocrine acinar cells. *J.Cell Biol.* 79, 533-545.

Iwatsuki, N. & Petersen, O. H. (1979a). Direct visualization of cell to cell coupling: transfer of fluorescent probes in living mammalian pancreatic acini. *Pflugers Arch.* 380, 277-281.

Iwatsuki, N. & Petersen, O. H. (1979b). Pancreatic acinar cells: the effect of carbon dioxide, ammonium chloride and acetylcholine on intercellular communication. *J.Physiol* 291, 317-326.

James, P. H., Pruschy, M., Vorherr, T. E., Penniston, J. T., & Carafoli, E. (1989). Primary structure of the cAMP-dependent phosphorylation site of the plasma membrane calcium pump. *Biochemistry* 28, 4253-4258.

Jayaraman, T., Ondriasova, E., Ondrias, K., Harnick, D. J., & Marks, A. R. (1995). The inositol 1,4,5-trisphosphate receptor is essential for T-cell receptor signaling. *Proc.Natl.Acad.Sci.U.S.A* 92, 6007-6011.

Jensen, R. T. (1994). Receptors on pancreatic acinar cells. In *Physiology of the Gastrointestinal Tract*, ed. Johnson, L. R., pp. 1377-1446. Raven Press, New York.

Johansson, J. S. & Haynes, D. H. (1992). Cyclic GMP increases the rate of the calcium extrusion pump in intact human platelets but has no direct effect on the dense tubular calcium accumulation system. *Biochim.Biophys.Acta* 1105, 40-50.

Johansson, J. S., Nied, L. E., & Haynes, D. H. (1992). Cyclic AMP stimulates Ca^{2+}-ATPase-mediated Ca2+ extrusion from human platelets. *Biochim.Biophys.Acta* 1105, 19-28.

Johnson, P., Tepikin, A., & Erdemli, G. (2002). Role of mitochondria in Ca^{2+} homeostasis of mouse pancreatic acinar cells. *Cell Calcium* 32, 59.

Kamouchi, M., Philipp, S., Flockerzi, V., Wissenbach, U., Mamin, A., Raeymaekers, L., Eggermont, J., Droogmans, G., & Nilius, B. (1999). Properties of heterologously expressed hTRP3 channels in bovine pulmonary artery endothelial cells. *J.Physiol* 518 Pt 2, 345-358.

Kanno, T. (1972). Calcium-dependent amylase release and electrophysiological measurements in cells of the pancreas. *J.Physiol* 226, 353-371.

Kasai, H., Li, Y. X., & Miyashita, Y. (1993). Subcellular distribution of Ca^{2+} release channels underlying Ca^{2+} waves and oscillations in exocrine pancreas. *Cell* 74, 669-677.

Kim, E., DeMarco, S. J., Marfatia, S. M., Chishti, A. H., Sheng, M., & Strehler, E. E. (1998). Plasma membrane Ca^{2+} ATPase isoform 4b binds to membrane-associated guanylate kinase (MAGUK) proteins via their PDZ (PSD-95/Dlg/ZO-1) domains. *J.Biol.Chem.* 273, 1591-1595.

Kim, J. Y., Kim, K. H., Lee, J. A., Namkung, W., Sun, A. Q., Ananthanarayanan, M., Suchy, F. J., Shin, D. M., Muallem, S., & Lee, M. G. (2002). Transporter-mediated bile acid uptake causes Ca^{2+}-dependent cell death in rat pancreatic acinar cells. *Gastroenterology* 122, 1941-1953.

Kiselyov, K., Xu, X., Mozhayeva, G., Kuo, T., Pessah, I., Mignery, G., Zhu, X., Birnbaumer, L., & Muallem, S. (1998). Functional interaction between $InsP_3$ receptors and store-operated Htrp3 channels. *Nature* 396, 478-482.

Kohut, M., Nowak, A., Nowakowska-Duiawa, E., & Marek, T. (2002). Presence and density of common bile duct microlithiasis in acute biliary pancreatitis. *World J.Gastroenterol.* 8, 558-561.

Komhoff, M., Hollinshead, M., Tooze, J., & Kern, H. F. (1994). Brefeldin A induced dose-dependent changes to Golgi structure and function in the rat exocrine pancreas. *Eur.J.Cell Biol.* 63, 192-207.

Krause, E., Pfeiffer, F., Schmid, A., & Schulz, I. (1996). Depletion of intracellular calcium stores activates a calcium conducting nonselective cation current in mouse pancreatic acinar cells. *J.Biol.Chem.* 271, 32523-32528.

Kruger, B., Albrecht, E., & Lerch, M. M. (2000). The role of intracellular calcium signaling in premature protease activation and the onset of pancreatitis. *Am.J.Pathol.* 157, 43-50.

Kuo, T. H., Liu, B. F., Yu, Y., Wuytack, F., Raeymaekers, L., & Tsang, W. (1997). Co-ordinated regulation of the plasma membrane calcium pump and the sarco(endo)plasmic reticular calcium pump gene expression by Ca^{2+}. *Cell Calcium* 21, 399-408.

Lankisch, T. O., Nozu, F., Owyang, C., & Tsunoda, Y. (1999). High-affinity cholecystokinin type A receptor/cytosolic phospholipase A_2 pathways mediate Ca^{2+} oscillations via a positive feedback regulation by calmodulin kinase in pancreatic acini. *Eur.J.Cell Biol.* 78, 632-641.

Lee, M. A., Dunn, R. C., Clapham, D. E., & Stehno-Bittel, L. (1998). Calcium regulation of nuclear pore permeability. *Cell Calcium* 23, 91-101.

Lee, M. G., Xu, X., Zeng, W., Diaz, J., Wojcikiewicz, R. J., Kuo, T. H., Wuytack, F., Racymaekers, L., & Muallem, S. (1997). Polarized expression of Ca^{2+} channels in pancreatic and salivary gland cells. Correlation with initiation and propagation of $[Ca2+]_i$ waves. *J.Biol.Chem.* 272, 15765-15770.

Li, W., Llopis, J., Whitney, M., Zlokarnik, G., & Tsien, R. Y. (1998). Cell-permeant caged $InsP_3$ ester shows that Ca^{2+} spike frequency can optimize gene expression. *Nature* 392, 936-941.

Liu, H. S., Jan, M. S., Chou, C. K., Chen, P. H., & Ke, N. J. (1999). Is green fluorescent protein toxic to the living cells? *Biochem.Biophys.Res.Commun.* 260, 712-717.

Liu, X. & Ambudkar, I. S. (2001). Characteristics of a store-operated calcium-permeable channel: sarcoendoplasmic reticulum calcium pump function controls channel gating. *J.Biol.Chem.* 276, 29891-29898.

Lockwich, T. P., Liu, X., Singh, B. B., Jadlowiec, J., Weiland, S., & Ambudkar, I. S. (2000). Assembly of Trp1 in a signaling complex associated with caveolin- scaffolding lipid raft domains. *J.Biol.Chem.* 275, 11934-11942.

Lutz, M. P., Piiper, A., Gaisano, H. Y., Stryjek-Kaminska, D., Zeuzem, S., & Adler, G. (1997). Protein tyrosine phosphorylation in pancreatic acini: differential effects of VIP and CCK. *Am.J.Physiol* 273, G1226-G1232.

Lutz, M. P., Sutor, S. L., Abraham, R. T., & Miller, L. J. (1993). A role for cholecystokinin-stimulated protein tyrosine phosphorylation in regulated secretion by the pancreatic acinar cell. *J.Biol.Chem.* 268, 11119-11124.

Ma, H. T., Patterson, R. L., van Rossum, D. B., Birnbaumer, L., Mikoshiba, K., & Gill, D. L. (2000). Requirement of the inositol trisphosphate receptor for activation of store-operated Ca^{2+} channels. *Science* 287, 1647-1651.

Ma, R., Pluznick, J., Kudlacek, P., & Sansom, S. C. (2001). Protein kinase C activates store-operated Ca^{2+} channels in human glomerular mesangial cells. *J.Biol.Chem.* 276, 25759-25765.

Marrero, I., Sanchez-Bueno, A., Cobbold, P. H., & Dixon, C. J. (1994). Taurolithocholate and taurolithocholate 3-sulphate exert different effects on cytosolic free Ca^{2+} concentration in rat hepatocytes. *Biochem.J.* 300 (Pt 2), 383-386.

Matozaki, T., Goke, B., Tsunoda, Y., Rodriguez, M., Martinez, J., & Williams, J. A. (1990). Two functionally distinct cholecystokinin receptors show different modes of action on Ca^{2+} mobilization and phospholipid hydrolysis in isolated rat pancreatic acini. Studies using a new cholecystokinin analog, JMV-180. *J.Biol.Chem.* 265, 6247-6254.

Matozaki, T., Martinez, J., & Williams, J. A. (1989). A new CCK analogue differentiates two functionally distinct CCK receptors in rat and mouse pancreatic acini. *Am.J.Physiol* **257**, G594-G600.

McCormack, J. G. & Denton, R. M. (1990). Intracellular calcium ions and intramitochondrial Ca^{2+} in the regulation of energy metabolism in mammalian tissues. *Proc.Nutr.Soc.* **49**, 57-75.

Michaelis, M. L., Bigelow, D. J., Schoneich, C., Williams, T. D., Ramonda, L., Yin, D., Huhmer, A. F., Yao, Y., Gao, J., & Squier, T. C. (1996). Decreased plasma membrane calcium transport activity in aging brain. *Life Sci.* **59**, 405-412.

Missiaen, L., Van Acker, K., Parys, J. B., De Smedt, H., Van Baelen, K., Weidema, A. F., Vanoevelen, J., Raeymaekers, L., Renders, J., Callewaert, G., Rizzuto, R., & Wuytack, F. (2001). Baseline cytosolic Ca^{2+} oscillations derived from a non-endoplasmic reticulum Ca^{2+} store. *J.Biol.Chem.* **276**, 39161-39170.

Missiaen, L., Vanoevelen, J., Parys, J. B., Raeymaekers, L., De Smedt, H., Callewaert, G., Erneux, C., & Wuytack, F. (2002a). Ca^{2+} uptake and release properties of a thapsigargin-insensitive nonmitochondrial Ca^{2+} store in A7r5 and 16HBE14o- cells. *J.Biol.Chem.* **277**, 6898-6902.

Missiaen, L., Vanoevelen, J., Van Acker, K., Raeymaekers, L., Parys, J. B., Callewaert, G., Wuytack, F., & De Smedt, H. (2002b). Ca^{2+} signals in Pmr1-GFP-expressing COS-1 cells with functional endoplasmic reticulum. *Biochem.Biophys.Res.Commun.* **294**, 249-253.

Mitchell, K. J., Pinton, P., Varadi, A., Tacchetti, C., Ainscow, E. K., Pozzan, T., Rizzuto, R., & Rutter, G. A. (2001). Dense core secretory vesicles revealed as a dynamic Ca^{2+} store in neuroendocrine cells with a vesicle-associated membrane protein aequorin chimaera. *J.Cell Biol.* **155**, 41-51.

Mogami, H., Nakano, K., Tepikin, A. V., & Petersen, O. H. (1997). Ca^{2+} flow via tunnels in polarized cells: recharging of apical Ca^{2+} stores by focal Ca^{2+} entry through basal membrane patch. *Cell* **88**, 49-55.

Monteith, G. R., Wanigasekara, Y., & Roufogalis, B. D. (1998). The plasma membrane calcium pump, its role and regulation: new complexities and possibilities. *J.Pharmacol.Toxicol.Methods* **40**, 183-190.

Motta, P. M., Macchiarelli, G., Nottola, S. A., & Correr, S. (1997). Histology of the exocrine pancreas. *Microsc.Res.Tech.* **37**, 384-398.

Muallem, S. (1989). Calcium transport pathways of pancreatic acinar cells. *Annu.Rev.Physiol* **51**, 83-105.

Muallem, S., Beeker, T., & Pandol, S. J. (1988a). Role of Na^+/Ca^{2+} exchange and the plasma membrane Ca^{2+} pump in hormone- mediated Ca2+ efflux from pancreatic acini. *J.Membr.Biol.* **102**, 153-162.

Muallem, S. & Lee, M. G. (1997). High $[Ca^{2+}]_i$ domains, secretory granules and exocytosis. *Cell Calcium* **22**, 1-4.

Muallem, S., Schoeffield, M. S., Fimmel, C. J., & Pandol, S. J. (1988b). Agonist-sensitive calcium pool in the pancreatic acinar cell. II. Characterization of reloading. *Am.J.Physiol* **255**, G229-G235.

Mulderry, P. K. (1996). Intracellular Microinjection: A Powerful Tool in the Study of Neuronal Gene Expression and Function. *Methods* **10**, 292-300.

Nathanson, M. H., Fallon, M. B., Padfield, P. J., & Maranto, A. R. (1994). Localization of the type 3 inositol 1,4,5-trisphosphate receptor in the Ca^{2+} wave trigger zone of pancreatic acinar cells. *J.Biol.Chem.* **269**, 4693-4696.

Nedergaard, M. (1994). Direct signaling from astrocytes to neurons in cultures of mammalian brain cells. *Science* **263**, 1768-1771.

Neher, E. & Augustine, G. J. (1992). Calcium gradients and buffers in bovine chromaffin cells. *J.Physiol* **450**, 273-301.

Nelson, G., Paraoan, L., Spiller, D. G., Wilde, G. J., Browne, M. A., Djali, P. K., Unitt, J. F., Sullivan, E., Floettmann, E., & White, M. R. (2002). Multi-parameter analysis of the kinetics of NF-kappaB signalling and transcription in single living cells. *J.Cell Sci.* **115**, 1137-1148.

Niederau, C., Niederau, M., Luthen, R., Strohmeyer, G., Ferrell, L. D., & Grendell, J. H. (1990). Pancreatic exocrine secretion in acute experimental pancreatitis. *Gastroenterology* **99**, 1120-1127.

Nishiyama, A. & Petersen, O. H. (1974). Pancreatic acinar cells: membrane potential and resistance change evoked by acetylcholine. *J.Physiol* 238, 145-158.

Nishizuka, Y. (1984). The role of protein kinase C in cell surface signal transduction and tumour promotion. *Nature* 308, 693-698.

Norman, J. (1998). The role of cytokines in the pathogenesis of acute pancreatitis. *Am.J.Surg.* 175, 76-83.

Opie, E. L. (1901). The etiology of acute hemorrhagic pancreatitis. *Johns Hopkins Hospital Bulletin* 121, 182-188.

Palade, P., Dettbarn, C., Volpe, P., Alderson, B., & Otero, A. S. (1989). Direct inhibition of inositol-1,4,5-trisphosphate-induced Ca^{2+} release from brain microsomes by K^+ channel blockers. *Mol.Pharmacol.* 36, 664-672.

Pandol, S. J. & Schoeffield-Payne, M. S. (1990). Cyclic GMP mediates the agonist-stimulated increase in plasma membrane calcium entry in the pancreatic acinar cell. *J.Biol.Chem.* 265, 12846-12853.

Pandol, S. J. & Schoeffield, M. S. (1986). 1,2-Diacylglycerol, protein kinase C, and pancreatic enzyme secretion. *J.Biol.Chem.* 261, 4438-4444.

Pandol, S. J., Schoeffield, M. S., Fimmel, C. J., & Muallem, S. (1987). The agonist-sensitive calcium pool in the pancreatic acinar cell. Activation of plasma membrane Ca^{2+} influx mechanism. *J.Biol.Chem.* 262, 16963-16968.

Parekh, A. B. & Penner, R. (1995). Depletion-activated calcium current is inhibited by protein kinase in RBL-2H3 cells. *Proc.Natl.Acad.Sci.U.S.A* 92, 7907-7911.

Parekh, A. B. & Penner, R. (1997). Store depletion and calcium influx. *Physiol Rev.* 77, 901-930.

Park, M. K., Ashby, M. C., Erdemli, G., Petersen, O. H., & Tepikin, A. V. (2001a). Perinuclear, perigranular and sub-plasmalemmal mitochondria have distinct functions in the regulation of cellular calcium transport. *EMBO J.* 20, 1863-1874.

Park, M. K., Lomax, R. B., Tepikin, A. V., & Petersen, O. H. (2001b). Local uncaging of caged Ca^{2+} reveals distribution of Ca^{2+}-activated Cl^- channels in pancreatic acinar cells. *Proc.Natl.Acad.Sci.U.S.A* 98, 10948-10953.

Park, M. K., Petersen, O. H., & Tepikin, A. V. (2000). The endoplasmic reticulum as one continuous Ca^{2+} pool: visualization of rapid Ca^{2+} movements and equilibration. *EMBO J.* 19, 5729-5739.

Patterson, R. L., van Rossum, D. B., & Gill, D. L. (1999). Store-operated Ca^{2+} entry: evidence for a secretion-like coupling model. *Cell* 98, 487-499.

Peng, J. B., Chen, X. Z., Berger, U. V., Vassilev, P. M., Tsukaguchi, H., Brown, E. M., & Hediger, M. A. (1999). Molecular cloning and characterization of a channel-like transporter mediating intestinal calcium absorption. *J.Biol.Chem.* 274, 22739-22746.

Penniston, J. T. & Enyedi, A. (1998). Modulation of the plasma membrane Ca^{2+} pump. *J.Membr.Biol.* 165, 101-109.

Perez-Martin, G., Gomez-Cerezo, J., Codoceo, R., Olveira, A., Conde, P., Garces, M. C., Barbado, F. J., & Vazquez, J. J. (1998). Bilirubinate granules: main pathologic bile component in patients with idiopathic acute pancreatitis. *Am.J.Gastroenterol.* 93, 360-362.

Perez-Terzic, C., Pyle, J., Jaconi, M., Stehno-Bittel, L., & Clapham, D. E. (1996). Conformational states of the nuclear pore complex induced by depletion of nuclear Ca^{2+} stores. *Science* 273, 1875-1877.

Petersen, C. C., Toescu, E. C., & Petersen, O. H. (1991a). Different patterns of receptor-activated cytoplasmic Ca^{2+} oscillations in single pancreatic acinar cells: dependence on receptor type, agonist concentration and intracellular Ca^{2+} buffering. *EMBO J.* 10, 527-533.

Petersen, C. C., Toescu, E. C., Potter, B. V., & Petersen, O. H. (1991b). Inositol triphosphate produces different patterns of cytoplasmic Ca^{2+} spiking depending on its concentration. *FEBS Lett.* 293, 179-182.

Petersen, O. H. (1975). Proceedings: Electrical coupling between pancreatic acinar cells. *J.Physiol* 250, 2P-4P.

Pfeiffer, F., Sternfeld, L., Schmid, A., & Schulz, I. (1998). Control of Ca^{2+} wave propagation in mouse pancreatic acinar cells. *Am.J.Physiol* **274**, C663-C672.

Piiper, A., Stryjek-Kaminska, D., Klengel, R., & Zeuzem, S. (1997). CCK, carbachol, and bombesin activate distinct PLC-beta isoenzymes via Gq/11 in rat pancreatic acinar membranes. *Am.J.Physiol* **272**, G135-G140.

Pinton, P., Pozzan, T., & Rizzuto, R. (1998). The Golgi apparatus is an inositol 1,4,5-trisphosphate-sensitive Ca^{2+} store, with functional properties distinct from those of the endoplasmic reticulum. *EMBO J.* **17**, 5298-5308.

Pollo, D. A., Baldassare, J. J., Honda, T., Henderson, P. A., Talkad, V. D., & Gardner, J. D. (1994). Effects of cholecystokinin (CCK) and other secretagogues on isoforms of protein kinase C (PKC) in pancreatic acini. *Biochim.Biophys.Acta* **1224**, 127-138.

Pollock, W. K., Sage, S. O., & Rink, T. J. (1987). Stimulation of Ca^{2+} efflux from fura-2-loaded platelets activated by thrombin or phorbol myristate acetate. *FEBS Lett.* **210**, 132-136.

Porat, A. & Elazar, Z. (2000). Regulation of intra-Golgi membrane transport by calcium. *J.Biol.Chem.* **275**, 29233-29237.

Powers, R. E., Grady, T., Orchard, J. L., & Gilrane, T. B. (1993). Different effects of hyperstimulation by similar classes of secretagogues on the exocrine pancreas. *Pancreas* **8**, 58-63.

Powers, R. E., Johnson, P. C., Houlihan, M. J., Saluja, A. K., & Steer, M. L. (1985). Intracellular Ca^{2+} levels and amylase secretion in Quin 2-loaded mouse pancreatic acini. *Am.J.Physiol* **248**, C535-C541.

Putney, J. W., Jr. (1986). A model for receptor-regulated calcium entry. *Cell Calcium* **7**, 1-12.

Putney, J. W., Jr. & McKay, R. R. (1999). Capacitative calcium entry channels. *Bioessays* **21**, 38-46.

Raraty, M., Ward, J., Erdemli, G., Vaillant, C., Neoptolemos, J. P., Sutton, R., & Petersen, O. H. (2000). Calcium-dependent enzyme activation and vacuole formation in the apical granular region of pancreatic acinar cells. *Proc.Natl.Acad.Sci.U.S.A* **97**, 13126-13131.

Raraty, M. G., Petersen, O. H., Sutton, R., & Neoptolemos, J. P. (1999). Intracellular free ionized calcium in the pathogenesis of acute pancreatitis. *Baillieres Best.Pract.Res.Clin.Gastroenterol.* **13**, 241-251.

Renard, P., Percherancier, Y., Kroll, M., Thomas, D., Virelizier, J. L., Arenzana-Seisdedos, F., & Bachelerie, F. (2000). Inducible NF-kappaB activation is permitted by simultaneous degradation of nuclear IkappaBalpha. *J.Biol.Chem.* **275**, 15193-15199.

Rickard, J. E. & Sheterline, P. (1985). Evidence that phorbol ester interferes with stimulated Ca^{2+} redistribution by activating Ca^{2+} efflux in neutrophil leucocytes. *Biochem.J.* **231**, 623-628.

Rizo, J. & Sudhof, T. C. (2002). Snares and munc18 in synaptic vesicle fusion. *Nat.Rev.Neurosci.* **3**, 641-653.

Rizzuto, R., Brini, M., Murgia, M., & Pozzan, T. (1993). Microdomains with high Ca2+ close to IP3-sensitive channels that are sensed by neighboring mitochondria. *Science* **262**, 744-747.

Rizzuto, R., Brini, M., Pizzo, P., Murgia, M., & Pozzan, T. (1995). Chimeric green fluorescent protein as a tool for visualizing subcellular organelles in living cells. *Curr.Biol.* **5**, 635-642.

Robb-Gaspers, L. D., Burnett, P., Rutter, G. A., Denton, R. M., Rizzuto, R., & Thomas, A. P. (1998). Integrating cytosolic calcium signals into mitochondrial metabolic responses. *EMBO J.* **17**, 4987-5000.

Rosado, J. A. & Sage, S. O. (2000a). Phosphoinositides are required for store-mediated calcium entry in human platelets. *J.Biol.Chem.* **275**, 9110-9113.

Rosado, J. A. & Sage, S. O. (2000b). The actin cytoskeleton in store-mediated calcium entry. *J.Physiol* **526 Pt 2**, 221-229.

Rutter, G. A., Fasolato, C., & Rizzuto, R. (1998). Calcium and organelles: a two-sided story. *Biochem.Biophys.Res.Commun.* **253**, 549-557.

Saez, J. C., Connor, J. A., Spray, D. C., & Bennett, M. V. (1989). Hepatocyte gap junctions are permeable to the second messenger, inositol 1,4,5-trisphosphate, and to calcium ions. *Proc.Natl.Acad.Sci.U.S.A* **86**, 2708-2712.

Saluja, A. K., Bhagat, L., Lee, H. S., Bhatia, M., Frossard, J. L., & Steer, M. L. (1999). Secretagogue-induced digestive enzyme activation and cell injury in rat pancreatic acini. *Am.J.Physiol* **276**, G835-G842.

Saluja, A. K., Donovan, E. A., Yamanaka, K., Yamaguchi, Y., Hofbauer, B., & Steer, M. L. (1997). Cerulein-induced in vitro activation of trypsinogen in rat pancreatic acini is mediated by cathepsin B. *Gastroenterology* **113**, 304-310.

Saluja, A. K., Saluja, M., Printz, H., Zavertnik, A., Sengupta, A., & Steer, M. L. (1989). Experimental pancreatitis is mediated by low-affinity cholecystokinin receptors that inhibit digestive enzyme secretion. *Proc.Natl.Acad.Sci.U.S.A* **86**, 8968-8971.

Sandberg, K., Ji, H., Iida, T., & Catt, K. J. (1992). Intercellular communication between follicular angiotensin receptors and Xenopus laevis oocytes: medication by an inositol 1,4,5- trisphosphate-dependent mechanism. *J.Cell Biol.* **117**, 157-167.

Santella, L. & Kyozuka, K. (1997). Effects of 1-methyladenine on nuclear Ca^{2+} transients and meiosis resumption in starfish oocytes are mimicked by the nuclear injection of inositol 1,4,5-trisphosphate and cADP-ribose. *Cell Calcium* **22**, 11-20.

Satoh, A., Shimosegawa, T., Fujita, M., Kimura, K., Masamune, A., Koizumi, M., & Toyota, T. (1999). Inhibition of nuclear factor-kappaB activation improves the survival of rats with taurocholate pancreatitis. *Gut* **44**, 253-258.

Schafer, C., Ross, S. E., Bragado, M. J., Groblewski, G. E., Ernst, S. A., & Williams, J. A. (1998). A role for the p38 mitogen-activated protein kinase/Hsp 27 pathway in cholecystokinin-induced changes in the actin cytoskeleton in rat pancreatic acini. *J.Biol.Chem.* **273**, 24173-24180.

Scheele, G., Adler, G., & Kern, H. (1987). Exocytosis occurs at the lateral plasma membrane of the pancreatic acinar cell during supramaximal secretagogue stimulation. *Gastroenterology* **92**, 345-353.

Schmid, R. M. & Adler, G. (2000). NF-kappaB/rel/IkappaB: implications in gastrointestinal diseases. *Gastroenterology* **118**, 1208-1228.

Senninger, N. (1992). Bile-induced pancreatitis. *Eur.Surg.Res.* **24 Suppl 1**, 68-73.

Shull, G. E. (2000). Gene knockout studies of Ca^{2+}-transporting ATPases. *Eur.J.Biochem.* **267**, 5284-5290.

Shuttleworth, T. J. (1996). Arachidonic acid activates the noncapacitative entry of Ca^{2+} during $[Ca^{2+}]_i$ oscillations. *J.Biol.Chem.* **271**, 21720-21725.

Siegel, G., Sternfeld, L., Gonzalez, A., Schulz, I., & Schmid, A. (2001). Arachidonic acid modulates the spatiotemporal characteristics of agonist-evoked Ca^{2+} waves in mouse pancreatic acinar cells. *J.Biol.Chem.* **276**, 16986-16991.

Sienaert, I., De Smedt, H., Parys, J. B., Missiaen, L., Vanlingen, S., Sipma, H., & Casteels, R. (1996). Characterization of a cytosolic and a luminal Ca^{2+} binding site in the type I inositol 1,4,5-trisphosphate receptor. *J.Biol.Chem.* **271**, 27005-27012.

Silverman, N. & Maniatis, T. (2001). NF-kappaB signaling pathways in mammalian and insect innate immunity. *Genes Dev.* **15**, 2321-2342.

Stauffer, P. L., Zhao, H., Luby-Phelps, K., Moss, R. L., Star, R. A., & Muallem, S. (1993). Gap junction communication modulates $[Ca^{2+}]_i$ oscillations and enzyme secretion in pancreatic acini. *J.Biol.Chem.* **268**, 19769-19775.

Steer, M. (1999). Primary Intracellular Events in Pancreatitis. In *Acute Pancreatitis Novel Concepts in Biology and Therapy*, eds. Buchler, M. W., Uhl, W., Friess, H., & Malfertheiner, P., pp. 3-12. **Blackwell Science.**

Stehno-Bittel, L., Perez-Terzic, C., & Clapham, D. E. (1995). Diffusion across the nuclear envelope inhibited by depletion of the nuclear Ca^{2+} store. *Science* **270**, 1835-1838.

Steinle, A. U., Weidenbach, H., Wagner, M., Adler, G., & Schmid, R. M. (1999). NF-kappaB/Rel activation in cerulein pancreatitis. *Gastroenterology* **116**, 420-430.

Strange, R. (1984). Hepatic Bile Flow. *Physiological Reviews* **64**, 1055-1102.

Streb, H., Heslop, J. P., Irvine, R. F., Schulz, I., & Berridge, M. J. (1985). Relationship between secretagogue-induced Ca^{2+} release and inositol polyphosphate production in permeabilized pancreatic acinar cells. *J.Biol.Chem.* **260**, 7309-7315.

Streb, H., Irvine, R. F., Berridge, M. J., & Schulz, I. (1983). Release of Ca^{2+} from a nonmitochondrial intracellular store in pancreatic acinar cells by inositol-1,4,5-trisphosphate. *Nature* **306**, 67-69.

Strehler, E. E., Strehler-Page, M. A., Vogel, G., & Carafoli, E. (1989). mRNAs for plasma membrane calcium pump isoforms differing in their regulatory domain are generated by alternative splicing that involves two internal donor sites in a single exon. *Proc.Natl.Acad.Sci.U.S.A* **86**, 6908-6912.

Sugawara, H., Kurosaki, M., Takata, M., & Kurosaki, T. (1997). Genetic evidence for involvement of type 1, type 2 and type 3 inositol 1,4,5-trisphosphate receptors in signal transduction through the B-cell antigen receptor. *EMBO J.* **16**, 3078-3088.

Tando, Y., Algul, H., Wagner, M., Weidenbach, H., Adler, G., & Schmid, R. M. (1999). Caerulein-induced NF-kappaB/Rel activation requires both Ca^{2+} and protein kinase C as messengers. *Am.J.Physiol* **277**, G678-G686.

Tepikin, A. V., Voronina, S. G., Gallacher, D. V., & Petersen, O. H. (1992a). Acetylcholine-evoked increase in the cytoplasmic Ca^{2+} concentration and Ca^{2+} extrusion measured simultaneously in single mouse pancreatic acinar cells. *J.Biol.Chem.* **267**, 3569-3572.

Tepikin, A. V., Voronina, S. G., Gallacher, D. V., & Petersen, O. H. (1992b). Pulsatile Ca^{2+} extrusion from single pancreatic acinar cells during receptor-activated cytosolic Ca^{2+} spiking. *J.Biol.Chem.* **267**, 14073-14076.

Thibault, O., Hadley, R., & Landfield, P. W. (2001). Elevated postsynaptic $[Ca^{2+}]_i$ and L-type calcium channel activity in aged hippocampal neurons: relationship to impaired synaptic plasticity. *J.Neurosci.* **21**, 9744-9756.

Thorn, P., Gerasimenko, O., & Petersen, O. H. (1994). Cyclic ADP-ribose regulation of ryanodine receptors involved in agonist evoked cytosolic Ca^{2+} oscillations in pancreatic acinar cells. *EMBO J.* **13**, 2038-2043.

Thorn, P., Lawrie, A. M., Smith, P. M., Gallacher, D. V., & Petersen, O. H. (1993a). Ca^{2+} oscillations in pancreatic acinar cells: spatiotemporal relationships and functional implications. *Cell Calcium* **14**, 746-757.

Thorn, P., Lawrie, A. M., Smith, P. M., Gallacher, D. V., & Petersen, O. H. (1993b). Local and global cytosolic Ca^{2+} oscillations in exocrine cells evoked by agonists and inositol trisphosphate. *Cell* **74**, 661-668.

Thorn, P. & Petersen, O. H. (1993). Calcium oscillations in pancreatic acinar cells, evoked by the cholecystokinin analogue JMV-180, depend on functional inositol 1,4,5- trisphosphate receptors. *J.Biol.Chem.* **268**, 23219-23221.

Tinel, H., Cancela, J. M., Mogami, H., Gerasimenko, J. V., Gerasimenko, O. V., Tepikin, A. V., & Petersen, O. H. (1999). Active mitochondria surrounding the pancreatic acinar granule region prevent spreading of inositol trisphosphate-evoked local cytosolic Ca^{2+} signals. *EMBO J.* **18**, 4999-5008.

Toescu, E. C., Lawrie, A. M., Petersen, O. H., & Gallacher, D. V. (1992). Spatial and temporal distribution of agonist-evoked cytoplasmic Ca^{2+} signals in exocrine acinar cells analysed by digital image microscopy. *EMBO J.* **11**, 1623-1629.

Toescu, E. C. & Petersen, O. H. (1995). Region-specific activity of the plasma membrane Ca^{2+} pump and delayed activation of Ca^{2+} entry characterize the polarized, agonist-evoked Ca^{2+} signals in exocrine cells. *J.Biol.Chem.* **270**, 8528-8535.

Torgerson, R. R. & McNiven, M. A. (2000). Agonist-induced changes in cell shape during regulated secretion in rat pancreatic acini. *J.Cell Physiol* **182**, 438-447.

Trepakova, E. S., Csutora, P., Hunton, D. L., Marchase, R. B., Cohen, R. A., & Bolotina, V. M. (2000). Calcium influx factor directly activates store-operated cation channels in vascular smooth muscle cells. *J.Biol.Chem.* **275**, 26158-26163.

Tsien, R. Y. (1981). A non-disruptive technique for loading calcium buffers and indicators into cells. *Nature* **290**, 527-528.

Tsunoda, Y. & Tashiro, Y. (1999). Distinct characteristics of receptor-operated Ca^{2+} influx and refilling in pancreatic acinar cells. *Biochem.Biophys.Res.Commun.* **256**, 579-583.

Tsunoda, Y., Yoshida, H., Africa, L., Steil, G. J., & Owyang, C. (1996). Src kinase pathways in extracellular Ca^{2+}-dependent pancreatic enzyme secretion. *Biochem.Biophys.Res.Commun.* **227**, 876-884.

Urunuela, A., Manso, M. A., de la Mano, A. M., Sevillano, S., Orfao, A., & De, D., I (2002). Asynchronous impairment of calcium homoeostasis in different acinar cells after pancreatic duct obstruction in rat. *Clin.Sci.(Lond)* **102**, 615-622.

Usachev, Y. M., DeMarco, S. J., Campbell, C., Strehler, E. E., & Thayer, S. A. (2002). Bradykinin and ATP accelerate Ca^{2+} efflux from rat sensory neurons via protein kinase C and the plasma membrane Ca^{2+} pump isoform 4. *Neuron* **33**, 113-122.

Valentijn, K. M., Gumkowski, F. D., & Jamieson, J. D. (1999). The subapical actin cytoskeleton regulates secretion and membrane retrieval in pancreatic acinar cells. *J.Cell Sci.* **112 (Pt 1)**, 81-96.

Van Baelen, K., Vanoevelen, J., Missiaen, L., Raeymaekers, L., & Wuytack, F. (2001). The Golgi PMR1 P-type ATPase of Caenorhabditis elegans. Identification of the gene and demonstration of calcium and manganese transport. *J.Biol.Chem.* **276**, 10683-10691.

Vaquero, E., Gukovsky, I., Zaninovic, V., Gukovskaya, A. S., & Pandol, S. J. (2001). Localized pancreatic NF-kappaB activation and inflammatory response in taurocholate-induced pancreatitis. *Am.J.Physiol Gastrointest.Liver Physiol* **280**, G1197-G1208.

Vennekens, R., Hoenderop, J. G., Prenen, J., Stuiver, M., Willems, P. H., Droogmans, G., Nilius, B., & Bindels, R. J. (2000). Permeation and gating properties of the novel epithelial Ca^{2+} channel. *J.Biol.Chem.* **275**, 3963-3969.

Voets, T., Prenen, J., Fleig, A., Vennekens, R., Watanabe, H., Hoenderop, J. G., Bindels, R. J., Droogmans, G., Penner, R., & Nilius, B. (2001). CaT1 and the calcium release-activated calcium channel manifest distinct pore properties. *J.Biol.Chem.* **276**, 47767-47770.

Voronina, S., Longbottom, R., Sutton, R., Petersen, O. H., & Tepikin, A. (2002a). Bile acids induce calcium signals in mouse pancreatic acinar cells: implications for bile-induced pancreatic pathology. *J.Physiol* **540**, 49-55.

Voronina, S., Sukhomlin, T., Johnson, P. R., Erdemli, G., Petersen, O. H., & Tepikin, A. (2002b). Correlation of NADH and Ca^{2+} signals in mouse pancreatic acinar cells. *J.Physiol* **539**, 41-52.

Wagner, A. C., Metzler, W., Hofken, T., Weber, H., & Goke, B. (1999). p38 map kinase is expressed in the pancreas and is immediately activated following cerulein hyperstimulation. *Digestion* **60**, 41-47.

Wakui, M., Potter, B. V., & Petersen, O. H. (1989). Pulsatile intracellular calcium release does not depend on fluctuations in inositol trisphosphate concentration. *Nature* **339**, 317-320.

Ward, J. B., Sutton, R., Jenkins, S. A., & Petersen, O. H. (1996). Progressive disruption of acinar cell calcium signaling is an early feature of cerulein-induced pancreatitis in mice. *Gastroenterology* **111**, 481-491.

Warnat, J., Philipp, S., Zimmer, S., Flockerzi, V., & Cavalie, A. (1999). Phenotype of a recombinant store-operated channel: highly selective permeation of Ca^{2+}. *J.Physiol* **518 (Pt 3)**, 631-638.

Whitcomb, D. C., Gorry, M. C., Preston, R. A., Furey, W., Sossenheimer, M. J., Ulrich, C. D., Martin, S. P., Gates, L. K., Jr., Amann, S. T., Toskes, P. P., Liddle, R., McGrath, K., Uomo, G., Post, J. C., & Ehrlich, G. D. (1996). Hereditary pancreatitis is caused by a mutation in the cationic trypsinogen gene. *Nat.Genet.* **14**, 141-145.

Williams, J. A. (1980). Regulation of pancreatic acinar cell function by intracellular calcium. *Am.J.Physiol* **238**, G269-G279.

Williams, J. A. (2001). Intracellular signaling mechanisms activated by cholecystokinin- regulating synthesis and secretion of digestive enzymes in pancreatic acinar cells. *Annu.Rev.Physiol* **63**, 77-97.

Williams, J. A. & Hotman, S. R. (1986). Stimulus-Secretion coupling in pancreatic acinar cells. In *The exocrine pancreas*, eds. Go, V. L. W., Gardner, J. D., Brooks, F. P., Lebenthal, E., Magno, E. P., & Scheele, G. A., pp. 109-140. Raven Press, New York.

Williams, J. A. & Lee, M. (1974). Pancreatic acinar cells: use of Ca^{2+} ionophore to separate enzyme release from the earlier steps in stimulus-secretion coupling. *Biochem.Biophys.Res.Commun.* **60**, 542-548.

Yao, Y., Ferrer-Montiel, A. V., Montal, M., & Tsien, R. Y. (1999). Activation of store-operated Ca^{2+} current in Xenopus oocytes requires SNAP-25 but not a diffusible messenger. *Cell* **98**, 475-485.

Yoo, S. H. & Albanesi, J. P. (1990). Inositol 1,4,5-trisphosphate-triggered Ca^{2+} release from bovine adrenal medullary secretory vesicles. *J.Biol.Chem.* **265**, 13446-13448.

Yoo, S. H. & Jeon, C. J. (2000). Inositol 1,4,5-trisphosphate receptor/Ca^{2+} channel modulatory role of chromogranin A, a Ca^{2+} storage protein of secretory granules. *J.Biol.Chem.* **275**, 15067-15073.

Yue, L., Peng, J. B., Hediger, M. A., & Clapham, D. E. (2001). CaT1 manifests the pore properties of the calcium-release-activated calcium channel. *Nature* **410**, 705-709.

Yule, D. I., Baker, C. W., & Williams, J. A. (1999). Calcium signaling in rat pancreatic acinar cells: a role for Galphaq, Galpha11, and Galpha14. *Am.J.Physiol* **276**, G271-G279.

Yule, D. I., Kim, E. T., & Williams, J. A. (1994). Tyrosine kinase inhibitors attenuate "capacitative" Ca^{2+} influx in rat pancreatic acinar cells. *Biochem.Biophys.Res.Commun.* **202** , 1697-1704.

Yule, D. I., Lawrie, A. M., & Gallacher, D. V. (1991). Acetylcholine and cholecystokinin induce different patterns of oscillating calcium signals in pancreatic acinar cells. *Cell Calcium* **12**, 145-151.

Yule, D. I., Stuenkel, E., & Williams, J. A. (1996). Intercellular calcium waves in rat pancreatic acini: mechanism of transmission. *Am.J.Physiol* **271**, C1285-C1294.

Zhang, B. X., Zhao, H., Loessberg, P., & Muallem, S. (1992). Activation of the plasma membrane Ca^{2+} pump during agonist stimulation of pancreatic acini. *J.Biol.Chem.* **267**, 15419-15425.

Zhou, W., Shen, F., Miller, J. E., Han, Q., & Olson, M. S. (1996). Evidence for altered cellular calcium in the pathogenetic mechanism of acute pancreatitis in rats. *J.Surg.Res.* **60**, 147-155.

Zolle, O., Lawrie, A. M., & Simpson, A. W. (2000). Activation of the particulate and not the soluble guanylate cyclase leads to the inhibition of Ca^{2+} extrusion through localized elevation of cGMP. *J.Biol.Chem.* **275**, 25892-25899.

Zweifach, A. & Lewis, R. S. (1995). Slow calcium-dependent inactivation of depletion-activated calcium current. Store-dependent and -independent mechanisms. *J.Biol.Chem.* **270**, 14445-14451.